

University of Alberta

**Development of an Injectable Implant System for Local
Delivery of Camptothecin**

By

Arash Hatefi



A thesis

**submitted to the Faculty of Graduate Studies and Research in partial fulfillment of
the requirements for the degree of**

Doctor of Philosophy

In

Pharmaceutical Sciences

Faculty of Pharmacy and Pharmaceutical Sciences

Edmonton, Alberta

Fall, 2002



National Library
of Canada

Acquisitions and
Bibliographic Services

395 Wellington Street
Ottawa ON K1A 0N4
Canada

Bibliothèque nationale
du Canada

Acquisitions et
services bibliographiques

395, rue Wellington
Ottawa ON K1A 0N4
Canada

Your file Votre référence

Our file Notre référence

The author has granted a non-exclusive licence allowing the National Library of Canada to reproduce, loan, distribute or sell copies of this thesis in microform, paper or electronic formats.

The author retains ownership of the copyright in this thesis. Neither the thesis nor substantial extracts from it may be printed or otherwise reproduced without the author's permission.

L'auteur a accordé une licence non exclusive permettant à la Bibliothèque nationale du Canada de reproduire, prêter, distribuer ou vendre des copies de cette thèse sous la forme de microfiche/film, de reproduction sur papier ou sur format électronique.

L'auteur conserve la propriété du droit d'auteur qui protège cette thèse. Ni la thèse ni des extraits substantiels de celle-ci ne doivent être imprimés ou autrement reproduits sans son autorisation.

0-612-81199-9

Canada

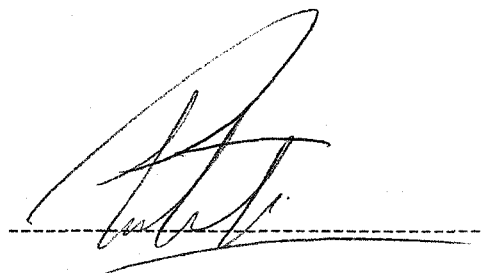
University of Alberta

Library Release Form

Name of Author: Arash Hatefi
Title of Thesis: Development of an Injectable Implant System for Local Delivery of Camptothecin
Degree: Doctor of Philosophy
Year Degree Granted: 2002

Permission is hereby granted to the University of Alberta library to lend or sell such copies for private scholarly, or scientific research purpose only.

The author reserves all other publication and other rights in association with the copyright in the thesis, and except as herein before provided, neither the thesis nor any substantial portion thereof may be printed or otherwise reproduced in any material form whatever without the author's written permission.

A handwritten signature in black ink, appearing to read 'Arash Hatefi', is written over a horizontal dashed line.

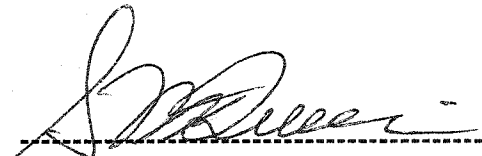
3118 Pharmacy-Dentistry Centre
University of Alberta
Edmonton, AB T6G 2N8

Date: Oct. 1/02

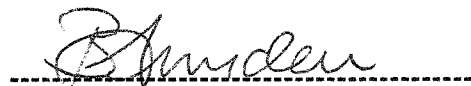
University of Alberta

Faculty of Graduate Studies and Research

The undersigned certify that they have read, and recommended to the Faculty of Graduate Studies and Research for acceptance, a thesis entitled **Development of an Injectable Implant System for Local Delivery of Camptothecin** submitted by **Arash Hatefi** in partial fulfillment of the requirements for the degree of **Doctor of Philosophy in Pharmaceutical Sciences**.



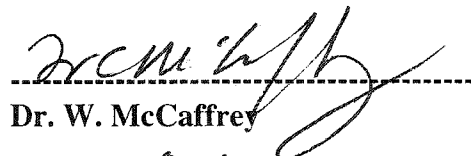
Dr. S. McQuarrie (Supervisor)



Dr. B. Amsden (Co-supervisor)



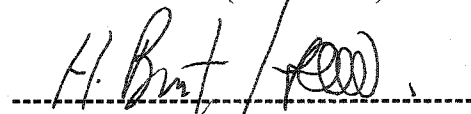
Dr. G. G. Miller



Dr. W. McCaffrey



Dr. L. I. Wiebe (Chairman)



Dr. H. Burt (External Examiner)

Date: Sep. 29/02

Dedications

This manuscript is dedicated to

*My beloved father, mother and sister, whose encouragements have
given me motivation, confidence and determination.*

*Dr. Brian Amsden who educated me patiently and guided me all
along.*

Abstract

Camptothecin is a potent anticancer drug which is highly water insoluble and sensitive to aqueous media. This drug decomposes via hydrolysis to less potent by-products which can cause serious side effects. These situations may be best treated using localized sustained release chemotherapy. This method of drug delivery will reduce the extent of undesirable side effects such as anaphylaxis and emboli formation. Furthermore, if the drug is delivered intra-tumorally, enhanced drug effectiveness may result. The principal aim of this research is to develop a material which possesses both a hydrophobic and polar nature, is syringeable, and biodegrades relatively quickly. A localized drug delivery system composed of a lipid block (long chain alcohols) and a biodegradable polyester (ϵ -caprolactone) was developed which was capable of solubilizing and stabilizing camptothecin while delivering it in a sustained fashion. The effects of the initiator's chemical structure on the rheology, crystallinity and melting point of the synthesized oligomers were investigated. It was found that oligo(ϵ -caprolactone) initiated with oleyl alcohol had the shortest degradation time in comparison to the other synthesized oligomers. This polymeric system can provide the lipophilic and polar environment necessary to incorporate this poorly water soluble drug (camptothecin) and maintain its stability within the delivery system after being injected into the simulated body fluid.

Acknowledgements

The present research has been fulfilled by the collaboration of a group of people and organizations. I would like to thank:

- My supervisors, Dr. Brian Amsden and Dr. Steve McQuarrie, for their support, guidance and insight without which it was not possible to accomplish this research. I specifically, would like to thank Dr. Amsden for providing research materials, financial assistance, responding to my emails and invaluable guidance. Despite the 3500 km distance between us, I am very grateful that I had his support at all times.
- Dr. Daneshtalab
- Dr. Loebenberg and all his graduate and post graduates
- Dr. Lavasanifar
- Dr. Jamali and all his graduate and post graduate students
- Don Whyte
- NSERC organization for providing financial support
- Dr. Xu in the Faculty of Chemical Engineering
- Faculty of Pharmacy and Pharmaceutical Sciences staff members
- And last but not least, faculty members from whom I have learned during the Ph.D. program.

TABLE OF CONTENTS

1.	CAMPTOTHECIN DELIVERY METHODS.....	1
1.1.	INTRODUCTION.....	2
1.1.1.	MECHANISM OF ACTION.....	3
1.1.2.	OTHER CLINICAL APPLICATIONS OF CPT.....	4
1.1.3.	PHYSICAL PROPERTIES OF CPT.....	5
1.1.4.	STRUCTURE ACTIVITY RELATIONSHIP.....	5
1.1.5.	CHEMICAL MODIFICATION.....	6
1.1.6.	PHARMACOKINETICS.....	8
1.2.	DELIVERY SYSTEMS.....	8
1.2.1.	POLYMER CONJUGATED CAMPTOTHECIN.....	9
1.2.2.	MICRO- AND NANO-PARTICLE ENCAPSULATED CPT.....	14
1.2.3.	LIPOSOMES, MICELLES, MINIEMULSIONS.....	17
1.3.	SUMMARY.....	20
1.4.	REFERENCES.....	28
2.	BIODEGRADABLE INJECTABLE IN-SITU FORMING DELIVERY SYSTEMS.....	37
2.1.	INTRODUCTION.....	38
2.2.	THERMOPLASTIC PASTES.....	39
2.3.	IN-SITU CROSSLINKED SYSTEMS.....	42
2.3.1.	THERMOSETS.....	42
2.3.2.	PHOTOCROSSLINKED GELS.....	44
2.3.3.	ION-MEDIATED GELATION.....	45

2.4.	IN-SITU POLYMER PRECIPITATION	47
2.4.1.	SOLVENT REMOVAL PRECIPITATION.....	47
2.4.2.	THERMALLY-INDUCED SOL/GEL TRANSITIONS.....	52
2.5.	IN-SITU SOLIDIFYING ORGANOGELS	57
2.6.	SUMMARY	59
2.7.	REFERENCES	73
3.	DEVELOPMENT AND CHARACTERIZATION OF AN INJECTABLE IMPLANT SYSTEM	89
3.1.	INTRODUCTION	90
3.1.1.	VISCOSITY.....	91
3.1.2.	DEGREE OF POLYMERIZATION.....	93
3.1.3.	POLYMERIZATION OF EPSILON-CAPROLACTONE.....	93
3.1.4.	HYPOTHESIS.....	95
3.1.5.	OBJECTIVES.....	95
3.2.	MATERIALS	96
3.3.	METHODS	96
3.3.1	POLYMER SYNTHESIS.....	96
3.3.2	POLYMER PURIFICATION.....	97
3.3.3	INSTRUMENTAL ANALYSIS.....	97
3.4.	RESULTS AND DISCUSSION	98
3.4.1.	DETERMINATION OF SUFFICIENT POLYMERIZATION TIME.....	100
3.4.2.	DETERMINATION OF SUFFICIENT POLYMERIZATION TEMPERATURE.....	100

3.4.3.	EFFECTS OF INITIATOR'S CHEMICAL STRUCTURE ON THE POLYMER PROPERTIES.....	101
3.4.3.1.	EFFECTS ON T_m AND CRYSTALLINITY.....	103
3.4.3.2.	EFFECTS ON MELT VISCOSITY.....	105
3.4.4.	OLIGOMER SYNTHESIS AND CHARACTERIZATION WITH DESIRED T_m	106
3.5.	CONCLUDING REMARKS	109
3.6.	REFERENCES	136
4.	CPT SOLUBILITY, STABILITY AND RELEASE.....	140
4.1.	INTRODUCTION	141
4.1.1.	POLYMER DEGRADATION.....	141
4.1.2.	POLYMERIC DRUG DELIVERY.....	143
4.1.3.	OBJECTIVES.....	146
4.2.	MATERIALS	147
4.3.	METHODS	147
4.3.1.	DIFFERENTIAL SCANNING CALORIMETRY.....	147
4.3.2.	CPT SOLUBILITY IN PCL AND PLGA (50:50).....	148
4.3.3.	MANUFACTURE OF PASTE FORMULATIONS.....	148
4.3.4.	HPLC ANALYSIS OF CPT.....	148
4.3.5.	EVALUATION OF IN-VITRO DRUG RELEASE.....	149
4.3.6.	EXAMINATION OF THE STABILITY OF CPT IN CL OLIGOMERS.....	149
4.4.	RESULTS AND DISCUSSION	150
4.4.1.	CPT SOLUBILITY IN OLIGOMERS.....	150

4.4.2.	EFFECTS OF CPT LOADING ON OLIGOMER	
	PHYSICAL PROPERTIES.....	152
4.4.3.	CPT STABILITY.....	152
4.4.4.	IN-VITRO STUDIES.....	153
4.5.	CONCLUDING REMARKS.....	156
4.6.	REFERENCES.....	174
5.	GENERAL DISCUSSION AND CONCLUSIONS.....	178
5.1.	HISTORY.....	179
5.2.	GENERAL DISCUSSION.....	180
5.3.	CONCLUSIONS.....	186
5.4.	FUTURE PERSPECTIVE.....	186
5.5.	REFERENCES.....	188
6.	APPENDICES	
	Appendix A.....	190
	Appendix B.....	207
	Appendix C.....	220
	Appendix D.....	241
	Appendix E.....	249
	Appendix F.....	254

LIST OF FIGURES

Figure 1.1.	Camptothecin (lactone and carboxylate form) and its analogs.....	22
Figure 1.2.	Chemical structure of PEG- α -CPT.....	23
Figure 1.3.	Glucuronic acid conjugated to 9-AC (glucuronide prodrug).....	24
Figure 2.1.	Cumulative release of taxol from taxol loaded PDLLA-PEG-PDLLA cylinders into PBS albumin buffer at 37°C.....	60
Figure 2.2.	Cumulative release of taxol from 20% taxol loaded PDLLA:PCL blends and PCL into PBS albumin buffer at 37°C.....	61
Figure 2.3.	Taxol release profiles. PCL and PCL:MePEG blend at 30% taxol loading.....	62
Figure 2.4.	In vitro drug release from formulations containing 5% flurbiprofen in PBS at 37°C.....	63
Figure 2.5.	Delivery of various proteins from a photopolymerized PEG-PLA hydrogel.....	64
Figure 2.6.	Release of metronidazole from thermally gelled liposome/alginate hydrogels.....	65
Figure 2.7A.	Release of FITC-BSA from the high molecular weight 50:50 PLGA system in PBS.....	66
Figure 2.7B.	Release of FITC-BSA from the low molecular weight 50:50 PLGA system in PBS.....	67

Figure 2.8.	In vitro vancomycin release from both poloxamer 407 gels at 37°C.....	68
Figure 2.9.	Release of MMC from pluronic F-127 gel at 37°C.....	69
Figure 2.10:	Cumulative amount of MMC released as a function of time at 37°C from xyloglucan gels.....	70
Figure 3.1.	Chemical structure of the DL-lactide, glycolide and ϵ -caprolactone and their corresponding polymers.....	110
Figure 3.2.	a) Synthesis of ϵ -caprolactone. b) Mechanism of ring opening polymerization of ϵ -caprolactone.....	111
Figure 3.3.	The transestrification of PCL. a) Back-biting caused by intramolecular transestrification, b) Scrambling caused by intermolecular estrification.....	112
Figure 3.4.	A) Chemical structure of GMO; B) Chemical structure of Vitamin D..	113
Figure 3.5.	A) DSC analysis of ϵ -caprolactone monomer. B) DSC thermogram of the polymerized PCL after 8 hours. C) DSC thermogram of the polymerized PCL after 12 hours.....	114
Figure 3.6.	DSC thermogram of the polymerized PCL after 24 hours. Polymerization time and temperature were 24hrs and 120°C respectively. The M/I ratio was 8.....	115
Figure 3.7.	DSC thermogram of the PCL polymerized at 110°C. The M/C ratio, M/I ratio, time of polymerization and type of initiator were 1000, 8, 24hrs and 1-butanol respectively.....	116
Figure 3.8.	DSC thermogram of the synthesized PCL at 140°C. The M/C ratio, M/I ratio, time of polymerization and type of initiator were 1000, 8, 24hrs and 1-butanol respectively.....	117

Figure 3.9.	DSC thermogram of the synthesized PCL at 80°C. The M/C ratio, M/I ratio, time of polymerization and type of initiator were 1000, 8, 24hrs and 1-butanol respectively.....	118
Figure 3.10.	Typical IR spectrum of CL-oligomers.....	119
Figure 3.11.	Effects of varying the number of carbons in initiator's chain on the degree of crystallinity.....	120
Figure 3.12.	Effects of varying the number of carbons in initiator's chain on the melting point.....	121
Figure 3.13.	Chemical structure of PCL initiated with 1-butanol (primary alcohol) and 2-butanol (secondary alcohol).....	122
Figure 3.14.	Effect of the initiator's chemical structure on the viscosity of the polymers at 50°C.....	123
Figure 3.15.	NMR graph for 2-butanol the initiator.....	124
Figure 3.16.	NMR graph for CL oligomer initiated by 2-butanol. Multiplets at $\delta=1.5$ and $\delta=3.75$ corresponds to the presence of unreacted initiator (2-butanol).....	125
Figure 3.17.	The chemical structure of PCL initiated by 1-Butanol and its corresponding NMR graph.....	126
Figure 3.18.	The chemical structure of PCL initiated by 2-Butanol and its corresponding NMR graph.....	127
Figure 4.1.	Schematic illustration of the principle of surface and bulk erosion.....	157
Figure 4.2.	A) Idealized diffusion-controlled matrix release system. B) Idealized diffusion-controlled reservoir release system.....	158

Figure 4.3.	Model of Helen and Baker describing drug release from thin biodegradable polymer films under going bulk erosion (curve: Erossion+Diffusion).....	159
Figure 4.4.	A typical calibration curve for HPLC analysis of CPT.....	160
Figure 4.5.	HPLC analysis of CPT at pH=7.4. Peaks with Retention Time of 4.05 & 9.59 correspond to carboxylate and lacotne forms of CPT.....	161
Figure 4.6.	Thermal behaviour of CL oligomer initiated by A)oleyl alcohol, and B) 2-dodecanol.....	162
Figure 4.7.	A) Thermal behaviour of PLGA. No endotherm was observed due to amorphous nature of PLGA. T _g was determined to be around 40°C. B) DSC analysis of CPT. The melting point of CPT determined to be 265.5 °C.....	163
Figure 4.8.	DSC analysis of CL oligomer initiated with ethanol mixed with CPT.....	164
Figure 4.9.	DSC analysis of PLGA mixed with CPT. Drug/ PLGA ratio of 3.5mg/100mg.....	165
Figure 4.10.	HPLC analysis of CPT after incorporation into CL oligomers and incubation in PBS (pH=7.4) for two months.....	166
Figure 4.11.	Cumulative release profile of CPT± SD from CL oligomers initiated with ethyl alcohol, 1-dodecanol, 2-dodecano and oleyl alcohol. The drug load was 5mg per 100mg of oligomers. A) Amount releases versus time, B) Amount released versus square root of time for the short time approximation.....	167
Figure 4.12.	Cumulative release profile of CPT± SD from PLGA samples. The drug load was 1.5 and 5 mg per 100mg of PLGA.....	168

LIST OF TABLES

Table 1.1.	Rates of hydrolysis and IC50 values of PEG-amino acid-CPTs.....	25
Table 1.2.	Activity of PEG-CPT derivatives against P388/0 leukemia <i>in vivo</i>	26
Table 1.3.	Concentration of CPT in five organs and tumors of mice treated for 30 min with CPT liposome aerosol.....	27
Table 2.1.	Properties of the Pluronic copolymers.....	71
Table 2.2.	Biodegradable <i>In-Situ</i> Solid Forming Delivery Systems.....	72
Table 3.1.	Melting point of the diblock oligomer (GMO-CL) with varying reactant composition.....	128
Table 3.2.	Theoretical \overline{Mn} calculated by the following formula: $\overline{M}_n = 114.14 \times \frac{M}{I} + M_{wi}$ for unpurified CL oligomers.....	129
Table 3.3.	Effects of the number of carbons and position of OH group in the initiator's chain, on the crystallinity and melting point.....	130
Table 3.4.	Comparison of the melt viscosity of polymerized ϵ -caprolactone at 50 °C by using different initiators. Oligomers were not purified after synthesis.....	131
Table 3.5.	Polymerized and characterized CL oligomers with desired melting point.....	132

Table 3.6.	Comparison of the \overline{Mn} calculated from $^1\text{H-NMR}$ and GPC for CL oligomers after purification.....	133
Table 3.7.	Melt viscosity data for polymerized ϵ -caprolactone followed by purification.....	134
Table 3.8.	Melting point and molecular weight comparison between unpurified (M/I=8) and purified (M/I=2, 1-4) oligomers.....	135
Table 4.1.	Categories of polymeric systems for controlled release.....	169
Table 4.2.	Drug loaded samples for <i>in vitro</i> studies. In all samples in every 100mg of polymer 5 mg drug was loaded, unless stated otherwise.....	170
Table 4.3.	Investigation of the solubility of CPT in CL oligomers initiated with different initiators.....	171
Table 4.4.	Effect of CPT loading on the melting point of unloaded CL oligomers.....	172
Table 4.5.	Effects of viscosity and crystallinity on the diffusivity of CPT from different vehicles.....	173

LIST OF ABBREVIATIONS

A549	Human lung carcinoma cells
ANOVA	Analysis of variance
CA-755	Adenocarcinoma 755
CD	Circular dichroism
CL	ϵ -caprolactone
CMC	Critical micelle concentration
CPT	Camptothecin
D	Diffusivity
DLPC	Dilauroylphosphatidylcholine
DMPC	Dimyristoylphosphatidylcholine
DMPG	Dimyristoylphosphatidylglycerol
DMSO	Dimethyl sulfoxide
DPPC	Dipalmitoyl phosphatidylcholine
DSC	Differential scanning calorimetry

Gly	Glycine
GPC	Gel permeation chromatography
HCPT	10-hydroxycamptothecin
HMG-CoA	3-hydroxy-3-methylglutaryl-co-enzyme A
HPLC	High performance liquid chromatography
HPMA	N-(2-hydroxypropyl) methacrylamide
HPMC	Hydroxypropylmethylcellulose
HT-29	Human colon cancer cells
ILS	Increase in Life Span
L1210	Leukemia Cells
LCST	Lower critical solution temperature
LS174T	Human colon adenocarcinoma cells
M109	Madison lung carcinoma cells
MePEG	Methoxy(polyethylene glycol)
MIA-PaCa-2	Human pancreas carcinoma cells
μg	Microgram

ml or mL	Millilitre
mM	Milli mole
MMC	Mitomycin C
Mn	Number average molecular weight
Mw	Weight average molecular weight
MWD	Molecular weight distribution
NIPAAM	N-isopropyl acrylamide
nm	Nanometer
NMP	N-methyl-2-pyrrolidone
P388	Leukemia cells
PBS	Phosphate buffer silane
PC-3	Human prostate carcinoma cells
PCL	Poly (ϵ -caprolactone)
PDLLA	Poly (DL-lactide)
PEG	Poly (ethylene glycol)

PEO	Poly(ethylene oxide)
PLA	Poly (Lactic Acid)
PLG or PLGA	Poly (Lactic-co-Glycolic Acid)
PMA	Polymethacrylic acid
PPO	Poly (propylene oxide)
SAIB	Sucrose acetate isobutyrate
SKOV3	Human ovary adenocarcinoma cells
SLN	Solid Lipid Nanoparticles
TEAA	Triethyl amine acetate
THP-1	Myeloid leukemia
T_g	Glass transition temperature
T_m	Melting temperature
Topo-I	Topoisomerase-I
9-AC	9-Aminocamptothecin
9-NC	9-Nitrocamptothecin

Chapter 1
Camptothecin Delivery Methods

A version of this chapter is published in *Pharmaceutical Research*.
A. Hatefi, B. Amsden, Camptothecin delivery systems. *Pharm. Res.* 19 (10):1387-1397
(2002).

1.1. Introduction

Compounds found in nature (e.g., plant alkaloids or flavonoids) display a wide range of diversity in terms of their structures and physical and biological properties. The function of these compounds in plants, fungi and marine organisms are still not widely understood. Currently, it is believed that many of these compounds act in defence of the detrimental effects of toxins and/or carcinogens found in the plant (1,2) or attack by outside predators (3). During the period 1950-1959, M. E. Wall *et al.*, saved thousands of plant ethanolic extracts. One of the extracts thus saved and stored was prepared from the leaves of *Camptotheca acuminata*, Nyssaceae, a tree that grows in southeastern provinces of China (4). Camptothecin (the extract) is an indole alkaloid with a pentacyclic ring, which is highly unsaturated (Fig. 1.1). On treatment with alkali, the compound readily opens forming an open lactone sodium salt shown in Fig. 1.1 (2). On acidification, the extremely water-soluble sodium salt is readily re-converted to the lactone. The parent compound, however, is extremely water-insoluble and, indeed, is insoluble in virtually all organic solvents except dimethyl sulfoxide (DMSO) in which it exhibits moderate solubility. This insolubility in most biocompatible solvents has made it very difficult to deliver this drug into the body through the conventional routes such as oral, and intravenous or intramuscular injection.

The antitumor activity of camptothecin was demonstrated in a CA-755 (Adenocarcinoma 755) assay (4). This test involves the implantation of a measurable solid tumor into a host mouse and measuring the survival time and inhibition of the tumor growth in response to the anticancer drug. Later, it was shown that camptothecin possesses the ability to halt the growth of a wide range of animal and human tumors (5-7) and is remarkably active in the life prolongation of mice treated with L1210 leukemia cells (8).

In preliminary pharmacologic and clinical evaluation of camptothecin sodium (1970, Baltimore Cancer Research Centre) (9), sixteen patients with various advanced solid tumors were chosen. At intervals of 2-4 weeks they received 35 single i.v. injections of 0.5-10.0 mg/kg of camptothecin. In five patients, partial remissions (>50% mass decrease) and in six others objective responses were noted. Most of the responses

occurred in patients with advanced and often refractory gastro-intestinal carcinoma. Toxicity consisted of alopecia, mild gastrointestinal symptoms, hemorrhagic cystitis, and dose-limiting myelosuppression. These side effects were generally tolerable (9).

Dozens of clinical trials are being conducted worldwide using camptothecin and its derivatives with broad application against a wide variety of tumors. For example, camptothecin treatment of tumor-bearing mice (i.e., lung, ovarian, breast, pancreas, and stomach cancers) resulted in complete remissions in nearly 80% of the lines examined (10). These studies also showed that CPT was more effective than any of the clinically available anticancer drugs tested, which included such drugs as 5-fluorouracil, doxorubicin, methotrexate, vincristine and vinblastine.

Camptothecin thus appears to be a promising drug. However, it has experienced several barriers in making it into clinical use. In this review, we discuss the mechanism of action and the stability problems of camptothecin, and side effects associated with it. Different delivery strategies that have been examined to solve these problems are discussed in terms of their potential for success.

1.1.1. Mechanism of Action

Camptothecin (CPT) induces its cytotoxicity by inhibiting both DNA and RNA synthesis in mammalian cells. The inhibition of RNA synthesis results in shortened RNA chains and is rapidly reversible upon drug removal (11). The inhibition of DNA synthesis, on the other hand, is only partially reversible upon drug removal. Another prominent effect of camptothecin is the rapid fragmentation of cellular DNA in cultured mammalian cells. This is accomplished by stabilization of the binding of topoisomerase I to DNA, leading to DNA fragmentation. This mechanism is unique to camptothecin. Hsiang *et al.* (1985), demonstrated that camptothecin blocks the rejoining step of the breakage-rejoining reaction of mammalian DNA topoisomerase I (Topo I).

The various mechanisms of resistance to anticancer drugs reported in the literature have been described (12). Upon exposure to natural product drugs, tumor cells can acquire resistance to structurally and functionally unrelated drugs. The classical form of drug resistance is caused by P-glycoprotein, a protein inserted in the plasma

membrane that acts as an ATP driven efflux pump. Acquisition of resistance to CPT does not correlate with the presence of P-glycoprotein. CPT has been shown to bypass the P-glycoprotein mediated multidrug resistance phenotype (13), which limits the long-term usefulness of many antineoplastic agents. With regard to camptothecin, some mammalian cell lines selected for resistance to CPT exhibit decreased levels of topo I, which in turn, results in a decreased number of DNA single-strand breaks compared with wild-type cells. Decreases in topo I levels have also been associated with rearrangement and hypermethylation of the topo I gene, as well as the presence of mutations in the topo I gene (14).

Most recently, camptothecin and camptothecin derivatives are being combined with other chemotherapeutic agents and other therapeutic modalities. Preclinical experimental studies suggest that when combined with other agents, radiation or hyperthermia, camptothecin may demonstrate a synergistic antitumor activity (15). The involvement of topoisomerase I in DNA repair suggests that camptothecins may have clinical application as radiation sensitizers. It has been shown *in vitro* that camptothecins can enhance radiation-induced cytotoxicity (16). At present, phase-I clinical trials are in progress to assess combinations of radiation therapy and topoisomerase I targeting agents (17).

1.1.2. Other Clinical Applications of Camptothecin (CPT)

Other than as anticancer agents, another utility for topoisomerase I inhibitors may be their antiviral activity as reported by Takahashi *et al.* (18). Topoisomerase I activity is involved in HIV-reverse transcriptase function. Priel *et al.* (19), showed that inhibition of topo I by CPT can block the development of retroviral-induced malignancies in mice. Tests of antitumor and antiviral activity of camptothecins in the treatment of HIV-associated malignancies such as Kaposi's sarcoma and HIV-associated lymphoma are in clinical trials. Vollmer-Haase *et al.* (20) also observed that in one patient with progressive multifocal leukoencephalopathy, CPT showed anti-infective activity against the JC papovavirus. In a study by Clements *et al.* (1999) (21), it was shown that CPT is not only capable of inhibiting the endothelial cell growth in a non-toxic manner, but also

it can inhibit angiogenesis. This observation demonstrates that besides the tumoricidal activity, CPT may have indirect antitumor activity due its anti-angiogenic activity. Another application of camptothecin entrapped in liposomes was recently explored against Leishmaniasis by Proulx *et al.* (2001) (22). The main reservoirs of parasites in visceral leishmaniasis are macrophages of the liver and spleen. These macrophages have a tendency to take up liposomes. Thus, the use of liposomes represents a strategic approach for accumulation of drugs within these tissues to more efficiently treat this parasitic infection.

1.1.3. Physical Properties of Camptothecin (CPT)

Camptothecin has a high melting point (264-267 °C), and has a molecular weight of 348.11 obtained by high-resolution mass spectroscopy, corresponding to the formula $C_{20}H_{16}N_2O_4$ (2). It gives an intense blue fluorescence under UV and is optically active ($[\alpha]_D^{20}$, +31.3 °). The partition coefficient, $\log P_{o/w}$ (octanol/water), for this compound has been determined to be 1.74 ($\log P_{o/w} = 1.74$) (23).

1.1.4. Structure-Activity Relationship

One important structural requirement for successful interaction with the topoisomerase I target and antitumor potency *in vivo* is a closed α -hydroxylactone moiety (6). Unfortunately, this functionality hydrolyses under physiological conditions, i.e., at pH 7 or above, with the lactone ring readily opening to yield the inactive carboxylate form of the drug (24). Ring opening of camptothecin is thought to result in a loss of activity due to the following three reasons. First of all, the carboxylate form displays decreased membrane associations. Comparison of the membrane affinity of camptothecin with that of its carboxylate form indicates that ring opening produces a greater than two-fold reduction in membrane associations. Secondly, ring opening results in a charged drug species, and charged species exhibit limited diffusivity through cell lipid bilayer domains of low dielectric constant; hence, ring opening of camptothecins results in agents with altered diffusivity characteristics. Finally, evidence from cell-free experiments indicates that ring opening results in significantly attenuated activity

towards the topoisomerase-I target (24). In summary, decreased cell membrane binding, decreased membrane diffusibility, and decreased intrinsic potency against the topoisomerase target all contribute to explain the reduction in cytotoxic activity which accompanies lactone ring opening of camptothecin.

The second structural requirement for successful interaction with the topoisomerase I target and antitumor potency *in vivo* is for the compound to be in its 20-(S) form. Camptothecin occurs in two different enantiomeric forms, 20-S and 20-R, indicating the particular arrangement of atoms and groups in space around the chiral centre (C₂₀) of this molecule. Wani *et al.* (1987) (25) demonstrated that the 20-(R) form of the compound was inactive, both in topoisomerase I inhibition and in *in vivo* assays, while the 20-(S) form of the compound had great potency in inhibiting human colon cancer xenografts in nude mice.

1.1.5. Chemical Modification

Camptothecin has also been chemically modified with the aim of finding a derivative with improved chemotherapeutic activity. Modified camptothecins examined with this goal in mind include 9-aminocamptothecin (9-AC) and 9-nitrocamptothecin (9-NC). Substitutions at carbons 9 and 10 (Fig. 1.1) by amino groups lead to compounds with greater *in vivo* activity. 9-AC is a water-insoluble camptothecin derivative with impressive preclinical activity (26). The results observed in experiments with 9-AC were comparable to those observed in native CPT experimental treatments. However, 9-AC achieved the onset of a complete remission with lower total dose and within a shorter time period, and no pattern of emerging resistance was observed in tumor-bearing mice (27). 9-NC is an intermediate of CPT synthetic conversion into 9-AC. This camptothecin analog can also be metabolically converted *in vivo* to 9-AC. In preclinical studies, this analog has shown excellent anticancer activity in nude mice bearing human tumor xenografts (28).

Two other camptothecin derivatives that have been approved in the United States for use in solid tumors are irinotecan (CPT-11) and topotecan (29). CPT-11 and topotecan are both water-soluble and potent derivatives of camptothecin. CPT-11 is a

prodrug which possesses limited antitumor activity, but is converted by the enzyme carboxylesterase to a very active compound (SN-38) *in vivo*. SN-38 is reported to be anywhere from 200 to 1000 times more potent than CPT-11 (30). Topotecan was made water-soluble by the presence of a stable, basic side chain at carbon 9 of the A ring. It can be administered without the severe and unpredictable side effects that are associated with camptothecin sodium. Like camptothecin, the lactone ring in topotecan is sensitive to pH change and hydrolyses into inactive carboxylate form in basic environment. Another analog of CPT is 10-hydroxycamptothecin (HCPT). In a topo I inhibition assay, HCPT has been shown to be more active than either CPT or topotecan. Its IC₅₀ (the minimum drug concentration that inhibits cleavable complex formation by 50%) is 0.106 μM , as compared to 0.677 μM (0.236 $\mu\text{g/mL}$) for CPT, and 1.110 μM for topotecan (31).

Progress has been made via chemical modification of camptothecin to improve its solubility in aqueous media. This is important in terms of delivering this drug in an effective dosage form. However, despite all the chemical modifications specified above, the camptothecin derivatives still contain a terminal lactone ring that makes them susceptible to ring opening in aqueous solutions by under going a rapid, pH-dependent, non-enzymatic hydrolysis to form an open ring hydroxy carboxylic acid (24). In each case, the open ring carboxylate form is inactive.

BN 80915 a new camptothecin homologue, wherein a seven-membered β -hydroxylactone replaces the six-membered α -hydroxylactone of the parent compound, has been reported recently (32). BN 80915 has shown enhanced plasma stability and activity in animal models and represents the only lactone ring modification known that conserves both the capacity to inhibit topo-I and the antitumor activity. This new derivative is not a substrate for P-glycoprotein and MDR² protein; the two drug efflux pumps most commonly associated with resistance of tumor cells to antineoplastic agents. BN 80915 hails a new generation of camptothecin derivatives and can be used as a template for the elaboration of new anticancer agents.

1.1.6. Pharmacokinetics

As discussed previously, the equilibrium between lactone and open salt forms of camptothecins is pH-dependent, favoring ring closure with increasing acidity. In addition, this equilibrium between open and closed forms is also affected by the preferential binding of serum albumin to the salt form (33). This preference of albumin for the carboxylate form results in a rapid ring opening of circulating CPT. Other blood components, such as erythrocyte membranes and lipoproteins, bind to CPTs, favoring the closed lactone form (33).

Very little of the chemotherapeutic activity of CPT is associated with the open salt, as illustrated by experiments with this form. A closed lactone ring is an essential pharmacophore for activity against cancer cells. The low anticancer activity of the open salt form in animals also is consistent with the failure of clinical trials with the sodium salt of CPT (34). Owing to the association of the chemotherapeutic activity of CPT with lactone and of mainly toxic responses with the open salt form, the goal of pharmacokinetic and metabolic studies must be to assist in the development of dosing regimens optimal for tumor uptake of CPTs.

In an attempt to establish the optimal schedule of administration numerous trials have been conducted (35). It appears that large doses of camptothecin and its derivatives given at large intervals are not greatly effective. It has been shown that the camptothecins require a prolonged schedule of administration given continuously at low doses or frequently fractioned dosing schedules in order to spare normal haematopoietic cells and mucosal progenitor cells with low topoisomerase-I levels while preserving efficacy (36). To achieve this type of prolonged schedule of administration, different delivery systems have been designed. In the following we review these systems and discuss the advantages and disadvantages associated with them.

1.2. Delivery Systems

The development of new drug delivery systems such as liposomes (37-38), microspheres (39-40), micelles (41-42) and injectable pastes (43), has received considerable attention in the field of cancer therapy. This interest has been ignited by the

advantages these delivery systems possess, such as ease of application, localized delivery for a site-specific action and prolonged delivery periods. Moreover, decreased body drug dosage with concurrent reduction in possible undesirable side effects common to most forms of systemic delivery, and improved patient compliance and comfort have put them in the spotlight. In this part of the review, the various strategies used to stabilize camptothecin in its lactone form are outlined. These strategies help to preserve the drug's anticancer activity with a view towards reducing its adverse effects.

1.2.1. Polymer Conjugated Camptothecin

As discussed earlier, camptothecin is extremely insoluble in water and is also insoluble in many organic solvents. This feature has severely restricted its clinical application (44). However, there has been increased interest in pursuing water-soluble CPT derivatives, because of their superior antitumor activity against *in vitro* human cancers and *in vivo* animal xenografts. Most attempts at producing water-soluble derivatives of CPT have been limited to making substitutions on the A and B rings (e.g., 9-AC and CPT-11) (45). These temporary chemical modifications are devised to alter the aqueous solubility and biodistribution of the parent drug, while keeping its inherent pharmacological properties intact. Some of these derivatives show quite good pharmacokinetics and efficacy, but the toxicological effects of these substitutions are controversial (46). These prodrugs are designed to dissociate *in vivo*, in a predictable fashion, to the active drug by either an enzymatic mechanism or simple hydrolysis initiated under physiological pH conditions. Another strategy would be to attach the camptothecin to a polymer carrier.

Greenwald *et al.* (1996), attempted to solubilize 20(S)-camptothecin as a non-ionic α -alkoxy ester transport form (prodrug) and demonstrated enhanced circulatory retention as well as sustained therapeutic release of native drug (47). This was achieved by condensation of camptothecin with poly(ethylene glycol) (PEG) 40 kDa dicarboxylic acid in the presence of diisopropylcarbodiimide. The result of this synthesis was a mixture of camptothecin mono and disubstituted esters in a ratio of approximately 2:1. All their studies utilized the mixture of mono and disubstituted esters. Examination of the physical properties of the mono and disubstituted esters mixture provided rates of hydrolysis in

water, buffer, and rat and human plasma. It was demonstrated that aqueous formulations were able to stand for 24hrs with less than 10% hydrolysis occurring due to the low rate of hydrolysis at room temperature. Furthermore, less than 5% loss of PEG camptothecin was observed in aqueous solutions (pH=5.6) maintained at 4 °C for over 6 months. This finding indicates easy formulation and storage of the transport form. *In vivo* studies employing P388-treated mice with this transport form (administered i.p. as an aqueous solution) produced a remarkable rate of 200% increase in life expectancies (ILS) and a cure rate of 80% at a dose of 16 mg/kg camptothecin equivalents with no acute toxicity. Pharmacokinetic studies of the transport form were done (i.v.) using CD-1 mice and displayed a blood $t_{1/2\alpha}$ of less than 15 minutes, but more significantly a $t_{1/2\beta}$ of 3.6 hrs, with detectable amounts still present after 24 hrs. This result confirms that the transport form circulates to release camptothecin over a substantial period of time. Finally, in an experiment performed with the transport form, in PBS buffer containing human serum albumin, results revealed that at physiologic pH the modified lactone ring structure does not engage in hydrolytic ring opening.

Conover *et al.* (1997), continued their studies to assess the efficacy of PEG- α -conjugated camptothecin (prodrug, Fig. 1.2) (48). Circulatory retention studies were performed in non-tumor bearing mice injected intravenously with 300 mg/kg of PEG- α -camptothecin. The results revealed that PEG- α -CPT was retained in the circulation for a prolonged period of time and this was attributed to the high molecular weight of PEG. Therapeutic efficacy was evaluated in both a murine P388/0 leukemia and a colorectal HT-29 carcinoma xenograft model. Five intraperitoneal injections of 3.2 mg/kg/day 20-(S)-camptothecin equivalents of PEG- α -camptothecin in their leukemia model resulted in significant survival over untreated controls ($P < 0.001$), with a mean time to death of treated versus control of 2.94 and a cure rate of 80% ($n=20$). The colorectal carcinoma xenograft model demonstrated that 2-3 mg/kg/day 20-(S)-camptothecin equivalents of PEG- α -camptothecin given 5 days a week for 5 weeks could reduce an initial tumor burden of 300 mm³ by more than 90% without any signs of overt toxicity. It was concluded that a water-soluble polymeric transport carrier for CPT, based on poly(ethylene glycol) esters, both stabilizes and extends the circulatory exposure of CPT. In addition, PEG may function to

decrease the toxicity and increase the therapeutic efficacy of CPT by a combination of lactone stabilization and slow release. In both studies mentioned above a heterogeneous mixture of mono and disubstituted ester prodrug of PEG- α -camptothecin were used and therefore are not clinically suitable. Moreover, with respect to patient compliance, daily injection of this type of dosage form may be considered as a disadvantage.

Conover *et al.* (1998), prepared a new homogeneous form of disubstituted CPT, PEG- β -camptothecin. The employment of a bifunctional spacer group (glycine) in the PEG prodrug strategy yielded a water-soluble non-ionic α -amidoester prodrug (49). *In vitro* P388 (Leukemia cells) cell toxicity for PEG- β -camptothecin ($IC_{50}=12nM$) was in the expected range for a prodrug that releases CPT ($IC_{50}=7nM$). The *in vitro* half-life of hydrolysis of PEG- β -CPT to CPT at 37 °C is 40 hrs in pH 7.4 phosphate buffer and 6 hrs in rat plasma. In this study, the *in vivo* circulatory retention, antitumor activity and tissue biodistribution of PEG-conjugated camptothecin-20-O-glycinate was evaluated. Nontumor-bearing mice injected intravenously with 875 mg/kg of PEG- β -CPT were employed for circulatory retention studies. Antitumor activity of the prodrug in nude mouse xenograft models was determined both intraperitoneally and intravenously. Biodistribution studies were performed in nude mice bearing colorectal carcinoma xenografts with tritium-labelled PEG- β -CPT and CPT injected intravenously. PEG- β -CPT showed a blood $t_{1/2\alpha}$ of approximately 6 minutes and a $t_{1/2\beta}$ of 10.2 hrs and significant antitumor activity was seen in all treated xenograft models. Ideally, it would be desirable for release of the drug to occur only in the vicinity of tumor cells, thereby sparing normal cells from concomitant destruction. By using labelled CPT, it appeared that more labelled CPT accumulated in solid tumors when delivered in the PEG- β -CPT form. This greater preference for tumor tissue was at least ten times more than normal tissue. It has already been demonstrated that macromolecules greater than roughly 50 kDa, circulating for extended periods, show substantial tumor accumulation (50). One reason for this enhanced accumulation of drug is the greater permeability of neovasculature in tumors (51-52) and the second reason is the absence of effective lymphatic drainage in tumor tissue (53). The combination of increased tumor vascular permeability with insufficient tissue drainage

results in what is termed “the enhanced permeability and retention effect”, which is thought to be a universal solid tumor phenomenon for macromolecular drugs (50). Therefore, by conjugating PEG to CPT-20-O-glycinate a homogenous water-soluble prodrug was produced with an extended circulatory life and altered biodistribution. This modification generates greater tumor accumulation as compared to unconjugated CPT, and produces significant antitumor activity. Since the amount and form of the CPT reaching the tumor site can be affected by the use of different amino acids within the PEG-CPT conjugate, further studies are necessary.

An investigation was undertaken by Conover *et al.* (1999), to determine the impact of various amino acid spacers on the activity of PEG-CPT conjugates (54). Using the P388/0 murine leukemia cell line, the *in vitro* biological efficacy of the PEG-conjugated CPT compounds was tested. The kinetic properties for the PEG conjugate series and the cytotoxicities of CPT and the PEG-amino acid conjugates are shown in Table 1.1 In PBS (pH 7.4) at room temperature, among the PEG-amino acid conjugates tested, the proline, alanine, and leucine derivatives appeared quite stable. A murine ascites model against mouse lymphoid neoplasm cells (P388/0) was used to monitor and assess the *in vivo* anticancer activity of the synthesized PEG-amino acid conjugates. mice were injected with P388/0 cells and then treated intraperitoneally for five consecutive days. The *in vivo* screen results are shown in Table 1.2. The 20 mg/kg total dose level of native CPT was toxic with a mean time to death of 8.1 days. This resulted in an ILS (Increase in Life Span) of -35.2% with no cures. Significant antitumor activity was observed against HT-29 (human colon cancer cells), A549 (human lung carcinoma cells), SKOV3 (human ovary adenocarcinoma cells), PC-3 (human prostate carcinoma cells), LS174T (human colon adenocarcinoma cells), MIA-PaCa-2 (human pancreas carcinoma cells) and M109 (Madison lung carcinoma cells) tumors in mice when treatment regimens of PEG-alanine-CPT were used. The results showed that both the PEG-CPT conjugates’ degradation and *in vivo* activity were altered by using specific amino acid spacers. Different mechanisms such as simple changes in circulatory dissociation rates to more complicated intratumoral, extracellular or even intracellular release can be responsible for differences in *in vivo* activities of PEG-CPT conjugates.

Recently, Caiolfa *et al.* (55), synthesized two soluble N-(2-hydroxypropyl) methacrylamide (HPMA) copolymers to contain CPT (5 wt% and 10 wt%). The α -hydroxyl group of CPT was linked to the polymers through a Glycine-Phenyl alanine-Leucine-Glycine spacer. This arrangement first makes it possible for esterases and proteases at the tumor site to cleave the drug from the polymer and release it slowly, and secondly prevents this water-soluble derivative of CPT in plasma from deactivating. To determine the tumor and tissue distribution, nude mice bearing HT29 human colon carcinoma were injected intravenously with radiolabeled free and bound CPT. Antitumor activity of the CPT-conjugates was also followed *in vivo* on the same animal model.

Results showed that, *in vitro*, CPT-conjugates were fairly stable in simulated physiologic fluids and plasma and native body enzymes such as elastase and cysteine-proteases were able to release the active drug. Total cell exposure to the drug released from polymer conjugates and free unconjugated CPT was measured. It was shown that the cell exposure to CPT was always 3-7 fold lower in the case of polymer conjugate than that measured after administration of unconjugated CPT. To assess the biodistribution of the conjugates, HT29 human colon carcinoma bearing mice were injected intravenously with [³H]CPT-conjugate and free [³H]CPT. More than 90% tumor inhibition, some complete tumor regressions, and no toxic deaths were observed after repeated intravenous administration of CPT-conjugates.

In a series of studies by Harada *et al.* (2000 & 2001), therapeutic efficacy, tumor targeting, drug release kinetics and dose dependent pharmacokinetics of T-0128 was evaluated (56,57). T-0128 is a macromolecular prodrug comprised of T-2513 (7-ethyl-10-aminopropoxy-CPT) bound to carboxymethyl dextran through a Gly-Gly-Gly linker. This molecule has a molecular weight of 130 kDa with weak anionic charge. Macromolecules greater than 70 kDa with weak anionic charges are shown to circulate in the blood for a long time. It was shown that the triplet glycine (Gly) linker could be cleaved by lysosomal cathepsin B to release T-2513 slowly and steadily which resulted in improved therapeutic efficacy.

To increase the stability of lactone ring and efficacy of CPT *in vivo*, Singer *et al.* (2000 & 2001) investigated the conjugation of hydroxyl group positioned at carbon 20 in

CPT structure to poly(L-glutamic acid) (58,59). Poly(L-glutamic acid) has many advantages over the other currently available polymers. Due to its anionic characteristic it enhances the solubility of CPT. It is biodegradable and has multiple available conjugation sites for drugs allowing for higher drug loading concentration. This conjugate showed an increased maximum tolerated dose and substantial antitumor activity. Application of conjugated polymers to increase the solubility of camptothecins has not only been limited to CPT, but other derivatives of CPT such as 9-AC have been explored as well (60). In a study by Leu *et al.* (1999), glucuronide derivative of 9-AC was prepared which was 80 times more soluble than CPT in pH 4 (61) (Fig. 1.3). 9-AC and glucuronic acid were linked via a self-immolative carbamate spacer. Glucuronide prodrug was selected due to two important reasons. First, the hydrophilicity of this functional group and second the glucuronide prodrug can be selectively activated at tumor cells targeted with β -glucuronidase antibody conjugates.

Overall, polymer bound camptothecin has shown a clear advantage in terms of improving drug stability, tumor accumulation and sustained release over the unconjugated free drug. Toxicity data on some of the conjugated polymers and spacers is still required, however. Moreover, further studies to determine the pharmacological characteristics and therapeutic window of these CPT-conjugates is necessary. One drawback is that they still have the requirement for frequent administration in order to be effective (once a day for 5 days), and, although enhanced tumor accumulation occurs, there is still a significant amount of drug not reaching the tumor.

1.2.2. Micro- and Nanoparticle Encapsulated Camptothecin

The development of controlled release formulations which consist of encapsulated CPT seems to be a promising strategy, especially with the use of biodegradable and biocompatible poly(lactide-co-glycolide) (PLGA) (62). These polymer devices are designed to be implanted or injected directly at the tumor site. Possibilities for the local administration of microspheres or nanoparticles containing CPTs are direct injection into a tumor (63), or implantation during surgery (64). There are a few tumors which can be accessible by the first route. Examples of these are those found in the prostate, skin, and

oral cavity. Additionally, there are times that the complete removal of cancer cells is not possible even after surgical excision. In this case, local application of microspheres/nanoparticles which are capable of slowly releasing a drug for an extended period after surgery may increase the probability of complete regression of residual cancer cells (65-66).

CPT is released from these polymer devices by a combination of diffusion and polymer degradation. PLGA is composed of lactic and glycolic acids and can be obtained in many different molecular weights. A free carboxylic end group can be found at the end of each PLGA polymer chain. When hydrolysed, PLGA is degraded into acidic oligomers and monomers. This hydrolysis step involves the imbibition of water into the polymer system, which in turn causes the device to swell. As a result of the degradation and imbibition of water, the microenvironmental pH within large specimens of PLGA is acidic (67). Since CPT is in its active lactone form at low pH, this phenomenon may favor the stabilization of camptothecin within the delivery device.

Shenderova *et al.* (1997), utilized PLGA microspheres as 10-Hydroxycamptothecin slow-release carriers (68). An oil-in-water emulsion-solvent evaporation method was used to encapsulate 10-HCPT in PLGA 50:50 (50 mole % lactic acid) microspheres. They observed that the lactone form of the drug was retained within PLGA microspheres for more than 10 weeks (>95% lactone) under a simulated physiological environment and it was concluded that PLGA microspheres have the ability to stabilize 10-HCPT within the device prior to being released. Application of PLGA for the stabilization of 10-HCPT has been demonstrated in another work by Mallery *et al.* (2001) (69) in a murine human oral squamous cell carcinoma regression model. Therefore, PLGA has the potential to stabilize other analogues within this class of chemotherapeutic agents such as CPT, topotecan, and irinotecan.

Based on this work, Ertl *et al.* (1999), developed CPT-containing-microspheres with sustained release properties by varying the method of solvent evaporation in order to study the influence of drug-loading on microsphere size, encapsulation efficiency and especially the release profile of the incorporated drug (70). In this study a special type of PLGA, the H-series, containing more carboxylic end chains than the non-H-series, was

selected for encapsulation of CPT. Stabilization of the CPT-lactone during release from H-PLGA microspheres as well as during the encapsulation process was investigated. The results showed that CPT was molecularly dispersed in the PLGA matrix at 1.2% drug load and above this concentration, CPT crystals started to form in the polymer matrix. The release profile of CPT from the PLGA microspheres was biphasic, comprising a burst delivering 20-35% of the total drug mass within the first 5 hours, the amount of drug released in this burst phase increasing with drug loading. The burst phase was followed by exponentially declining delivery of CPT releasing a total of 40-75% of the originally loaded drug within 100 h. It was determined that the CPT-lactone form was maintained during preparation and storage.

Another possible strategy is to use CPT-loaded nanoparticles as injectable and targetable delivery systems. For example, Yang *et al.* (1999), investigated the specific passive drug targeting of CPT after intravenous injection by incorporation into solid lipid nanoparticles (SLN) (71). A CPT loaded SLN suspension was prepared by high-pressure homogenization. This suspension consisted of 0.1%(w/w) camptothecin, 2.0%(w/w) stearic acid, 1.5%(w/w) soybean lecithin and 0.5%(w/w) poloxamer™ 188. *In vitro* drug release was investigated in pH 7.4 phosphate buffer saline at 37 °C and the results showed that this system was capable of releasing the drug for up to a week. In tested organs such as the liver, heart, spleen, lung, kidney and brain, the mean residence times of CPT-SLN were much higher than those of a camptothecin control solution (more than 10%), especially in the brain and heart. The release of CPT from CPT-SLN exhibited a diffusional release profile and the CPT-lactone form was protected from hydrolysing to the carboxylate form. It was concluded that the SLN may allow a reduction in dosage and a decrease in systemic toxicity, and thus may be a promising carrier and drug targeting system for lipophilic antitumor drugs. Unfortunately, a lack of toxicity data and the non-selective accumulation of drug in vital organs are some important disadvantages associated with this system.

In an attempt to improve the dissolution rate and cytotoxicity of camptothecin, it was incorporated into oxidized-cellulose (OC) microspheres by a spray drying method (72). Oxidized cellulose with different carboxylic content (7, 13 & 20%) was used to prepare microspheres. The size of microspheres were reported to be in the range of 1.25-

1.52± 0.4µm. The results of release studies in buffer pH 7.4 revealed that the dissolution of CPT was faster from microsphere formulations compared to physical mixtures and free CPT. In *in vitro* cytotoxicity studies against human derived RPMI-8402 lymphoid and THP-1 myeloid leukemia cell lines, more effective results were observed from OC microsphere formulations of CPT in comparison to free CPT. Unfortunately, the time to release 50% CPT from OC-microspheres was between 19-37 hrs which may not satisfy the need for long term drug release for optimum antineoplastic activity *in vivo*.

1.2.3. Liposomes, Micelles, Miniemulsions

Early studies of CPT and lipid based formulations demonstrated that the insoluble parent compound, CPT, was readily soluble in various lipids, while maintaining its biological activity (73-74). These findings suggest that liposomes or emulsions may be an effective delivery vehicle for these drugs.

It has been demonstrated that camptothecin binds to membranes by intercalating between the acyl chains of the phospholipid membrane while at the same time it remains stable (75). To prove this, stability profiles were determined for CPT and its analogues both free in solution and bound to dimyristoylphosphatidylcholine (DMPC) and dimyristoylphosphatidylglycerol (DMPG) bilayers. Due to the drug's lactone ring penetration into the liposome's lipid bilayer, and hence reduced contact with water molecules, the lipid bilayer can keep CPT in its active lactone form. This approach may be applied for increasing the half-life of the biologically active lactone form of the intercalated agent in blood circulation (76-77).

Lundberg (1998), devised oleic acid esters of CPT and analogues such as 10-HCPT and SN-38 which were capable of being incorporated into liposome bilayers and submicron lipid emulsions (78). This esterification process with oleic acid was chosen to make more lipophilic derivatives of the parent drugs. Small unilamellar liposomes and submicron lipid emulsions were prepared from DPPC (dipalmitoyl phosphatidylcholine), PEG and polysorbate 80 and characterized for size and colloidal stability. Subsequently, the esterified CPT and its analogues were incorporated into the liposomes with the mean efficiency ranging from 1.4 to 10.5%. The *in vitro* cytotoxic action of the parent drugs

added as DMSO-ethanol solutions and their ester derivatives in liposomes and lipid emulsions was evaluated. In terms of activity, both parent drugs and the corresponding fatty acid derivatives were very similar. The esters in lipid carriers showed more activity against T-47D (breast cancer cells) and Caco 2 cells (colon adenocarcinoma cells) than the parent drugs, with IC_{50} values of ~ 1 and $3\mu M$ respectively.

Application of the 9-NC derivative delivered by a liposome aerosol has previously been reported in the treatment of human breast, colon and lung cancer xenografts in nude mice (79-80). Following this work, Koshkina *et al.* (1999), analyzed the pharmacokinetics and tissue distribution of inhaled CPT formulated in dilauroylphosphatidylcholine (DLPC) liposomes (81). It was speculated that by depositing CPT within the lungs where there is little albumin (82) and with rapid transit to sites of cancer, more of the active lactone form of the drug would reach the tumor cells. Table 1.3 shows a quantitative comparison of aerosol dosing with previously reported oral, intravenous and intramuscular dosing of CPT in mice (83). The aerosol consisted of CPT in liposomes, while for the other routes of administration CPT was dispersed as a fine emulsion in Intralipid 20 (soya bean oil + egg yolk phospholipids + glycerol). This table shows that the tissue concentrations of CPT were considerably greater after aerosol treatment at 30 minutes than after administration by the other routes. At 120 minutes, the drug concentrations in mice treated by the non-aerosol routes were three to ten times greater in the non-aerosol treated animals. Therefore, it was concluded that despite the 50-fold greater dose of the drug given in non-aerosol groups, the aerosol provided quicker penetration and relatively larger concentrations in the five organs and tumors of the mice that were examined. This study clearly suggests that liposomal aerosol delivery of CPT has advantages over the other routes of administration (i.e., oral, i.m., i.v.) due to two reasons. First, the low concentration of albumin in tracheal and bronchial surface liquids is 1-2% of the albumin concentration in plasma (0.5-0.7 mg/mL). Second, the faster penetration of drug into the tumor tissues may help to preserve more lactone form of the drug.

Following their study, Koshkina *et al.* (2001), modulated the respiratory physiology through the addition of 5% CO_2 to the air source used to generate CPT entrapped liposome aerosols (84). The CO_2 enriched aerosol not only increased pulmonary ventilation but also

increased deposition of the inhaled particles. Results of this study showed that a significantly higher concentration of CPT was found in mice organs exposed to 5% CO₂-air aerosols compared to organs of mice exposed to normal air aerosols.

Other advantages of using liposomes for CPT delivery to the body are: (a) enhancement of drug cellular internalization, (b) decreased unwanted systemic toxicity and (c) increased drug solubility in biological fluids. Despite all these advantages, these systems still presently suffer from a lack of selectivity in targeting tumor cells and, although the efficiency of CPT delivery into the tumor tissues has been improved, the need for sustained delivery of the drug in low dosages for a long period of time is still unsatisfied. Moreover, the leakiness of liposomes and their clearance by the circulatory macrophages and hence, relatively short half-life is, a major disadvantage of this type of delivery system.

In addition to liposomes, micelle solutions and microemulsions have also been proposed as efficient strategies for drug delivery. The solubilization capacity, simple method of preparation, and potential increase in the permeability of the drug through biological membranes by the micellar solutions and microemulsions offer some potential advantages as delivery systems (85).

Different formulations of CPT were designed by Cortesi *et al.* (1997), firstly to increase the solubility of camptothecin in body fluids and secondly to reduce the toxicities associated with the administration of this drug (85). In their work they described (a) the preparation and characterization of liposome-associated CPT, (b) the preparation of micellar solutions and microemulsions containing CPT and (c) the *in vitro* performances of these three delivery systems on cultured human leukaemic K562 cells. The results revealed that the prepared microemulsion composed of a surfactant (Labrasol®), oil (isostearyl-isostearate) and water was stable, single phase, transparent liquid system and optimal formulation for CPT. All three micellar solutions, liposomes and microemulsion were able to release CPT effectively and showed antiproliferative activity on K562 cells. Their efficacy was similar or slightly enhanced in comparison with that exerted by the free drug.

Recently, amphiphilic diblock copolymer micelles have received considerable attention among fellow scientists due to their capability to solubilize hydrophobic drugs

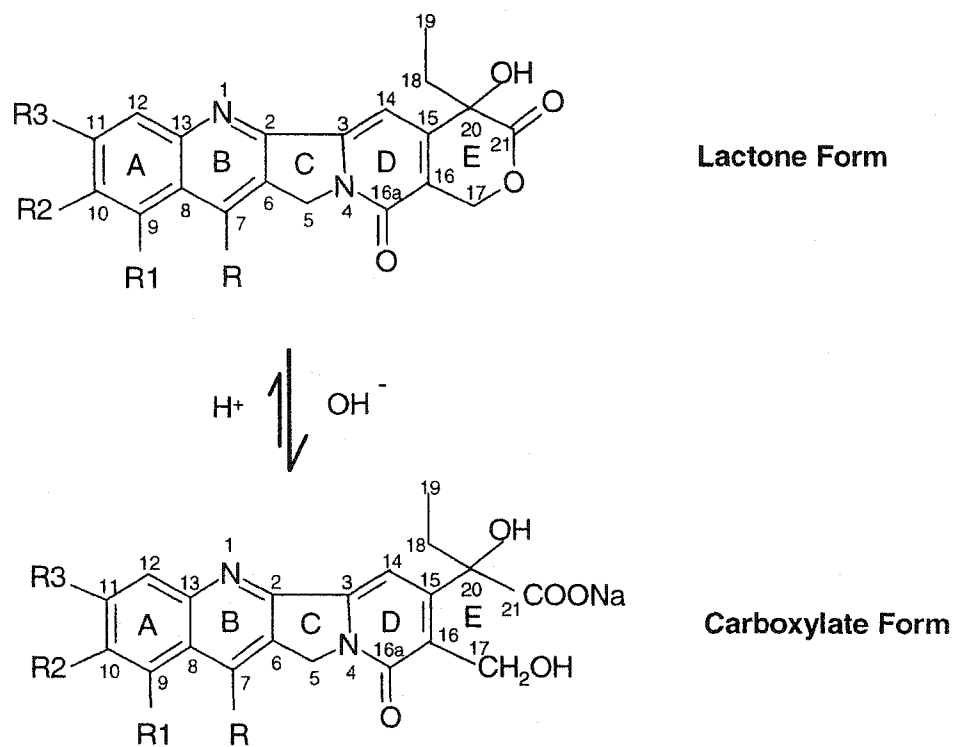
and increase their circulation time (86). The hydrophobic drugs can be either covalently attached to block copolymers to form micellar structures or can be physically incorporated inside the hydrophobic moiety of polymeric micelles (87). For example, Kowan *et al.* (1994), used the diblock copolymer, poly(aspartic acid)-block-polyethylene glycol as a micellar carrier for the anticancer drug adriamycin for intravenous administration (87). In another study by Zhang *et al.* (1996), a diblock copolymer of poly(DL-lactide)-block-(methoxy polyethylene glycol) was investigated as a potential micellar solubilizer and carrier for taxol (88). It was shown that factors such as higher poly (DL-lactide) (PDLLA) content and higher molecular weight of the copolymer have a significant role in the solubilization of taxol. This result emphasizes on the fact that taxol interacts strongly with the hydrophobic PDLLA segment of the micelle. These studies point to the future direction of new camptothecin delivery systems using micelles, which may emerge in near future.

1.3. Summary

Recently, numerous studies have focused on designing new drug delivery systems for camptothecin and other antitumor drugs. This effort is mainly done because of the scarce selectivity and high toxicity that characterize many antitumor drugs. Due to this fact, many of these drugs, which are presently in clinical use, are limited in their dosage and effectiveness. In this respect, the preparation and characterization of specialized delivery systems, such as liposomes, microspheres, microemulsions, micellar solutions, polymer conjugated CPT were proposed, which could be taken as a starting point for future utilization in experimental therapy.

Unfortunately, all of the delivery systems mentioned above suffer from the lack of selectivity; therefore, the whole body is exposed to the cytotoxic drug. The ability to inject a drug incorporated into a polymer to a localized site and have the polymer form a semi-solid drug depot has a number of advantages. Among these advantages is ease of application and localized, prolonged drug delivery. For these reasons a large number of *in situ* setting polymeric delivery systems have been developed and investigated for use in delivering a wide variety of drugs. In the next chapter we introduce the various strategies that have been used to prepare *in situ* setting systems, and outline their

advantages and disadvantages as localized drug delivery systems.



Camptothecin: R=R1=R2=R3=H

10-Hydroxycamptothecin: R=R1=R3=H, R2=OH

10-Methoxycamptothecin: R=R1=R3=H, R2=OMe

9-Nitrocamptothecin: R=R2=R3=H, R1=NO₂

9-Aminocamptothecin: R=R2=R3=H, R1=NH₂

Topotecan: R=R3=H, R1=CH₂NH(CH₃)₂

Irinotecan (CPT-11): R1=R3=H, R=C₂H₅, R2=C₁₁H₁₉O₂

Figure 1.1. Camptothecin (lactone and carboxylate form) and its analogs.

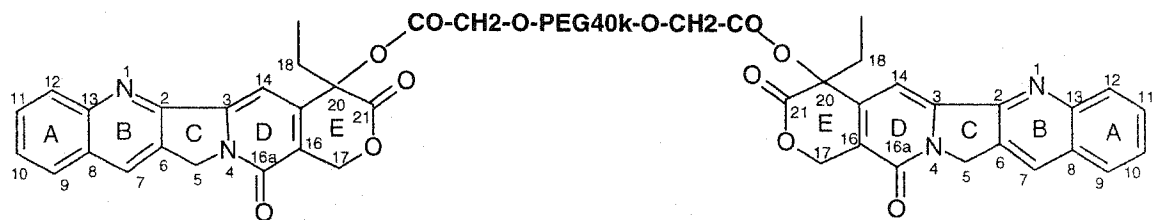


Figure 1.2. Chemical structure of PEG- α -CPT. Reproduced from reference 48

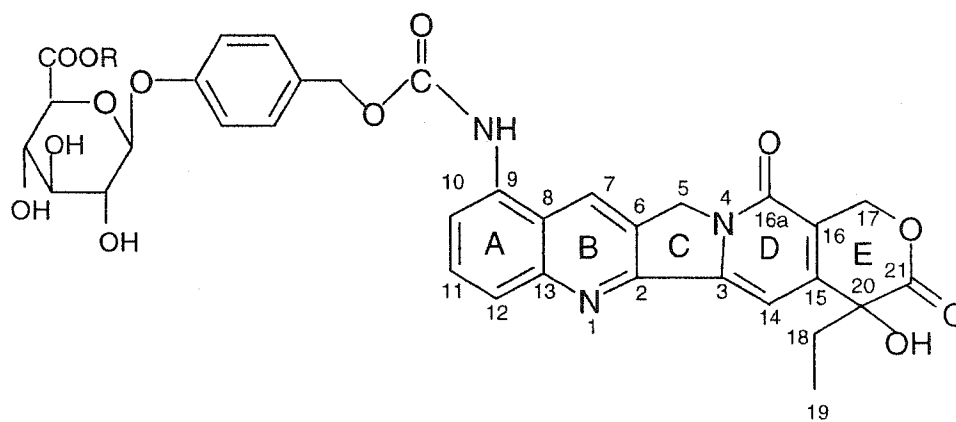


Figure 1.3. Glucuronic acid conjugated to 9-AC (glucuronide prodrug).
Reproduced from reference 61.

Table 1.1. Rates of hydrolysis and IC₅₀ values of PEG-amino acid-CPTs.
Reproduced from reference 54.

Amino acid spacer	IC ₅₀ (nM) ^a	%buffer hydrolysis in 24 h ^b	t _{1/2} (h) ^c	
			Rat plasma	Human Plasma
none (native CPT)	7	-----	-----	-----
glycine	34	>10	9	4
alanine	16	<10	15	7
phenylalanine	27	>10	9	2
methionine	7	>10	6	3
glutamate (Ome)	16	>10	21	9
leucine	358	<10	25	4
proline	3000	<10	113	6

^a All experiments were carried out in duplicate on P388/0 cells:STD of measurement \pm 10

^b PBS buffer (pH 7.4) at 37 °C.

^c These results represent the half lives (\pm 10) by disappearance of the PEG-conjugates.

Table 1.2. Activity of PEG-CPT derivatives against P388/0 leukemia *in vivo*.
Reproduced from reference 54.

Test Compound	Total Dose ^a (mg/kg)	Medium time to death (days) [cures/group]	Mean time to death (days) ^b	% ILS ^c
Control	-----	12.0 [0/10]	12.5± 1.3	-----
CPT	20 ^d	8.5 [0/10]	8.1±1.3	-35.2
PEG-gly-CPT	20	40.0 [6/10]	28.2± 15.3	125.6
PEG-ala-CPT	20	22.0 [0/10]	21.7± 1.6	73.6
PEG-phe-CPT	20	27.0 [1/10]	26.8± 8.6	114.4
PEG-met-CPT	20	32.0 [4/10]	31.1±10.0	148.8
PEG-glu-CPT	20	20.0 [0/10]	19.7±0.7	57.6
PEG-leu-CPT	20	22.0 [0/10]	22.4±1.0	79.2
PEG-pro-CPT	20	13.0 [0/10]	13.1±1.2	4.8

Derivatives were given daily (i.p.×5), following an injection of P388/0 cells into the abdominal cavity with survival monitored for 40 days.

Animals surviving at 40 days were considered cured.

^a Equivalent dose of CPT

^b Kaplan-Meier estimates with survivors uncensored.

^c ILS is $(T/C-1) \times 100$

^d Toxic dose level

Table 1.3. Concentration of CPT in five organs and tumors of mice treated for 30 min with CPT liposome aerosol at a dose of 0.081 mg/kg and in five organs and tumors of mice treated by the oral, intravenous and intramuscular routes with tritiated CPT in a lipid dispersion at a dose of 4 mg/kg. Reproduced from reference 81

Organ	Aerosol		Oral		Intravenous		Intramuscular	
	30min	90min	30min	90min	30min	90min	30min	90min
Lungs	310	17	43	5.3	32	36	44	170
Tumor	26	6.8	31	6.0	36	56	42	57
Brain	61	9.0	37	2.7	12	4	27	74
Blood	26	3.2	39	5.3	23	19	60	144
Liver	103	42.9	137	21.3	50	54	105	118
Kidney	95	7.2	243	210	109	146	176	294
Mean	104	14.4	88	42	44	53	76	143
SD	106	14.7	86	83	35	50	56	85

1.4. References

- [1]- M. E. Wall and M. Wani, Camptothecin and Taxol: Discovery to clinic. *Cancer Res.* 55 (1995) 753-760.
- [2]- M. E. Wall and M. Wani. Plant antitumor agents I. The isolation and structure of camptothecin, a novel alkaloid leukemia and tumor inhibitor from *Camptotheca acuminata*. *J. Am. Chem. Soc.* 88 (1966) 3888-3890.
- [3]- B. C. Giovanella, J. S. Stehlin, DNA topoisomerase I-targeted chemotherapy of human colon cancer in xenografts. *Science* 246 (1989) 1046-1048.
- [4]- M. E. Wani, P. E. Ronman, Plant antitumor agents 18: Synthesis and biological activity of camptothecin analogs. *J. Med. Chem.* 23 (1980) 554-560.
- [5]- B. C. Giovanella, H. R. Cheng, Complete growth inhibition of human cancer xenografts in nude mice by treatment with 20-S-camptothecin. *Cancer Res.* 51 (1991) 3052-3055.
- [6]- H. T. Abelson, S. Penman, Selective interruption of high molecular weight RNA synthesis in Hela cells by camptothecin. *Nature New Biol.* 237 (1972) 144-146.
- [7]- T. G. Burke, Z. Mi, Ethyl substitution at the 7-position extends the half-life of 10-hydroxy-CPT in the presence of human serum albumin. *J. Med. Chem.* 36 (1993) 2580-2582.
- [8]- M. E. Wall, M. C. Wani, Camptothecin and analogues: from discovery to clinic, In: M. Potmesol, H. Pinedo (eds.), *Camptothecins: new anticancer agents*. CRC Press, 1995, pp. 21.
- [9]- Y. Sugimoto, S. Tsukahara, Decreased expression of topoisomerase I in camptothecin-resistant tumor cell lines as determined by a monoclonal antibody. *Cancer Res.* 50 (1990) 6925-6930.
- [10]- B. C. Giovanella, H. R. Cheng, Complete growth inhibition of human cancer

xenografts in nude mice by treatment with 20-S-camptothecin. *Cancer Res.* 51 (1991) 3052-3055.

[11]- H. T. Abelson, S. Penman, Selective interruption of high molecular weight RNA synthesis in Hela cells by camptothecin. *Nature New Biol.* 237 (1972) 144-146.

[12]- W. B. Pratt, R. W. Ruddon. *The anticancer drugs.* The Oxford University Press, New York, 1994.

[13]- M. Potmesil, Camptothecins: From bench research to hospital wards. *Cancer Res.* 54 (1994) 1431-1439.

[14]- I. Madelaine, S. Prost, Sequential modifications of topoisomerase I activity in a camptothecin resistant cell line established by progressive adaptation. *Biochem. Pharmacol.* 45 (1993) 339-348.

[15]- P. Pantazis, Preclinical studies of water insoluble camptothecin congeners: cytotoxicity, development of resistance and combination treatments. *Clinic. Cancer Res.* 1 (1995) 1235-1244.

[16]- M. R. Mattern, G. A. Hofmann, F. L. McCabe, R. K. Johnson, Synergistic cell killing by ionizing γ -radiation and topo-I inhibitor topotecan. *Cancer Res.* 51 (1991) 5813-5816.

[17]- A. Yokoyama, K. Shimokata, Y. Kurita, N. Saijo, Dose finding study of irinotecan and cisplatin plus concurrent radiotherapy for unresectable stage III nonsmall cell lung cancer. *Brit. J. Cancer* 78 (1998) 257-262.

[18]- H. Takahashi, M. Matsuda, A. Kojima, T. Sata, T. Andoh, T. Kurata, K. Nagashima, W. W. Hall, Human immunodeficiency virus type-I reverse transcriptase-Enhancement of activity by interaction with cellular topo-I. *Proc. Natl. Acad. Sci.* 92 (1995) 5694-5698.

[19]- E. Priel, E. Aflalo, G. Chechelnitzsky, D. Benharroch, M. Aboud, S. Segal, Inhibition of retrovirus-induced disease in mice by camptothecin. *J. Virol.* 67 (1993) 3624-3629.

- [20]- J. Vollmer-Haase, P. Young, E. B. Ringelstein, Efficacy of camptothecin in progressive multifocal leucoencephalopathy. *Lancet* 349 (1997) 1366-1370.
- [21]- M. K. Clements, C. B. Jones, M. Cumming, S. S. Daoud, Antiangiogenic potential of camptothecin and topotecan. *Cancer Chemotherap. Pharmacol.* 44 (1999) 411-416.
- [22]- ME. Proulx, A. Desormeaux, J-F. Marquis, M. Olivier, M. G. Bergeron, Treatment of visceral leishmaniasis with sterically stabilized liposomes containing camptothecin. *Antimicrob. Agents Chemotherap.* 45 (2001) 2623-2627.
- [23]- C. Hansch, Comparative QSAR: Understanding hydrophobic interactions. *ACS Symp. Series* 606 (1995) 254-262.
- [24]- C. Jaxel, K. W. Kohn Structure activity study of the actions of camptothecin derivatives on mammalian topoisomerase I. *Cancer Res.* 49 (1989) 5077--5082.
- [25]- M. C. Wani, A. W. Nicholas, Plant antitumor agents 28. Resolution of a key tricyclic synthon: total synthesis and antitumor activity of 20-(S)- and 20-(R)-camptothecin. *J. Med. Chem.* 30 (1987) 2317-2319.
- [26]- C. H. Takimoto, J. Wright, Clinical applications of the camptothecins. *Biochem. Biophys. Acta* 1400 (1998) 107-119.
- [27]- M. Potmesil, M. E. Wall, M. Wani, R. Silber, J. S. Stehlin, B. C. Giovanella, 9-amino and 10,11-methylenedioxy camptothecins in the treatment of human cancer xenografts. *Proc. Am. Assoc. Cancer Res.* 32 (1991) 337.
- [28]- P. Pantazis, J. A. Early, A. J. Kozielski, J. T. Mendoza, H. R. Hinz, B. C. Giovanella, Regression of human breast carcinoma tumors in immunodeficient mice treated with 9-nitrocamptothecin: Differential response of nontumorigenic and tumorigenic human breast cells *in vitro*. *Cancer Res.* 53 (1993) 1577-1582.
- [29]- G. J. Creemers, B. Lund, J. Verweij, Topoisomerase I inhibitors: topotecan and irinotecan. *Cancer Treatment Rev.* 20 (1994) 73-96.

- [30]- Y. Kawato, M. Aonuma, Y. Hirota, Intracellular roles of SN-38, a metabolite of the camptothecin derivative CPT-11, in the antitumor effect of CPT-11. *Cancer Res.* 51 (1991) 4187-4191.
- [31]- R. Zhang, Y. Li, Q. Cai, T. Liu, H. Sun, B. Chambless, Preclinical pharmacology of the natural product anticancer agent 10-hydroxycamptothecin, an inhibitor of topo I. *Cancer Chemother. Pharmacol.* 41 (1998) 257-267.
- [32]- A. K. Larsen, C. Gilbert, G. Chyzak, S. Y. Plisov, I. Naguibneva, Unusual potency of BN 80915, a novel fluorinated E-ring modified camptothecin, toward human colon carcinoma cells. *Cancer Res.* 61 (2001) 2961-2967.
- [33]- Z. Mi, T. G. Burke, Differential interactions of camptothecin lactone and carboxylate forms with human blood components. *Biochemistry* 33 (1994) 10325-10336.
- [34]- F. M. Muggia, P. J. Creaven, Phase I clinical trial of weekly and daily treatment with camptothecin : Correlation with preclinical studies. *Cancer Chemother. Rep.* 56 (1972) 515-521.
- [35]- E. Rowinsky, L. Grochow, D. Ettinger, Phase I and pharmacologic study of CPT-11, a semisynthetic topoisomerase I-targeting agent, on a single dose schedule. *Proc. Am. Soc. Clin. Oncol.* 11 (1992) 115.
- [36]- J. O'Leary, F. M. Muggia. Camptothecins: A review of their development and schedules of administration. *Eur. J. Cancer* 34 (1998) 1500-1508.
- [37]- A. Sharma, U. S. Sharma, liposomes in drug delivery: progress and limitations. *Int. J. Pharm.* 154 (1997) 123-140.
- [38]- L. Chen, R. N. Apte, Characterization of PLGA microspheres for the controlled delivery of IL-1 for tumor immunotherapy. *J. Controlled Release* 43 (1997) 261-272.
- [39]- J. L. Cleland, A. J. S. Jones, Stable formulations of recombinant human growth

hormone and interferon gamma for microencapsulation in biodegradable polymers. Pharm. Res. 13 (1996) 1462-1473.

[40]- X. Zhang, J. K. Jackson, H. M. Burt, Development of amphiphilic diblock copolymers as micellar carriers of taxol. Int. J. Pharm. 132 (1996) 195-206.

[41]- H. Alkan-Onyuksel, S. Ramakrishnan, A mixed micellar formulation suitable for the parenteral administration of taxol. Pharm. Res. 11 (1994) 206-212.

[42]- C. I. Winternitz, J. K. Jackson, Development of a polymeric surgical paste formulation for taxol. Pharm. Res. 13 (1996) 368-375.

[43]- M. Wall, M. Wani, Camptothecin and taxol: from discovery to clinic. J. Ethnopharmacol. 51 (1996) 239-254.

[44]- M. Wall, M. Wani, Camptothecin and taxol: from discovery to clinic. J. Ethnopharmacol. 51 (1996) 239-254.

[45]- W. Kingsbury, J. Boehm, Synthesis of water soluble (aminoalkyl)camptothecin analogues: Inhibition of topoisomerase I and antitumor activity. J. Med. Chem. 34 (1991) 98-107.

[46]- J. Supko, L. Malspeis, Pharmacokinetics of the 9-amino and 10,11-methylenedioxy derivatives of camptothecin in mice. Cancer Res. 53 (1993) 3062-3069.

[47]- R. B. Greenwald, C. W. Gilbert, Drug delivery systems: water soluble Taxol-2-poly(ethylene glycol) ester prodrugs-design and *in vivo* effectiveness. J. Med. Chem. 39 (1996) 424-431.

[48]- C. D. Conover, A. Pendri, R. B. Greenwald, Camptothecin delivery systems: antitumor activity of a camptothecin-20-O-polyethylene glycol ester transport form. Anticancer Res. 17 (1997) 3361-3368.

[49]- C. D. Conover, R. B. Greenwald, Camptothecin delivery systems: enhanced efficacy and tumor accumulation of camptothecin following its conjugation to

polyethylene glycol via a glycine linker, *Cancer Chemother. Pharmacol.* 42 (1998) 407-414.

[50]- H. Maeda, L. Seymour, Conjugates of anticancer agents and polymers: advantages of macromolecular therapeutics *in vivo*. *Bioconjug. Chem.* 3 (1992) 351-358.

[51]- A. Trouet, Increased activity of drugs by linking to carriers. *Eur. J. Cancer* 14 (1978) 105.

[52]- L. Seymour, Passive tumor-targeting of soluble macromolecules and drug conjugates. *Crit. Rev. Ther. Drug Carrier Syst.* 9 (1992) 135.

[53]- H. Dvorak, J. Nagy, Identification and characterization of the blood vessels of solid tumors that are leaky to circulating macromolecules. *Am. J. Pathol.* 138 (1988) 95-104.

[54]- C. D. Conover, R. B. Greenwald, Camptothecin delivery systems: the utility of amino acid spacers for the conjugation of camptothecin with polyethylene glycol to create prodrugs. *AntiCancer Drug Design* 14 (1999) 499-506.

[55]- VR. Caiolfa, M. Zamai, A. Fiorino, E., Frigerio, C. Pellizzoni, R. d'Argy, A. Ghiglieri, MG. Castelli, M. Farao, E. Pesenti, M. Gigli, F. Angelucci, A. Suarato, Polymer-bound camptothecin: initial biodistribution and antitumour activity studies. *J. Controlled Release* 65 (2000) 105-119.

[56]- M. Harada, H. Sakakibara, T. Yano, T. Suzuki, S. Okuno, Determinants for the drug release from T-0128, camptothecin analogue-carboxymethyl dextran conjugate. *J. Controlled Release* 69 (2000) 399-412.

[57]- M. Harada, J-I. Murata, Y. Sakamura, H. Sakakibara, S. Okuno, T. Suzuki, Carrier and dose effects on the pharmacokinetics of T-0128, a camptothecin analogue-carboxymethyl dextran conjugate, in non-tumor and tumor-bearing rats. *J. Controlled Release* 71 (2001) 71-86.

[58]- J. W. Singer, P. de Vries, R. Bhatt, J. Tulinsky, P. Klein, C. Li, L. Milas, R. A. Lewis, S. Wallace, Conjugation of camptothecin to poly-(L-glutamic acid). *Annal. New York Acad. Sci.* 922 (2000)136-150.

- [59]- J. W. Singer, R. Bhatt, J. Tulinsky, K. R. Buhler, E. Heasley, P. Klein, P. de Vreis. Water-soluble poly-(L-glutamic acid)-Gly-camptothecin conjugates enhance camptothecin stability and efficacy *in vivo*. *J. Controlled Release* 74 (2001) 243-247.
- [60]- S. Sakuma, ZR. Lu, P. Kopeckova, J. Kopecek, Biorecognizable HEMA copolymer-drug conjugates for colon-specific delivery of 9-aminocamptothecin. *J. Controlled Release* 75 (2001) 365-379.
- [61]- Y-L. Leu, S. R. Roffler, J-W. Chern, Design and synthesis of water-soluble glucuronide derivatives of camptothecin for cancer prodrug monotherapy and antibody-directed enzyme prodrug therapy. *J. Med. Chem.* 42 (1999) 3623-3628.
- [62]- A. A. Ignatius, L. E. Claes, *In vitro* biocompatibility of bioresorbable polymers: poly(L,DL, lactide) and poly (L-lactide-co-glycolide). *Biomaterials* 17 (1996) 831-839.
- [63]- D. F. Emerich, S. R. Winn, P. Snodgrass, D. LaFreniere, M. Agostino, T. Wiens, H. Xiong, Injectable chemotherapeutic microspheres and Glioma II: Enhanced survival following implantation into deep inoperable tumors. *Pharm. Res.* 17 (2000) 776-781.
- [64]- A. Roalland, *Pharmaceutical particulate carriers: Therapeutic applications*. Marcel Dekker, New York, 1993.
- [65]- H. Brem, L. Piatadosi, Placebo controlled trial of safety and efficacy of intraoperative controlled delivery by biodegradable polymers of chemotherapy for recurrent gliomas. *Lancet* 345 (1995) 1008-1012.
- [66]- L. K. Fung, M. Shin, Chemotherapeutic drugs released from polymers: Distribution of 1,3-bis (2-chloroethyl)-1-nitrosourea in the rat brain. *Pharm. Res.* 13 (1996) 671-682.
- [67]- S. Cohen, H. Bernstein, *Microparticulate systems for the delivery of proteins and vaccines*. Marcel Dekker, New York, 1996.
- [68]- A. Shenderova, T. G. Burke, S. P. Schwendeman, Stabilization of 10-Hydroxycamptothecin in poly(lactide-co-glycolide) microsphere delivery vehicles. *Pharm. Res.* 14 (1997) 1406-1414.

- [69]- S. R. Mallery, A. Shenderova, P. Pei, S. Begum, J. R. Ciminieri, R. F. Wilson, B. C. Casto, D. E. Schuller, M. A. Morse, Effects of 10-hydroxycamptothecin, delivered from locally injectable poly(lactide-co-glycolide) microspheres, in a murine human oral squamous cell carcinoma regression model. *Anticancer Res.* 21 (2001) 1713-1722.
- [70]- B. Ertl, P. Platzer, Poly(D,L-lactide-co-glycolide) microspheres for sustained delivery and stabilization of camptothecin. *J. Controlled Release* 61 (1999) 305-317.
- [71]- S. C. Yang, L. F. Lu, Body distribution in mice of intravenously injected camptothecin solid lipid nanoparticles and targeting effect on brain. *J. Controlled Release* 59 (1999) 299-307.
- [72]- V. Kumar, J. Kang, R. J. Hohi, Improved dissolution and cytotoxicity of camptothecin incorporated into oxidized-cellulose microspheres prepared by spray drying. *Pharm. Dev. Technol.* 6 (2001) 459-467.
- [73]- S. M. Sugarman, Lipid-complexed camptothecin: formulation and initial biodistribution and antitumor activity studies. *Cancer Chemother. Pharmacol.* 37 (1996) 531-538.
- [74]- T. G. Burke, Liposomal stabilization of camptothecin's lactone ring. *J. Am. Chem. Soc.* 114 (1992) 8318-8319.
- [75]- T. G. Burke, A. K. Mishra, Lipid bilayer partitioning and stability of camptothecin drugs. *Biochem.* 32 (1993) 5352-5364.
- [76]- D. L. Emerson, Liposomal delivery of camptothecins. *Pharm. Sci. Tech. Today* 3 (2000) 205-209.
- [77]- T. G. Burke, X. Gao, Stabilization of topotecan in low pH liposomes composed of Distearylphosphatidylcholine. *J. Pharm. Sci.* 83 (1994) 967-969.
- [78]- B. B. Lundberg, Biologically active camptothecin derivatives for incorporation into liposome bilayers and lipid emulsions. *Anti-cancer Drug Design* 13 (1998) 453-461.

- [79]- V. Knight, N. V. Koshkina, Anticancer effect of 9-nitrocamptothecin liposome aerosol on human cancer xenografts in nude mice. *Cancer Chemother. Pharmacol.* 44 (1999) 177-185.
- [80]- N. V. Koshkina, J. C. Walderp, Anticancer effect of 9-nitrocamptothecin aerosol delivery on human cancer xenograft models. *Proc. of the 89th annual meeting of the Am. Assoc. Cancer Res.* 39 (1998) 278.
- [81]- N. V. Koshkina, B. E. Gilbert, Distribution of camptothecin after delivery as a liposome aerosol or following intramuscular injection in mice. *Cancer Chemother. Pharmacol.* 44 (1999) 187-192.
- [82]- J. C. Patton Mechanisms of macromolecule absorption by the lungs. *Adv. Drug Delivery Rev.* 19 (1996) 3-20.
- [83]- E. A. Ahmed, S. Jacob, Influence of route of administration on [3H]-camptothecin distribution and tumor uptake in CASE-bearing nude mice: whole body autoradiographic studies. *Cancer Chemother. Pharmacol.* 39 (1996) 122-129.
- [84]- N. V. Koshkina, V. Knight, B. E. Gilbert, E. Golunski, L. Roberts, J. C. Waldrep, Improved respiratory delivery of the anticancer drugs, camptothecin and paclitaxel, with 5% CO₂-enriched air: pharmacokinetic studies. *Cancer Chemother. Pharmacol.* 47 (2001) 451-456.
- [85]- R. Cortesi, E. Esposito, Formulation study for the antitumor drug camptothecin: liposomes, micellar solutions and a microemulsion. *Int. J. Pharm.* 159 (1997) 95-103.
- [86]- G. Kwon, M. Yokoyama, T. Okano, Y. Sakurai, K. Kataoka, Biodistribution of micelle-forming polymer drug conjugates. *Pharm. Res.* 10 (1993) 970-974.
- [87]- G. Kwon, S. Suwa, M. Yokoyama, T. Okano, Y. Sakurai, K. Kataoka, Enhanced tumor accumulation and prolonged circulation times of micelle-forming poly(ethyleneoxide-aspartate) block copolymer-adriamycin conjugates. *J. Controlled Release* 29 (1994) 17-23.
- [88]- X. Zhang, J. K. Jackson, H. M. Burt, Development of amphiphilic diblock copolymers as micellar carriers of taxol. *Int. J. Pharm.* 132 (1996) 195-206.

Chapter 2

Biodegradable Injectable *In Situ* Forming Delivery Systems

A version of this chapter is published in *Journal of Controlled Release*.

A. Hatefi, B. Amsden. Biodegradable Injectable In-Situ Forming Drug Delivery Systems, *J. Controlled Release* 80:9-28 (2002).

2.1. Introduction

The development of new injectable drug delivery systems has received considerable attention over the past few years (1-3). This interest has been sparked by the advantages these delivery systems possess, which include ease of application, localized delivery for a site-specific action (4-6), prolonged delivery periods, decreased body drug dosage with concurrent reduction in possible undesirable side effects common to most forms of systemic delivery, and improved patient compliance and comfort. Initial studies examined delivery systems such as emulsions (7-9), liposomes (10-13), biodegradable microspheres (14-16) and micelles (17,18). Although these formulations have demonstrated some success in certain applications, there still is room for improvement.

Emulsions are used extensively in parenteral products but usually not in long acting formulations because of the stability problems accompanying this dosage form. The possibility of the dispersion breakdown or dissolution in the surrounding body fluid has made emulsions a poor choice for long acting formulations (19). Liposomes are not a promising dosage form for long acting formulations as well. Local retention of liposome-entrapped drugs is likely to be longer than that of free drugs, but it may not always be long enough to maintain local therapeutic drug levels, due in part to rapid clearance by macrophages and other cells (20,21). Other problems, such as stability issues, sterilization problems and often-low drug entrapment, have played an important role in limiting the utility of liposomes (22). Microspheres are easy to deliver to the site of action but they have several inherent disadvantages. These include the need for reconstitution before injection, a relatively complicated manufacturing procedure to produce a sterile, stable, and reproducible product, and the possibility of microsphere migration from the site of injection (23-27). Micelles, which are also prone to migration, suffer from the fact that there are a large number of variables, which influence micelle properties. Controlling factors like core block length and corona outer shell length, which significantly influence drug loading and size distribution, at the same time is almost impossible. Furthermore, the stability of micelles is highly dependent on their critical micelle concentration (CMC), which is the minimum polymer concentration

required for micelle formation. The lower the value of the CMC, the greater the thermodynamic stability of micelles in dilute solutions. Once diluted below the CMC, micelles begin to spontaneously disassemble into single chains (27,28). Therefore, dilution upon injection, as well as interaction with lipid components in the blood, may result in dose dumping.

With these shortcomings in mind, injectable, *in situ* setting semi-solid drug depots are being developed as alternative delivery systems. These implant systems are made of biodegradable products, which can be injected via a syringe into the body and once injected, solidify to form a semi-solid depot (29-31). Our goal in this paper is to outline the different strategies used to prepare *in situ* setting drug depots and comment on their advantages and disadvantages. In this review, semi-solid biodegradable injectable implant systems are divided into four categories based on the mechanism of achieving solidification *in vivo*: 1) thermoplastic pastes, 2) *in situ* crosslinked systems, 3) *in situ* precipitation, and 4) *in situ* solidifying organogels. The coverage of the literature is not encyclopedic; rather, a few select examples have been chosen to highlight certain points. The discussion will emphasize some of the practical issues, problems and unique challenges that are associated with these injectable implant systems.

2.2. Thermoplastic Pastes

Thermoplastic pastes are polymer systems, which are injected into the body as a melt and form a semi-solid upon cooling to body temperature. They are characterized as having a low melting point, ranging from 25 to 65 °C, and an intrinsic viscosity from 0.05 to 0.8 dL/g, measured at 25 °C (32). It has been reported that an intrinsic viscosity below 0.05 dL/g may fail to significantly impart a delayed release profile to a drug, and a carrier copolymer with an intrinsic viscosity above 0.8 dL/g may be too viscous to be easily administered through a needle (33). The facile injectability of these systems, when heated slightly above their melting point, is due to their low molecular weight and low T_g (glass transition temperature). These polymeric systems flow easily when pushed or stretched by a load, usually at elevated temperatures. They mostly hold their shape at room temperature and can be formed into different shapes by applying heat (34).

Bioerodible thermoplastic pastes could be prepared from such monomers as D,L-lactide, glycolide, ϵ -caprolactone, trimethylene carbonate, dioxanone and ortho esters (33,35). Polymers and copolymers of these monomers have been extensively used in a number of biomedical areas, from carriers of pharmaceutical compounds (36) to surgical sutures (37), ocular implants (38), soft tissue repair (39,40) and augmentation materials [41,42]. They therefore have a demonstrated track record of biocompatibility and thus are attractive starting points for new material development. Specific examples of the use of these materials are given in the following paragraphs.

Walter *et al.*, placed a Taxol™-loaded poly [bis(p-carboxyphenoxy)propane-sebacic acid] implant beside brain tumors or within tumor resection sites and demonstrated the effectiveness of the method in rats after surgery (43). In an effort to develop a means of avoiding surgery and circumventing the invasiveness of Walter's method, Zhang *et al.*, developed a thermoplastic triblock polymer system composed of poly(D,L-lactide)-*block*-poly(ethylene glycol)-*block*-poly(D,L-lactide) and blends of low molecular weight poly(D,L-lactide) and poly (ϵ -caprolactone) for the local delivery of paclitaxel (44). Both polymeric systems were capable of releasing Taxol™ for a long period of time (greater than 60 days)(Fig. 2.1), albeit at a very low rate. The advantages of using this system over systemic administration of Taxol™ are reduced side effects due to the local delivery of Taxol™ to the tumor site. There are some noteworthy disadvantages associated with this polymeric system. The melting points of these polymeric pastes were greater than 60 °C, therefore the temperature of the paste at the time of injection was at least 60 °C. This temperature can be very painful for a patient and increases the chance of necrosis and scar tissue formation at the site of injection (45). The second disadvantage is the very slow rate of drug release (40% drug mass released after 60 days when the block copolymer was used and 35% drug mass released after 30 days when the blend of PDLLA and PCL were used)(Fig. 2.2). This slow rate of release, which had a significant impact on the efficacy of the polymeric paste formulation to inhibit the tumor growth, may be due to the high molecular weight of PCL, the high degree of crystallinity in the synthesized polymer (PCL) or the affinity of the drug for the polymer versus the aqueous phase.

Dordunoo *et al.*, attempted to overcome the problem of slow Taxol™ release by using poly(ϵ -caprolactone) of molecular weight 10-20 kDalton as a polymeric paste (46). To enhance Taxol release, they examined the effect on the rate of drug release of water-soluble additives such as gelatin, albumin, methylcellulose, dextran and sodium chloride. Cylindrical pellets of Taxol™-loaded paste were prepared by melt extrusion and suspended in phosphate buffered saline for *in vitro* studies. Addition of the water-soluble additives significantly improved the rate of drug release, especially when gelatin or albumin was used. The authors suggested that the enhanced rate of drug release in the case of gelatin or albumin emanated from the fact that these two additives are water swellable as well as soluble. The swelling of such additives inside the polymeric paste, increased the water imbibitions into the polymer and hence, produced a higher rate of drug dissolution and release. An alternative explanation is that the enhanced release may not have anything to do with swelling, but may be a result of increased Taxol™ solubility in the release medium due to its binding to proteins. Taxol™ has low water solubility (0.2 $\mu\text{g/mL}$), and the addition of proteins such as albumin can increase the water solubility of Taxol™ up to 3.7 $\mu\text{g/mL}$ (46). In *in vivo* studies, pastes containing Taxol™-gelatin particles were prepared and heated to 60 °C and then extruded at the tumor site of eight DBA/2j female mice. Tumor mass was reduced $63 \pm 27\%$ with respect to controls. This system has some limiting disadvantages, however. Low molecular weight poly(ϵ -caprolactone) has a degree of crystallinity of between 50-70% (47). This high degree of crystallinity would impede the diffusion of the drug within the cylinder. Further, the paste was heated to 60 °C to bring it into a molten state and make it injectable through a needle. This temperature can invoke scar tissue formation, which in turn can encapsulate the polymeric paste and inhibit the diffusion of Taxol™ to the surrounding tumor cells.

In another approach Winternitz *et al.*, added methoxy(polyethylene glycol) (MePEG) in amounts up to 30% to the poly(ϵ -caprolactone) (PCL) paste, which brought down the melting point from 55 to around 50 °C and increased the crystallinity of the polymer from 42% to 51% (48). Taxol showed a biphasic *in vitro* release profile composed of a burst phase during the first couple of days followed by a much slower

release rate (Fig. 2.3). The addition of MePEG increased the amount of water taken up by the polymer blends but decreased the rate of Taxol™ release. This was attributed to an increased degree of crystallinity of PCL resulting in a polymer, which degrades more slowly, and a decreased Taxol diffusion coefficient due to the increased tortuosity of the diffusional pathway (48). Nevertheless, this delivery system, with slight changes with respect to polymer composition, was tested in human prostate LNCaP tumors grown subcutaneous in castrated athymic male mice and promising results were obtained (49).

Thermoplastic injectable implants have even been used for delivery of pharmaceutically active agents into the eye (50). An injectable implant system was developed by Davis *et al.*, made of copolymers of PCL and PEG which was capable of being injected through a 25 gauge needle when heated to 50 °C. This invention avoids the hazards of eye surgery to insert the drug delivery device and also avoids possible intraocular chemical reactions. The only problem that this system bears is the temperature of the paste at the time of injection (50 °C), which appears to be too high for the eye environment. It is claimed that *in vivo* compatibility and degradation life times in the eye can be ascertained by injecting the sterilized paste into both the anterior chamber and vitreous cavity of laboratory rabbits' eyes. Absence of experimental data or examples, regarding the *in vivo* compatibility of this system, emphasizes the necessity for further studies.

2.3. In Situ Crosslinked Systems

Crosslinked polymer networks can be formed *in situ* in a variety of ways, forming solid polymer systems or gels. Means of accomplishing this end include free radical reactions initiated by heat (thermosets) or absorption of photons, or ionic interactions between small cations and polymer anions.

2.3.1. Thermosets

Thermoset polymers can flow and be molded when initially constituted, but after heating, they set into their final shape. This process is often called “curing” and involves the formation of covalent crosslinks between polymer chains to form a macromolecular

network. Reheating a cured polymer only degrades the polymer (34). This curing is usually initiated chemically upon addition of heat. In two U.S. patents, Dunn *et al.* introduced the application of thermoset systems (39,40). Unfortunately, there have not been many articles written regarding the application of chemically initiated thermoset systems for the delivery of pharmaceutically active agents into the body. This may be due to the limitations and adverse effects associated with it (51). In particular, the reaction conditions for *in vivo* applications are quite stringent, including a narrow range of physiologically acceptable temperatures, requirement for nontoxic monomers and/or solvents, moist and oxygen-rich environments, the need for rapid processing, and clinically suitable rates of polymerization (52). In this part of the review, the characteristics of thermoset systems and the application of photoinitiated thermoset systems will be investigated.

Dunn *et al.*, used biodegradable copolymers of D,L-lactide or L-lactide with ϵ -caprolactone to prepare a thermosetting system for prosthetic implants and slow release drug delivery systems. This system is liquid outside the body and is capable of being injected via a syringe and needle and once inside the body, it cures (53). The multifunctional polymers in their thermosetting system were first synthesized via copolymerization of either D,L-lactide or L-lactide with ϵ -caprolactone using a multifunctional polyol initiator and a catalyst (e.g., peroxides) to form polyol terminated liquid prepolymers. This prepolymer was then converted to an acrylic ester-terminated prepolymer. Curing the liquid acrylic-terminated pre-polymer is initiated by the addition of either benzoyl peroxide or N,N-dimethyl-p-toluidine, prior to injection into the body. After introduction of the initiator, the polymer system is injected and polymer solidification occurs. The estimated time of reaction is between 5 to 30 minutes (54).

The advantage of using this system is its facile syringeability. There are a couple of disadvantages accompanied with this system, which have limited its application. When a bioactive agent (e.g., flurbiprofen) was incorporated into this system, a burst in drug release during the first hour was observed (Fig. 2.4). This burst was due to the lag time for solidification of the polymer. While the cross-linking reaction inside the body is in process and the polymer is in liquid form, the drug can diffuse out of the system more

rapidly, thereby causing the burst. This high concentration of drug at the site of reaction may result in the appearance of side effects of the drug. Furthermore, the heat released upon curing (up to 94 °C have been reported for poly(methyl methacrylate) used as a prosthetic bone cement (57)) due to the exothermic nature of the crosslinking reaction, can cause necrosis to the surrounding tissues (51,55,56,57). Finally, introduction of free radical producing agents such as benzoyl peroxide into the body may induce tumor promotion (58-60).

2.3.2. Photocrosslinked Gels

Photopolymerizable, degradable biomaterials provide many advantages over chemically initiated thermoset systems. In this approach, prepolymers are introduced to the desired site via injection and photocured *in situ* with fiber optic cables (52). This approach has many advantages. Photoinitiated reactions provide rapid polymerization rates at physiological temperatures. Further, because the initial materials are liquid solutions or moldable putties, the systems are easily placed in complex shaped volumes and subsequently reacted to form a polymer of exactly the required dimensions. These characteristics have encouraged the investigation of using this system for tissue engineering (56), orthopedic applications (61), cell transplantation (62), local drug delivery (63,64), dentistry (65,66), and tissue adhesion prevention (67-68).

Hubbell *et al.*, described a photopolymerizable biodegradable hydrogel as a tissue contacting material and controlled release carrier (69). This system consisted of a macromer with at least two free radical-polymerizable regions (PEG-oligoglycolyl-acrylates), a photosensitive initiator (eosin dye) and a light source (ultraviolet or visible light). By exposing the mixture of macromers and photoinitiator to the light source, the macromer undergoes rapid crosslinking and forms a network. These networks can be used to entrap water-soluble drugs and enzymes and deliver them at a controlled rate. Use of an argon laser as a light source offers a greater depth and degree of polymerization, less time is required and an enhancement of the physical properties of the polymer is realized. These advantages are offset by reports that the increased polymerization caused by the laser results in increased shrinkage and brittleness of the

polymer (70).

As an example of the drug delivery capabilities of this approach, the delivery of various proteins from a photopolymerized PEG-PLA hydrogel is illustrated in Figure 2.5 (71). Release of the proteins from these hydrogels was relatively rapid, with completion achieved within 5 days. The release rate was dependent on protein molecular weight, decreasing as molecular weight increased. The release was diffusionally controlled for molecules below a critical molecular weight. For the larger immunoglobulin G, release required the degradation of the hydrogel structure to afford larger openings within the gel to allow for diffusion. Thus, to achieve prolonged release, this delivery system is best suited for large drug molecules.

2.3.3. Ion-mediated Gelation

Alginates are natural polymers, which have been widely investigated for drug delivery (72). Alginates form a gel upon contact with divalent cations such as calcium ions. They can be used directly as a drug carrier or as a carrier of another delivery system such as liposomes (73). Liposomes are capable of increasing the local retention of liposome-entrapped drugs over that of free drugs. However, site retention may not always be long enough to maintain local therapeutic levels, due in part to rapid clearance of the liposomal vesicles by macrophages. In order to overcome this problem Cui *et al.* used thermally sensitive Ca-loaded vesicles, capable of releasing Ca^{2+} when heated to body temperature, along with Na-alginate to form a fluid suspension that gels at 37 °C. 1,2-bis(palmitoyl)-glycero-3-phosphocoline (DPPC) and 1,2-bis(myristoyl)-glycero-3-phosphocoline (DMPC) were used to prepare both Ca-loaded and drug loaded phospholipid vesicles. The molar ratio of DPPC:DMPC was adjusted to 9:1 to bring the melting point of the liposomes below body temperature. It is well known that the permeability of the phospholipid bilayers is strongly temperature dependent (74,75). At temperatures below the lipid chain melting transition, phospholipid bilayers are relatively impermeable to multivalent ions. However, phospholipid permeability has been shown to be several orders of magnitude higher at the melting temperature (74). The addition of drug-filled liposomes to the formulation resulted in a hydrogel that

released entrapped drug (metronidazole) in a controlled manner. Drug release was characterized by a rapid burst-type release followed by a slower controlled release of drug from the hydrogel matrix. Metronidazole was released more rapidly from the 15% DMPC liposome than from the pure DPPC liposome due to the difference in bilayer permeability of the two compositions at the experimental temperature (37 °C)(Fig. 2.6). This approach clearly improved the half-life of the liposomes and proved to be advantageous for certain local delivery applications in which *in situ* gelation is required (76,77). The disadvantages of using this system are a short shelf life due to the slow leakage of Ca^{2+} from the liposomes and a large amount of drug released in the initial release burst.

Recently, Westhaus *et al.* (2001) (78), introduced thermally triggered Ca^{2+} release from liposomes to form Ca-alginate hydrogels, and a protein-based system in which triggered release of calcium activates transglutaminase enzyme-catalyzed cross-linking of proteins. The fundamentals of this system are the same as the Cui *et al.* hydrogel system mentioned above and has the same problem of calcium leakage out of the liposomes and hence, the same problem with a short shelf life.

Alginate has been used for ophthalmic drug delivery as well (79). The human eye has enough calcium ions to induce alginate gelation. In a study by Cohen *et al.*, it was demonstrated that an aqueous solution of sodium alginate could gel in the eye without the addition of external calcium ions or other bivalent/polyvalent cations. The concentration of CaCl_2 in lacrimal fluid is 0.008 % w/v. Using this calcium to cause gelation of an alginate-pilocarpine solution; pilocarpine was delivered to the eye in a sustained fashion. Unfortunately, this method of delivery is restricted to the eye due to the lack of calcium concentration in other tissues.

Despite these applications, there are two important factors, which have limited the use of calcium alginate for drug delivery purposes. The first factor is their potential immunogenicity and the second is the long time required for their *in vivo* degradation (80,81). For example, cytotoxicity and the nonbiodegradable nature of calcium alginate wound dressings induce a chronic foreign-body reaction (80).

2.4. In situ Polymer Precipitation

Another strategy that has been utilized to produce an injectable drug delivery depot is the phenomenon of polymer precipitation from solution. This precipitation can be induced by solvent-removal (82,83), a change in temperature (84,85), or a change in pH (86,87).

2.4.1. Solvent-Removal Precipitation

Dunn *et al.*, introduced an *in vivo* setting system made of biodegradable polymers (88), which has been used for human as well as veterinary purposes (89-94). This injectable implant system is comprised of a water insoluble biodegradable polymer, such as poly(D,L-lactide), poly(D,L-lactide-co-glycolide) and poly(D,L-lactide-co- ϵ -caprolactone), dissolved in a water miscible, physiologically compatible solvent. Upon injection into an aqueous environment, the solvent diffuses into the surrounding aqueous environment while water diffuses into the polymer matrix. Since the polymer is water insoluble, it precipitates upon contact with the water and results in a solid polymeric implant. Solvents which have been used in this approach include N-methyl-2-pyrrolidone, propylene glycol, acetone, dimethyl sulfoxide, tetrahydrofuran, 2-pyrrolidone, and triacetin, but the most preferred are N-methyl-2-pyrrolidone (NMP) and dimethyl sulfoxide (DMSO) because of their pharmaceutical precedence (95). Due to the number of disadvantages inherent in this system, it has not been extensively investigated or endorsed by fellow pharmaceutical scientists.

One of the problems is the possibility of a burst in drug release especially during the first few hours after injection into the body. Since this injectable implant system is administered as a liquid, it is reasonable to assume that there is a lag between the injection and the formation of the solid implant. During this lag time the initial burst of drug may exceed the plasma concentration achieved using conventional implant systems. This initial burst of drug has been linked to tissue irritation and sometimes to systemic toxicity. Due to this unwanted phenomenon, the use of this system has been limited only to drugs with a narrow therapeutic index.

In order to control the burst effect four factors have been examined: the

concentration of polymer in the solvent (96), the molecular weight of the polymer (29), the solvent used (29,82,97), and the addition of a surfactant (98). All of these parameters influence the rate of precipitation of the polymer. For example, Lambert and Peck examined the influence of solvent, polymer molecular weight, and polymer concentration on FITC-bovine serum albumin release from poly(D,L-lactide-co-glycolide) (PLGA) precipitated from solution as spheres (29). They found that, for a high PLGA (75-115,000 Dalton) molecular weight, the higher the polymer loading in the solvent (10 to 20 %), the smaller the burst effect, and the higher the capability of solvent to dissolve the polymeric system the greater the burst effect (Fig. 2.7A). By using a lower molecular weight PLGA (10-15,000 Dalton), much greater concentrations (33.5 to 40 %) of polymer in solution were obtainable, and as a consequence, the initial burst of drug released was eliminated (Fig. 2.7B). The effect of solvent choice, however, was not as clearly defined. For the high molecular weight polymer case, DMSO provided the greatest burst effect at a given polymer concentration, while the opposite effect was observed for the low molecular weight polymer. Finally, Chandrashekar *et al.*, have reported that the addition of a diblock of PLGA-PEG of relatively low molecular weight (5000 Dalton) was effective in reducing the burst of small drug molecules. For example, the initial burst (% released after 24 hours) of leuprolide acetate in PLGA dissolved in DMSO (50% PLGA, 50% DMSO) was reduced from 50% to 34% of the initially loaded concentration when injected subcutaneously into rats (98) with the incorporation of 10% PLGA-PEG in place of 10% of the PLGA. Similar results were reported for floxuridine, lidocaine, and lidocaine HCl. The reduction in the burst effect was most notable for the water soluble lidocaine HCl, whose initial burst decreased from 82 % to 30%. While the reductions are significant, there still remains a large burst effect with this approach.

Another problem with this system is the use of DMSO and NMP, which are highly controversial solvents. There are extensive toxicity data for oral, intraperitoneal and intravenous administration of these solvents, but not for subcutaneous or intramuscular use (99). In a recent study (100), poly(lactide) or PLGA was dissolved in NMP, DMSO or 2-pyrrolidone and injected intramuscularly into Sprague-Dawley rats. It was shown that these solvents are myotoxic and can damage muscles. Chandrashekar *et*

al. (1996) (101) and Singh *et al.* (1997) (102), tried propylene glycol and triacetin respectively. However, triacetin suffers from the same problems of NMP and DMSO and propylene glycol is not recommended due to its hemolytic potential (103,104). Eliaz *et al.* (2000), utilized glycofurol as a solvent to deliver soluble necrosis factor receptor from an *in situ* forming PLGA implants *in vivo* (105). Glycofurol is another solvent, which has been used in parenteral products (106). Unfortunately, little toxicological data are available in the literature (107). The only data uncovered were intravenous LD₅₀'s of 3.8 g/kg in the mouse (108) and 2.0-4.3 g/kg in the rat (109).

Poly(acrylic acid) and its derivatives have also been examined as precipitating polymers. Haglund *et al.* (110), investigated the use of poly(ethylene glycol) and poly(methacrylic acid) or poly(acrylic acid) as an injectable drug delivery system. Albumin-FITC and pheniramine were chosen as high and low molecular weight model drugs, respectively. Since the system is poorly soluble in an aqueous environment, at least 50% ethanol (preferably 60-80%) was added to keep the solution clear. After injection into the body, the ethanol diffuses out and water diffuses into the system, causing the dissolved polymeric network to collapse and precipitate. A similar approach was investigated by Ismail *et al.* (111), who examined water-soluble polymers such as hydroxypropylmethylcellulose (HPMC)-carbopol system and polymethacrylic acid (PMA)-polyethyleneglycol (PEG) for plasmid DNA delivery. Carbopol is a pH dependent polymer, which forms a low viscosity gel in alkaline environment (e.g., pH=7.4) and stays in solution in acidic pH. The addition of HPMC, a viscosity inducing agent, to carbopol reduces the carbopol concentration and hence the solution acidity while preserving the viscosity of the *in-situ* gelling system. This system gels upon an increase in pH when injected. The second appraised system consisted of a mixture of PMA and PEG dissolved in NMP/ethanol/buffer (1:1:2 ratio). Although the conformational analysis of the released pDNA from these systems showed no sign of degradation *in-vitro*, it was shown that the physical stability of pDNA was compromised (conversion from super coil to open circular form). Both systems were capable of releasing the pDNA but with a 35-70% drug burst in the first couple of hours followed by little to no subsequent release. The lack of significant release beyond the burst phase

indicates a strong interaction between the pDNA and the polymers used, which holds a portion of the pDNA within the polymer matrix. The collapse of the polymer network due to the removal of solvent (ethanol) causes a significant change in the volume of the system, which in turn causes the rapid release of the drug, especially when the drug is soluble in alcohol. Moreover, the outburst of the alcoholic solvent at the site of injection is likely to cause tissue irritation. Additionally, the *in vitro* release profiles of Ismail *et al.* was compared by using a two-way ANOVA . It is noteworthy that the use of two-way ANOVA to compare dissolution profiles is not recommended by the FDA. This is due to the fact that in dissolution profile data all the time points are dependent on each other and this violates the ANOVA assumption of independence between dissolution time points, and the time effect, which is not of interest, consumes too many degrees of freedom in the analysis (112).

In-situ forming injectable microspheres is a different approach introduced by Jain *et al.* (2000) (113). This system is comprised of a stable dispersion of PLGA-solvent solution microglobules (premicrospheres) dispersed in a continuous oil phase. Upon injection into the body, water penetration into the system while the PLGA solvent diffuses out hardens the microglobules into solid microspheres. To prepare this system PLGA was first dissolved in triacetin and a solution of PEG 400 and the drug (e.g., myoglobin Mw=16,950 or cytochrome c Mw=12,327) was added into followed by an addition of Tween 80. This mixture, called oil phase I, was added into a mixture of Span 80 and Miglyol 812 (oil phase II) dropwise with continuous homogenization to form the premicrospheres. Drug entrapment efficiency was reported to be between 60-90% by varying the PEG 400 and drug concentration in the formulation. The effects of using different vehicles were investigated and compared (triacetin with triethyl citrate and Miglyol 812 with soybean oil). It was shown that there is no effect in myoglobin release profile when the different vehicles were used. Overall, both systems were able to release the drugs in a sustained fashion for 15 days with a burst in the drug release of between 30-50 % during the first day. This was attributed to the free and unencapsulated drug present in the vehicle. The molecular weight of the drug had an impact on the *in vitro* release rate, and circular dichroism (CD) spectroscopy showed no sign of physical

instability in the proteins' native conformation. Although the system is readily injectable, the same can be said about the injection of drug-loaded PLGA hardened microspheres in a suitable vehicle, which would not have the disadvantage of the presence of an undesirable solvent phase.

These examples illustrate that the burst effect obtained depends on the nature of the drug incorporated (82). For hydrophobic drugs, the burst effect depends on the affinity of the drug for the solvent-water phase versus the solvent-polymer phase. If the drug has a higher affinity for the solvent-water phase, which initially surrounds the device, then a high burst effect will be observed. For hydrophilic drugs, such as FITC-bovine serum albumin, which are injected as suspensions in the polymer-solvent solution, the burst effect is determined by the number of drug particles which reside at the implant surface during polymer precipitation. This is affected by the viscosity of the solution, which governs particle settling, and the degree of mixing of the solution. Viscosity increases as polymer molecular weight and concentration increase, for a given solvent. Viscosity is also influenced by the polymer-solvent interaction. The greater the affinity of the polymer for the solvent, the greater the expansion of the polymer chain in solution and thus the greater the number of polymer chain entanglements which produces a more viscous solution. The burst effect is thus a complex situation and difficult to predict *a priori*.

A non-polymeric approach using the same precipitation strategy has also been developed. Smith and Tipton (114) introduced sucrose acetate isobutyrate (SAIB), a noncrystalline, viscous compound, which dissolves in solvents such as DMSO and ethanol, to form a solution having the same viscosity of vegetable oil (50-200 cP). SAIB is reported to be bioerodible and essentially insoluble in water. Upon injection of SAIB dissolved in, for example, ethanol at 50% concentration, into tissue, the solution increases dramatically as the solvent diffuses away. The SAIB then forms a depot, which sustains the release of the drug. Drugs that have been examined for release by this system include gonadotropin hormone (115), chlorhexidine, doxycycline, diclofenac, flurbiprofen, naproxen, and theophylline (116). Although sustained release is achieved, the same problems inherent with the polymeric systems exist with this system, i.e. high

initial burst, relatively rapid release rates, and use of controversial solvents. Furthermore, although SAIB has been approved as a food additive, it has not received approval as a parenteral compound.

2.4.2. Thermally-induced Sol/Gel Transitions

Many polymers undergo abrupt changes in solubility in response to changes in environmental temperature (117,118,119). This physical characteristic has been employed to form drug depots by using polymer systems, which undergo a sol-gel transition upon injection into the body.

Poly(N-isopropyl acrylamide) (poly(NIPAAM)) is an example of a thermosensitive polymer. It exhibits the phenomenon of lower critical solution temperature (LCST) phase separation. Reviews of polyNIPAAM and its gel applications are numerous (120,121,122). PolyNIPAAM shows a very well defined LCST at about 32 °C, which can be shifted to body temperature by formulating polyNIPAAM based gels with salts and surfactants (123,124). Although numerous poly(N-alkylacrylamides) and polymers possess LCSTs (125,126), polyNIPAAM is unique with respect to the sharpness of its almost discontinuous transition, which is usually observed only with ionizable polymers (127). These features make poly(NIPAAM) an interesting potential material for use in *in situ* setting drug delivery. However, acrylamide based polymers with quaternary ammonium in their structure, in general, are not suitable for implantation purposes due to cell toxicity (128). The observation that acrylamide-based polymers activate platelets on contact with blood (129), along with the poorly understood metabolism of polyNIPAAM and its non-degradability (130), make it difficult to win FDA approval. Therefore, the vast majority of the drug delivery systems which employ LCST, use block copolymers of poly(ethylene oxide) (PEO) and poly(propylene oxide) (PPO) simply because of FDA approval (131).

Triblock PEO-PPO-PEO copolymers (Pluronics®, or Poloxamers®) are available in a variety of lengths and are of particular interest, as their gelation phenomena have been extensively studied (132,133,134). The properties of some Pluronic copolymers frequently used in drug delivery studies are collected in Table 2.1

(135). It is significant to note that, although most of the Pluronics listed in Table 2.1 have a LCST well above normal body temperature, they do exhibit gelation at body temperature in concentrated solutions (136). However, application of concentrated polymer solutions (>16 wt%) in drug delivery may be disadvantageous as it changes the osmolality of the formulation, kinetics of gelation, and causes discomfort in ophthalmic applications due to vision blurring and crusting (137). Since F127 has been reported to be the least toxic of the commercially available Pluronics® (138), it has been used most extensively in drug delivery studies. One other reason for the popularity of Pluronics® is its inhibitory effect on P-glycoprotein (139,140). Certain Pluronics®, e.g., P85, strikingly increase the cytotoxicity of drugs such as daunorubicin, against multidrug cell overexpressing P-glycoprotein (141). It appears that unimers of Pluronics are able to inhibit P-glycoprotein. The mechanism of inhibition is unclear, but it may be related to the changes at a membrane level induced by Pluronics. This may inhibit P-glycoprotein or enhance cellular uptake of drugs (142).

Veyries *et al.* (143), demonstrated the possibility of controlled release of vancomycin from Pluronic® F127. They investigated Poloxamer® 407 (Pluronic® F127) 25% formulations aimed at prolonging the residence time of vancomycin, a time dependent antibiotic, in a body site with a high infectious risk. It appeared that neither the rheological properties of the Poloxamer® matrices nor the antibacterial activity of vancomycin was altered by their combination. Two formulations were prepared, one saturated and one unsaturated (solubilized) with vancomycin. *In vitro*, the dispersed form (saturated) exhibited prolonged release, with a lower diffusion coefficient of vancomycin compared to the solubilized form (4.7×10^{-8} vs 2.1×10^{-7} cm^2s^{-1}) (Fig. 2.8). In rats, a single dose was well tolerated and resulted in a high local concentration for 24 hrs (>131 mg/L), followed by lower but effective antibacterial levels for at least 8 days. Based on the release profiles, good preservation of vancomycin activity, good tolerability in rats, and ease of administration, it was concluded that Poloxamer® 407 might be useful as a vancomycin delivery vehicle for local prophylaxis of infections, especially in prosthetic surgery. In another study by Miyazaki *et al.*, the antitumor effect of Pluronic® F-127 containing Mitomycin C (MMC) on sarcoma-180 ascites tumor

mice was evaluated (144). The Pluronic® F-127 gels were evaluated as a sustained release vehicle for intraperitoneal administration of MMC in order to enhance the therapeutic effects of MMC. Tumor cell injections were made on day 0 and injections of MMC in 25% (w/w) Pluronic® F-127 on day 1, both intraperitoneally. A prolongation of the life span of tumor-bearing mice following injection of therapeutic Pluronic® F-127 was noted, and Pluronic® F-127 containing MMC was therapeutically more active than free drug. The *in vitro* release experiments indicated that Pluronic® gel might serve as rate-controlling barrier and be useful as a vehicle for sustained release preparations of MMC to be administered intraperitoneally (Fig 2.9).

As discussed previously, Pluronic® concentrations above 16 wt% may show toxicity particularly when intended for intraperitoneal administration. This problem led the Miyazaki's group to study the potential of natural polymers as vehicles for drug delivery. Xyloglucan polysaccharide derived from tamarind seeds is composed of a (1-4)- β -D-glucan backbone chain, which has (1-6)- α -D-xylose branches that are partially substituted by (1-2)- β -D-galactoxylose. When partially degraded by β -galactosidase, the resultant product exhibits thermally reversible gelation in dilute aqueous solutions [145]. An important difference between the gelation properties of the xyloglucan gels and block copolymers such as Pluronic® F-127 from a toxicity viewpoint is that xyloglucan forms gels at much lower concentrations. In an *in vitro* study, the cumulative release of MMC from an aqueous solution of concentration 0.025% (w/v) and from xyloglucan gels with gel concentrations of 0.5, 1 and 1.5% (w/w) was compared at 37 °C (Fig. 2.10). It was determined that the *in vitro* release of MMC from xyloglucan gels is diffusionally controlled. The figure demonstrates that the system has the potential for sustained drug release. The advantage of xyloglucan gel is its gel formation at low concentrations. However, there is no published information on their biodegradability or tissue biocompatibility, which may limit its suitability for use.

Beside the two examples given above, Poloxamer® 407 has been studied in a series of papers for controlled delivery of low and high molecular weight bioactive agents such as melanotan-I (146), lidocaine (147), ibuprofen (148), pilocarpine (149) and

interleukin-2 (150). One important drawback of Poloxamer® 407 is hypertriglyceridemia induction following intraperitoneal injection. Johnston *et al.* in two studies (151,152), demonstrated that Poloxamer® 407 injected into rats by intraperitoneal injection resulted in sustained hypercholesterolemia and hypertriglyceridemia. This phenomenon was due to stimulation of 3-hydroxy-3-methylglutaryl-co-enzyme A (HMG-CoA) reductase activity in the liver by the Poloxamer® vehicle. Thus, elevated levels of plasma cholesterol and triglycerides resulting from the chronic administration of Poloxamer® containing drug formulations to patients may potentially hinder therapeutic outcome.

Jeong *et al.* in 1997 (130,153), reported a hydrogel consisting blocks of poly(ethylene oxide) and poly(L-lactic acid). Aqueous solutions of these copolymers exhibited temperature-dependent reversible gel-sol transitions. The advantage of this system over solvent-removal gelation is the absence of any organic solvent. Unfortunately, this system can only be loaded with bioactive molecules in an aqueous phase at an elevated temperature (around 45 °C), where it forms a sol. This loading procedure limits the nature of the drugs that can be incorporated in the delivery system to those that are not prone to hydrolysis. Moreover, this temperature can cause protein denaturation.

Jeong *et al.* (154), also designed another thermo-responsive hydrogel made of PEG-PLGA-PEG tri-block copolymers. This type of polymer mixture demonstrates phase separation behavior as the temperature increases above the LCST. The polymer is in sol form at room temperature and once inside the body, it turns into a gel and forms a viscous polymer solution. No organic solvent is required for this system but it bears the problem common to sol-gel systems, which is the high initial burst effect. When a polymer system goes through the sol/gel process, it shrinks and its volume changes dramatically. This phenomenon can exude significant amounts of the encapsulated bioactive agent out of the hydrogel and create an initial burst.

Chenite *et al.*, developed a novel hydrogel system composed of neutral solutions of chitosan (155). Chitosan is obtained by alkaline deacetylation of chitin, a natural component of shrimp or crab shells. Chitosan is a biocompatible pH-dependent cationic

polymer, which remains dissolved in aqueous solution up to a pH of 6.2. Neutralization of chitosan aqueous solutions to a pH exceeding 6.2 leads to the formation of a hydrated gel-like precipitate. In this study, pH-gelling cationic polysaccharide solutions were transformed into thermally sensitive pH-dependent gel-forming aqueous solutions, without any chemical modification or crosslinking. This was done by addition of polyol salts bearing a single anionic head, such as glycerol-, sorbitol-, fructose- or glucose-phosphate salts to chitosan aqueous solutions. This system was examined for delivery of biologically active growth factors *in vivo* as well as encapsulation of living chondrocytes for tissue engineering. Although this transformation has solved the non-degradability problem of chitosan and can be considered as an advantage for this system, there is a lack of data presented regarding the volume change of the hydrogel and release profile data for the growth factor. Therefore, its suitability as a drug delivery vehicle requires further examination.

Other thermally sensitive polymer systems have also been developed. For example, the concept of stereocomplex formation was exploited recently to form a novel hydrogel, based on self-assembling of enantiomeric lactic acid oligomers grafted to dextran (156). L- and D- lactic acid oligomers were coupled to dextran, yielding dex-(L)lactate and dex-(D)lactate, respectively. Upon dissolving each product in water separately and mixing the solutions, a hydrogel formed at room temperature. Although no drug delivery applications have been demonstrated to date, this approach can be manipulated for delivering pharmaceutically active agents into the body without the need for crosslinking agents and organic solvents. In two reports, one published in *Science* (1998) and the other in *Nature* (1999), protein domains were used to form hydrogels. Petka *et al.*, used recombinant DNA methods to create artificial proteins that undergo reversible gelation in response to changes in pH or temperature (157). The proteins consisted of terminal leucine zipper domains flanking a central, flexible, water-soluble polyelectrolyte segment. Formation of coiled-coil aggregates of the terminal domains in near-neutral aqueous solutions triggers formation of a three-dimensional polymer network. Dissociation of the coiled-coil aggregates through elevation of pH or temperature causes dissolution of the gel and showing viscous behavior. Wang *et al.*,

reported a hybrid hydrogel system assembled from water-soluble synthetic polymers and a well-defined protein-folding motif, the coiled coil (158). These hydrogels undergo temperature-induced collapse owing to the cooperative conformational transition of the coiled-coil protein domain. Such new systems are still in the development stage and need more experimental studies.

2.5. *In Situ* Solidifying Organogels

Organogels or oleaginous gels are composed of water-insoluble amphiphilic lipids, which swell in water and form various types of lyotropic liquid crystals. The nature of the liquid crystalline phase formed depends on the structural properties of the lipid, temperature, nature of the drug incorporated, and the amount of water in the system (159). The amphiphilic lipids examined to date for drug delivery are primarily glycerol esters of fatty acids, for example glycerol monooleate, glycerol monopalmitostearate, and glycerol monolinoleate which are waxes at room temperature. These compounds form a cubic liquid crystal phase upon injection (159) into an aqueous medium. The cubic phase consists of a three-dimensional lipid bilayer separated by water channels. This liquid crystalline structure is gel-like and highly viscous.

This gel forming nature has been used to form drug depot systems for the delivery of both water soluble and water insoluble drugs. For example, Ericsson *et al.* (160) used a glycerol monooleate system to deliver somatostatin subcutaneously in rabbits while Yim *et al.* developed a formulation for interferon- α composed primarily of aluminum monostearate and peanut oil (19), and Gao *et al.* (161,162) demonstrated the use of a glycerol palmitostearate (Precirol) system to deliver the lipophilic drugs levonorgestrel and ethinyl estradiol. The equilibrium water content of the organogel formed is typically approximately 35 %, which therefore produces relatively short release duration for hydrophilic drugs. For the somatostatin example given above, somatostatin release lasted for only 6 hours. Much more sustained release can be achieved using a lipophilic drug. In the work of Gao *et al.* (161,162), *in vitro* release of levonorgestrel was observed for up to 14 days (162), while *in vivo* studies of levonorgestrel in the organogel injected subcutaneously into rabbits demonstrated an

estrus blockage for up to 40 days (161).

Although they can be formulated with a low concentration of water, the viscosity of the system is reduced by mixing with vegetable oils. Reducing the viscosity in this manner eases injectability and increases the release duration, particularly for lipophilic drugs. For example, Gao *et al.* found that incorporating glycolized apricot kernel oil (Labrafil 1944 CS) reduced the *in vitro* release rate of levonorgestrel, from 36.2 $\mu\text{g}/\text{cm}^2$ to 19.9 $\mu\text{g}/\text{cm}^2$ at day 14 for 0% and 20% oil incorporation respectively (162). Lipophilic drug release from these organogels is also dependent upon the solubility of the drug in the cubic phase. If the drug concentration exceeds its solubility in the cubic phase then drug particles will form. The presence of these solid particles has been demonstrated to produce zero-order release kinetics, with a rate which increases as particle size decreases (162).

Another advantage of these systems is that they are biodegradable. Biodegradation occurs through the action of lipases (163) and for the glycerol palmitostearate/Labrafil 1944 CS system, requires between 5 to 6 weeks (161). An inflammatory reaction was observed for this system, which lasted for 7 days and then dissipated.

Organogels thus are a promising injectable delivery system for lipophilic compounds. There are some disadvantages inherent to this approach. Purity of waxes and stability of oils are the major issues that need to be addressed. There are number of waxes such as carnauba wax, wool wax, spermaceti wax and esparto wax, used for cosmetic purposes but not for parenteral applications. Only beeswax is readily available in various purification grades. Oils usually need a stabilizer, antioxidant and preservative to increase their shelf life and stability. Moreover, the difference between the melting point of waxes and oils makes this system susceptible to phase separation. Labrafil and Precirol are a mixture of many different vegetable oils and glyceryl esters of fatty acids, respectively. Unfortunately, there is still concern over the purity and lack of toxicity data for these waxes and oils. Another drawback is the need to apply heat to mix the oil and wax phase. Temperatures of up to 60 °C for 30 minutes have been used (161,164). Temperatures this high can easily reduce the potency of some drugs.

2.6. Summary

We have reviewed a large cross-section of biodegradable *in-situ* forming drug delivery systems for local delivery of drugs (Table 2). These delivery systems have unique challenges associated with their development that are related to drug stability, drug release kinetics and the conditions under which the system is delivered to the body. The continuous advances in biotechnology and drug development will produce more pharmaceutically active agents that will be difficult to administer by conventional means, and an increased demand for controlled or site-specific delivery system is anticipated.

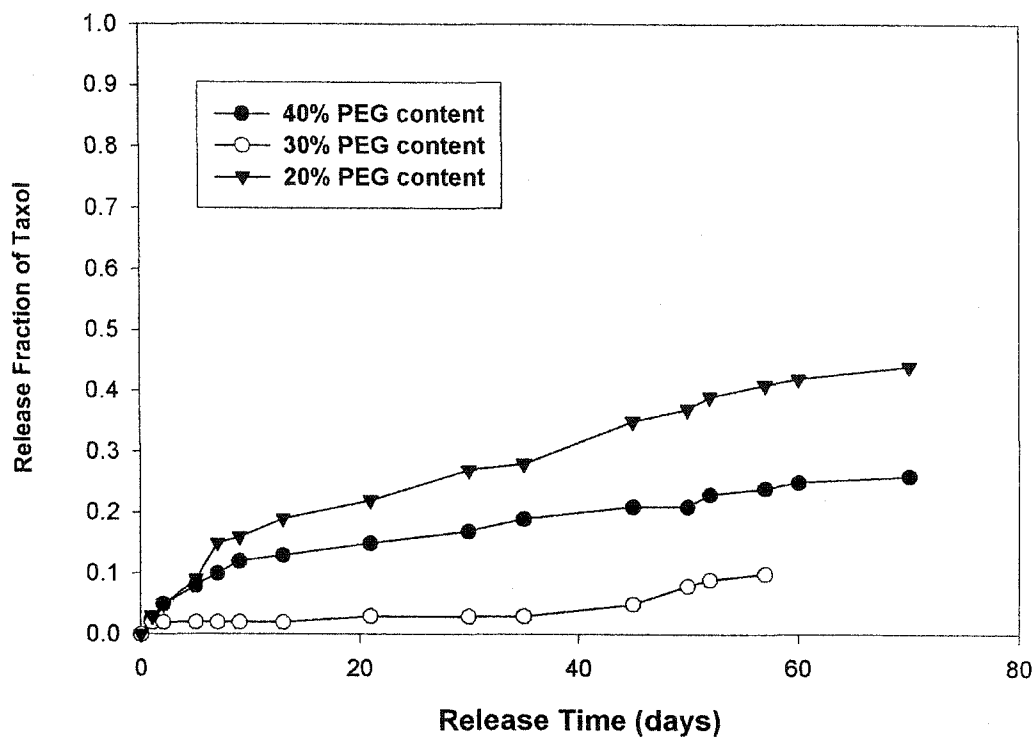


Figure 2.1: Cumulative release of taxol from taxol loaded PDLLA-PEG-PDLLA cylinders into PBS albumin buffer at 37 °C. Reproduced from reference 44.

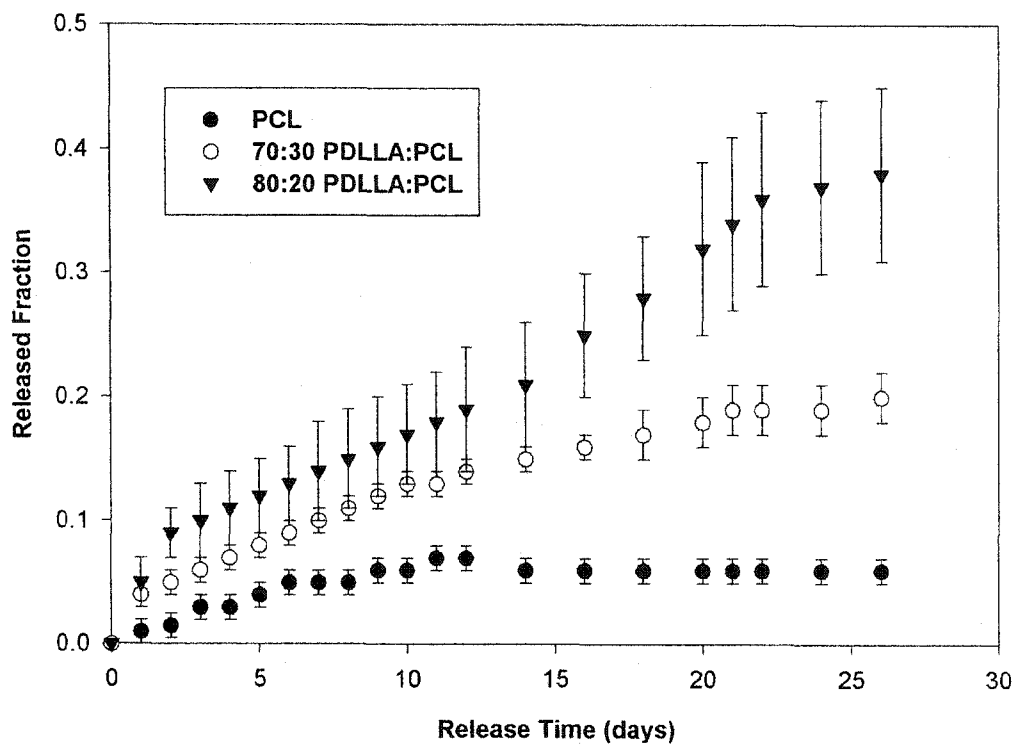


Figure 2.2: Cumulative release of taxol from 20% taxol loaded PDLLA:PCL blends and PCL into PBS albumin buffer at 37 °C. The error bars represent the S.D. of 4 samples.
 Reproduced from reference 44.

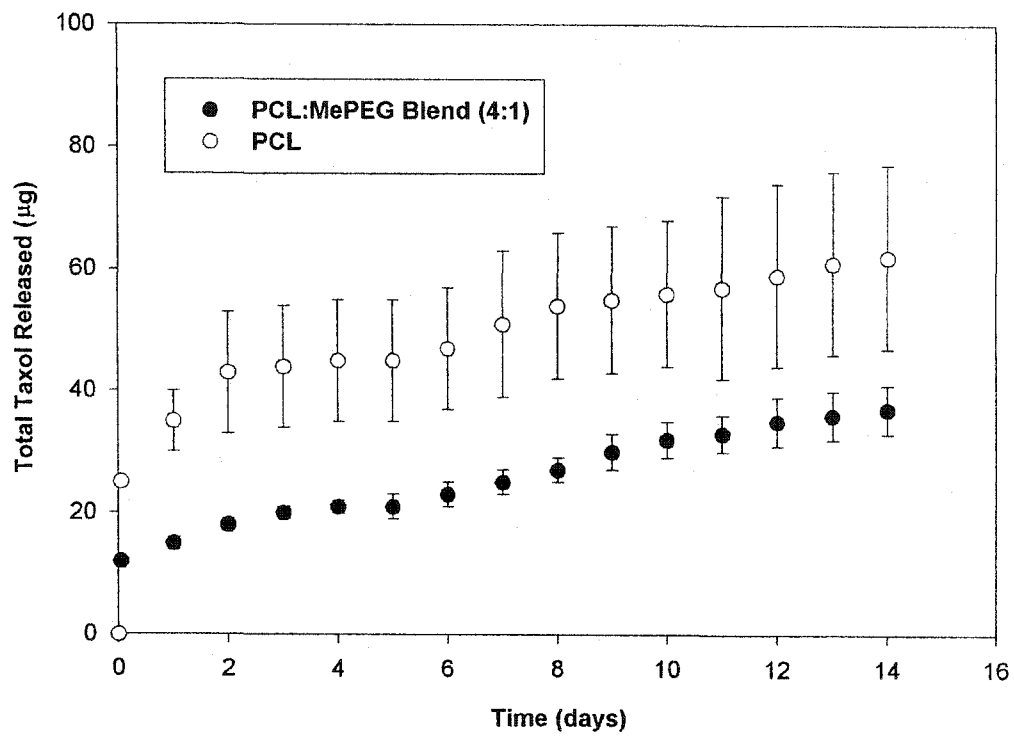


Figure 2.3: Taxol release profiles. PCL and PCL:MePEG blend at 30% taxol loading. Reproduced from reference 48.

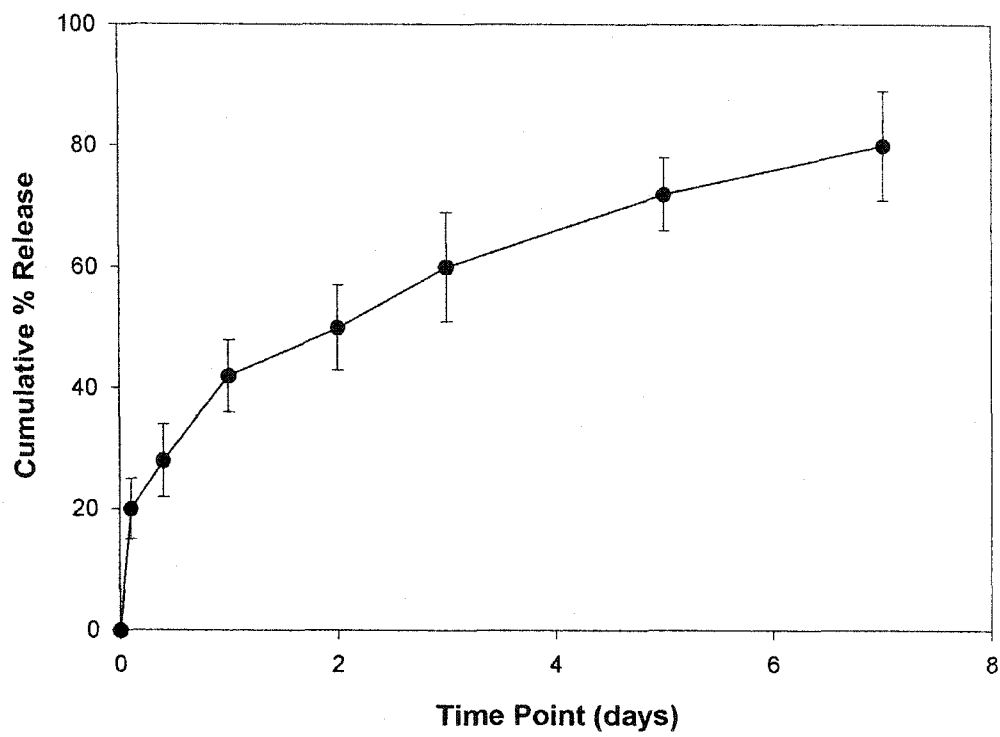


Figure 2.4: *In vitro* drug release from formulations containing 5% flurbiprofen in PBS at 37 °C. Reproduced from reference 54.

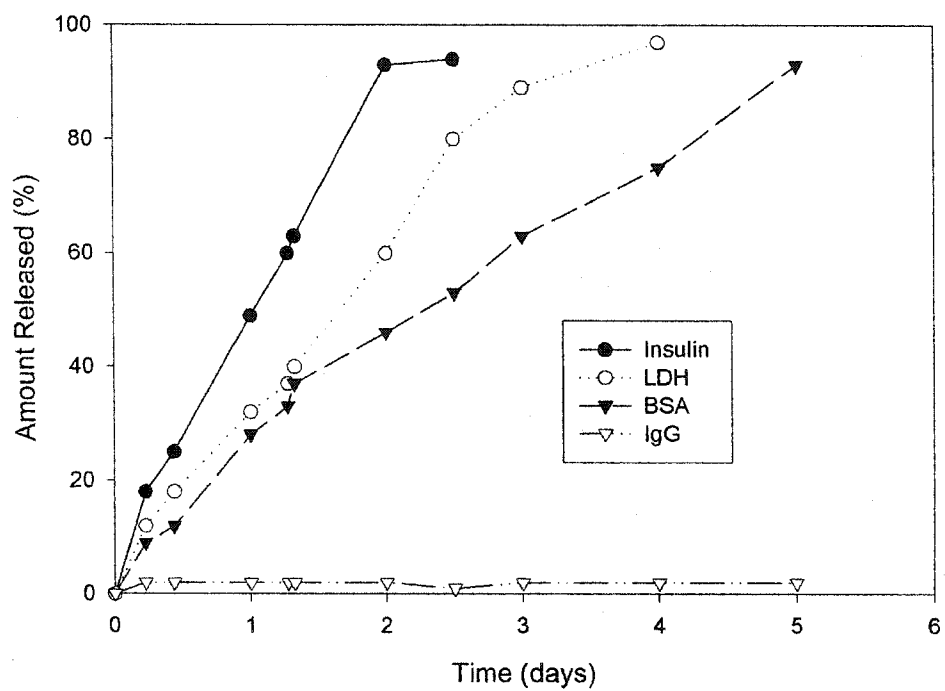


Figure 2.5: Delivery of various proteins from a photopolymerized PEG-PLA hydrogel. Reproduced from reference 71.

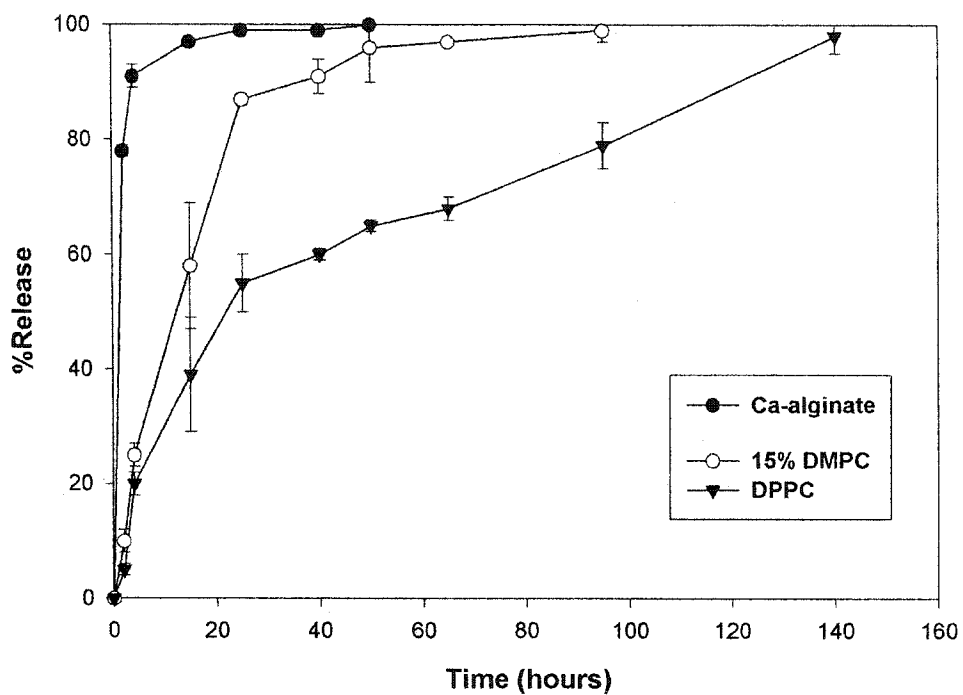


Figure 2.6: Release of metronidazole from thermally gelled liposome/alginate hydrogels. Sealed dialysis bags containing one part Ca-loaded liposomes, one part drug-loaded liposomes (DPPC or 15% DMPC) and three parts sodium alginate (2%) were inserted into 37 °C buffer at time zero. The control was a metronidazole-infused calcium alginate (2%). Reproduced from reference 73.

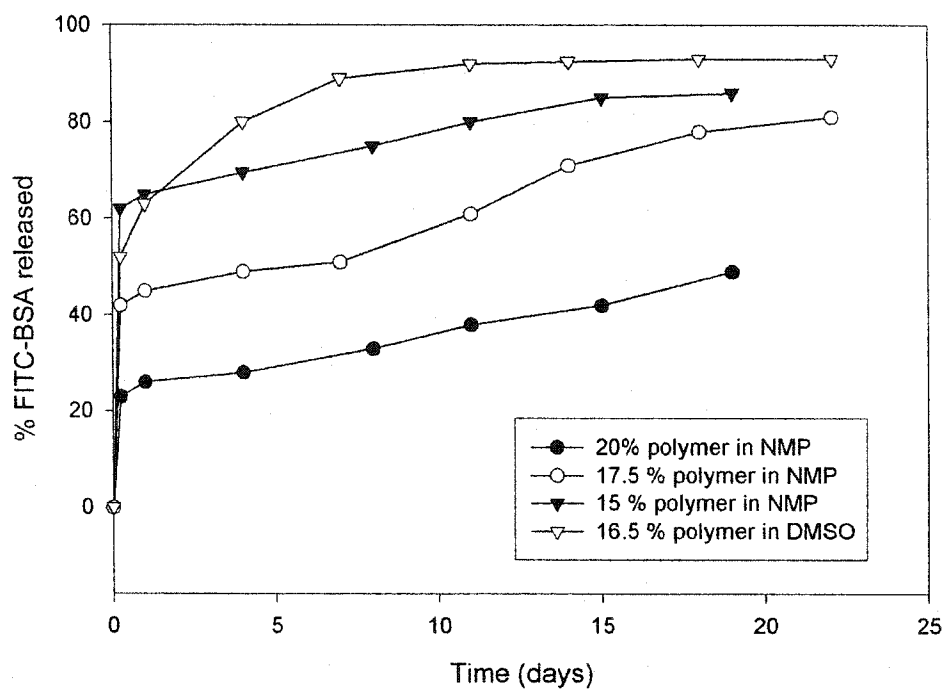


Figure 2.7A: Release of FITC-BSA from the high molecular weight 50:50 PLGA system in PBS. Error bars indicate standard deviation (n=3). The initial burst of the high molecular weight 50:50 PLGA in NMP is found to be inversely proportional to polymer percent and is followed by close to zero order release for up to two weeks. Reproduced from reference 29.

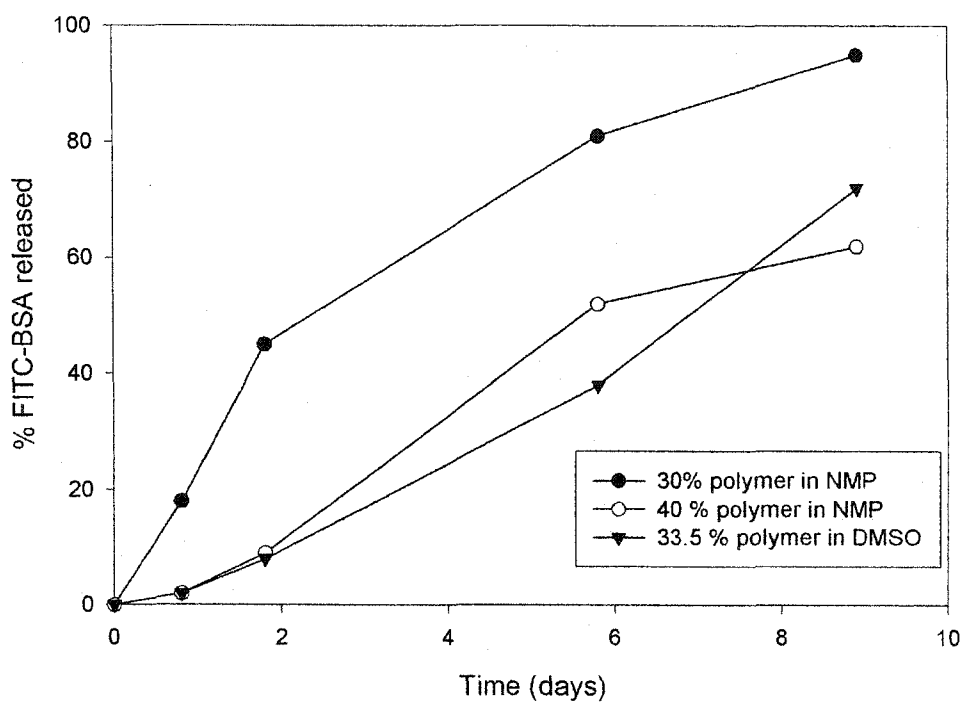


Figure 2.7B: Release of FITC-BSA from the low molecular weight 50:50 PLGA system in PBS. Error bars indicate standard deviation (n=3). Reproduced from reference 29.

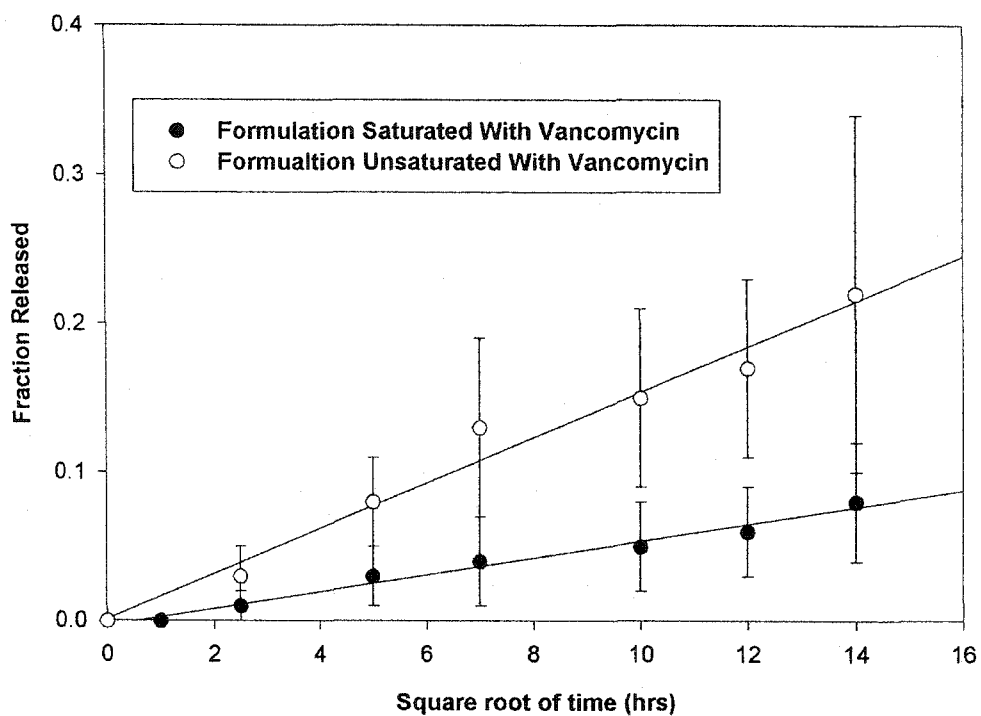


Figure 2.8: *In vitro* vancomycin release from both poloxamer 407 gels at 37 °C. Values were measured by HPLC and are expressed as a fraction of vancomycin released in the receptor compartment versus the square root of time.
Reproduced from reference 143.

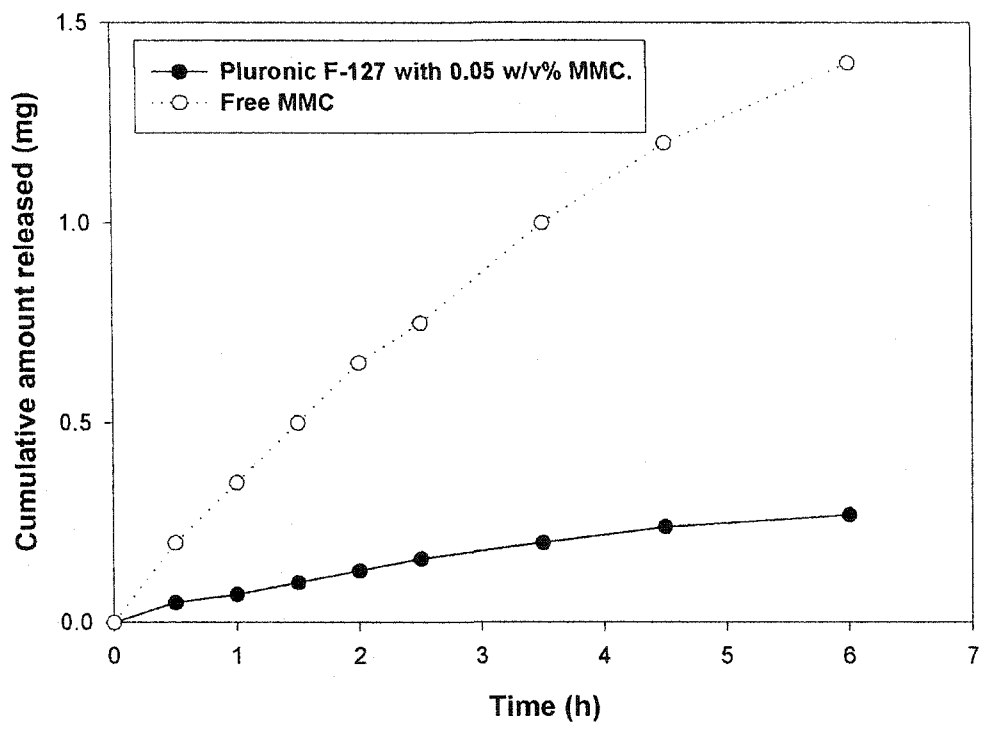


Figure 2.9: Release of MMC from pluronic F-127 gel at 37 °C. Each value represents the mean of three experiments. Reproduced from reference 144.

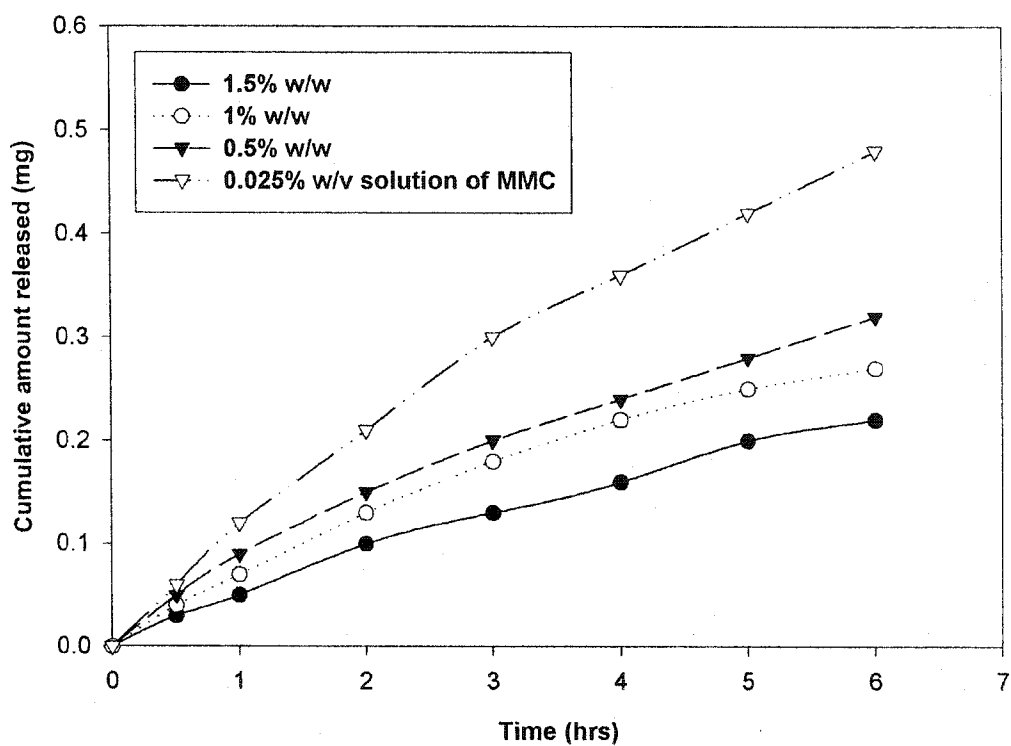


Figure 2.10: Cumulative amount of MMC released as a function of time at 37 °C from xyloglucan gels of concentrations 0.5, 1 and 1.5% containing an initial concentration of 0.025% (w/v) and from 0.025% (w/v) solution of MMC. Reproduced from reference 145.

Table 2.1: Properties of the Pluronic copolymers. Reproduced from reference 135.

Copolymer ^a	Composition	Average Mw	M _{ppo}	PEO(wt%)	CP ^b (°C)	HLB ^c
L64	EO ₁₃ PO ₃₀ EO ₁₃	2900	1740	50	58	12-18
F68	EO ₇₆ PO ₂₉ EO ₇₆	8400	1680	80	>100	>24
F88	EO ₁₀₃ PO ₃₉ EO ₁₀₃	11400	2280	80	>100	>24
P103	EO ₁₇ PO ₆₀ EO ₁₇	4950	3465	30	86	7-12
P104	EO ₂₇ PO ₆₁ EO ₂₇	5900	3540	40	81	12-18
P105	EO ₃₇ PO ₅₆ EO ₃₇	6500	3250	50	91	12-18
P108	EO ₁₃₂ PO ₃₀ EO ₁₃₂	14600	2920	80	>100	>24
F127	EO ₁₀₀ PO ₆₅ EO ₁₀₀	12600	3780	70	>100	18-23
L122	EO ₁₂ PO ₆₇ EO ₁₂	5000	3600	20	19	1-7

a: L, F and P indicate liquid, flakes and paste, respectively.

b: Cloud point in aqueous 1 wt% solution.

c: Hydrophilic-lipophilic balance.

Table 2.2: Biodegradable *In-Situ* Solid Forming Delivery Systems.

Delivery Systems	Common Problems	Common Materials Used
1- Thermoplastic Pastes	1- High temperature at the time of injection.	PLA, PLGA & PCL. Stannous Octoate as catalyst. Alcohols as initiator.
2- In situ Crosslinked Systems		
A: Thermosets	1- Unacceptable level of heat released during the reaction. 2- Burst in drug release. 3- Toxicity of un-reacted monomers.	Oligomers of PLA, PDLLA & PCL. Polyols as initiator and peroxides as curing agent.
B: Photocrosslinked Gels	1- Shrinkage and brittleness of the polymer due to high degree of crosslinking.	PGA, PLA, PCL & PEG. Initiators such as eosin dye Light source (e.g., UV or laser)
C: Ion Mediated Gelation	1- Low shelf life. 2- Burst in drug release. 3- Degradation Time	Alginates. Gelling agent (e.g., Ca ²⁺).
3- In Situ Polymer Precipitation		
A: Solvent-Removal Precipitation	1- Burst in drug release. 2- Application of organic solvents.	PDLLA, PCL & PLA. Solvents (e.g., DMSO or NMP).
B: Thermally-Induced Sol/Gel Transition	1- Burst in drug release.	NIPAAM, PEG, PLA, PLGA & Chitosan., Pluronic
4- Organogels	1- Stability of oils and purity of waxes. 2- Lack of toxicity data 3- Phase separation	Oils such as peanut oil & Labrafil. Waxes (Beeswax)

2.7. References

[1]- J. Heller, Polymers for controlled parenteral delivery of peptides and proteins. *Adv. Drug Deliv. Rev.* 10 (1993) 163-204.

[2]- R. Langer, New methods of drug delivery. *Science* 249 (1990) 1527-1533.

[3]- K. R. Reddy, Controlled release, pegylation, liposomal formulations: New mechanisms in the delivery of injectable drugs. *Ann. Pharmacother.* 34 (2000) 915-922.

[4]- A. J. Tipton, R.L. Dunn, *In situ* gelling systems, in: J. H. Senior, M. Radomsky (eds), *Sustained release injectable products*. Interpharm Press, Denver, 2000, pp. 71-102.

[5]- L. E. Hollister, Site-specific drug delivery to central nervous system. *Nuorobiol. aging* 10(5) (1989) 631; discussion 648-650.

[6]- R. J. Levy, L. Vinod, S. A. Strickberger, T. Underwood, J. Davis, Controlled release implant dosage forms for cardiac arrhythmias: review and perspectives. *Drug Deliv.* 3 (1996) 137-142.

[7]- L. C. Collins-Gold, R. T. Lyons, L. C. Batholow, Parenteral emulsions for drug delivery. *Adv. Drug Deliv. Rev.* 5 (1990) 189-208.

[8]- S. S. Davis, L. Illum, Colloidal drug delivery systems: opportunities and challenges, in: E. Tomlinson, S. S. Davis (eds), *Site-specific drug delivery*. Wiley, New York, 1986 pp. 210-224.

[9]- A. T. Florence, D. Whitehill, The formulation and stability of multiple emulsions. *Int. J. Pharm.* 11 (1982) 277-308.

[10]- T. M. Allen, C. B. Hansen, L. S. S. Guo, Subcutaneous administration of liposomes: A comparison with the intravenous and intraperitoneal routes of injection. *Biochim. Biophys. Acta.* 1150 (1993) 9-16.

[11]- P. M. Anderson, S. E. Katsanis, S. F. Sencer, D. Hasz, B. Bostrom, Depot

characteristics and biodistribution of interleukin-2 liposomes: Importance of route of administration. *J. Immunother.* 12 (1992) 19-31.

[12]- A. Bonetti, E. Chatelut, S. Kim, An extended-release formulation of methotrexate for subcutaneous administration. *Cancer Chemother. Pharmacol.* 33 (1994) 303-306.

[13]- A. Sharma, U. S. Sharma, liposomes in drug delivery: progress and limitations. *Int. J. Pharm.* 154 (1997) 123-140.

[14]- A. Shendrova, T. G. Burke, S. P. Schwendeman, Stabilization of 10-hydroxycamptothecin in poly(lactide-co-glycolide) microsphere delivery vehicles. *Pharm. Res.* 14(10) (1997) 1406-1414.

[15]- L. Chen, R. N. Apte, S. Cohen, Characterization of PLGA microspheres for the controlled delivery of IL-1 for tumor immunotherapy. *J. Controlled Release* 43 (1997) 261-272.

[16]- J. L. Cleland, A. J. S. Jones, Stable formulations of recombinant human growth hormone and interferon gamma for microencapsulation in biodegradable polymers. *Pharm. Res.* 13 (1996) 1462-1473.

[17]- X. Zhang, J. K. Jackson, H. M. Burt, Development of amphiphilic diblock copolymers as micellar carriers of taxol. *Int. J. Pharm.* 132 (1996) 195-206.

[18]- H. Alkan-Onyuksel, S. Ramakrishnan, H. B. Chai, J. M. Pezzuto, A mixed micellar formulation suitable for the parenteral administration of taxol. *Pharm. Res.* 11 (1994) 206-212.

[19]- Z. Yim, M. A. Zupon, I. A. Chaudry, Stable oleaginous gel. U.S. Patent 4,851,220, July 25, 1989.

[20]- I. A. J. M. Woudenberg, M. T. Kate, G. Storm, E. W. M. van Etten, Administration of liposomal agents and the phagocytic function of the mononuclear phagocyte system. *Int. J. Pharm.* 162 (1998) 5-10.

[21]- S. M. Moghimi, Opsono-recognition of liposomes by tissue macrophages. *Int. J.*

pharm. 162 (1998) 11-18.

[22]- A. Sharma, U. S. Sharma, Liposomes in drug delivery: progress and limitations. Int. J. Pharm. 154 (1997) 123-140.

[23]- A. J. Tipton, S. M. Fujita, A biodegradable injectable delivery system for nonsteroidal anti-inflammatory drugs. Pharm. Res. Supp. 9 (1991) S-196.

[24]- C. Allen, A. Eisenberg, D. Maysinger, Nano-engineering block copolymer aggregates for drug delivery. Colloids and surfaces B: Biointerfaces 16 (1999) 3-27.

[25]- M. S. Espuelas, P. Legrand, J. M. Irache, C. Gamazo, A. M. Orecchinioni, J. Ph. Devissaguet, P. Ygartua, Poly caprolactone nanospheres as an alternative way to reduce amphotericin B toxicity. Int. J. Pharm. 158 (1997) 19-27.

[26]- R. Herrero-Vanrell, E. Barcia, S. Negro, M. F. Refojo, Development of gancyclovir microspheres from poly DL-Lactide-co-glycolide for the treatment of AIDS-related cytomegalovirus retinitis. S.T.P. Pharma. Sci. 8 (4) (1998) 237-240.

[27]- C. Allen, A. Eisenberg, D. Maysinger, Copolymer drug carriers: conjugates, micelles and microspheres. S.T.P. Pharma. Sci. 9(1) (1999) 139-151.

[28]- A. T. Florence, D. Atwood(eds.), Physicochemical principles of pharmacy. Macmillan Press LTD, Hampshire, London, 1998, pp. 224-234.

[29]- W. J. Lambert, K. D. Peck, Development of an *in situ* forming biodegradable poly-lactide-co-glycolide system for the controlled release of proteins. J. Controlled Release 33 (1995) 189-195.

[30]- W. R. Gombotz, D. K. Pettit, Biodegradable polymers for protein and peptide drug delivery. Bioconjug. Chem. 6 (1995) 332-351.

[31]- D. A. Wood, Biodegradable drug delivery systems. Int. J. Pharm. 7 (1980) 1-18.

[32]- R. S. Bezwada, Liquid copolymers of epsilon-caprolactone and lactide. U.S. Patent

5,442,033, August 15, 1995.

[33]- R. S. Bezwada, S. C. Arnold, liquid absorbable copolymers for parenteral applications. U.S. Patent 5,653,992, August 5, 1997.

[34]- P. C. Painter, M. M. Coleman (eds.), Fundamentals of polymer science. Technomic Publishing Co, Lancaster, PA, 1994, pp. 4-5.

[35]- S. Einmahl, F. Behar-Cohen, C. Tabatabay, M. Savoldelli, F. D. Hermies, D. Chauvaud, J. Heller, R. Gurny, A viscous bioerodible poly(ortho ester) as a new biomaterial for intraocular application. *J. Biomed. Mater. Res.* 50 (2000) 566-577.

[36]- J. K. Jackson, W. Min, T. F. Cruz, S. Cindric, L. Arsenault, DD. Von Hoff, D. Degan, H. M. Burt, Polymer-based drug delivery system for the antineoplastic agent bis(maltolato)oxovanadium in mice. *Br. J. Cancer* 75 (7) (1997) 1014-1020.

[37]- S. J. Holland, B. J. Tighe, P. L. Gould, Polymers for biodegradable medical devices. 1- The potential of polyesters as controlled macromolecular release systems. *J. Controlled Release* 4 (1986) 155-180.

[38]- A. A. Deshpande, J. Heller, R. Gurny, Bioerodible polymers for ocular drug delivery. *Crit. Rev. Ther. Drug Carrier Syst.* 15 (4) (1998) 381-420.

[39]- R. L. Dunn, J. P. English, D. R. Cowsar, D. D. Vanderbelt, Biodegradable in-situ forming implants and methods of producing the same. U.S. Patent 5,278,201, January 11, 1994.

[40]- R. L. Dunn, J. P. English, D. R. Cowsar, D. D. Vanderbelt, Biodegradable in-situ forming implants and methods of producing the same. U. S. Patent 5,278,202, January 11, 1994.

[41]- A. G. Scopelianos, R. S. Bezwada, S. C. Arnold, Injectable liquid copolymers for soft tissue repair and augmentation. U. S. Patent 5,824,333, October 20, 1998.

[42]- E. Janzen, M. J. Hoekstra, R. P. Dutrieux, Injectable compositions for soft tissue augmentation. U.S. Patent 5,523,291, June 4, 1996.

- [43]- K. A. Walter, M. A. Cahan, A. Gur, B. Tyler, J. Hilton, O. M. Colvin, P. C. Burger, A. Domb, H. Brem, Interstitial Taxol delivered from a biodegradable polymer implant against experimental malignant glioma. *Cancer Res.* 54 (1994) 2207-2212.
- [44]- X. Zhang, J. K. Jackson, W. Wong, W. Min, T. Cruz, W. L. Hunter, H. M. Burt, Development of biodegradable polymeric paste formulations for Taxol: an *in vivo* and *in vitro* study. *Int. J. Pharm.* 137 (1996) 199-208.
- [45]- F. Liu, B.C. Wilson, Hyperthermia and photodynamic therapy, in: I. Tannock, R. P. Hill (eds.), *Basic science of oncology*. McGraw-Hill, New York, 1998, pp. 443-453.
- [46]- S. K. Durdanoo, A. M. C. Oktaba, W. Hunter, W. Min, T. Cruz, H. M. Burt, Release of Taxol from poly caprolactone pastes: effect of water soluble additives. *J. Controlled Release* 44 (1997) 87-94.
- [47]- C. G. Pitt, Poly- ϵ -caprolactone and its copolymers, in: M. Chasin, R. Langer (eds.), *Biodegradable polymers as drug delivery systems*. Marcel Decker, New York, 1990, pp.71-120.
- [48]- C. I. Winternitz, J. K. Jackson, J. K. Jackson, A. M. Oktaba, H. M. Burt, Development of a polymeric surgical paste formulation for taxol. *Pharm. Res.* 13 (3) (1996) 368-375.
- [49]- J. K. Jackson, M. E. Gleave, V. Yago, E. Beraldi, W. L. Hunter, H. M. Burt, The suppression of human prostate tumor growth in mice by the intratumoral injection of a slow-release polymeric paste formulation of Paclitaxel. *Cancer Res.* 60 (2000) 4146-4151.
- [50]- P. A. Davis, Cousins S, Biodegradable injectable drug delivery polymer. U.S. Patent 5,384,333, January 24, 1995.
- [51]- S. J. Peter, J. A. Nolley, M. S. Widmer, J. E. Merwin, M. J. Yaszemski, A. W. Yasko, P. S. Engel, A. G. Mikos, *In vitro* degradation of a poly(propylene fumarate)/ β -tricalcium phosphate composite orthopedic scaffold. *Tissue Eng.* 3 (1997) 207-215.
- [52]- A. K. Burkoth, K. S. Anseth, A review of photocrosslinked polyanhydrides: in-situ forming degradable networks. *Biomaterials* 21 (2000) 2395-2404.

- [53]- R. L. Dunn, J. P. English, D. R. Cowsar, D. D. Vanderbilt, Biodegradable in-situ forming implants and methods for producing the same. U.S. Patent 5,340,849, August 23, 1994.
- [54]- L. A. Moore, R. L. Norton, S. L. Whitman, R. L. Dunn, An injectable biodegradable drug delivery system based on acrylic terminated poly ϵ -caprolactone. The 21st Ann. Meeting Society Biomater., CA, USA, 1995.
- [55]- G. Sund , J. Rosequist, Morphological changes in bone following implantation of methyl methacrylate. *Acta Orthop. Scand.* 54 (1983) 148-156.
- [56]- J. S. Temenoff, A. G. Mikos, Injectable biodegradable materials for orthopedic tissue engineering. *Biomaterials* 21 (2000) 2405-2412.
- [57]- G. Biehl, U. Hanser, J. Harms, Experimental studies on heat development in bone during polymerization of bone cement. Intra-operative measurement of temperature in normal blood circulation and in bloodlessness. *Arch. Orthop. Unfallchir.* 78 (1974) 62-69.
- [58]- M. A. Saleem, S. I. Ahmed, Tephrosia purpurea ameliorates benzoyl peroxide-induced coetaneous toxicity in mice: Diminution of oxidative stress. *Pharm. Pharmacol. Commun.* 5 (7) (1999) 455-461.
- [59]- I. B. Gimenez-Conti, R. L. Binder, D. Johnston, T. J. Slaga, Comparison of the skin tumor-promoting potential of different organic peroxides in SENCAR mice. *Toxicol. Appl. Pharmacol.* 149(1) (1998) 73-79.
- [60]- J. L. Zhao, Y. Sharma, M. L. Chatterjee, R. Agarwal, Inhibitory effect of a flavonoid antioxidant silymarin on benzoyl peroxide-induced tumor promotion, oxidative stress and inflammatory response in SENCAR mouse skin. *Carcinogenesis* 21(4) (2000) 811-816.
- [61]- S. He, M. J. Yaszemski, A. W. Yasko, P. S. Engel, A. G. Mikos, Injectable biodegradable polymer composites based on poly(propylene fumarate) crosslinked with poly(ethylene glycol)-dimethacrylate *Biomaterials* 21 (2000) 2389-2394.
- [62]- L. J. Suggs, A. G. Mikos, Development of poly(propylene fumarate-co-ethylene

glycol) as an injectable carrier for endothelial cells. *Cell Transplant* 8 (1999) 345-350.

[63]- S. Lu, K. S. Anseth, Photopolymerization of multilaminated poly(HEMA) hydrogels for controlled release. *J. Controlled Release* 57 (1999) 291-300.

[64]- J. A. Hubbell, Hydrogel systems for barriers and local drug delivery in the control of wound healing. *J. Controlled Release* 39 (1996) 305-313.

[65]- K. S. Anseth, S. M. Newman, C. N. Bowman, Polymeric dental composites: properties and reaction behaviour of multimethacrylate dental restorations. *Biopolymers* 122 (1995) 177-217.

[66]- I. E. Ruyter, H. Oysaed, Composites for use in posterior teeth composition and conversation. *J. Biomed. Mater. Res.* 21 (1987) 11-23.

[67]- J. L. Hill-West, S. M. Chowdhury, M. J. Slepian, J. A. Hubbell, Inhibition of thrombosis and intimal thickening by in-situ photopolymerization of thin hydrogel barriers. *Proc. Natl. Acad. Sci.* 91 (1994) 5967-5971.

[68]- A. S. Sawhney, C. P. Pathak, J. J. van Rensburg, R. C. Dunn, J. A. Hubbell, Optimization of photopolymerized bioerodible hydrogel properties for adhesion prevention. *J. Biomed. Mater. Res.* 28 (1994) 831-838.

[69]- J. A. Hubbell, C. P. Pathak, A. S. Sawhney, N. P. Desai, J. L. Hill, Photopolymerizable biodegradable hydrogels as tissue contacting materials and controlled release carriers. U.S. Patent 5,410,016, April 25, 1995.

[70]- M. G. Fleming, W. A. Maillet, Photopolymerization of composite resin using the argon laser. *J. Can. Dent. Assoc.* 65(8) (1999) 447-450.

[71]- J. L. West, J. A. Hubbell, Localized intravascular protein delivery from photopolymerized hydrogels. *Proceed. Intern. Symp. Control. Rel. Bioact. Mater.* 22 (1995) 17-18.

[72]- T. X. Viegas, L. E. Reeve, R. L. Henry, Medical uses of in-situ formed gels. U.S. Patent 5,318,780, June 7, 1994.

[73]- H. Cui, P. B. Messerlith, Thermally triggered gelation of alginate for controlled release, in: I. McCulloch, S. W. Shalaby (eds.), Tailored polymeric materials for controlled delivery systems. American Chemical Society, Washington DC, 1998, pp. 203-211.

[74]- D. Papahadjopoulos, K. Jacobsen, S. Nir, T. Isac, Phase transitions in phospholipid vesicles. *Biochim. Biophys. Acta* 311 (1973) 330.

[75]- D. Marsh, A. Watts, P. F. Knowles, Cooperativity of phase transition in single bilayer and multi bilayer lipid vesicles. *Biochim Biophys Acta* 465(3) (1977) 500-514.

[76]- P. G. Kibat, Y. Igari, M. A. Wheatley, H. N. Eisen, R. Langer, Enzymatically activated microencapsulated liposomes can provide pulsatile drug release. *FASEB J.* 4, (1990) 2533-2539.

[77]- W. A. Soskolne, Subgingival delivery of therapeutic agents in the treatment of periodontal diseases. *Crit. Rev. Oral Biol. Med.* 8 (1997) 164-174.

[78]- E. Westhaus, P. B. Messerlith, Triggered release of calcium from lipid vesicles: a bioinspired strategy for rapid gelation of polysaccharide and protein hydrogels. *Biomaterials* 22 (2001) 453-462.

[79]- S. Cohen, E. Lobel, A. Trevigoda, Y. Peled, A novel in-situ forming drug delivery system from alginates undergoing gelation in the eye. *J. Controlled Release* 44 (1997) 201-208.

[80]- Y. Suzuki, Y. Nishimura, M. Tanihara, K. Suzuki, Y. Shimizu, Y. Yamawaki, Y. Kakimaru, Evaluation of a novel alginate gel dressing: cytotoxicity to fibroblasts *in vitro* and foreign-body reaction in pig's skin *in vivo*. *J. Biomed. Mater. Res.* 39 (1998) 317-322.

[81]- A. B. G. Lansdown, M. J. Payne, An evaluation of the local reaction and biodegradation of calcium sodium alginate (kaltostat) following subcutaneous implantation in the rat. *J. R. Coll. Surg. Edinb.* 39 (1994) 284-288.

[82]- N. H. Shah, A. S. Railkar, F. C. Chen, R. Tarantino, S. Kumar, M. Murjani, D. Palmer, M. H. Infeld, A. W. Malick, A biodegradable injectable implant for delivering

micro and macromolecules using poly(lactic-co-glycolic)acid copolymers. *J. Controlled Release* 27 (1993) 139-147.

[83]- R. E. Eliaz, J. Kost, Characterization of a polymeric PLGA-injectable implant delivery system for the controlled release of proteins. *J. Biomed. Mater. Res.* 50 (2000) 388-396.

[84]- B. Jeong, Y. H. Bae, S. W. Kim, In-situ gelation of PEG-PLGA-PEG triblock copolymer aqueous solutions and degradation thereof. *J. Biomed. Mater. Res.* 50 (2000) 171-177.

[85]- A. Paavola, J. Yliruusi, P. Rosenberg, Controlled release and dura mater permeability of lidocaine and ibuprofen from injectable poloxamer-based gels. *J. Controlled Release* 52(1-2) (1998) 169-178.

[86]- R. A. Siegel, B. A. Firestone, pH-dependent equilibrium swelling properties of hydrophobic poly-electrolyte copolymer gels. *Macromolecules* 21 (1988) 3254-3259.

[87]- T. Tanaka, Phase transitions in ionic gels. *Phys. Rev. Lett.* 45 (1980) 1636-1639.

[88]- R. L. Dunn, J. P. English, D. R. Cowsar, D. P. Vanderbelt, Biodegradable in-situ forming implants and methods of producing the same. U.S. Patent 4,938,763, July 3, 1990.

[89]- R. Dunn, G. Hardee, A. Polson, A. Bennett, S. Martin, R. Wardley, W. Moseley, N. Krinick, T. Foster, K. Frank, S. Cox, In-situ forming biodegradable implants for controlled release veterinary applications. *Controlled Release Society, Inc. Proc. Intern. Symp. Rel. Bioact. Mater.*, 1995, 22.

[90]- E. G. Duysen, S. L. Whitman, N. L. Krinick, S. M. Fujita, G. L. Yewey, An injectable, biodegradable delivery system for antineoplastic agents. *AAPS, Pharm. Res.*, American Association Of Pharmaceutical Scientists, Presentation #7575, 1994.

[91]- J. M. Sherman, S. M. Fujita, Localized delivery of bupivacaine from Atrigel formulations for the management of postoperative pain. *AAPS, Pharm. Res.*, American Association Of Pharmaceutical Scientists, Presentation # 7574, 1994.

[92]- R. L. Dunn, G. L. Yewey, E. G. Duysen, K. R. Frank, W. E. Huffer, R. Pieters, Bone regeneration with the Atrigel polymer system. Portland Bone Symp., Portland, Oregon, 1995.

[93]- K. R. Frank, E. G. Duysen, G. L. Yewey, W. E. Huffer, R. Pieters, Controlled release of bioactive growth factors from a biodegradable delivery system. Pharm. Res., American Association Of Pharmaceutical Scientists, Presentation # 2070, 1994.

[94]- B. K. Lowe, R. L. Norton, E. L. Keeler, K. R. Frank, A. J. Tipton, The effects of Gamma irradiation on poly D,L-lactide as a solid and in N-methyl 2-pyrrolidone solutions. The 19th Ann. Meeting Society Biomater., AL, USA, 1993.

[95]- R. L. Dunn, A. J. Tipton, G. L. Southard, J. A. Rogers, Biodegradable polymer composition. U.S. Patent 5,599,552, February 4, 1997.

[96]- M. L. Radomsky, G. Brouwer, B. J. Floy, D. J. Loury, F. Chu, A. J. Tipton, L. M. Sanders, The controlled release of Ganirelix from the Atrigel injectable implant system. Proc Intern. Symp. Control. Rel. Bioact. Mater. 20, (1993) 458-459.

[97]- M. L. Shively, A. T. Bennett, B. A. Coonts, W. D. Renner, J. L. Southard, Physico-chemical characterization of polymeric injectable implant delivery system. J. Controlled Release 33 (1995) 237-243.

[98]- B. L. Chandrashekar, M. Zhou, E. M. Jarr, R. L. Dunn, Controlled release liquid delivery compositions with low initial drug burst. U.S. Patent 6,143,314, 2000.

[99]- M. A. Royals, S. M. Fujuta, G. L. Yewey, J. Rodriguez, P. C. Schultheiss, R. L. Dunn, Biocompatibility of a biodegradable in-situ forming implant system in rhesus monkeys. J. Biomed. Mater. Res. 45 (1999) 231-239.

[100]- H. Kranz, G. A. Brazeau, J. Napaporn, R.L. Martin, W. Millard, R. Bodmeier, Myotoxicity studies of injectable biodegradable in-situ forming drug delivery systems. Int. J. Pharm. 212 (2001) 11-18.

[101]- G. Chandrashekar, N. Udupa, Biodegradable injectable implant systems for long term drug delivery using poly(lactic-co-glycolic) acid copolymers. J. Pharm. Pharmacol. 48 (1996) 669-674.

[102]- U. V. Singh, N. Udupa, R. Kamath, P. Umadevi, Enhanced antitumor efficacy of methotrexate poly(lactic-co-glycolic) acid injectable gel implants in mice bearing sarcoma-180. *Pharm. Sci.* 3 (1997) 133-136.

[103]- R. Cherng-Chyi Fu, D. M. Lidgate, J. L. Whatley, T. McCullough, The biocompatibility of parenteral vehicles *In vivo* // *In vitro* screening comparison and the effect of excipients on haemolysis. *J. Parent. Sci. Tech.* 41(5): (1987) 164-168.

[104]- N. J. Medlicott, K. A. Foster, K. L. Audus, S. Gupta, V. J. Stella, Comparison of the effects of potential parenteral vehicles for poorly water soluble anticancer drugs. *J. Pharm. Sci.* 87(9) (1998) 1138-1143.

[105]- R. E. Eliaz, D. Wallach, J. Kost, Delivery of soluble tumor necrosis factor receptor from in-situ forming PLGA implants: *in vivo*. *Pharm. Res.* 17(12) (2000) 1546-1550.

[106]- A. H. Kibbe, A. Wade, P. J. Weller, Hand book of pharmaceutical excipients. Washington, D.C.: American Pharmaceutical Association; London, England: Pharmaceutical Society of Great Britain, 1994, pp.127.

[107]- M. A. Crowther, A. Pilling, K. Owen, The evaluation of glycofurol as a vehicle for use in toxicity studies. *Hum. Exp. Toxicol.* 16 (1997) 406.

[108]- A. J. Spiegel, M. M. Noseworthy, Use of non-aqueous solvents in parenteral products. *J. Pharm. Sci.* 52 (1963) 917-926.

[109]- V. R. Budden, U. G. Kuhl, G. Buschmann, Studies on pharmacodynamic activity of several drug solvents. *Arzneimittel-forschung-Drug Res.* 28 (1978) 1571-1579.

[110]- B. O. Haglund, J. Rajashree, K. J. Himmelstein, An in-situ gelling system for parenteral delivery. *J. Controlled Release* 41 (1996) 229-235.

[111]- F. A. Ismail, J. Napaporn, J. A. Hughes, G. A. Brazeau, *In situ* gel formulations for gene delivery: Release and myotoxicity studies. *Pharm. Dev. Tech.* 5 (2000) 391-397.

[112]- T. O'Hara, A. Dunne, J. Butler, J. Devane, A review of methods used to compare dissolution profile data. *Pharm. Sci. Technol. To.* 1(5) (1998) 214-223.

[113]- R. A. Jain, C. T. Rhodes, A. M. Railkar, A. W. Malick, N. A. Shah, Controlled release of drugs from injectable *in situ* formed biodegradable PLGA microspheres: effect of various formulation variables. *Eur. J. Pharm. Biopharm.* 50 (2000) 257-262.

[114]- D. A. Smith, A. J. Tipton, A novel parenteral delivery system. *Pharm. Res.* 13(9) (1996) 300.

[115]- P. J. Burns, J. W. Gibson, A. J. Tipton, Compositions suitable for controlled release of the hormone GNRH and its analogs. U.S. Patent 6,051,558, April 18, 2000.

[116]- A. J. Tipton, High viscosity liquid controlled delivery system as a device. U.S. Patent 5,968,542, October 19, 1999.

[117]- R. A. Stile, W. R. Burghardt, K. E. Healy, Synthesis and characterization of injectable poly (N-isopropylacrylamide)-based hydrogels that support tissue formation *in vitro*. *Macromolecules* 32 (1999) 7370-7379.

[118]- A. S. Hoffman, Applications of thermally reversible polymers and hydrogels in therapeutics and diagnostics. *J. Controlled Release*, 6 (1987) 297-305.

[119]- Y. H. Bae, T. Okano, R. Hsu, S. W. Kim, Thermosensitive polymers as on-off switches for drug release. *Makromol. Chem. Rapid Commun.*, 8(10) (1987) 481-485.

[120]- H. G. Schild, Poly(N-isopropylacrylamide): experiment, theory and application. *Prog. Polym. Sci.* 17 (1992) 163-249.

[121]- S. Hirotsu, Coexistence of phases and the nature of first order phase transition in poly(N-isopropylacrylamide) gels. *Adv. Polym. Sci.* 110 (1993) 1-26.

[122]- M. Irie, Stimuli responsive poly(N-isopropylacrylamide). Photo and chemical induced phase transitions. *Adv. Polym. Sci.* 110 (1993) 49-65.

[123]- J. Eliassaf, Aqueous solutions of poly((N-isopropylacrylamide). *J. Appl. Polym. Sci.* 22 (1978) 873-874.

[124]- H. G. Schild, D. A. Tirrell, Microcalorimetric detection of lower critical solution temperatures in aqueous polymer solutions. *J. Phys. Chem.* 94 (1990) 4352-4356.

- [125]- L. D. Taylor, L. D. Cerankowski, Preparation of films exhibiting a balanced temperature dependence to permeation by aqueous solutions: A study of lower consolute behavior. *J Polym Sci, Part A: Polym. Chem.* 13 (1975) 2551-2570.
- [126]- I. Y. Galaev, B. Mattiasson, Thermoreactive water soluble polymers, non-ionic surfactants, and hydrogels as reagents in biotechnology. *Enzyme Microb. Technol.* 15 (1993) 345-366.
- [127]- S. Hirotsu, Y. Hirokawa, T. Tanaka, Volume-phase transitions of ionized N-isopropylacrylamide gels. *J. Chem. Phys.* 87 (1987) 1392-1395.
- [128]- F. Hoffman, J. Cinatl Jr., H. Kabickova, J. Cinatl, J. Kreuter, F. Stieneker, Preparation, characterization and cytotoxicity of methylmethacrylate copolymer nanoparticles with permanent positive surface charge. *Int. J. Pharm.* 157 (1997) 189-198.
- [129]- E. W. Merrill, R. W. Pekala, Hydrogel for blood contact, in: Peppas NA (ed.) *Hydrogels in medicine and pharmacy*. CRC Press Vol. III, 1987, pp. 9.
- [130]- B. Jeong, Y. H. Bae, D. S. Lee, S. W. Kim, Biodegradable block copolymers as injectable drug delivery systems. *Nature* 388 (1997) 860-862.
- [131]- BASF Performance Chemicals, FDA and EPA status, BASF Corporation, North Mount Olive, New Jersey, 1993.
- [132]- P. Alexandridis, T. A. Hatton, Poly(ethylene oxide)-poly(propylene oxide)-poly(ethylene oxide) block copolymer surfactants in aqueous solutions and at interfaces: Thermodynamics, structure, dynamics and modeling. *Colloid Surfaces A* 96 (1995) 1-46.
- [133]- P. Wang, T. P. Johnston, Kinetics of sol-to-gel transition for Pluronic polyols. *J Appl. Polym. Sci.* 43 (1991) 283-292.
- [134]- P. Alexandridis, Amphiphilic copolymers and their applications. *Curr Opin Colloid Interface Sci.* 1 (1996) 490-501.
- [135]- L. E. Bromberg, E. S. Ron, Temperature-responsive gels and thermogelling polymer matrices for protein and peptide delivery. *Adv. Drug Deliv. Rev.* 31 (1998) 197-221.

[136]- K. Zhang, A. Khan, Phase behavior of poly(ethylene oxide)-poly(propylene oxide)-poly(ethylene oxide) triblock copolymers in water. *Macromolecules* 28 (1995) 3807-3812.

[137]- A. Joshi, S. Ding, K. J. Himmelstrin, Reversible gelation compositions and methods of use. U.S. Patent 5,252,318, October 12, 1993.

[138]- R. G. Laughlin (ed.), *The aqueous phase behavior of surfactants*. Academic Press, London, 1994.

[139]- D. W. Miller, E. V. Batrakova, T. O. Waltner, V. Y. Alakhov, A. V. Kabanov, Interactions of Pluronic block copolymers with brain microvessel endothelial cells: evidence of two potential pathways for drug absorption. *Bioconj. Chem.* 8 (1997) 649-657.

[140]- E. V. Batrakova, V. Y. Han, V. Y. Alakhov, D. W. Miller, A. V. Kabanov, Effects of Pluronic block copolymers on drug absorption Caco-2 cell monolayers. *Pharm. Res.* 15 (1998) 850-855.

[141]- V. Yu. Aladhov, E. Yu. Moskaleva, E. V. Batrakova, A. V. Kabanov, Hypersensitization of multidrug resistant human ovarian carcinoma cells by Pluronic P85 block copolymer. *Bioconj. Chem.* 7 (1996) 209-216.

[142]- G. S. Kwon, T. Okano, Soluble self-assembled block copolymers for drug delivery. *Pharm Res* 16(5) (1999) 597-600.

[143]- M. L. Veyries, G. Couarraze, S. Geiger, F. Agnely, L. Massias, B. Kunzli, F. Faurisson, B. Rouveix, Controlled release of vancomycin from Poloxamer 407 gels. *Int. J. Pharm.* 192 (1999) 183-193.

[144]- S. Miyazaki, Y. Ohkawa, M. Takada, D. Attwood, Antitumor effect of Pluronic F-127 gel containing Mitomycin C on Sarcoma-180 ascites tumor. *Chem. Pharm. Bull.* 40 (1992) 2224-2226.

[145]- F. Suisha, N. Kawasaki, S. Miyazaki, M. Shirakawa, K. Yamatoya, M. Sasaki, D. Attwood, Xyloglucan gels as sustained release vehicles for the intraperitoneal administration of mitomycin C. *Int. J. Pharm.* 172 (1998) 27-32.

[146]- R. Bhardwaj, J. Blanchard, Controlled release delivery system for the α -MSH analog Melanotan-I using Poloxamer 407. *J. Pharm. Sci.* 85(9) (1996) 915-919.

[147]- A. Paavola, J. Yliruusi, Y. Kajimoto, E. Kalso, T. Wahlstrom, P. Rosenberg, Controlled release of lidocaine from injectable gels and efficacy in rat sciatic nerve block. *Pharm. Res.* 12(12) (1995) 1997-2002.

[148]- A. Paavola, P. Tarkkila, M. Xu, T. Wahlstrom, J. Yliruusi, P. Rosenberg, Controlled release gel of Ibuprofen and Lidocaine in epidural use-Analgesia and systemic absorption in pigs. *Pharm. Res.* 15(3) (1998) 482-487.

[149]- S. D. Desai, J. Blanchard, Evaluation of Pluronic F-127-based sustained release ocular delivery systems for pilocarpine using the albino rabbit eye model. *J. Pharm. Sci.* 87(10) (1998) 1190-1195.

[150]- T. P. Johnston, M. Punjabi, C. J. Froelich, Sustained delivery of interleukin-2 from Poloxamer 407 gel matrix following intraperitoneal injection in mice. *Pharm. Res.* 9(3) (1992) 425-434.

[151]- Z. G. M. Wout, T. P. Johnston, E. A. Pec, J. A. Maggiore, R. H. Williams, P. Palicharla, Poloxamer 407 mediated changes in plasma cholesterol and triglycerides following intraperitoneal injection to rats. *J. Parenteral Sci. Tech.* 46(6) (1992) 192-200.

[152]- T. P. Johnston, W. K. Palmer, Mechanism of poloxamer 407 induced hypertriglyceridemia in the rat. *Biochem. Pharmacol.* 46(6) (1993) 1037-1042.

[153]- B. Jeong, Y. K. Choi, Y. H. Bae, G. Zentner, S. W. Kim, New biodegradable polymers for injectable drug delivery systems. *J. Controlled Release* 62 (1999) 109-114.

[154]- B. Jeong, Y. H. Bae, S. W. Kim, Drug release from biodegradable injectable thermosensitive hydrogel of PEG-PLGA-PEG triblock copolymers. *J. Controlled Release* 63 (2000) 155-163.

[155]- A. Chenite, C. Chaput, D. Wang, C. Combes, M. D. Buschmann, C. D. Hoemann, J. C. Leroux, B. L. Atkinson, F. Binette, A. Selmani, Novel injectable neutral solutions of chitosan form biodegradable gels in-situ. *Biomaterials* 21 (2000) 2155-2161.

[156]- S. J. De Jong, S. C. De Smedt, M. W. C. Wahls, J. Demeester, J. J. Kettenes, W. E. Hennink, Novel self-assembled hydrogels by stereocomplex formation in aqueous solution of enantiomeric lactic acid oligomers grafted to dextran. *Macromolecules* 33 (2000) 3680-3686.

[157]- W. A. Petka, J. L. Harden, K. P. McGrath, D. Wirtz, D. A. Tirrell, Reversible hydrogels from self-assembling artificial proteins. *Science* 281 (1998) 389-392.

[158]- C. Wang, R. J. Stewart, J. Kopecek, Hybrid hydrogels assembled from synthetic polymers and coiled-coil protein domains. *Nature* 397 (1999) 417-420.

[159]- S. Engstrom, L. Engstrom, "Phase behavior of the lidocaine-monoolein-water system," *Int. J. Pharm.* 79 (1992) 113-122.

[160]- B. Ericsson, P. O. Ericsson, J. E. Lofroth, S. Engstrom, Cubic phases as drug delivery systems for peptide drugs. *ACS Symposium Series*, 469 (1991) 251-265.

[161]- Z. Gao, W. R. Crowley, A. J. Shukla, J. R. Johnson, J. F. Reger, Controlled release of contraceptive steroids from biodegradable and injectable gel formulations: *In vivo* evaluation. *Pharm. Res.* 12(6) (1998) 864-868.

[162]- Z. Gao, A. J. Shukla, J. R. Johnson, W. R. Crowley, Controlled release of contraceptive steroid from biodegradable and injectable gel formulations: *In vitro* evaluation. *Pharm. Res.* 12(6) (1995) 857-864.

[163]- L. Appel, K. Engle, J. Jensen, L. Rajewski, G. Zentner, An *in vitro* model to mimic *in vivo* subcutaneous monoolein degradation. *Pharm. Res.* 11(10) (1994) S-217.

[164]- C. M. Chang, R. Bodmeier, Effect of dissolution media and additives on the drug release from cubic phase delivery systems. *J. Controlled Release* 46(1997) 215-222.

Chapter 3

Development and Characterization of an Injectable Implant System

A version of this chapter and the next chapter are ready for submission to Pharmaceutical Research for publication. It will be submitted after a patent is filed.

3.1. Introduction

Based on the discussion of the preceding chapter, a means of delivering camptothecin, and other drugs with similar properties, for a prolonged period of time in a localized fashion is required. Of the methods currently investigated to achieve this type of delivery, thermoplastic polymer depots possess a number of advantages over the other strategies. These advantages include the lack of a potentially toxic solvent, no heat of reaction upon setting, facile syringeability, and degradability. The materials which have been developed for this purpose to date however, possess a number of disadvantages, particularly when considering a hydrophobic drug prone to hydrolysis. They contain hydrophilic polymers (1-3), such as poly(ethylene glycol), which promote water absorption into the drug depot and which increase the viscosity of the melt, making them difficult to inject through a needle, or they possess melt temperatures which are too high for tissue compatibility. For the purpose of this project, we are looking for a delivery vehicle with a low melting point, preferably slightly above body temperature (i.e., 38-41 °C), one which has a low viscosity when heated above its melting point, one which is hydrophobic, biodegradable and possesses a short degradation time (e.g., a few months) one which is capable of releasing CPT in a sustained fashion.

Polymers that degrade through hydrolysis are an important group of materials with an increasing number of applications. Currently, new applications for degradable polymers are actively being sought in biomaterials research (4,5). Biodegradable polymers such as poly(glycolide) (PGA), poly(L-lactide) (PLLA), poly(D,L-lactide) (PDLLA), poly(ϵ -caprolactone) (PCL) (Figure 3.1) and their copolymers find wide use in surgery and controlled drug delivery primarily due to their hydrolyzability and biocompatibility. PGA and PLLA have found applications mainly in temporary tissue and bone fixation where good mechanical strength is required. In contrast to PGA and PLLA, PDLLA is an amorphous polymer and is used mainly for controlled drug release applications rather than tissue fixation (6). ϵ -caprolactone (ϵ -CL) has proven to be a suitable monomer or comonomer for the preparation of a diversified family of homo- or copolymers with mechanical properties ranging from elastomeric to rigid (7). These elastomeric copolymers have good elongation characteristics, which make them

interesting for applications where both elasticity and degradability are required. Since one of the aspects of this project is the syringeability of the polymer through a 22-gauge needle, viscosity of the polymer at the time of injection is a crucial factor.

3.1.1. Viscosity

Viscosity is an expression of the resistance of fluid to flow; the higher the viscosity the greater the resistance. In Newtonian fluids, the shear stress is proportional to the shear rate:

$$\tau = \eta \cdot \dot{\gamma} \quad \text{(equation 3.1)}$$

where, τ is shear stress (the force per unit area required to bring about flow to a liquid), $\dot{\gamma}$ is shear rate (the difference of velocity between two planes of liquid separated by an infinitesimal distance) and η is viscosity (8). This formula suggests that the higher the viscosity of a liquid, the greater the force per unit area (shear stress) required to produce a certain rate of shear. Polymers usually do not behave like Newtonian fluids, however, a linear relationship between shear stress and shear rate has been observed in low molecular weight polymers (9). Accordingly, an objective of this work is to prepare a polymer with low viscosity, which can easily be pushed (low shear stress) through a needle.

The viscosity of a polymer is dependent on three factors: a) chemical structure of the polymer, b) molecular weight of the polymer, and c) temperature as it affects molecular motion (9). The chemical structure of a polymer and intermolecular interactions between polymer chains have a significant impact on polymer glass transition temperature (T_g). T_g marks a transition in polymer material characteristics. Below T_g the polymer behaves as a glass, and above T_g it behaves as a leathery material.

It is already established that the lower the glass transition temperature of the polymer the lower its viscosity at its melt state (9,10). T_g indicates an increase in polymer chain mobility in the solid state. Chain stiffness or flexibility determines chain mobility, which is characterized by the ease of rotation of constituents around the bonds

of the polymer backbone (9). Stiffer polymer chains and those with stronger intermolecular interactions would have a higher T_g (9). Bulky groups, such as benzene rings, in the backbone of the polymer chain, introduce a high energy barrier to bond rotation which can be overcome only at higher temperatures. Also, bulky pendent groups attached to the polymer backbone can increase the T_g through steric hinderance to bond rotations. Consequently, a flexible polymer chain which easily bends or slides over other polymer chains needs lower shear stress to flow resulting a low viscosity polymer bulk.

Molecular weight also is an important factor which affects the polymer T_g . Fox and Flory used a simple formula to demonstrate this idea:

$$T_g = T_g^\infty - \frac{K}{M_n} \quad \text{(equation 3.2)}$$

where, T_g^∞ is the glass transition temperature that would be obtained from a polymer of infinite molecular weight, $\overline{M_n}$ is the number average molecular weight of the polymer and K is a constant related to parameters describing the free volume. This formula clearly shows that by increasing the molecular weight of a polymer the T_g of the polymer increases and hence, the viscosity (9).

The relationship between viscosity and temperature is described clearly by Williams, Landel and Ferry (WLF) theory (9):

$$\log \frac{\eta}{\eta_g} = \frac{-C_1(T - T_g)}{C_2(T - T_g)} \quad \text{(equation 3.3)}$$

where η is viscosity, η_g is viscosity at glass transition temperature, C_1 and C_2 are constants and T is temperature in °K. Based on this theory, as the temperature increases the viscosity of the polymer melt decreases logarithmically.

3.1.2. Degree of Polymerization

To produce a low molecular weight polymer (oligomer) with a low melting point and hence low viscosity, close to body temperature the degree of polymerization (DP) needs to be controlled. Degree of polymerization is another way of describing chain length and equals to the number of structural units (monomers) in the chain. The relationship between T_m and DP has been given by Flory as (11):

$$\frac{1}{T_m} - \frac{1}{T_{m_0}} = \frac{2R}{\Delta H_f (DP)} \quad \text{(equation 3.4)}$$

in which T_m is the equilibrium melting point, T_{m_0} is the equilibrium melting point of a polymer of infinite molecular weight, ΔH_f is the enthalpy of fusion per monomer and DP is the degree of polymerization. This equation demonstrates that T_m is expected to decrease as the molecular weight of the polymer decreases. Therefore, it is desirable to have a low molecular weight polymer to reduce the melting point to the desired level of close to 37 °C.

3.1.3. Polymerization of ϵ -caprolactone

From this discussion, in order to achieve the desired goal of an easily syringeable polymeric delivery system, a low molecular weight polymer (oligomer) with a low T_g , which bears low viscosity when heated slightly above its desired melting point of 38-41 °C is required. Among all the degradable polyesters discussed above, poly(ϵ -caprolactone) has the lowest glass transition temperature. For comparison, the T_g of poly(caprolactone) is -65 °C while the T_g for PDLLA and PLLA is 58 and 65 °C respectively (12). Due to the linear and mostly hydrocarbon chemical structure of the polymer, one can expect to observe flexible polymer chains sliding over each other with low entanglement when melted. Poly(ϵ -caprolactone) is a semi-crystalline, highly hydrophobic and flexible polymer (13,14) (Figure 3.1). As it possesses many of the desired properties of an injectable polymer, ϵ -caprolactone was chosen as the starting point for our low molecular weight polymer.

ϵ -caprolactone is a lactone ring manufactured by oxidation of cyclohexanone with peracetic acid (15) (Figure 3.2a). There are at least four mechanisms that can be utilized to polymerize ϵ -caprolactone, categorized as anionic, cationic, coordination and radical (14-16). These methods can provide different degrees of control of molecular weight and molecular weight distribution, end group composition, and the chemical structure and sequence (block versus random) distribution of copolymers (14).

Among all the methods mentioned above, coordination polymerization is the most versatile method of preparing PCL (Figure 3.2b). Di-n-butyl zinc, stannous chloride and octoate, and alkoxides and halides are among the more frequently used catalysts for the polymerization process. Stannous octoate is the only catalyst approved by the FDA for use in the human body and substantial toxicological data are now available (17). With stannous octoate ($\text{Sn}(\text{Oct})_2$) promoted polymerization, the metal species is believed to function as the catalyst and water or an alcohol serves as the initiator (18) (Figure 3.2b). Although the major features of the mechanism of polymerization of cyclic esters (e.g., ϵ -caprolactone) with other initiators, have been established (19-21), the mechanism of $\text{Sn}(\text{Oct})_2$ induced polymerization is still under debate (22-24). Most investigators believe that stannous octoate merely complexes with the monomer, activating it in this way (18,25). Chain growth, according to this mechanism, which can be called "activated monomer mechanism", requires the nucleophilic attack of the -OH ended macromolecule on the carbonyl carbon atom of the cyclic ester complexed with stannous octoate (26).

Many different temperatures have been reported in the literature for the coordination polymerization of cyclic esters, ranging from 80-180 °C, but the most commonly used temperature range is 110-140 °C (27-29). It is well known from the anionic and cationic polymerization of ϵ -caprolactone that the ionic chain ends cause transesterification (Figure 3.3) even at moderate temperatures (e.g., 50 °C) (30,31). Intramolecular transesterification, i.e. "back-biting", causes degradation and formation of cyclic oligomers. Intermolecular transesterification modifies the sequence of copolymers, and both intra- and intermolecular transesterification broaden the molecular weight distribution. Transesterification has also been observed in ring-opening

polymerizations of lactones using stannous octoate as a catalyst (32). Therefore, conditions under which transesterification occurs need to be avoided. Kricheldorf et al. (32), reported that in the stannous octoate catalyzed ring opening polymerization of cyclic esters, no transesterification reactions occurred at reaction temperatures below 120 °C.

3.1.4. Hypothesis

One hypothesis of this work was that the chemical structure of the initiator would be another major factor defining the physicochemical properties of the low molecular weight (oligomer) CL. The initiator can be a small hydrophilic molecule like water or a large hydrophobic molecule such as stearyl alcohol or oleyl alcohol. The functional moiety necessary for the polymerization process of ϵ -caprolactone (CL) is an OH group which is present in water or alcohols. Since the initiator is part of the polymer chain it will participate in defining the final physicochemical properties of the synthesized oligomer. We believe that by addition of a small alcohol such as ethanol to the CL oligomer we do not expect to introduce any significant hydrophobicity to the oligomer chain while by adding oleyl alcohol to the CL oligomer we expect to change the hydrophobicity of the oligomer dramatically. Moreover, by introducing a big block of initiator to the CL oligomer it is probably more suitable to consider the CL oligomer as a diblock oligomer. To test this hypothesis, different initiators were used and their effects on enhancing the capability of the CL oligomer in dissolving CPT which has a hydrophobic polar nature, and stabilizing the active lactone ring by keeping the water out of the polymeric system was examined.

3.1.5. Objectives

The objectives in this portion of the study were as follows. First, the necessary temperature and time for polymerization of CL were determined. Second, the effect of the initiator's chemical structure on the degree of crystallinity, melting point and rheologic behaviour of the synthesized caprolactone oligomers was investigated. Finally, oligomers were synthesized using various initiators, their melting points adjusted to 39-42 °C and then characterized to determine their physicochemical properties.

To meet the first objective a sufficient time for polymerization was determined by keeping the M/I (Monomer/Initiator) ratio, the M/C (Monomer/Catalyst) ratio and the temperature of polymerization constant while varying the time of polymerization, and a sufficient temperature for polymerization reaction was found by keeping the M/I ratio, M/C ratio and time of polymerization constant and varying the temperature. To meet the second objective, by keeping the number of CL monomers in oligomer constant the effects of initiator's chemical structure on T_m , degree of crystallinity and rheologic behaviour were examined. Finally, based on the results from preliminary experiments, the M_w was manipulated to achieve the desired T_m and the oligomer properties were examined.

3.2. Materials

ϵ -caprolactone with 99% purity (Lancaster Inc.) was distilled over CaH_2 under reduced pressure. 20 mL glass ampoules (Kimble) were silanized with dichlorodimethylsilane (99%, Sigma, USA) and washed with methanol (99.9%, Fisher Scientific) and dried in an oven heated to 50 °C. Stannous octoate with 96% purity (ICN Laboratories Inc., Canada) was used as received and stored in a dry nitrogen atmosphere. Glyceryl monooleate (GMO 85%, Eastman Kodak, USA), Vitamin D (99%, Sigma, USA), dichloromethane (99.9%, Fisher Scientific), ethanol (99.9%, Fisher Scientific), 1-butanol (99.8%, Fisher Scientific), 2-butanol (99.5%, Sigma, USA), 1-octanol (99%, Sigma, USA), 2-octanol (97.8%, Sigma, USA), 1-dodecanol (99%, TCI, America), 2-dodecanol (99%, Aldrich, USA), stearyl alcohol (99%, Sigma, USA), and oleyl alcohol (99%, Sigma, USA) were used as received.

3.3. Methods

3.3.1. Polymer Synthesis

The synthesis of oligo(ϵ -caprolactone) was carried out by ring opening polymerization in the bulk (Figure 3.2b). Stannous octoate was used as a catalyst and various alcohols as the initiator. Thus a mixture of ϵ -caprolactone, catalyst and initiator

was charged into a 20 mL glass ampoule and vortex mixed. The sample size was adjusted around 18 mL to reduce the volume of void space remained at top of the ampoules. Nitrogen gas was bubbled into the mixture for 3-5 minutes and the ampoule was heat sealed under vacuum. The ampoule was transferred into a preheated oven (ranging from 80-140 °C) and the polymerization was carried out for several hours (ranging from 12-24 hrs).

3.3.2. Polymer Purification

A method was developed to purify and rid polymerized CL from unreacted monomers (if any), unreacted initiator and catalyst and yet result in an acceptable yield. 15g of as-reacted PCL was first dissolved in 3 mL dichloromethane or chloroform to form a clear solution. Then it was precipitated in 500 mL cold ethanol (4 °C), and left undisturbed at this temperature for 12 hours. Oligomers precipitated only in cold ethanol (4 °C) due to their low solubility at this temperature. The precipitate was collected by filtration and transferred into a vacuum oven which was filled with nitrogen to reduce the possibility of oxidation of the oligomer by atmospheric oxygen. Then it was dried at room temperature and under reduced pressure for 48 hrs.

3.3.3. Instrumental Analysis

The purity and molar composition of the synthesized polymers were determined from ¹H-NMR spectra using a Bruker AM 300 MHz spectrometer. For this purpose, the polymer was dissolved in CDCl₃ at a 5 mg/mL concentration and transferred into 5mm NMR tubes.

Fourier transform infrared (FTIR) spectroscopy is best for analysis of films and liquids, where the sample is maintained in intimate contact with the crystal. The oligomers were dissolved in chloroform (10-15 mg/mL) and placed on the crystal and the IR spectrum was obtained using an FTIR spectrometer (model 550, Nicolet).

The thermal transitions and heat of fusion were measured by using a differential scanning calorimeter (DSC) (Seiko-120). Samples (3-5 mg) were heated twice at a rate of 10 °C/min and cooled at a rate of 20 °C/min to ensure that the thermal history of the samples was similar. The degree of crystallinity of the different oligomers was evaluated

from the heat of fusion. By integrating the normalized area of the melting endotherm, determining the heat involved, and relating it to the reference 100% crystalline polymer (ϵ -caprolactone heat of fusion of 139.5 mJ/mg (33)), the relative crystallinity of the oligomer product was assessed. The melting point of the material was taken to be the onset of melting as illustrated by P. Gallagher (11). As this point also corresponds to the onset of crystallization, it is of more interest than the peak melting temperature which is often used to describe the melting point of polymers.

Rheologic properties were measured using a Haake Viscotester (VT550) at 45, 50 and 55 °C with cup and bob at the University of Alberta, Department of Chemical Engineering. Other viscosity measurements were done using a TA Rheometrics 500 at Queen's University, Department of Chemical Engineering by Darryl Night.

The weight average molecular weight (M_w), number average molecular weight (M_n), and molecular weight distribution of the polymers were identified by using gel permeation chromatography (GPC) (Pump: HP 1100 series; Differential refractometer: Waters 410; Dynamic Light Scattering Detector: Precision Detectors PD-2000 DLS) and Precision Detectors software. The column was an SEC Phenogel 5 μ 300x7.8mm purchased from Phenomenex, USA. The mobile phase was tetrahydrofuran (THF) with a flow rate of 1 mL/min. The injection volume was 20 μ l from a stock solution of polymer dissolved in THF (2 mg/mL). The temperature of system at the time of measurement was 35 °C and monodisperse polystyrene standard was used for initial system calibration.

The syringeability of the copolymers was confirmed by loading them into a 1 mL syringe and heating them to 55 °C to melt all the crystals in the polymer. Then, the loaded syringe was transferred into a preheated 46 °C oven and after 30 minutes incubation at this temperature they were manually pushed through a 22-gauge needle.

3.4. Results and Discussion

Glyceryl monooleate (GMO) is a glycerinated fatty acid and due to the presence of OH moiety in its chemical structure can be used as an initiator for the polymerization of ϵ -caprolactone (Figure 3.4a). Once polymerized with ϵ -caprolactone it provides lipophilic properties to the diblock oligomer, so the oligomer can more easily

incorporate lipophilic drugs. This material has a low melting point of 34 °C and once polymerized with ϵ -caprolactone can possibly produce a low viscosity material, due to its linear hydrocarbon structure. Inside the body it is expected that enzymes such as esterase catalyze the esteric bond between glycerin and oleate and produce glycerine and oleic acid, both of which are biocompatible. These characteristics made this material a good candidate to start with, for the purpose of this project. ϵ -caprolactone was polymerized in the presence of stannous octoate (catalyst) and GMO (initiator) at 140 °C for 24 hrs. Table 3.1 presents the thermal behaviour of the diblock oligomer versus the mass ratios.

Unfortunately, after polymerizing ϵ -caprolactone with GMO the resulting oligomer was a heterogenous (two phase) mixture with a clear phase on top and a white opaque precipitate on bottom of the polymerization vessel. This non-uniform mixture proved to compromise the reproducibility of the experiments. Commercially available GMO is a mixture of at least 5 different fatty acids (85% glyceryl monooleate) and the presence of 15% unknown impurities made this material unsuitable.

Vitamin D was the second initiator tried for polymerizing ϵ -caprolactone. Vitamin D is a molecule with an available hydroxyl group; it is a liquid at room temperature (low T_m) and lipophilic due to the presence of the cyclic rings in its chemical structure (Figure 3.4b). When polymerized with ϵ -caprolactone, it produced an orange colored oligomer with high viscosity at its melt state. This problem was attributed to the presence of the cyclic rings in the chemical structure of vitamin D. Since viscosity of the polymer at its melt state plays a significant role in this project, application of vitamin D as an initiator was abandoned. Due to these problems it was decided to start with simple initiators (e.g., 1-butanol) in a methodical approach.

As discussed previously, coordination polymerization is the most widely studied and simplest method of polymerization for ϵ -caprolactone. Veld et al. (34), investigated the polymerization of ϵ -caprolactone under various reaction times and temperatures. To determine the most suitable temperature and time in the polymerization process and confirm their results, the following experiments were conducted.

3.4.1. Determination of Sufficient Polymerization Time

To determine the sufficient time for the polymerization process, the monomer/initiator (M/I) ratio was kept constant at 8 mole/mole, because preliminary experiments indicated that this ratio produces CL oligomers with a melting point close to the desired melting point range for this project (38-41 °C). The monomer/catalyst (M/C) ratio was kept constant at 1000 mole/mole which is close to the M/C concentrations reported in the literature (34,35). 1-Butanol was used as an initiator and the polymerization temperature was 120 °C. Four samples were prepared in the manner described above with the time regimens for the polymerization process of 8, 12, 24, and 48 hrs. These samples were analyzed by DSC to identify the presence of detectable unreacted monomers. Figure 3.5A is a DSC analysis of pure ϵ -caprolactone which indicates that the monomer has a melting point of -1 °C. Once the monomer is completely polymerized, no endotherm corresponding to the melting point of the monomer should be observed. As can be seen in Figure 3.5B, which corresponds to the ϵ -caprolactone polymerized for 8 hrs, there are two distinct endotherms. One is related to the melting point of ϵ -caprolactone (around -5 °C) and the second is related to the PCL (around 30 °C). By increasing the time of the polymerization reaction it can clearly be seen that the endotherm related to monomer dwindles and gives rise to the endotherm related to the PCL (Figures 3.5C & 3.6). Based on the observed data it was concluded that the sufficient time of polymerization is 24 hrs and all the monomers are polymerized to PCL at this time point.

3.4.2. Determination of Optimal Polymerization Temperature

Various temperatures have been reported for the polymerization of ϵ -caprolactone ranging from 80-180 °C. To identify the sufficient temperature for the polymerization process the M/I ratio was again kept constant at 8 and M/C ratio at 1000. The time of polymerization was 24 hrs and temperatures of 80, 110, 120 and 140 °C were used. DSC analysis of data for polymerized ϵ -caprolactone at 110, 120 and 140 °C

showed no endotherm related to unreacted monomers. By comparing the DSC data obtained from the samples polymerized at 110 °C (Figure 3.7), 120 °C (Figure 3.6) and 140 °C (Figure 3.8) it can be observed that at 120 and 140 °C there is a broad peak (broad molecular weight distribution) which may be due to transesterification (36). Therefore, it was concluded that the sufficient temperature for the polymerization process is 110 °C. The peak broadening observed in Figures 3.6 and 3.8 can be attributed to the transesterification by-products produced at 120 and 140 °C. This finding confirms the result of the Kricheldorf et al.'s investigations discussed previously (31). The DSC analysis of polymerized ϵ -caprolactone at 80 °C for 24 hours showed no endotherm related to unreacted monomers (Figure 3.9) but when a sample was analyzed by ^1H NMR it was proved that still some unreacted monomers exist (Figures 1-3, Appendix C). Therefore, the most suitable temperature for the polymerization of ϵ -caprolactone was concluded to be 110 °C. The chemical structures of all the samples were also analyzed by IR spectroscopy (Figure 3.10). The C=O band at 1719 cm^{-1} and C-O band at 1162 cm^{-1} imply the presence of ester bonds in the chemical structure of CL-oligomers. Also the band at 3539 cm^{-1} shows the presence of the terminal O-H group in small molar ratio in comparison to the rest of the oligomer structure.

3.4.3. Effects of initiator's chemical structure on the polymer properties

In the preceding discussion, the sufficient conditions for the polymerization process by using 1-butanol as an initiator were determined. 1-butanol is a short chain alcohol with an OH group positioned on C₁, which is capable of opening the ϵ -caprolactone ring and producing a linear PCL chain. By using long chain primary alcohols (i.e., 1-octanol, 1-dodecanol and stearyl alcohol) and secondary alcohols (i.e., 2-butanol, 2-octanol and 2-dodecanol) as initiators in the polymerization process of ϵ -caprolactone, it was investigated whether the characteristics of the synthesized oligomers, such as degree of crystallinity, melting point and rheologic behaviour, were dependent on the nature of the initiator used. The M/C ratio of 1000 and M/I ratio of 8 were kept constant for all the synthesized polymers and the polymers were examined as synthesized without any purification.

It has already been shown that in Sn(Oct)₂ catalyzed polymerization of ε-caprolactone in the presence of an alcohol, the rate of conversion is 100% under certain conditions (heat of polymerization= 110 °C, M/C ratio= 1000, reaction time=24h, M/I ratio of 10), (34) which is in agreement with our results. Based on this fact, in the absence of back-biting reactions, the degree of polymerization (\overline{DP} , number of monomer units per chain of polymer) can be calculated from the following formula (37):

$$\overline{DP} = \frac{M}{I} \times \frac{\%Conversion}{100} \quad (\text{equation 3.5})$$

where, M is the number of moles of monomer and I is the number of moles of initiator.

Therefore, the \overline{Mn} of the polymer is:

$$\overline{M}_n = 114.14 \times \frac{M}{I} + M_{wi} \quad (\text{equation 3.6})$$

Where, \overline{Mn} is the number average molecular weight of polymer, M_{wi} is the molecular weight of initiator and 114.14 is the molecular weight of ε-caprolactone.

The theoretical molecular weights of the oligomers are shown in Table 3.2. Practically, the number average molecular weight (\overline{Mn}) of the oligomers can be calculated from the ¹H-NMR spectrum (34). The number average molecular weight can be calculated from the intensity ratios of the OCH₂ methylene proton signal (δ=4.05) and the HOCH₂ methylene proton signals (δ=3.65) in the ¹H-NMR spectra by using the following formula (34):

$$\left(\frac{\delta = 4.05}{\delta = 3.65} + 1 \right) \times 114.14 + M_{wi} = \overline{Mn} \quad (\text{equation 3.7})$$

where M_{wi} is the molecular weight of the initiator and 114.14 is the molecular weight of ϵ -caprolactone.

The results of theoretical \overline{Mn} were compared with \overline{Mn} of the oligomers obtained from NMR spectra and GPC (Appendix D, Figures 4-10 & Table 3.2). In synthetic polymerization reactions, the resultant macromolecules are heterodisperse. This means that they have different chain lengths and a range of molecular weights which can be described by average molecular weights (i.e., weight average and number average molecular weight) and weight distribution (8). Therefore, GPC provides more meaningful and realistic value for average molecular weight (Table 3.2). However, in light-scattering detection, the differential increment of refractive index (dn/dc) is used in calculating M_w and M_n while MWD is not affected by this constant. dn/dc changes with polymer composition as well as molecular weight. Since this value is unknown for oligo (ϵ -caprolactone), we used the same dn/dc value as determined for polystyrene (i.e., 0.184) which makes the accuracy of GPC results questionable. It can be used to calculate polydispersity, because this number is not affected by the dn/dc value. As determined and demonstrated in Table 3.2, all the MWD values are very close to each other. Therefore, the influence of low molecular weight fractions produced during the synthesizing process is not significant when comparing oligomers. In this case, by keeping the M/I ratio constant at 8, any changes observed in terms of melting point and degree of crystallinity, can be attributed to the differences between the chemical structures of the initiators.

3.4.3.1. Effects on T_m and Crystallinity

As mentioned earlier, Crescenzi et al. (33), determined the heat of fusion (ΔH_f) of 100% crystalline homopoly (CL) by means of DSC to be 139.5 mJ/mg. Using this value, the crystallinity of different CL oligomers was calculated. In this part of the study in order to compare the T_m of the oligomers, the midpoint of the DSC endotherms were considered as opposed to onset of melting. This is due to the fact that onset of melting is usually a range and hard to determine; and thereby subject to error, while DSC endotherm midpoint is usually a well defined point and can be determined with much

more accuracy. DSC analysis (Appendix A, Figures 1-7) revealed that, by increasing the number of carbons in the structure of the primary alcohol initiators, heat of fusion and degree of crystallinity of the synthesized oligomers increased. Also by increasing the number of carbons in the initiators chain from 4 (i.e., 1-butanol) to 12 (i.e., 1-dodecanol) the average melting point increased but statistical analysis of data showed no significant increase in melting point. However, when stearyl alcohol was used as an initiator, melting point increased significantly (Table 3.3, Figures 3.11 & 3.12). For example, using a 12-carbon initiator yielded a heat of fusion of 80.5 mJ/mg and a crystallinity of 57.7% while an 18-carbon initiator produced a heat of fusion of 86 mJ/mg and a crystallinity of 61.6%. Moreover, the structure of the initiator, whether linear (primary alcohol) or branched (secondary alcohol), influenced the polymer melting point, heat of fusion and crystallinity (Table 3.3, Figures 3.11 & 3.12). However, a statistical analysis of the data (two-tailed student t-test, $p < 0.05$) revealed that in secondary alcohols the degree of crystallinity and melting point didn't change significantly when the number of carbons in the initiator increased. Overall, there was a significant difference between CL oligomers initiated by primary alcohols and secondary alcohols in terms of degree of crystallinity and melting point. Those oligomers initiated using secondary alcohols had significantly lower melting points and degrees of crystallinity. The presence of a pendant CH_3 group in the structure of secondary alcohols may interfere with the hydrogen bonds and close alignment of the polymer chains and thereby reduce the degree of crystallinity and melting point.

Theoretically, we expected to observe a decrease in the degree of crystallinity and an increase in melting point as the number of carbons in the initiator's chain increased, especially in primary alcohols with a linear structure. As the number of carbons in the structure of initiator increases the melting point increases. For example, the melting point of 1-butanol is $-89.5\text{ }^\circ\text{C}$ whereas the melting point of stearyl alcohol is $61\text{ }^\circ\text{C}$. Inclusion of an initiator with higher melting point (i.e., stearyl alcohol) in the oligomer backbone can increase the melting point of the oligomer while the inclusion of 1-butanol may decrease the melting point of the oligomer. By introducing a non-polar hydrocarbon chain (i.e., initiator) to the polar structure of poly(ϵ -caprolactone) it is possible that the non-polar structure of the initiator interferes with the hydrogen bonds or

any polar bonds between the CL units in the backbone of CL-oligomer. This interference could inhibit the polymer chain alignment as well as decreasing the number of polar bonds in the bulk causing a reduced degree of crystallinity. Failing to observe a statistical difference among data does not mean that the different synthesized polymers are truly the same. The declaration of nonsignificance here probably means that the sample size was too small; that is, the same difference with a larger sample could be significant at the 5% level. Since the number of data obtained in each experiment was three (degree of freedom=2), it is possible that we made a type II error (failing to observe a statistical difference if a specified difference truly exists) due to the insufficient number of data which has a significant impact on the power (not making type II error) of the test (38). Since the degree of crystallinity has a great impact on the drug release profile and polymer degradation time, it is very important to characterize different synthesized polymers in terms of degree of crystallinity.

3.4.3.2. Effects on Melt Viscosity

Rheologic behaviour of these polymers also plays a significant role in this project. In order to be syringeable through a needle while heated slightly above its melting point, the polymer vehicle must have a low melt viscosity. Two factors such as the flexibility of the polymer backbone, which was discussed earlier, and the entanglement of the polymer chains with each other have a significant impact on the syringeability of the polymers (8). Primary alcohols can initiate the polymerization process of ϵ -caprolactone and produce a linear chain PCL. In the melt state these polymer chains can slide over each other with minimum entanglement. This low entanglement between the polymer chains eases the passage of polymer through the needle. In contrast, secondary alcohols with an OH group positioned on the C₂ of the initiator's chain produce a PCL with a pendent CH₃ in the backbone (Figure 3.13). The presence of this pendent group reduces the flexibility of the backbone chain as bond rotations are inhibited by steric hindrance and the number of configurations available to the chain becomes limited (9). Moreover, the smaller number of carbons in the structure of primary alcohols (e.g., 1-dodecanol) in comparison to their corresponding secondary alcohol (i.e., 2-dodecanol) can reduce the flexibility of the PCL chain and hence,

produce a higher melt viscosity (39). This increased viscosity can make the polymer move through the needle with difficulty.

To test this theory, different polymers were synthesized (Table 3.4) and their rheologic behaviour was investigated. The results revealed that all the synthesized polymers behaved like Newtonian fluids at their melt state at three different temperatures (45, 50 & 55 °C) (Appendix B, Figures 1-8). To compare the viscosity of the polymers shown in Table 3.4 with each other at a constant temperature (e.g., 50 °C) a plot of shear stress versus shear rate was produced with the slope of the line being the viscosity (Appendix B, Figures 9-16). Figure 3.14 shows that by increasing the number of carbons in the structure of the initiator, the viscosity of the polymer decreases and overall primary alcohols produce lower viscosity polymers than secondary alcohols.

This observation can be justified with the same argument delivered above. The introduction of a non-polar initiator into the polar structure of CL oligomers can interfere with the hydrogen bonds available between CL oligomer chains and facilitate their movement while it is melted. Perhaps the result of the rheology study can be another reason to believe that the explanation of reduced melting point and degree of crystallinity by increasing the number of carbons in initiator's chain is valid.

3.4.4. Oligomer Synthesis and Characterization with Desired T_m

One goal of this project was to produce CL oligomers with melting points slightly above body temperature. Knowing that melting point can be influenced by molecular weight, different M/I ratios were used. By changing the M/I ratio, different CL oligomers were synthesized using various initiators, and purified to obtain oligomers with a melting point in the desired range (Table 3.5). As can be seen in Table 3.5, a wide variety of initiators were used. Alcohols such as ethyl alcohol with two carbons (polar and hydrophilic) in its structure to oleyl alcohol with 18 carbons (polar and hydrophobic) were tested. Application of initiators with different hydrophobicities and structure introduces a broad range of hydrophobic nature to the structure of the synthesized CL oligomers. One of the initiators used for polymerization of ϵ -caprolactone was oleyl alcohol, which has the same number of carbons as stearyl alcohol but bears some distinct characteristics and must be differentiated from stearyl alcohol. Firstly, this initiator is

more hydrophobic than stearyl alcohol due to the C=C in the middle of the oleyl alcohol chain. Secondly, it has a lower melting point (5 °C) in comparison to stearyl alcohol which has a $T_m=65$ °C. This lower melting point is due to the presence of the C=C bond in its backbone.

After synthesis and the purification procedure the yield of the process was measured and found to vary from 20-40% (Table 3.5). This low yield emphasizes the production of a large number of low molecular weight oligomers which were solubilized and removed during the purification process leaving only oligomers with higher molecular weight. Only this portion of the oligomers were capable of precipitating and being collected. In order to collect a reasonable amount of oligomer with melting point in the desired range the M/I ratio of the oligomers initiated with 1-dodecanol, 2-dodecanol, stearyl alcohol, and oleyl alcohol had to be manipulated. The M/I ratio of these oligomers was increased from 2.1 up to 4 to produce enough oligomer with the desired melting point (Table 3.5). The CL oligomers initiated with the four-abovementioned initiators, didn't precipitate in cold ethanol when an M/I ratio of 2.1 was used. This may be attributed to the lower reactivity of these initiators in comparison to the small size initiators (i.e., ethanol and butanol). This lower reactivity can produce largely low molecular weight oligomers incapable of precipitating in cold ethanol and hence, no oligomer collection. Moreover, due to the presence of large number of initiator molecules in synthesized oligomers with M/I ratios of 2.1-4, some of these initiator molecules didn't participate in the polymerization process and were left unreacted. By comparing the NMR spectrum of CL-oligomer (Appendix C, Figure 1), 2-butanol (Figure 3.15) and CL oligomer initiated with 2-butanol (M/I=2.1) (Figure 3.16) it is obvious that no CL monomer is left at the end of the polymerization process while some unreacted initiator is present. These unreacted initiator molecules were removed by the purification process.

The composition and molecular weight of the CL oligomers were determined by NMR spectroscopy (Appendix C, Figures 11-19 & Table 3.6). Two typical NMR spectrum related to PCL initiated by 1-butanol (primary alcohol) and 2-butanol (secondary alcohol), and their corresponding chemical structure, are shown in Figures 3.17 and 3.18. The ^1H -NMR assignment of all CL-oligomers initiated with primary

alcohols is similar to 1-butanol-initiated CL-oligomer, and that of secondary alcohols is similar to 2-butanol- initiated CL-oligomer. The results of the calculated \overline{Mn} from the $^1\text{H-NMR}$ and GPC are compared in Table 3.6. \overline{Mn} values obtained with GPC were generally in agreement with those of NMR which confirm the production of oligo(ϵ -caprolactone). By comparing the \overline{Mn} obtained from GPC or NMR after purification with theoretical \overline{Mn} which is calculated based on unpurified oligomers it is obvious that the theoretical \overline{Mn} was much lower. It was speculated that when the low M/I ratios were used (i.e., 2.1-4) a very heterogeneous oligomer bulk was produced comprised of mainly very low molecular weight chains which were removed after purification leaving only higher molecular weight oligomer chains. The low yield of the purification process (20-40%) is another reason confirming this theory.

All the synthesized diblock oligomers were characterized in terms of their melting point and degree of crystallinity by using DSC (Appendix A, Figures 8-16, Table 3.6), molecular weight and molecular weight distribution by using GPC (Appendix D, Figures 1-8, Table 3.5), and melt viscosity using a rheometer (Table 3.7).

DSC results revealed that the synthesized diblock oligomers had melting points between 38-42 °C, which is in the desired range. Moreover, no sign of transesterification was observed in the DSC endotherms (no peak broadening). In this case the onset of melting was determined and reported, as this value is also the same as on set of crystallization. It is worth mentioning that the purified oligomers with T_m in the desired range (M/I= 2.1-4) had almost the same \overline{Mn} and T_m as unpurified oligomers (M/I= 8) mentioned above (Table 3.8). Basically, in both methods the same molecular weight oligomers with the same melting point, one with 100% yield and the other with on average 30% yield were produced. Although the purification method dramatically reduced the yield of the process but the resultant oligomer had a narrower MWD as shown in DSC graphs (Appendix A). This narrow MWD helps us to determine the onset of crystallization (same as onset of melting) with better pinpoint accuracy. Determination of onset of crystallization is important to us because it shows the

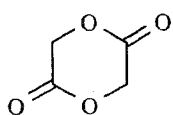
temperature at which the undesirable crystallization phenomenon occurs; thereby, it can be adjusted.

The GPC results showed that the molecular weight distribution of the oligomers was narrow and the molecular weight of all the oligomers were below 5000 daltons. Moreover, no distinct spectrum resulting from transesterification products was observed which was in agreement with the DSC results. A molecular weight of 5000 daltons is a critical point for caprolactone oligomers. It has been shown that at this molecular weight the caprolactone chains become small enough to diffuse out of the polymer bulk. Therefore, the polymer bulk becomes prone to fragmentation and faster degradation (40).

Table 3.7 summarizes the melt viscosity of the synthesized and purified oligomers. It is obvious that by increasing temperature the melt viscosity of oligomers decreases. Moreover, it can be observed that all the synthesized oligomers are in the melt state at 46 °C emphasizing the possibility of being syringeable at this temperature. By comparing the results of melt viscosity produced at 50 °C for purified and unpurified oligomers (Table 3.4 and 3.7) it is obvious that the unpurified oligomers are showing higher values than that of the purified oligomers. It was expected to observe lower melt viscosity for the unpurified oligomers due to the higher MWD. This anomaly can be attributed to the difference between the equipment used for measurements at the University of Alberta and Queen's University. Since two different rheometrics with two different sets of cup and bob were used, observation of this slight anomaly was expected.

3.5. Concluding Remarks

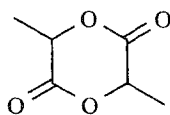
All the synthesized polymers mentioned above have a melting point in the desired range and they all are syringeable. They can all be used for the next part of the project, which focuses on the *in vitro* drug release studies. Among all these polymers four were chosen as the best candidates for further studies. CL oligomers initiated by oleyl alcohol and 2-dodecanol were chosen due to their low degree of crystallinity. PCL initiated with ethanol was another candidate chosen as a comparison sample. CL oligomer initiated by 1-dodecanol was another candidate and was chosen to be compared with CL oligomer initiated with 2-dodecanol. In this latter case we can study the effect of the initiator on the drug release profile.



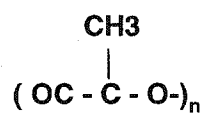
$C_4H_4O_4$
Mw=116.1



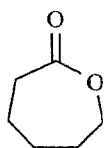
GLYCOLIDE



$C_6H_8O_4$
Mw=144.1



DL-LACTIDE



$C_6H_{10}O_2$
Mw=114.14



ε -CAPROLACTONE

Figure 3.1. Chemical structure of the DL-lactide, glycolide and ε-caprolactone and their corresponding polymers.

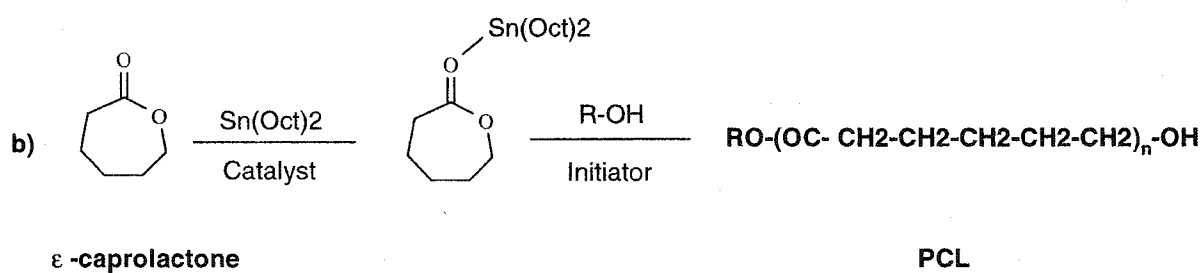
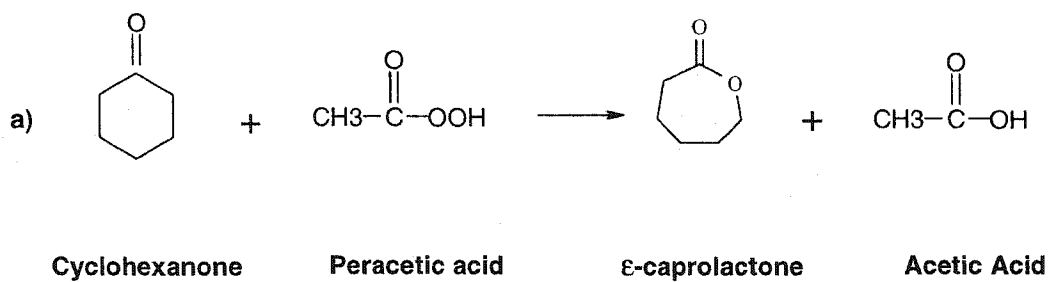


Figure 3.2. a) Synthesis of ε-caprolactone. b) Mechanism of ring opening polymerization of ε-caprolactone. Reproduced from reference 14.

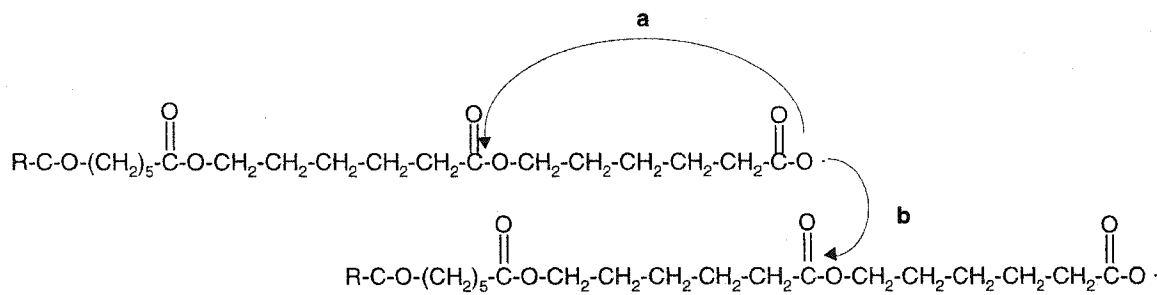
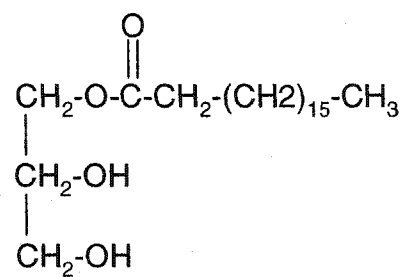


Figure 3.3. The transesterification of PCL. **a)** Back-biting caused by intramolecular transesterification, **b)** Scrambling caused by intermolecular transesterification. Reproduced from reference 14.

A)



B)

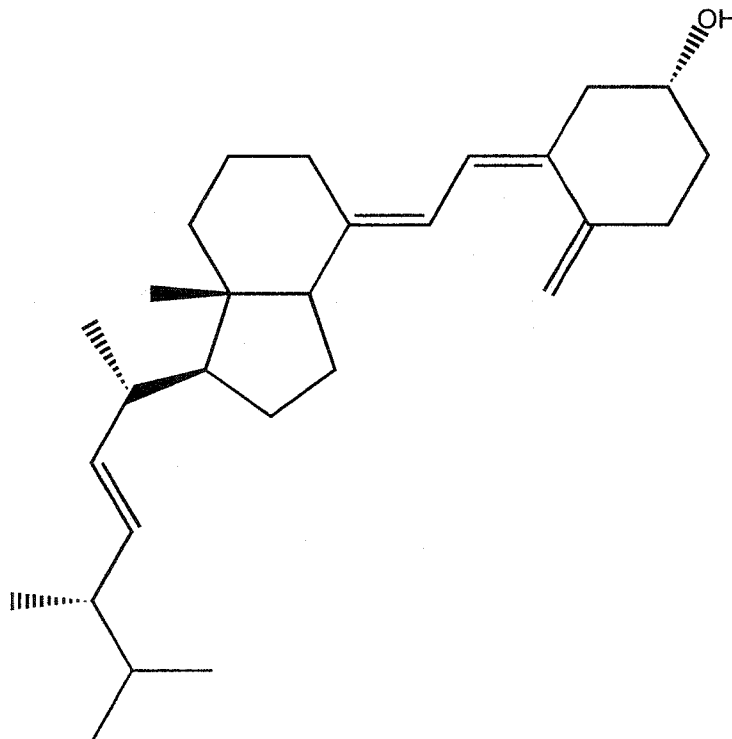


Figure 3.4. A) Chemical structure of Glyceril Mono Oleate (GMO); B) Chemical structure of Vitamin D.

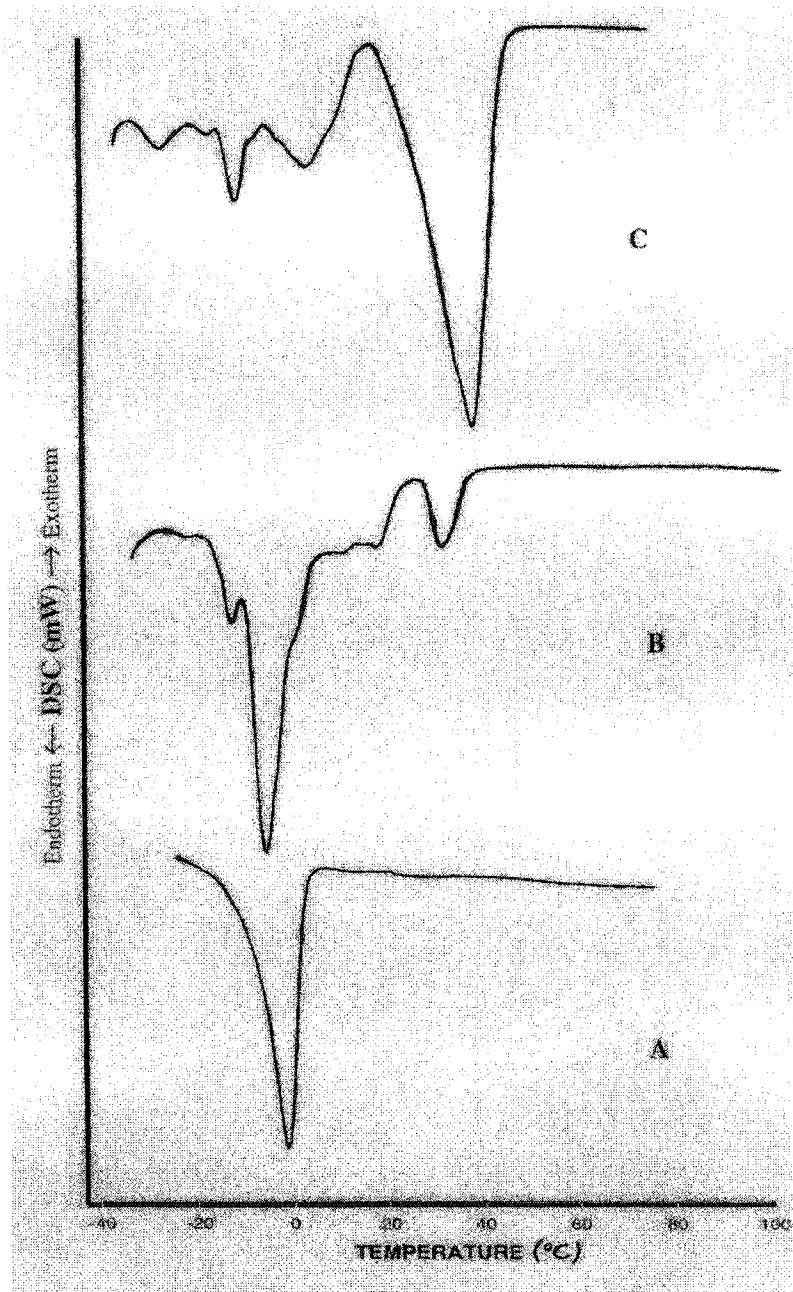


Figure 3.5. A) DSC scans of ϵ -caprolactone monomer. B) DSC scans of the polymerized PCL after 8 hours. C) DSC scans of the polymerized PCL after 12 hours.

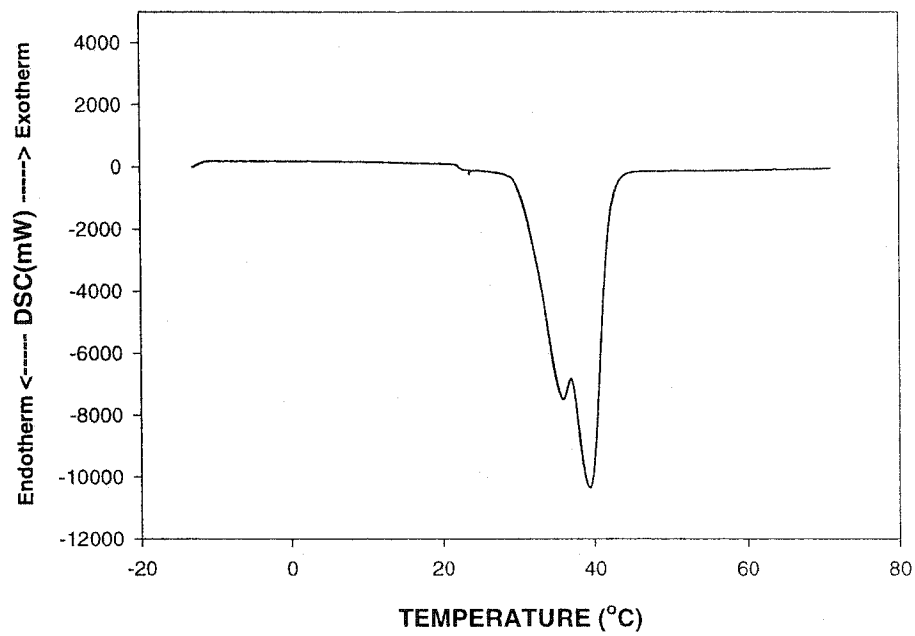


Figure 3.6. DSC scans of the polymerized PCL after 24 hours. Polymerization time and temperature were 24 hrs and 120 °C, respectively. The M/I ratio was 8.

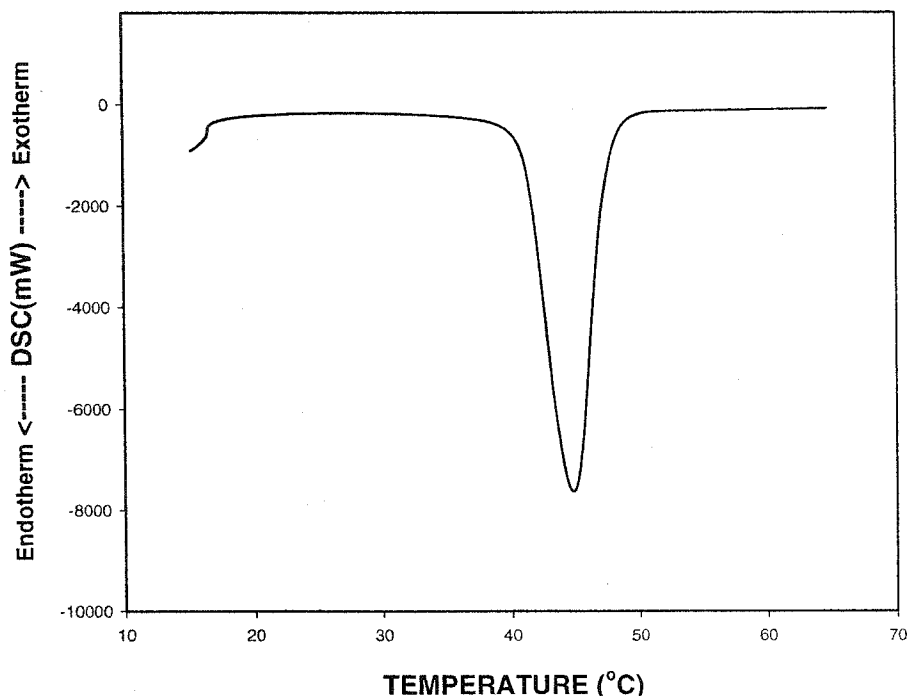


Figure 3.7. DSC scans of the PCL polymerized at 110 °C. The M/C ratio, M/I ratio, time of polymerization and type of initiator were 1000, 8, 24 hrs and 1-butanol, respectively.

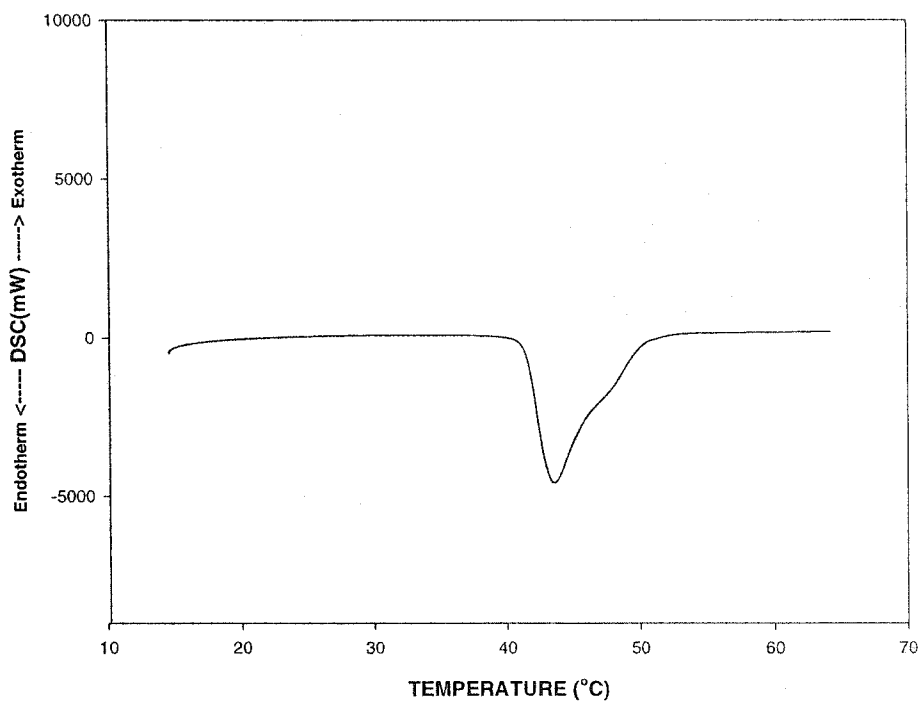


Figure 3.8. DSC scans of the synthesized PCL at 140 °C. The M/C ratio, M/I ratio, time of polymerization and type of initiator were 1000, 8, 24 hrs and 1-butanol, respectively.

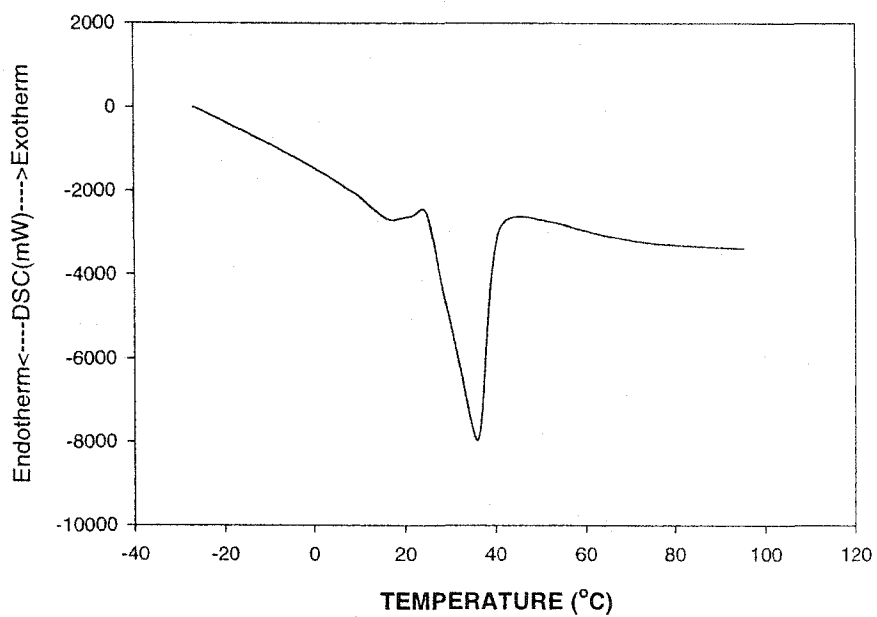


Figure 3.9. DSC scans of the synthesized PCL at 80 °C. The M/C ratio, M/I ratio, time of polymerization and type of initiator were 1000, 8, 24 hrs and 1-butanol, respectively.

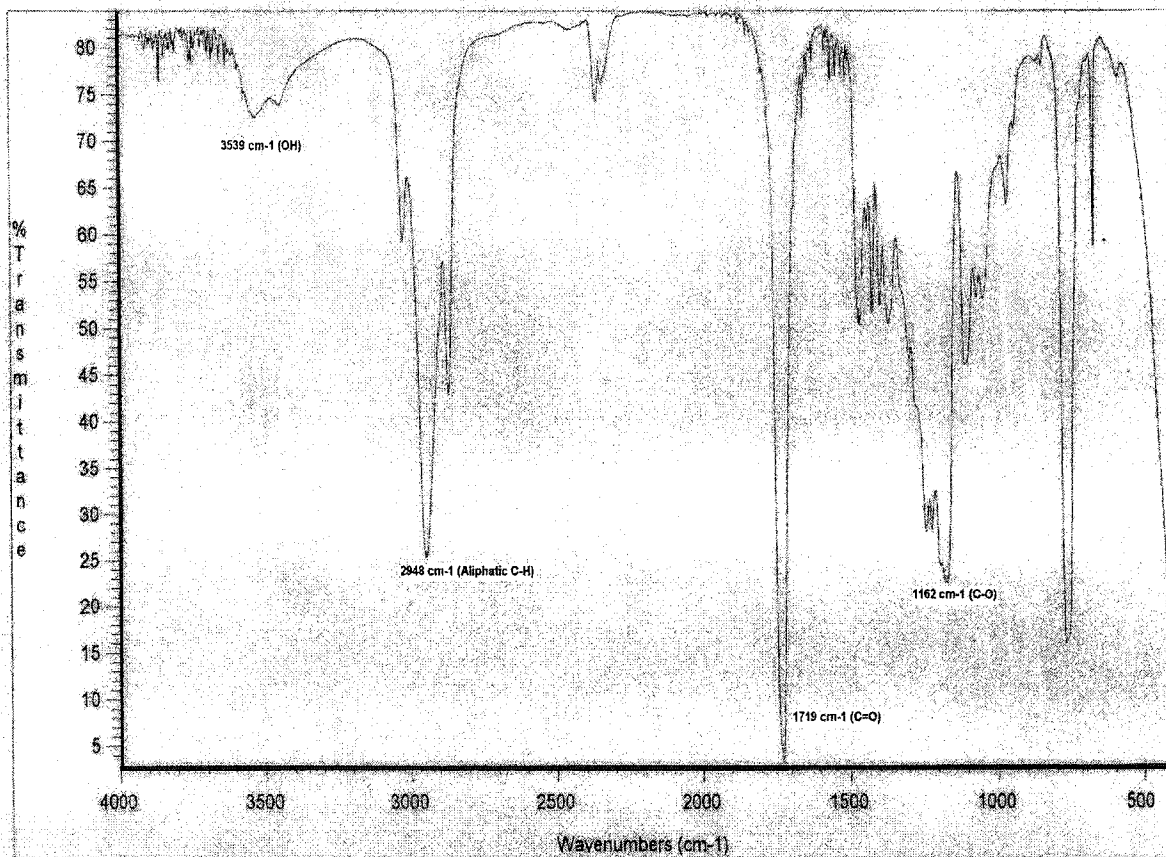


Figure 3.10. Typical IR spectrum of CL-oligomers. From the spectrum C-O shift at 1162 cm^{-1} , C=O shift at 1719 cm^{-1} , O-H shift at 3539 cm^{-1} and aliphatic C-H shift at 2948 cm^{-1} were assigned.

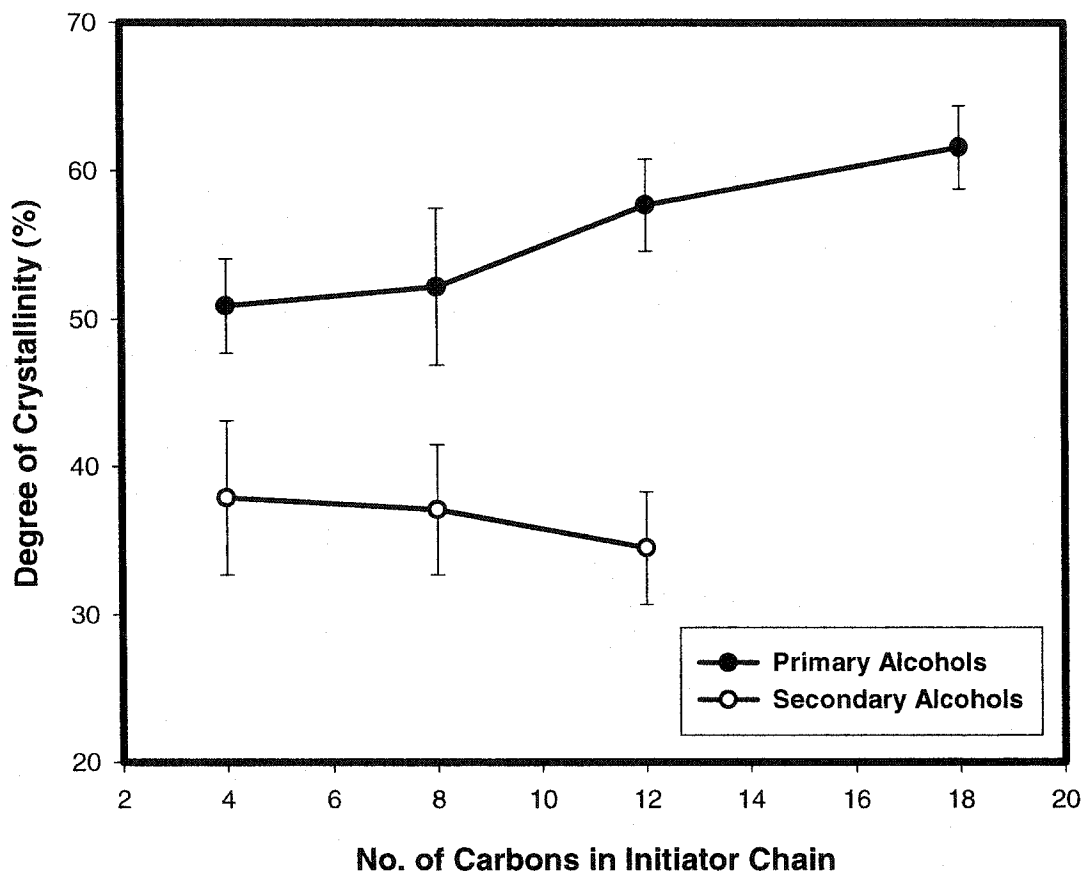


Figure 3.11. Effects of varying the number of carbons in initiator chain on the degree of crystallinity. Data are shown as average \pm standard deviation ($n=3$).

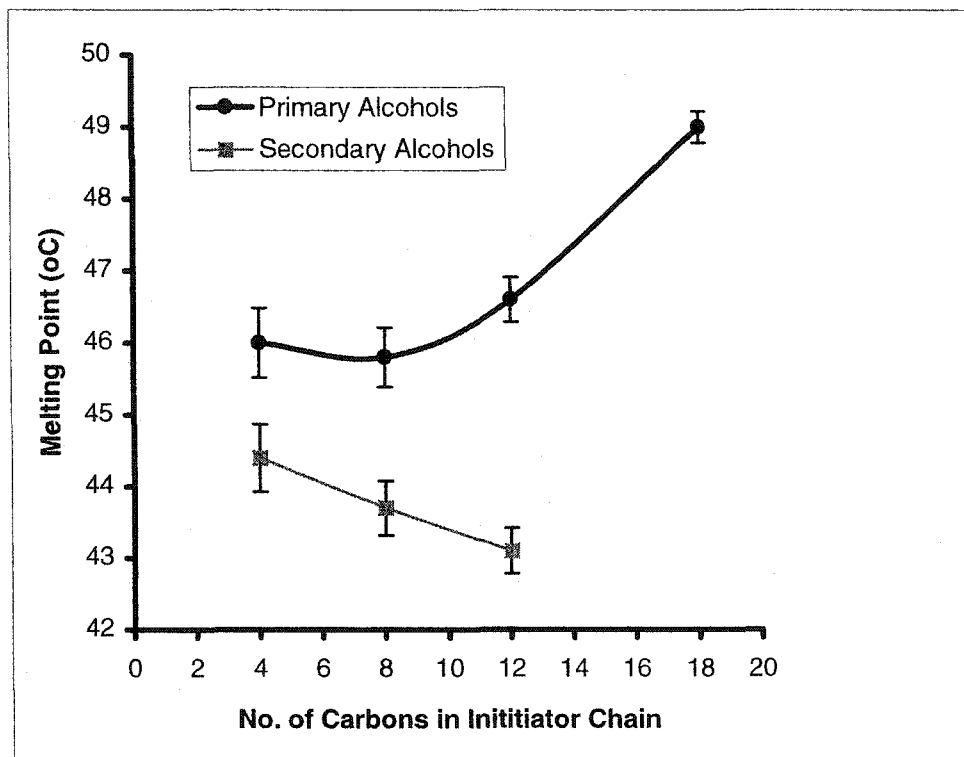
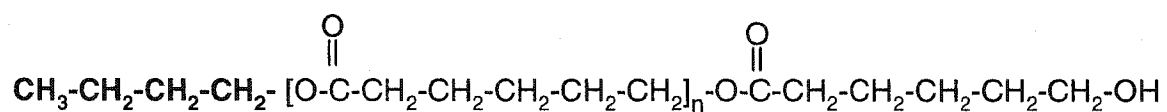
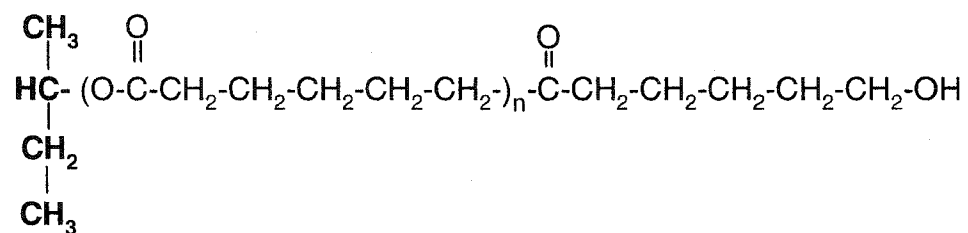


Figure 3.12. Effects of varying the number of carbons in initiator chain on the melting point of the oligomers. For better accuracy the melting point midpoint from DSC endotherms were used. Data are shown as average \pm standard deviation ($n=3$).



1-butanol (initiator)



2-butanol (initiator)

Figure 3.13. Chemical structure of PCL initiated with 1-butanol (primary alcohol) and 2-butanol (secondary alcohol).

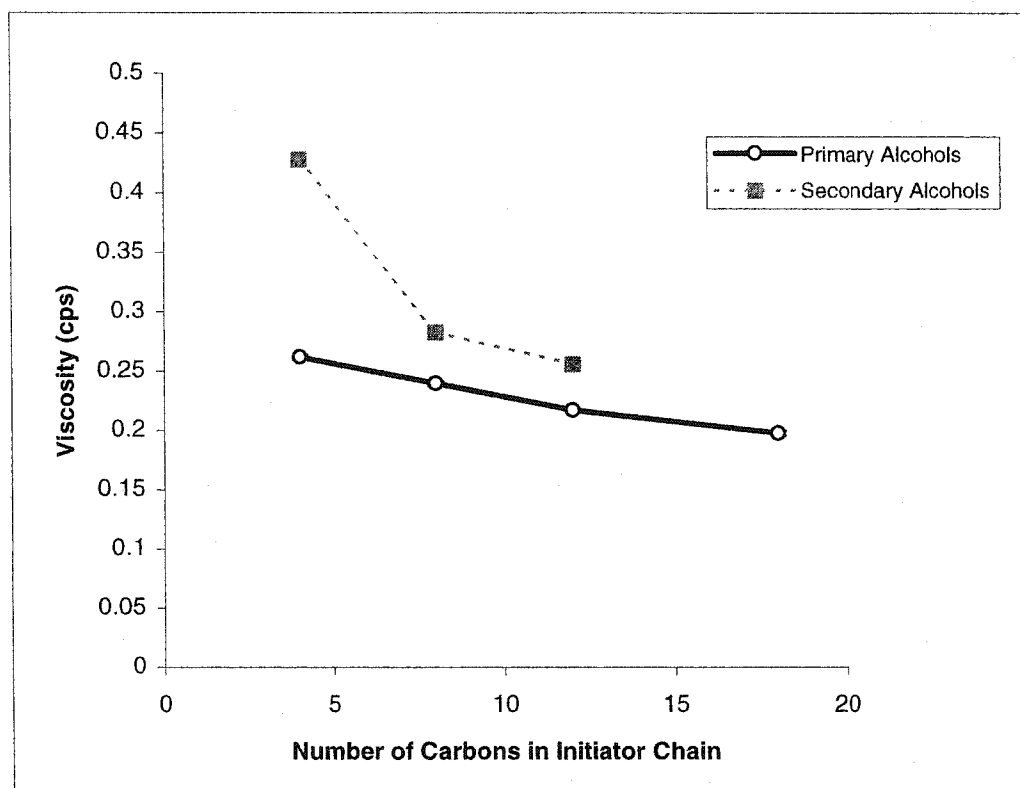


Figure 3.14. Effect of the initiator chemical structure on the viscosity of the polymers at 50 °C. Data are shown as average \pm standard deviation ($n=3$).

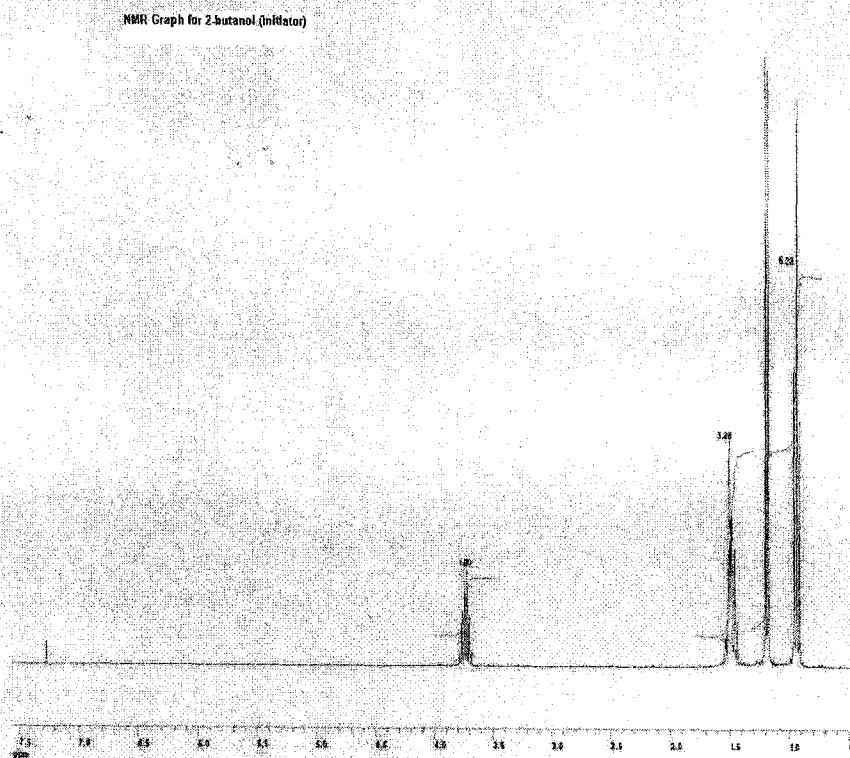


Figure 3.15. NMR spectrum for 2-butanol the initiator. Samples were prepared in CDCl_3 by using a 300 MHz NMR spectroscope.

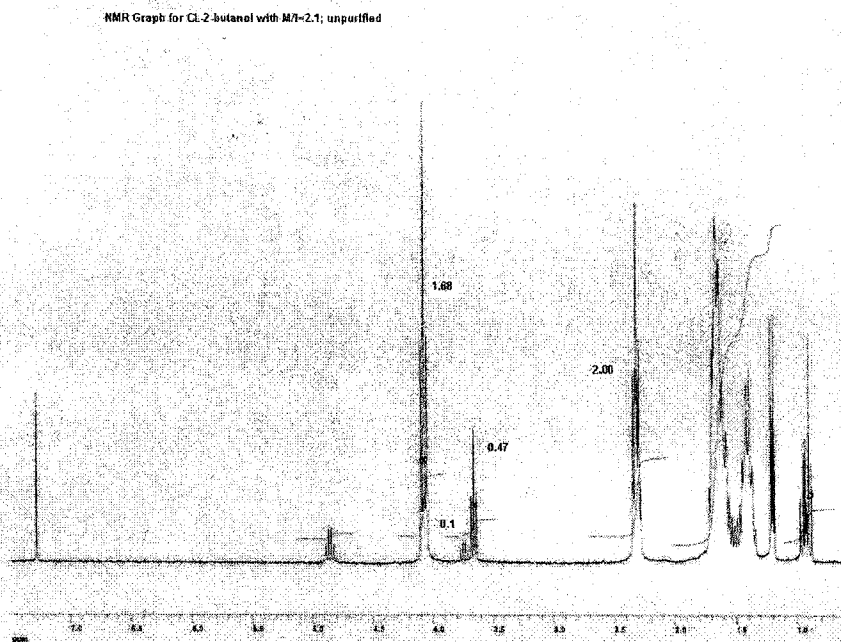


Figure 3.16. NMR spectrum for CL oligomer initiated by 2-butanol (M/I=2.1). Multiplets at $\delta=1.5$ and $\delta=3.75$ corresponds to the presence of unreacted initiator (2-butanol). Samples were prepared in CDCl_3 by using a 300 MHz NMR spectroscope.

Table 3.1. Melting point of the diblock oligomer (GMO-CL) with varying reactant composition. By polymerizing CL with GMO and increasing the CL/GMO molar ratio, the melting point increased.

Caprolactone/GMO (g/g)	Melting Point (°C)
0*	34
0.6	16.4
1	18.6
3	37.3
4	46.3
5	49.5
6	50.5
7	53.5

*Only GMO

Table 3.2. Theoretical \overline{Mn} calculated by the following formula:

$$\overline{M}_n = 114.14 \times \frac{M}{I} + M_{wi}$$
for unpurified CL oligomers. The closeness of MWD values of the oligomers to each other is indicative of narrow polydispersity.
All the GPC measurements were done in the University of Queens by Darryl Knight.

Initiator	Theoretical Mn	M _n by NMR	M _n By GPC	M _w by GPC	MWD*
1-butanol	988	1176	701	828	1.21
2-butanol	988	1097	763	871	1.15
1-octanol	1044	1171	630	732	1.16
2-octanol	1044	1230	872	988	1.14
1-dodecanol	1100	1240	966	1036	1.08
2-dodecanol	1100	1043	672	747	1.11
Stearyl alcohol	1184	1213	619	693	1.12

* Molecular Weight Distribution

Table 3.3. Effects of the number of carbons and position of OH group in the initiator's chain, on the crystallinity and melting point. Degree of crystallinity was calculated based on the ΔH of fusion obtained from the DSC scans.

Initiator	No. of Carbons in Initiator	M/C (mol/mol)	T _m (°C) Midpoint	T _m (°C) Onset	ΔH (mJ/mg)	Crystallinity %
1-Butanol	4	1000	46± 0.48	39.9±0.8	71.1±4.4	50.9± 3.2
2-Butanol	4	1000	44.4± 0.47	40.1±0.7	52.8±7.2	37.9± 5.2
1-Octanol	8	1000	45.8± 0.41	40.9±0.5	72.8±6.0	52.2± 4.3
2-Octanol	8	1000	43.7±0.38	38.4±0.6	51.7±6.1	37.1± 4.4
1-Dodecanol	12	1000	46.6± 0.3	39.1±0.7	80.5±4.3	57.7± 3.1
2-Dodecanol	12	1000	43.1± 0.32	37.8±0.9	48.1±5.2	34.5± 3.8
Stearyl Alcohol	18	1000	49± 0.22	44.5±0.6	85.9± 3.9	61.6± 2.8

Table 3.4. Comparison of the melt viscosity of polymerized ϵ -caprolactone at 50 °C by using different initiators. Oligomers were not purified after synthesis.

PCL No.	Initiator	Average Viscosity (cP) at 50 °C (n=3)	S.D.
1	1-butanol	0.262	0.002
2	2-butanol	0.428	0.004
3	1-octanol	0.240	0.002
4	2-octanol	0.283	0.002
5	1-dodecanol	0.217	0.001
6	2-dodecanol	0.256	0.002
7	stearyl alcohol	0.198	0.002

Table 3.5. Polymerized and characterized CL oligomers with desired melting point. M/C ratio was kept constant and by manipulating the M/I ratio the desired melting point was obtained. All the oligomers were purified after synthesis to remove any unreacted initiator. The low yield value is an indicative of the removal of not only unreacted initiators but very low molecular weight oligomers.

PCL No.	Initiator	M/C	M/I	Mw	Mn	MWD	Tm (°C)±SD Onset	ΔH (mJ/mg)	crystallinity %	Yield %
1	Ethanol	1000	2.1	1916	1366	1.402	41.7±0.4	114.82	82	29
2	1-Butanol	1000	2.1	2380	1945	1.226	40.2±0.62	107.25	76	21
3	2-Butanol	1000	2.1	3083	2776	1.111	41.8±0.52	117.65	84	23
4	1-Octanol	1000	2.1	2103	1844	1.141	40.8±0.56	124.66	89	27
5	2-Octanol	1000	2.1	2747	2219	1.238	40.4±0.66	105.95	75	25
6	1-Dodecanol	1000	3.4	2232	1893	1.179	39.6±0.77	110.40	79	34
7	2-Dodecanol	1000	2.6	2164	1717	1.261	39.5±0.48	94.60	67	30
8	Stearyl Alcohol	1000	4	1883	1209	1.557	40.2±0.68	Unidentified	Unidentified	45
9	Oleyl Alcohol	1000	3.2	2435	1575	1.545	37.9±0.51	93.12	66	40

Table 3.6. Comparison of the \overline{M}_n calculated from $^1\text{H-NMR}$ and GPC for CL oligomers after purification. The M_n obtained by GPC and NMR are very close to each other emphasizing the accuracy of these methods. Since the oligomers were purified and very low molecular weight oligomers were removed, the theoretical M_n is showing much lower values than those obtained by GPC and NMR.

PCL	Initiator	M_n Calculated by GPC	M_n Calculated by NMR	Theoretical M_n
P135	Ethanol	1366	1188	286
P136	1-Butanol	1945	1101	314
P144	2-Butanol	2776	1330	314
P138	1-Octanol	1844	1144	370
P145	2-Octanol	2219	2070	370
P152	1-Dodecanol	1893	1442	574
P156	2-Dodecanol	1717	1898	483
P153	Stearyl Alcohol	1209	1070	727
P143	Oleyl Alcohol	1575	1524	634

Table 3.7. Melt viscosity data at three different temperatures for polymerized ϵ -caprolactone followed by purification. The viscosity values were obtained by plotting shear stress versus shear rate obtained from the rheometer.

PCL No.	Initiator	Average Viscosity at 50 °C (cps)	S.D.	Average Viscosity at 48 °C (cps)	S.D.	Average Viscosity at 46 °C (cps)	S.D.
1	ethanol	0.157	0.013	0.187	0.015	0.206	0.019
2	1-octanol	0.120	0.005	0.134	0.008	0.146	0.010
3	2-octanol	0.210	0.015	0.250	0.020	0.273	0.023
4	1-dodecanol	0.102	0.030	0.114	0.031	0.121	0.026
5	2-dodecanol	0.130	0.005	0.148	0.006	0.166	0.012
6	stearyl alcohol	0.147	0.005	0.167	0.006	0.178	0.005
7	oleyl alcohol	0.110	0.005	0.127	0.002	0.132	0.005

Table 3.8. Melting point and molecular weight comparison between unpurified (M/I=8) and purified (M/I=2.1-4) oligomers. M/C ratio was kept constant at 1000 for the synthesized oligomers.

Initiator	M _n by NMR	T _m (°C)±SD Onset	M _n by NMR	T _m (°C)±SD Onset
	Purified Oligomers		Unpurified Oligomers	
1-Butanol	1101	40.2±0.62	1176	39.9±0.8
2-Butanol	1330	41.8±0.52	1097	40.1±0.7
1-Octanol	1144	40.8±0.56	1171	40.9±0.5
2-Octanol	2070	40.4±0.66	1230	38.4±0.6
1-Dodecanol	1442	39.6±0.77	1240	39.1±0.7
2-Dodecanol	1898	39.5±0.48	1043	37.8±0.9
Stearyl Alcohol	1070	40.2±0.68	1213	44.5±0.6

3.6. References

- [1]- M. K. Yeh, P. G. Jenkins, S. S. Davis, Improving the delivery capacity of microparticle systems using blends of poly(D-L-lactide-co-glycolide) and poly(ethylene glycol). *J. Controlled Release* 37 (1995) 1-9.
- [2]- C. I. Winternitz, J. K. Jackson, A. M. Oktaba, Development of a polymeric surgical paste formulation for Taxol. *Pharm. Res.* 13 (1996) 368-375.
- [3]- M. B. Sintzel, A. Merkli, J. Heller, Synthesis and analysis of viscous poly(ortho-ester) analogs for controlled drug release. *Int. J. Pharm.* 155 (1997) 263-269.
- [4]- I. Engelberg, J. Kohn, Physicochemical properties of degradable polymers used in medical applications. *Biomaterials* 12 (1991) 292.
- [5]- C. G. Pitt, Z-W. Gu, P. Ingram, R. W. Hendren, The synthesis of biodegradable polymers with functional side chains. *J. Polym. Sci. Part A Polym. Chem.* 25 (1987) 955.
- [6]- X. Zhang, U. P. Wyss, D. Pichora, M. F. A. Goosen, A mechanistic study of antibiotic release from biodegradable poly (D-L lactide) cylinders. *J. Controlled Release* 31 (1994) 129-144.
- [7]- M. Hiljanen-vainio, T. Karjalainen, J. Seppala, Biodegradable lactone copolymers. I. Characterization and mechanical behaviour of ϵ -caprolactone and lactide copolymers. *J. Appl. Polym. Sci.* 59 (1996) 1281-1288.
- [8]- A. Martin, *Physical Pharmacy*. Lea & Febiger, Malvern, PA, USA (1993).
- [9]- P. C. Painter, M. M. Coleman, *Fundamentals Of Polymer Science*. Technomic Publishing Co., Lancaster, PA, USA (1994).
- [10]- M. B. Roller, R. S. Bezwada, Liquid and low melt absorbable copolymers and their blends- Synthesis and rheology. *Med. Plastics Biomater.* (1996) 40-43.

- [11]- P. K. Gallagher, Thermoanalytical instrumentation, techniques, and methodology, In: E. A. Turi (ed.), Thermal characterization of polymeric materials. Academic Press, San Diego, 1997.
- [12]- D. H. Lewis, Controlled release of bioactive agents from lactide/glycolide polymers, In: M. Chasin, R. Langer (eds.), Biodegradable polymers as drug delivery systems. Marcel Decker, New York, 1990.
- [13]- C. G. Pitt, Y. T. Bao, A. L. Andradý, P. N. K. Samuel, The correlation of polymer-water and octanol-water partition coefficients: estimation of drug solubilities in polymers. *Int. J. Pharm.* 45 (1988) 1-11.
- [14]- C. G. Pitt, Poly ϵ -caprolactone and its copolymers. In M. Chasin, R. Langer (eds.), Biodegradable polymers as drug delivery systems. Marcel Decker, New York, 1990, pp.72-120.
- [15]- V. F. Jenkins, Caprolactone and its polymers. *Polym. Paint Colour J.* 167 (1977) 622-627.
- [16]- K. Ito, Y. Hashizuka, Y. Yamashita, Equilibrium cyclic oligomer formation in anionic polymerization of ϵ -caprolactone. *Macromolecules* 10 (1977) 821-825.
- [17]- S. Segal, Contraceptive subdermal implants, In: D. R. Mishell (ed.), Advances in fertility research. Raven Press, New York, 1982, pp. 117-137.
- [18]- A. Kowalski, A. Duda, S. Penczek, Kinetics and mechanism of cyclic esters polymerization initiated with tin(II) octoate. *Macromol. Rapid Commun.* 19 (1998) 567-572.
- [19]- A. Kowalski, A. Duda, S. Penczek, Polymerization of L,L-Lactide Initiated by Aluminum Isopropoxide Trimer or Tetramer. *Macromolecules* 7 (1998) 2114.
- [20]- A. Duda, S. Penczek, Polymerization of ϵ -caprolactone initiated by aluminum isoperoxide trimer and/or tetramer. *Macromolecules* 28 (1995) 5981.

- [21]- A. Hofman, S. Slomkowski, S. Penczek, Polymerization of ϵ -caprolactone with kinetic suppression of macrocycles. *Makromol. Chem. Rapid Commun.* 8 (1987) 387.
- [22]- H. R. Kricheldorf, I. Kreiser-Saunders, C. Boettcher, Poly lactones: 31. Sn(II)octoate-initiated polymerization of L-lactide: a mechanistic study. *Polymer* 36 (1995) 1253-1259.
- [23]- Y. J. Du, P. J. Lemstra, A. J. Nijenhuis, H. A. M. Van Aert, ABA type copolymers of lactide with poly(ethylene glycol)-kinetic-mechanistic and model studies. *Macromolecules* 28 (1995) 2124-2132.
- [24]- G. Schwach, J. Coudane, R. Engel, M. Vert, More about the polymerization of lactides in the presence of stannous octoate. *J. Polym. Sci., Part A: Polym. Chem.* 35 (1997) 3431.
- [25]- Y. Yamashita, T. Tsuda, H. Ishida, M. Hasegawa, Polymerization and copolymerisation of ϵ -caprolactone. *Kogyo Kagaku Zasshi* 71 (1968) 755-757.
- [26]- Y. J. Du, P. J. Lemstra, A. J. Nijenhuis, H. A. M. Van Aert, ABA type of copolymers of lactide with poly(ethylene glycol)-kinetic, mechanistic and model studies. *Macromolecules* 25 (1995) 2124.
- [27]- M. P. H. Vainio, P. A. Orava, J. V. Seppala, Properties of ϵ -caprolactone/DL-lactide copolymers with a minor ϵ -CL content. *J. Biomed. Mater. Res.* 34 (1997) 39-45.
- [28]- D. W. Grijpma, A. J. Pennings, Polymerization temperature effects on the properties of L-lactide and ϵ -caprolactone copolymers. *Polymer Bulletin* 25 (1991) 335.
- [29]- P. Cerrai, M. Tricoli, F. Andruzzi, M. Poci, M. Pasi, Polyether-polyester block copolymers by non-catalyzed polymerization of ϵ -caprolactone with poly(ethylene glycol), *Polymer* 30 (1989) 338-343.
- [30]- K. Ito, Y. Hashizuka, Y. Yamashita, Equilibrium cyclic oligomer formation in anionic polymerization of ϵ -caprolactone. *Macromolecules* 10 (1977) 821.

- [31]- S. Sosonowski, S. Slomkowski, S. Penczek, Kinetic of epsilon-caprolactone polymerization and formation of cyclic oligomers. *Makromol. Chem.* 184 (1983) 2159.
- [32]- H. R. Kricheldorf, C. Boettcher, K. U. Tonnes, *Poly lactones*.23. Polymerization of racemic and meso D-L-lactide with various organotin catalysts stereochemical aspects. *Polymer* 33 (1992) 2817.
- [33]- V. Crescenzi, G. Manzini, G. Calzolari, C. Borri, Thermodynamics of fusion of poly- β -propiolactone and poly- ϵ -caprolactone. *Eur. Polym. J.* 8 (1972) 449.
- [34]- P. J. A. I. Veld, E. M. Velner, P. V. D. Witte, J. Hamhuis, P. J. dijkstra, J. Feijen, Melt block copolymerisation of ϵ -caprolactone and L-lactide. *J. Polym. Sci., Part A: Polym. Chem.* 35 (1997) 219-226.
- [35]- K. Hiltunen, J. V. Seppala, M. Harkonen, Effect of catalyst and polymerization on the preparation of low molecular weight lactic acid polymers. *Macromolecules* 30 (1997) 373-379.
- [36]-H. L. Hseih, W. Wang, An improved process for ϵ -caprolactone containing block copolymers, In: J. E. McGrath (ed.), *Ring opening polymerization: kinetics, mechanisms and synthesis*. Washington D.C., ACS, 1985, pp.162.
- [37]- H. R. Kricheldorf, M. Berl, N. Scharnagl, *Poly(lactones)*. 9. Polymerization mechanism of metal alkoxide initiated polymerizations of lactide and various lactones. *Macromolecules* 21 (1988) 286-293.
- [38]- S. Bolton, *Pharmaceutical statistics*, Marcel Dekker Inc., New York, 1997.
- [39]- L. H. Sperling, *Introduction to physical polymer science*. John Wiley & Sons, New York, 1986.
- [40]- S. C. Woodward, P. S. Brewer, F. Moatamed, The intracellular degradation of poly(ϵ -caprolactone). *J. Biomed. Mater. Res.* 19 (1985) 437-444.

Chapter 4
CPT Solubility, Stability and Release

4.1. Introduction

One of the problems associated with the delivery of CPT is the low solubility of the drug in water. It is reported that at 37 °C, only 3.8 µg of CPT is soluble in one millilitre of water (1). Moreover, structure activity investigations elucidated that the preservation of the lactone ring of CPT is crucial for its anti-tumor activity (2). However, the delivery of the active form is quite challenging, since the lactone form exists in a pH dependent equilibrium with an open ring carboxylate form (2). At physiological pH more than 80% of the drug exists as the carboxylate form at equilibrium, whereas at a pH below 5, essentially the entire drug is in the lactone form (3). Furthermore, it has been shown that CPT requires a prolonged schedule of administration given continuously at low doses in order to spare normal haematopoietic cells and mucosal progenitor cells while at the same time maintaining drug efficacy (4). Therefore, this drug would benefit from a localized controlled release depot system. However, any depot developed would also need to maintain the CPT in its active form prior to being released. Additionally, it is desirable that the polymer carrier be biodegradable to eliminate the need for device retrieval at the end of the delivery period.

4.1.1. Polymer Degradation

The degradation of biodegradable polymers such as PCL and PLGA has been studied by many investigators (5-8). They biodegrade by hydrolysis of the readily accessible and hydrolytically unstable aliphatic-ester linkages. The degradation time varies from a few weeks for PLGA to 1-2 years for PCL.

Biodegradable polymers undergo three stages of degradation *in vitro* (9). These three stages are not discrete and may overlap with each other. The first stage is the hydration of the implant after being placed in the physiologic fluid. In this stage, the device absorbs water from the surrounding environment. During the first stage of degradation process no weight loss occurs. The diffusion of water into the implant depends on the mass, surface area and hydrophilicity/hydrophobicity of the implant and occurs over the period of days or months. Amorphous parts of the polymer hydrate readily while the crystalline segments are not prone to hydration. In the second stage of

degradation chemical cleavage of the polymer backbone occurs and results in a reduction in mechanical properties (e.g. strength). In this process, water molecules hydrolyse and covalent chemical bonds of the polymer such as esteric linkages (in the case of PLGA and PCL) and result in a reduction in average molecular weight (10,11). The third stage only applies to hydrophilic biomaterials such as PLGA and to some extent to PCL. PCL is much more hydrophobic than PLGA and the rate of water imbibition is much slower than PLGA. In this stage PLGA and PCL fragment into pieces of low molecular weight polymer due to the loss of mass integrity.

For biodegradable polymers two different erosion mechanisms have been proposed: 1) surface or heterogeneous erosion; and 2) bulk or homogeneous erosion (12) (Figure 4.1). In the case of surface eroding polymer matrices (e.g., polyanhydrides), the rate of polymer degradation is faster than the rate of the water imbibition by the polymer bulk. Therefore, degradation occurs on the superficial layers of the polymer. Consequently, erosion affects only the surface and not the inner parts of the matrix (heterogeneous process). In bulk eroding polymers (e.g., PLGA and PCL) water uptake by the system is much faster than polymer degradation and the polymer degrades slowly. Thus, the entire system is rapidly hydrated and polymer chains are cleaved throughout the polymer. Consequently, the erosion is not restricted to the polymer surface (homogeneous process) (13).

The degradation of such polymers thus depends on the initial molecular weight, degree of crystallinity, physical geometry of the specimen, and the physico-chemical environment (14,15). Molecular weight of the polymer plays a crucial role in the polymer degradation time. Since the high molecular weight polymer chains are water insoluble, it takes more time for water to hydrolyse and cleave these chains into small water soluble chains. Therefore, the higher the molecular weight the longer the degradation time (5). Crystallinity is known to play an important role in determining biodegradability because of the fact that the bulk crystalline phase is inaccessible to water and other permeants (16). The biodegradation rate is reduced by the decrease in accessible ester bonds. The physical geometry of the device determines its surface area to volume ratio. Geometries with large surface area and small volume degrade faster than those of small surface area and large volume. The physico-chemical environment is

another important factor which can affect the degradation rate. Factors such as temperature and pH are among the most important physico-chemical factors which can easily increase or decrease the polymer degradation time. The hydrolysis of polyesters can be either acid or base catalyzed. The degradation products of polymers such as PLGA or PCL bear a terminal carboxylic group which are capable of decreasing the pH inside the polymer bulk. The decreased pH and the generated carboxylic acids cause autocatalytic effects leading to the faster erosion inside poly(α -hydroxy acids) in comparison to their surface (17).

4.1.2. Polymeric Drug Delivery

Table 4.1 categorizes the various controlled release technologies, including physical as well as chemical systems (18). The drug carrier complex used for implanting or injecting at a specific site can be formulated as either a reservoir type or a matrix type of drug delivery system (19). Most biodegradable systems for site-specific delivery are of the matrix type, where the drug is homogeneously dissolved or dispersed throughout the polymer (20) (Figure 4.2A). Monolithic systems are probably the simplest and least expensive way to control the release of an active agent which is dispersed in an inert polymeric matrix (21). In reservoir systems (Figure 4.2B) a core of drug is surrounded by a swollen or non-swollen polymer film (20). The mechanism of drug release from these delivery systems can be a combination of solute diffusion, and polymer erosion and/or dissolution (19).

The release rate of drugs from a polymer implant can vary widely, and have been described by a variety of mathematical models. It is instructive to first examine diffusion-controlled release from a non-biodegradable polymer with constant permeability. Drug release from a diffusion controlled monolithic device made of non-biodegradable polymer can be discussed under two main categories: a) dissolved active agent case and b) dispersed active agent case. The former describes the situation in which the active agent is dissolved in the polymer at or below saturation level. For such a planar matrix of thickness δ , immersed in a well-agitated infinite medium, the amount of active agent released by time t is given by (22,23):

$$\frac{M_t}{M_\infty} = 1 - \sum_{n=0}^{\infty} \frac{8}{(2n+1)^2 \pi^2} \exp\left[\frac{-D_m(2n+1)^2 \pi^2 t}{\delta^2}\right] \quad (\text{equation 4.1})$$

where D_m is the diffusivity of drug in polymer and M_∞ is the amount released at infinite time; it is equal to the initial active agent loading less the amount in the device which is in equilibrium with the medium at infinite time. Important simplifications of this equation may be used if one is interested in avoiding the lengthy calculations of this series solution. For a slab, the expression for the initial stages of release is:

$$\frac{M_t}{M_\infty} = 4 \left(\frac{D_m t}{\pi \delta^2} \right)^{1/2} \quad \text{for} \quad 0 \leq \frac{M_t}{M_\infty} \leq 0.6 \quad (\text{equation 4.2})$$

and the long-time approximation is:

$$\frac{M_t}{M_\infty} = 1 - \frac{8}{\pi^2} \exp\left(\frac{-\pi^2 D_m t}{\delta^2}\right) \quad \text{for} \quad 0.4 \leq \frac{M_t}{M_\infty} \leq 1.0 \quad (\text{equation 4.3})$$

It is clear that when slabs of monolithic devices are kept at constant external concentration, the fractional release is proportional to the square root of time at early stages (up to 60%) and then decays exponentially.

In the dispersed active agent case, the initial active agent loading in the polymer exceeds its solubility in the polymer. The excess produces a separate phase at equilibrium. This phase is dispersed in the polymer and causes the release characteristics to be different from the dissolved active agent case. In these systems, dissolution of the drug may be the rate-limiting step of this release process. Therefore, several models have been proposed to describe this phenomenon. Higuchi (24) offered the first model for this type of device. Using this model the following expression for drug release from a slab has been derived (25):

$$\frac{M_t}{M_\infty} = \left[\frac{2C_s D t}{A \delta^2} \right]^{1/2} \quad \text{(equation 4.4)}$$

The fraction of drug released ($\frac{M_t}{M_\infty}$) from a slab of thickness δ , at time t , is dependent of the drug's diffusion coefficient (D), solubility in the matrix (C_s), and drug loading. Drug is initially removed from the surface regions of the polymer and consequently a progressively thicker drug-depleted layer forms adjacent to the surface of the device (26).

Based on the mathematical models presented above, the *in vitro* performance of a diffusion controlled release device can be determined by a number of factors. Some of these factors are properties of the polymer-active agent system, such as drug diffusivity in the polymer vehicle and solubility. Others are design factors such as active agent loading, device geometry and barrier thickness that may be controlled independently (22).

Diffusion of an active agent in polymers occurs through the amorphous polymeric regions. The diffusivity is related to the mobility of the polymer chains and, thereby, to the free volume of the system. The free volume concept was originally proposed by Cohen and Turnbull (1959) which considers diffusion to occur due to local density fluctuations in the liquid. These fluctuations periodically open voids in between of the liquid molecules into which a diffusing molecule may jump (22). The free volume is, in turn, dependent upon a number of factors, the most prominent being the temperature of the system relative to the glass transition temperature T_g . As the system temperature is lowered and approaches T_g , the free volume available for diffusion decreases, thereby decreasing the diffusivity (22). Increasing temperature also affects viscosity as described in chapter 3 (WLF theory). At a certain temperature a polymer with lower viscosity bears more free volume therefore facilitates drug diffusion through its chains. The presence of crystallites in polymers serve to increase the tortuosity of the diffusion paths and thereby reducing diffusivity. The diffusivity of the active agent is

also a function of its own characteristics. The most significant of these is the molecular weight of the diffusing species, with bigger molecules diffusing more slowly (27).

A factor not controlled by the designer of a controlled release system, but which nevertheless may have a significant influence on the release rate is the presence of a boundary layer on the surface of the device. The boundary layer serves as an extra diffusional resistance and can restrict or slow the transport of an active agent of low solubility. To avoid this, experimental studies in the laboratory are designed to be performed under well-stirred, infinite sink conditions.

Poly(ϵ -caprolactone) is a water insoluble polymer that undergoes hydrolytic backbone cleavage and is solubilized by conversion to small, water-soluble molecules. Drug release from such a matrix is complicated because it is a combination of diffusion and erosion mechanisms. Diffusional drug release in the absence of erosion was described by equations 4.1 to 4.4 assuming that the diffusivity of drug through the polymer chains is constant at all times. In biodegradable polymers, diffusivity changes due to the change in molecular weight of the polymer. As the chains cleave they become more flexible and mobile and therefore produce more free volume in between the chains. Increased free volume facilitates drug diffusion and thereby, the drug release rate increases. With no erosion, drug release slowly declines following the so-called $t^{-1/2}$ kinetics. However, because of polymer degradation which causes diffusivity to rise above the initial value, the normal decline is slowed and then in the final stages it may even be reversed (Figure 4.3) (27).

4.1.3. Objectives

One hypothesis of this work is that incorporation of CPT into a generally hydrophobic polymer carrier would enhance the stability of the as-yet unreleased drug while within the polymer. Another hypothesis is that the incorporation of an alkane block to the caprolactone initiator would provide an increase in CPT solubility within the oligomer. To facilitate the implantation of the polymer-drug depot, an injectable system has been designed. The presence of the dispersed active agent, in our case CPT, can promote the formation of drug crystals which in turn increases the viscosity of the polymer/drug mixture. This increase in viscosity is not desirable due to its negative

impact on the syringeability of the polymeric system. Therefore, we would like to have CPT dissolved in our delivery system without reaching its saturation point.

In this chapter the capability of the synthesized CL oligomers in solubilizing CPT and keeping it in its active lactone form is examined. Second, the release of CPT from PCLs initiated with different alcohols is investigated and compared with CPT release rates from PLGA (50:50 mole percent). PLGA (50:50) has been utilized in forming microspheres for stabilizing CPT (28), and this is used as a control to compare the performance of our system with other systems.

4.2. Materials

20-S-camptothecin (96% purity) was obtained from Aldrich (Milwaukee, WI). PLGA with an inherent viscosity of 0.19 dl/g ($M_n = 6000$ daltons) was purchased from Birmingham Polymers (Birmingham, AL). CL oligomers initiated with ethanol, 1-dodecanol, 2-dodecanol and oleyl alcohol were synthesized and purified as described in Chapter 2. 10 and 20 mL scintillation glass (Type I) vials with PTFE screw caps were purchased from Fisher Scientific. HPLC grade acetonitrile and water were purchased from Fisher Scientific. Analytical grade sodium chloride, di-sodium hydrogen phosphate, potassium dihydrogen phosphate, potassium chloride and Tween 80 were purchased from Sigma (USA).

4.3. Methods

4.3.1. Differential Scanning Calorimetry (DSC)

DSC was carried out using a Seiko 120 DSC. The heating rate was 10 °C/min and the drug/oligomer samples were weighed (10-15 mg) into crimped sealed aluminium sample pans.

4.3.2. CPT Solubility in PCL and PLGA (50:50)

Given amounts of CPT were weighed into 10 mL glass vials. Into each vial 100 mg of CL oligomer was added to prepare loading levels of 0-20% CPT. Aliquots of chloroform/methanol (8:2 v/v) were added to the vials and mixed until it formed a clear solution. Under constant stirring on a stirrer/heater, and a constant stream of nitrogen and mild heat (60 °C) the solvent was evaporated. The precipitant was transferred into a preheated vacuum oven (30 °C) and kept under vacuum for 24 hrs to remove any residual solvent (29). The samples were removed from the oven and cooled to room temperature and analyzed by DSC.

4.3.3. Manufacture of Paste Formulations

CPT, at loadings of 50% of its saturation concentration in CL oligomers (i.e., 5 mg CPT/100 mg oligomer) and PLGA (i.e., 1.5 mg CPT/100 mg PLGA), was thoroughly dissolved in a chloroform/methanol mixture (8:2 v/v). The solvent was evaporated and the mixture was rendered solvent free as explained above. The CPT loaded pastes were weighed into 1 mL syringes and stored at 4 °C.

4.3.4. HPLC Analysis of CPT

Carboxylate and lactone levels of CPT were determined by high performance liquid chromatography (HPLC), which allows separation of the two forms of the drug within a single chromatographic run. The HPLC system consisted of the following: a Chem Mate pump, a Basic Marathon auto sampler (Rose Scientific) fitted with a 100 µL sample loop, a Waters 470 scanning fluorescent detector with 360nm excitation and 440nm emission, and a Hewlett Packard 3390A integrator (Middleton, WI). The separation was carried out using a Phenomenex Hypersil BDS-C₁₈ reverse phase column. The mobile phase was composed of 26% by volume acetonitrile and 74% triethylamine acetate buffer (TEAA) (1% v/v triethylamine in water, adjusted to pH 5.5 with glacial acetic acid) and was delivered at a flow rate of 1.0 mL/min in all experiments. The mobile phase was filtered and vacuum degassed prior to use. Retention times of the carboxylate and lactone were around 4 and 9 minute, respectively. A calibration curve was prepared before each experiment for the conversion of total lactone and carboxylate

area to concentration. A typical calibration curve and chromatogram are shown in Figures 4.4 and 4.5.

4.3.5. Evaluation of *in Vitro* Drug Release

Drug release from the samples was carried out in phosphate buffer saline (PBS) (8mM Na₂HPO₄, 1mM KH₂PO₄, 137 mM NaCl, 3mM KCl, pH=7.4) containing Tween 80 (0.05% w/v) at 37 °C under perfect sink condition. Since CPT has poor solubility in water, Tween 80 was included to increase the solubility of CPT in PBS (28). 1 mL syringes loaded with drug/polymer mixture were placed in preheated oven (55 °C) for 30 minutes to bring the mixture to a complete liquid state. The syringes were then transferred into another preheated oven (47 °C) and kept for 30 minutes. While inside the oven one drop of each sample (~ 50 µl) (Table 4.2) was transferred into a 20 mL scintillation glass vial and quickly transferred into a 37 °C-preheated oven. 20 mL PBS (37 °C) was added to the vials and the vials then mounted on a rotary shaker Model 099A RD4524 (Fisher Scientific) which was already placed inside an oven (37 °C). The rotation speed was set to 10 rpm. The buffer was replaced at frequent time intervals initially to characterize the burst of the drug from samples, and then at less frequent intervals to examine the long-term release behaviour. Concentrations of both active lactone and carboxylate forms of CPT in the release media were determined by HPLC and used as the total amount released in each time point.

4.3.6. Examination of the Stability of CPT in CL Oligomers

The extent to which CPT remained stable in the CL oligomers was evaluated by three methods: 1) by extracting the drug from CL oligomers right after drug incorporation to ensure that the method of preparation had no effect on CPT stability, 2) by capturing the CPT in the release media before significant lactone to carboxylate conversion could take place, and 3) by extracting CPT from the CL oligomers after 2 months incubation in PBS (37 °C) to determine any significant lactone to carboxylate conversion.

In method one, 5 mg of the drug-loaded samples were weighed into a glass centrifuge tube. Chloroform 0.1 mL was added into the tube and mixed thoroughly to

dissolve the oligomer while the drug remained undissolved. 5 mL cold methanol was added to the centrifuge glass tube to completely dissolve the CPT while forcing the oligomer to precipitate. The centrifuge tube was stored in the freezer (-10 °C) for complete precipitation of the oligomers. Then, it was centrifuged for 3 minutes at 5000 rpm to collect the polymer sample into the bottom of the tube. 0.5 mL of the supernatant was taken out and diluted to 100 mL with TEAA buffer pH=6.1 and immediately analyzed by HPLC. In previous studies it was shown that the rate of lactone to carboxylate conversion is minimal at pH=6.5 (<8% of drug converts to carboxylate form in 10 minutes) and this gives enough time to the examiner to analyze the true composition of the drug before any significant conversion happens (28). In these studies, it was found that at pH=6.1 the rate of lactone to carboxylate is much slower than at pH=6.4 and it is more suitable to use this pH for the experiments (<1% of drug converts to carboxylate form in 10 minutes).

In the second method, drug-loaded samples were washed with water and exposed to PBS pH=6.1 for 10 minutes at 37 °C. The released CPT was immediately analyzed before significant lactone to carboxylate conversion could take place. By using this method, it was possible to determine not only what form of CPT is present in the samples, but also which form actually is released from the samples.

In the third method, samples were exposed to PBS pH 7.4 at 37 °C for 2 months. They were washed with pure water and CPT was extracted as explained in method 1. The drug was analyzed with HPLC for detection of any lactone to carboxylate conversion. By using this method, it was possible to determine whether PBS was able to penetrate through the oligomer chains and hydrolyse CPT.

4.4. Results and Discussion

4.4.1. CPT Solubility in Oligomers

To investigate the solubility of CPT in different CL oligomers and PLGA, the thermal behaviour of CL oligomers, PLGA and CPT was investigated separately. Figure 4.6A illustrates the thermal behaviour of CL oligomers initiated with oleyl alcohol. The

endotherm around 40 °C corresponds to the melting point of the polymer while the exotherm around 300 °C corresponds to oligomer decomposition. To confirm the thermal behaviour of the CL oligomer another sample (i.e., CL oligomer initiated with 2-dodecanol) was treated with heat in the same manner (Figure 4.6B). These oligomers clearly showed a melting point around 45 °C and decomposition point around 300 °C. The same method was utilized to determine the melting point and thermal behaviour of PLGA (Figure 4.7A) and CPT (Figure 4.7B).

The DSC analysis revealed that the melting point of CPT is around 265.5 °C which is in agreement with literature (265-267 °C) (28). By mixing CPT with CL oligomers, the drug can exist in the mixture either dissolved in the oligomer or undissolved (i.e., above saturation). In the first case (i.e., dissolved) no drug crystals exist in the mixture and DSC analysis of the drug/oligomer mixture is expected to show only one endotherm related to the melting point of the oligomer. In the second case where the drug is undissolved in oligomers and drug crystals are present in the drug/oligomer mixture, we expect to observe two separate endotherms, one related to oligomer melting point and the other related to CPT melting point (29).

Four different candidates (i.e., CL oligomer initiated by ethanol, 1-dodecanol, 2-dodecanol and oleyl alcohol) were chosen to investigate the effect of different initiators with different hydrophobicity on the solubility of CPT. The CL oligomer initiated by ethanol was the first tested and, as illustrated in Figure 4.8A, at a ratio of 9.2 mg CPT/100 mg oligomer, the drug remained dissolved in the oligomers. When the concentration of CPT in the oligomer increased to 9.8 mg/100mg a small endotherm related to CPT crystals appeared in the DSC spectrum (Figure 4.8B). To confirm this observation and make sure that the observed endotherm truly corresponds to CPT, the concentration of CPT in the oligomer was increased to 20 mg/100mg (Figure 4.8C). Ertl et al. (1999) (30), reported the same type of thermal behaviour for CPT dispersed in PLGA. CPT solubility in the other CL oligomers (Figures 1-4, Appendix E) and in PLGA (Figure 4.9) was determined in the same manner.

Table 4.3 summarizes the result of CPT solubility in CL oligomers initiated with different initiators and in PLGA. The CL oligomers can solubilize CPT up to 11 mg in each 100 mg of oligomer, which is at least 10000 times more than its solubility in water

(2.5 µg/mL) and 3 times more than PLGA. The results depicted in Table 4.3 do not show a clear difference of CPT solubility in the different CL oligomers. It was hypothesized that different CL oligomers with different hydrophobicity would show different CPT solubility. This lack of differentiation could be attributed to the insufficient sensitivity of our DSC instrument for this experiment, or may be an indication that CPT solubility is determined solely by its affinity for the CL component of the oligomer.

4.4.2. Effects of CPT Loading on Oligomer Physical Properties

The effect of CPT loading on the characteristics of the CL oligomers was investigated by determining the melting point changes. CL oligomers initiated with ethanol (the smallest initiator) and oleyl alcohol (the largest initiator) were chosen as two examples with different initiator, and alkane, chain sizes. In comparison to unloaded CL oligomers, the T_m of CPT-loaded-oligomers appeared to rise slightly but the increase was within the experimental error of the equipment (± 0.2 °C) and so the result is not considered significant (Table 4.4).

4.4.3. CPT Stability

Since carboxylate conversion limits bioavailability and efficacy of CPT, maintenance of the lactone structure during preparation and release is a prerequisite for improved therapy using injectable implants. Different methods of analysis have been developed by different investigators to capture both lactone and carboxylate form of CPT by a single chromatographic run (31-34). Among all four methods tried, the method suggested by Warner et al., was adopted due to its simplicity and high degree of reproducibility (34). As determined by isocratic reversed-phase HPLC, at pH= 6.1 the conversion of lactone to carboxylate is minimal (Appendix F, Figures 1-3). Working at this pH makes it possible to analyse the true configuration of CPT as is without any significant conversion.

The carboxylate form of CPT, which is more hydrophilic than the lactone form, has a retention time of around 4 minutes while that of the lactone form is around 9 minutes. Therefore, in a sample consisting of only the lactone form a lone peak at 9

minutes is expected (Appendix F, Figure 1). Since the kinetics of lactone to carboxylate conversion at pH=6.1 is slow, after 30 minutes a small peak related to carboxylate form of CPT appeared while the peak related to lactone form dwindled (Appendix F, Figures 2 & 3).

Based on this method, CPT after incorporation into the CL oligomers was analyzed and no lactone to carboxylate conversion was observed (Appendix F, Figures 4-6). The presence of one peak around 9 minutes emphasized the existence of the lactone form only. To confirm this finding, a drug-loaded CL oligomer was prepared and incubated in PBS pH=6.1 for 10 minutes and the released CPT was captured for configuration analysis. The results showed that only the lactone form of CPT is present in the prepared sample and it is only the lactone form which is released into the media (Appendix F, Figure 7). Overall, it was concluded that the preparation method does not have any harmful effect on the stability of CPT and it is only the lactone configuration of CPT which is releasing into the buffer medium.

During long-term drug release studies in PBS (two months), no conversion of lactone to carboxylate was observed (Figure 4.10). This result proves that the delivery system was capable of preserving the lactone ring of CPT from water even after incubation for two months in PBS pH=7.4. This finding can be explained by considering the hydrophobicity of the CL oligomers which limits water penetration into the device and thus prevents hydrolysis of the CPT molecules.

4.4.4. *In Vitro* Studies

For *in vitro* studies, drug-loaded oligomers with a concentration of 5 mg CPT in 100 mg of CL oligomer were prepared. As discussed above, this concentration is approximately 50% of the determined CPT saturation concentration in the oligomer. For the PLGA samples two different concentrations (i.e., 1.5 mg CPT/100 mg PLGA, & 5 mg CPT/100 mg PLGA) were prepared.

According to the release of drugs from monolithic solution systems we should expect that the *in vitro* release profile of CPT from CL oligomers follow the square root of time kinetics up to mass fraction released of 0.6 (i.e., diffusion controlled) (Figures 4.11 A & B). The slope of each line (mass released vs $t^{1/2}$, Equation 4.2) is directly

related to the diffusivity of CPT in each vehicle (Table 4.5). In the early stages, where the drug concentration is high and there has not been a significant polymer degradation and thereby, constant diffusivity; the release of the drug follows the square root of time. As time goes by, the drug concentration in the polymer bulk decreases and therefore, the rate of the release decays exponentially and doesn't follow the square root of time anymore (equation 4.3). Meanwhile, the polymer starts to degrade into smaller molecular weight chains providing more free volume for the drug molecules to diffuse, hence the diffusivity of the drug within the polymer increases producing an increase in drug release rate. The combination of these factors that work against each other in terms of drug diffusivity, has made it difficult to predict the real mechanism of release from biodegradable polymers.

Examination of the defining equation shows that device thickness is important in determining how fast the drug will be released. In the prepared samples the thickness and shape of the oligomer/drug droplets were slightly different as they were randomly placed on the bottom of the glass vials. It is possible that this difference between the thicknesses of samples is responsible for the different rates of drug release. However, the impact of thickness was minimized by preparing the samples in triplicate as this difference is randomly dispersed among all the samples. Therefore, the drug release rate from the oligomers was compared by assuming no significant thickness effect in drug release.

The CPT release profile from CL oligomers was analyzed statistically by comparing the slope of the lines in the release profile using two tailed student's t-test. The statistical analysis of results revealed that, overall, the drug release rate from the oligomers were different ($p < 0.05$). As discussed earlier, the degree of crystallinity has a significant impact on drug release. The degree of crystallinity of the drug loaded oligomers was calculated and no significant difference among different oligomers was observed (Table 4.5). It is noteworthy that all the samples that prepared for *in vitro* studies had a melting point close to 37 °C and at this temperature it is plausible to assume that the crystallinity of the oligomer vehicle is reduced over that reported in Table 4.5. Therefore, the effect of degree of crystallinity on drug release rate can be considered insignificant.

The second important factor which has an impact on drug release rate is the rheological behaviour of the oligomers. Oligomers with lower melt viscosity have more mobile chains, allowing the drug molecules to diffuse easier. Based on this fact the drug release profile of CPT from different oligomers was analysed. By comparing the slope of the release profile of CPT from different oligomers, the only non-significant difference was observed between CL-1-dodecanol (caprolactone oligomer initiated with 1-dodecanol) and CL-oleyl alcohol (caprolactone oligomer initiated with oleyl alcohol). It is obvious from Table 4.5 that CL-oleyl alcohol has almost the same melt viscosity as CL-1-dodecanol. This similarity can be interpreted into same free volume at a given temperature for both oligomers, allowing the drug molecules to release with the same pace. By analysing the rate of drug release from the other oligomers, it can be concluded that the lower the melt viscosity at a given temperature the higher the free volume and the faster the release rate (Table 4.5).

After 190 days of incubation in PBS (pH=7.4, 37 °C) it was only the CL-oleyl alcohol which showed signs of degradation while macroscopically the others remained intact. This faster rate of degradation can be attributed to the lower viscosity and lower melting point of the oligomer and thus a higher rate of water imbibition by the CL-oleyl alcohol block oligomers.

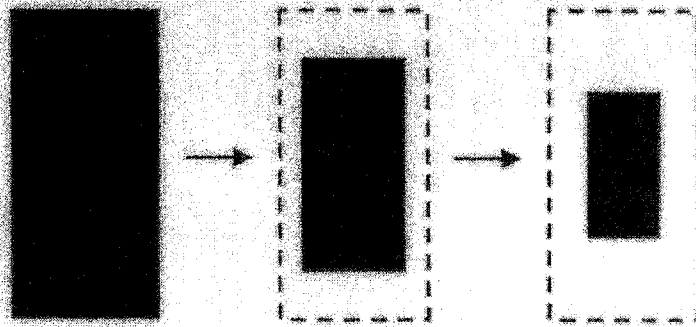
PLGA has a T_g of around 60 °C, therefore at the release conditions (37 °C) polymer is in its glassy state and drug release through the polymer chains is highly restricted (phase 1) (Figure 4.12.). This continues for a period of one month till water cleaves the esteric linkages inside the PLGA therefore \overline{M}_n and T_g of the oligomer decreases and it swells. This swelling changes the mobility of polymer chains and increases the water imbibition and the diffusivity of drug. All these changes lead to a significant release of drug in the second phase. The final stage is related to the release of drug from the fragmented pieces of polymer (phase 3) (14). This pattern of drug release which consisted of releasing drug in very small doses for a period of 30 days followed by a burst in drug release does not seem to be suitable for effective camptothecin delivery.

The statistical analysis of drug release from PLGA loaded with 1.5% drug (PLGA 1.5%) and PLGA loaded with 5% drug (PLGA 5%) by using repeated measure analysis showed that the rate of release from the latter was slower ($p < 0.05$). Higher load of CPT which is a hydrophobic drug in PLGA seems to delay the water imbibition process and therefore the drug released into the media with a slower pace.

4.5. Concluding Remarks

The newly developed delivery system provided a suitable carrier to preserve the active lactone form of drug and release of CPT in sustained fashion for a period of 190 days. The active lactone form was preserved mainly by hydrophobicity of the oligomers and depriving the drug from its aqueous surrounding. CL-oleyl alcohol seemed to be more suitable for CPT delivery than the other oligomers due to its lower degradation lifetime. This depot system might present an alternative to unpleasant repeated i.v. administration.

Surface erosion



Bulk erosion

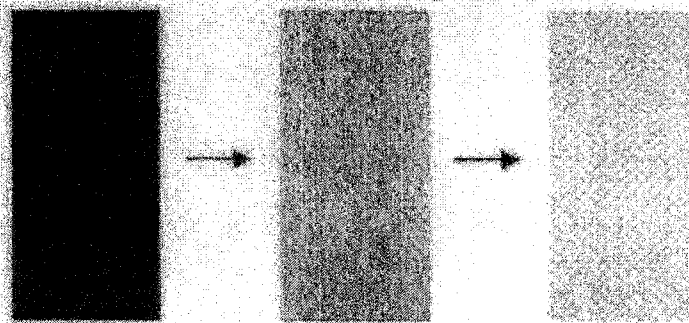
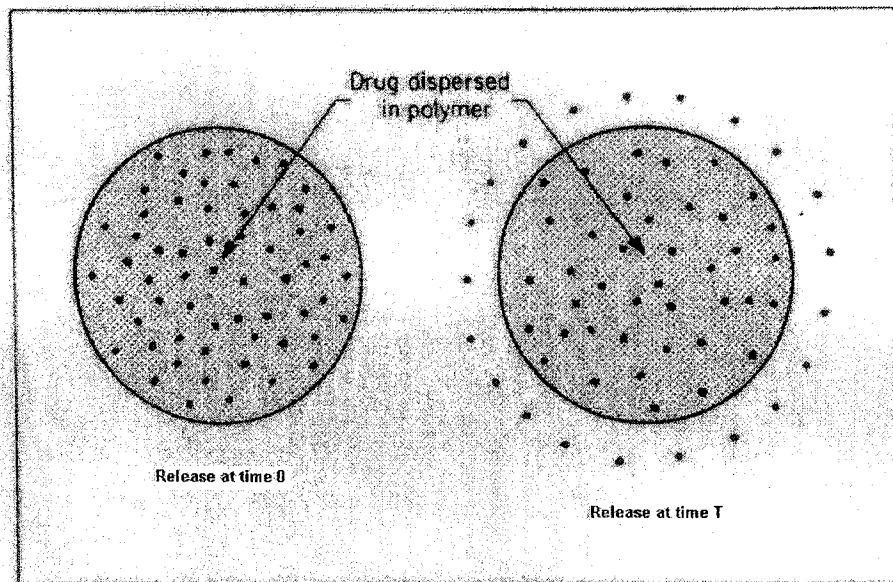


Figure 4.1. Schematic illustration of the principle of surface and bulk erosion. Reproduced from reference 13 with permission from Elsevier Science.

A)



B)

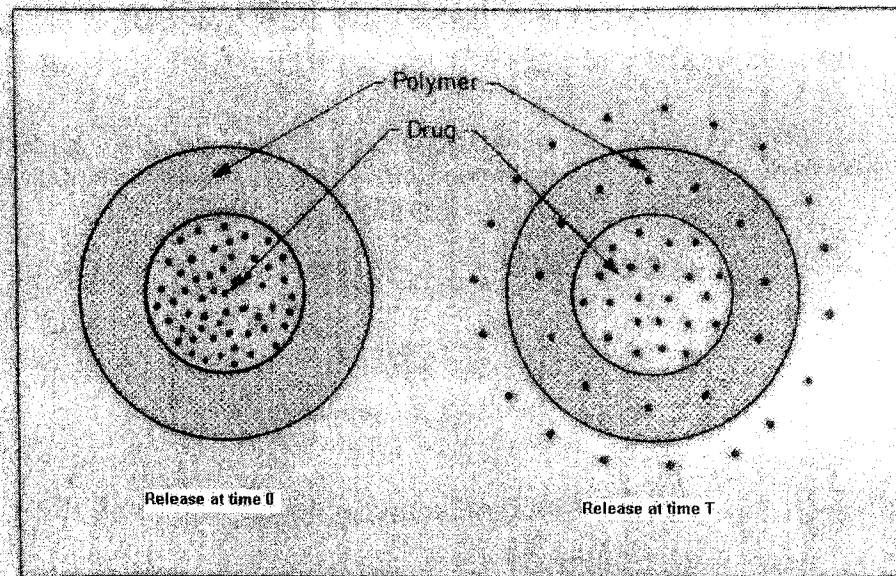


Figure 4.2. A) Idealized diffusion-controlled matrix release system. B) Idealized diffusion-controlled reservoir release system. Reproduced from reference 20.

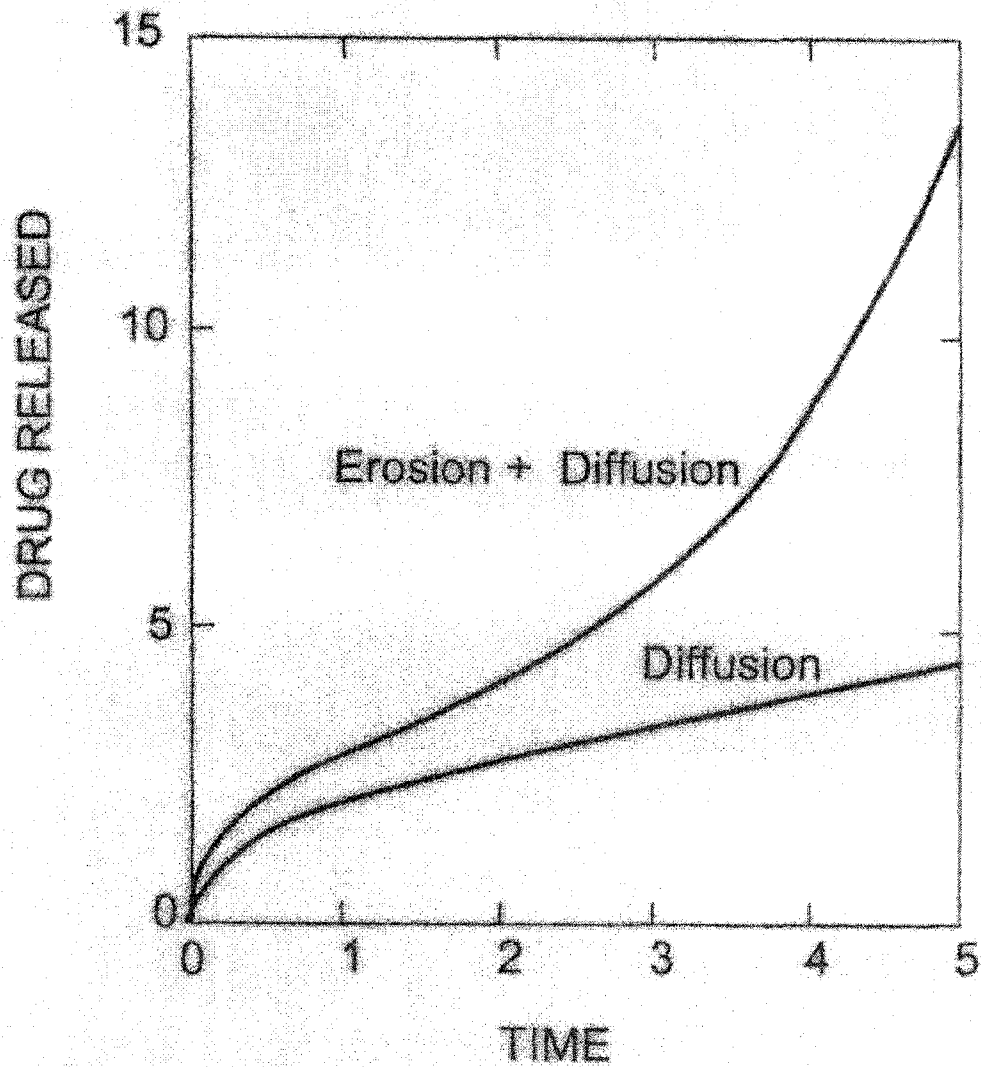


Figure 4.3. Model of Helen and Baker describing drug release from thin biodegradable polymer films under going bulk erosion (curve: Erosion+Diffusion). For comparison, also purely diffusion controlled release kinetics calculated using classical Higuchi equation are illustrated (curve: Diffusion). Reproduced from reference 13 with permission from Elsevier Science.

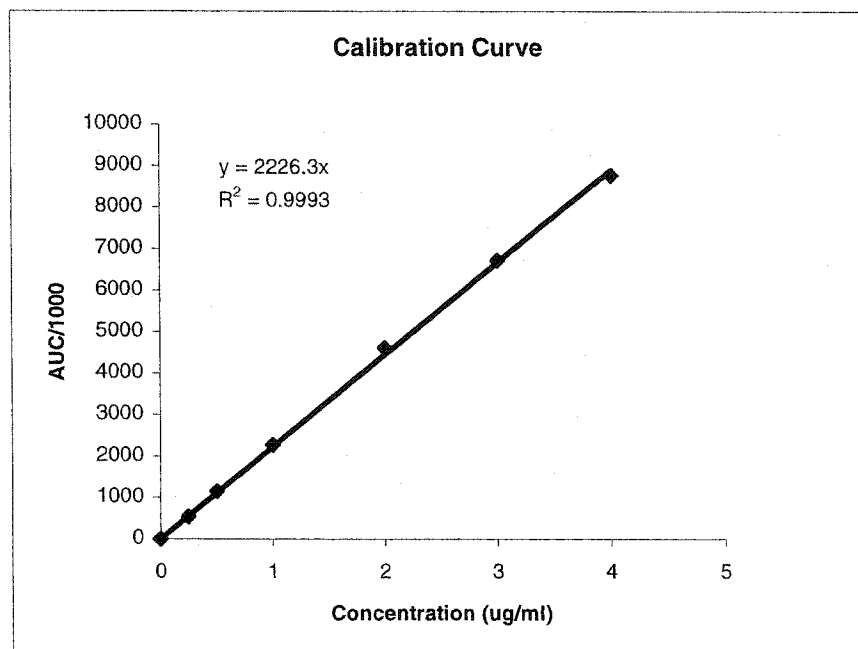


Figure 4.4. A typical calibration curve for HPLC analysis of CPT. Concentrations of 0.25, 0.5, 1, 2, 3 and 4 $\mu\text{g}/\text{mL}$ of CPT were prepared and used as calibration points.

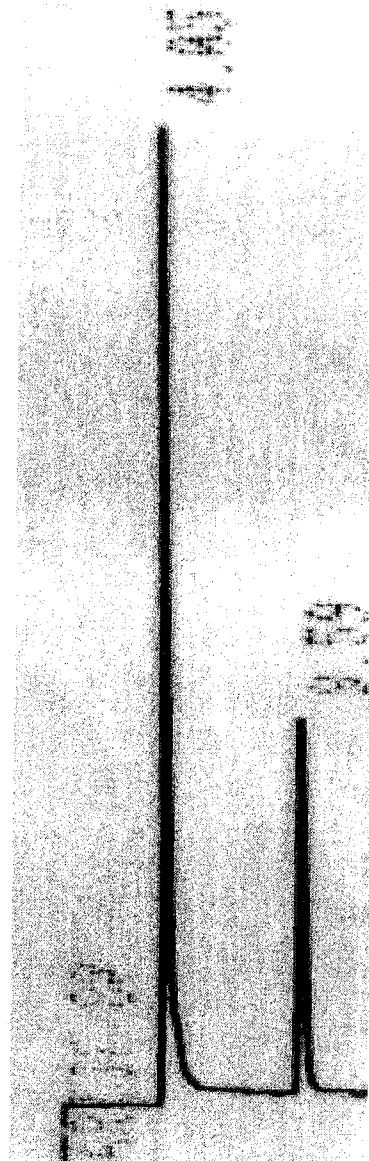
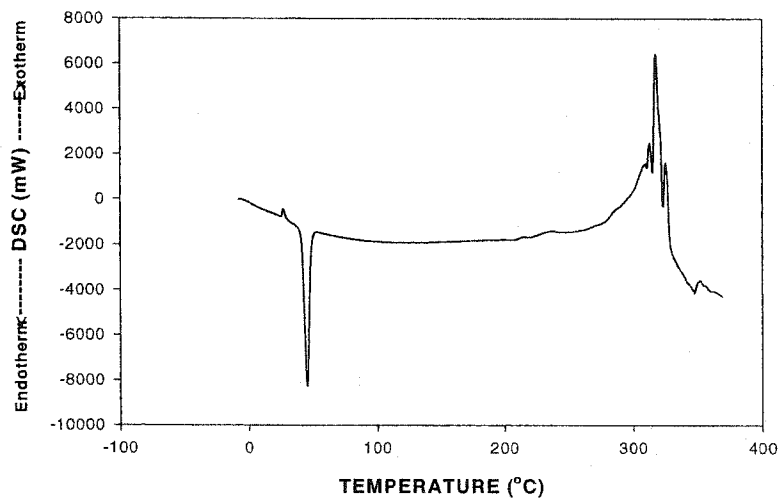


Figure 4.5. HPLC analysis of CPT at pH=7.4. Peaks with Retention Time of 4.05 & 9.59 minutes correspond to carboxylate and lactone forms of CPT.

A)



B)

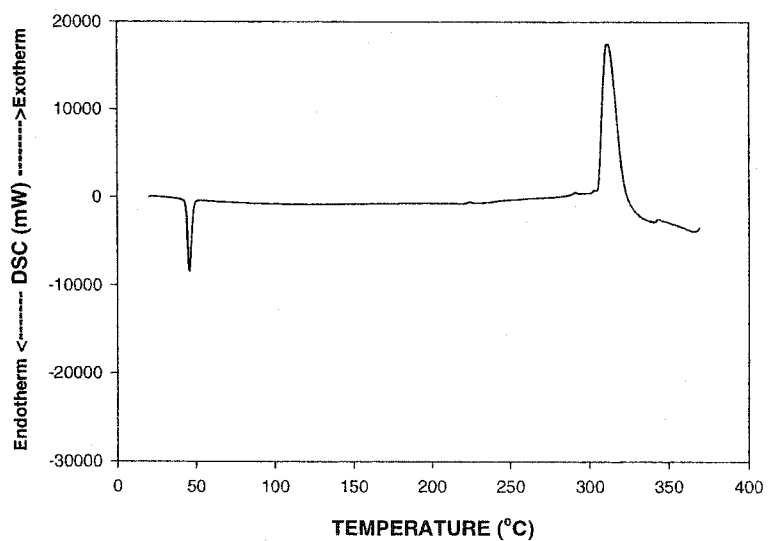
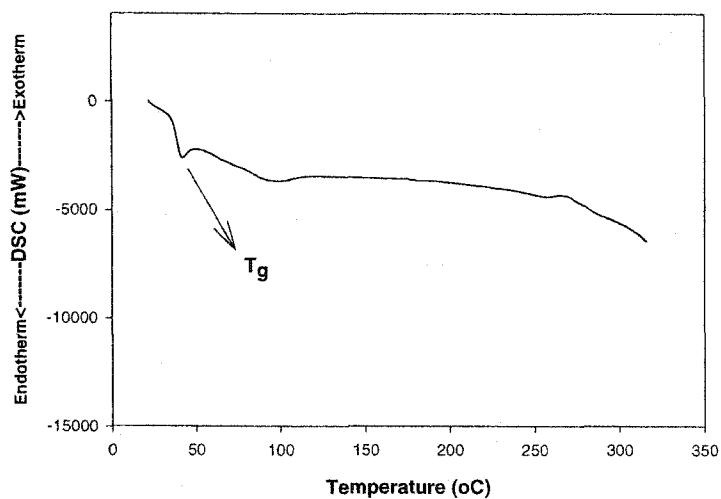


Figure 4.6. Thermal behaviour of CL oligomer initiated by A) oleyl alcohol, and B) 2-dodecanol. Endotherm around 40 °C corresponds to oligomer melting point and exotherm around 300 °C corresponds to oligomer decomposition.

A)



B)

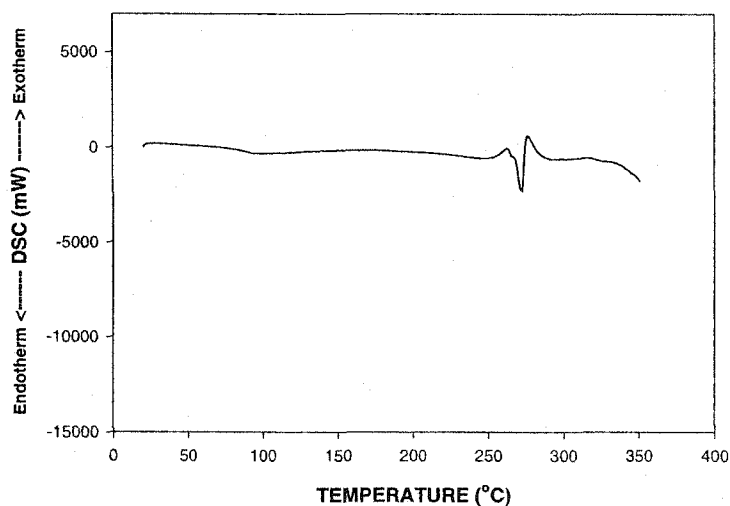
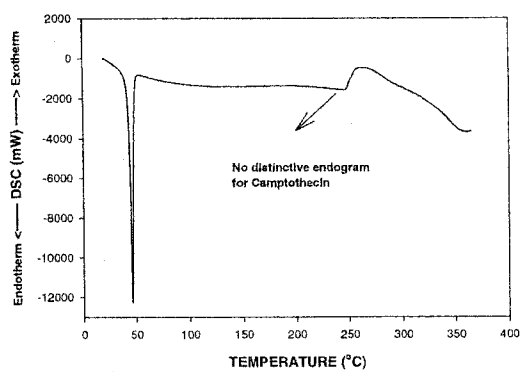
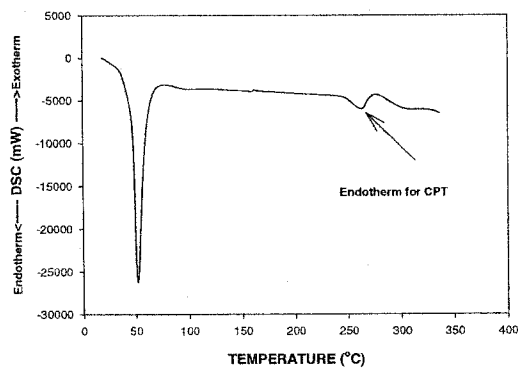


Figure 4.7. A) Thermal behaviour of PLGA. No endotherm was observed due to amorphous nature of PLGA. T_g was determined to be around 40 °C. B) DSC analysis of CPT. The melting point of CPT determined to be 265.5 °C.

A)



B)



C)

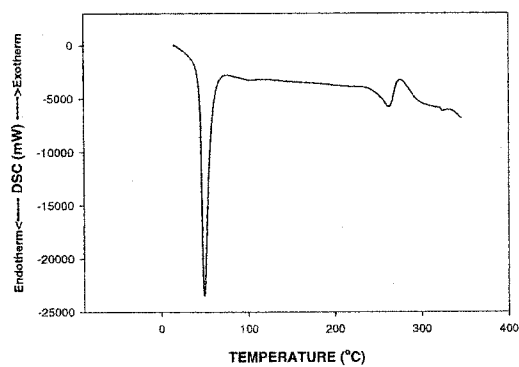


Figure 4.8. DSC analysis of CL oligomer initiated with ethanol mixed with CPT. Drug/ oligomer ratio of A) 9.2 mg/100 mg, B) 9.8 mg/100 mg, C) 20 mg/ 100 mg.

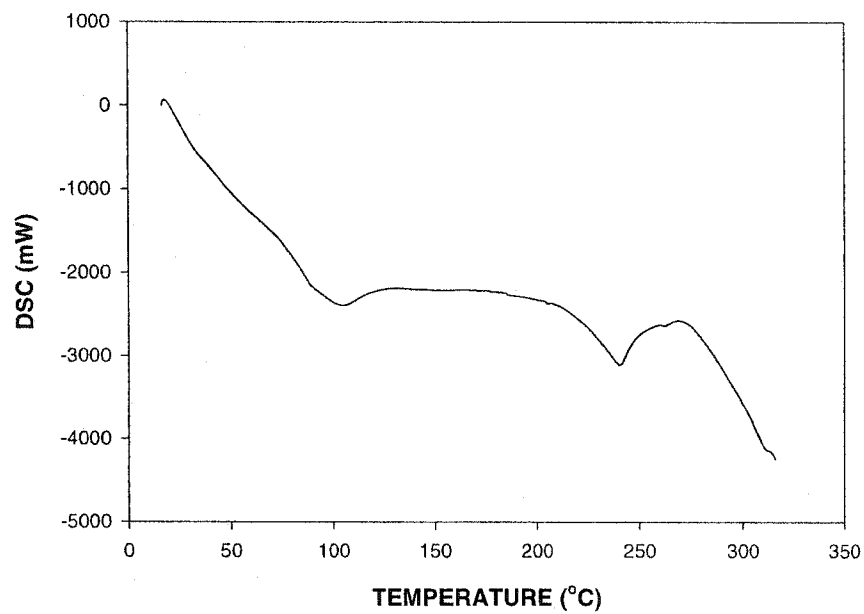


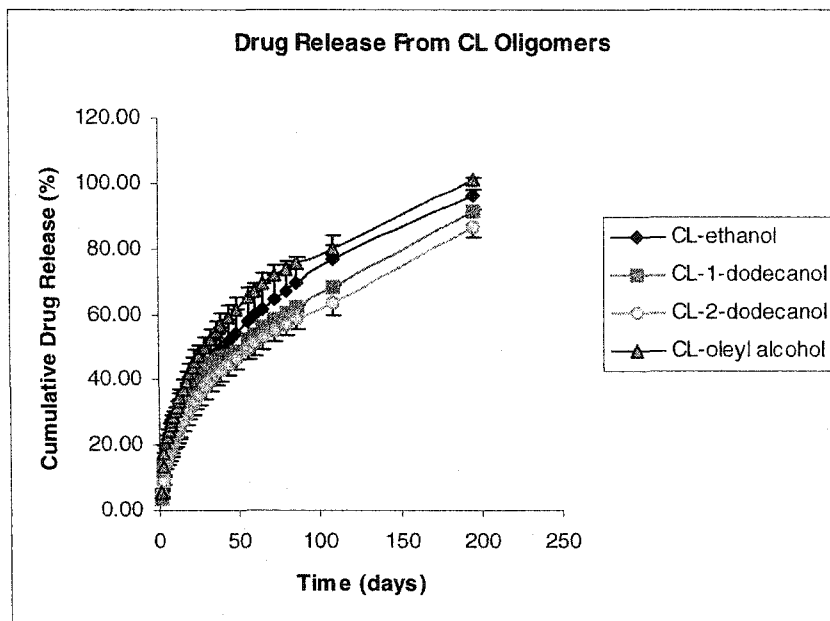
Figure 4.9. DSC analysis of PLGA mixed with CPT. Drug/ PLGA ratio of 3.5 mg/100 mg. Presence of an endotherm at 250 °C corresponds to the presence of the CPT crystals.



Figure 4.10. HPLC analysis of CPT after incorporation into CL oligomers and incubation in PBS (pH=7.4) for two months. (first injection, time=0 min). No retention time for carboxylate form was observed.

<u>Retention Time</u>	<u>Area %</u>	
9.50	100%	Lactone form

A)



B)

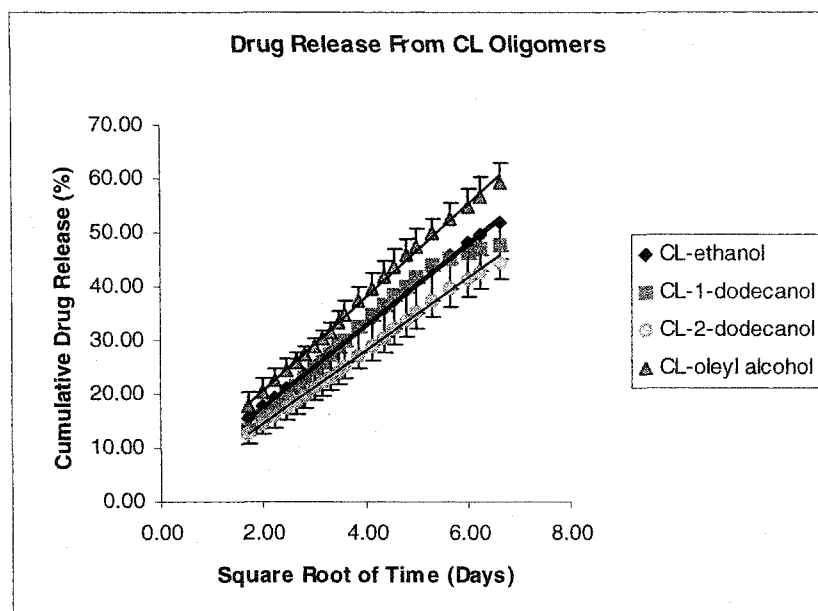


Figure 4.11. Cumulative release profile of CPT \pm SD from CL oligomers initiated with ethyl alcohol, 1-dodecanol, 2-dodecanol and oleyl alcohol ($n=3$). The drug load was 5 mg per 100 mg of oligomers. **A)** Amount releases versus time, **B)** Amount released versus square root of time for the short time approximation.

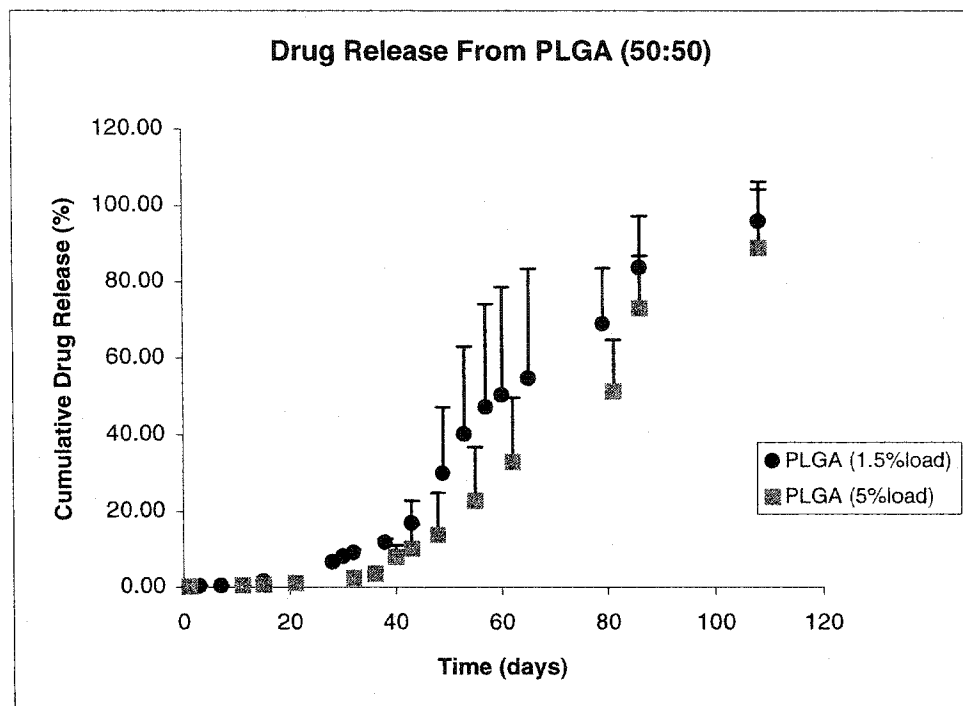


Figure 4.12. Cumulative release profile of CPT \pm SD from PLGA samples (n=3). The drug load was 1.5 and 5 mg per 100 mg of PLGA.

Table 4.1. Categories of polymeric systems for controlled release. Reproduced from reference 18.

I- Physical Systems

- A:** Reservoir systems with rate-controlling membrane
- 1- *Microencapsulation*
 - 2- *Macroencapsulation*
 - 3- *Membrane systems*
- B:** Reservoir systems without rate-controlling membrane
- 1- *Hollow fibres*
 - 2- *Poroplastic® ultramicroporous cellulose triacetate*
 - 3- *Porous polymeric substrate and foams*
- C:** Monolithic Systems
- 1- Physically dissolved in nonporous, polymeric matrix
 - a: *Nonerodible*
 - b: *Erodible*
 - c: *Environmental agent ingression*
 - d: *Degradable*
 - 2- Physically dispersed in nonporous, polymeric matrix
 - a: *Nonerodible*
 - b: *Erodible*
 - c: *Environmental agent ingression*
 - d: *Degradable*
- D:** Laminated Structures
- 1- *Reservoir layers chemically similar to outer control layers*
 - 2- *Reservoir layers chemically dissimilar to outer control layers*
- E:** Other Physical Methods
- 1- *Osmotic pumps*
 - 2- *Adsorption onto ion-exchange resins*

II- Chemical Systems

- A:** Chemical erosion of polymer matrix
- 1- *Heterogeneous*
 - 2- *Homogeneous*
- B:** Biological erosion of polymer matrix
- 1- *Heterogeneous*
 - 2- *Heterogeneous*
-

Table 4.2. Drug loaded samples for *in vitro* studies. In all samples in every 100 mg of polymer 5 mg drug was loaded, unless stated otherwise.

Sample Name	Sample No.	Sample Weight (mg)	Sample Drug Content (mg)*	Total Amount Remained (mg)**
PCL-ethanol (5% load)	1	16	0.800	0.027
	2	14.9	0.745	0.024
	3	15.2	0.760	0.009
PCL-1-dodecanol (5% load)	1	15.7	0.785	0.043
	2	15.4	0.770	0.021
	3	15.6	0.780	0.016
PCL-2-dodecanol (5% load)	1	16.3	0.815	0.017
	2	16.2	0.810	0.015
	3	16.1	0.805	0.023
PCL-Oleyl alcohol (5% load)	1	16.4	0.820	0
	2	16.1	0.805	0
	3	13.4	0.670	0
PLGA (1.5% load)	1	15	0.225	0
	2	15.8	0.237	0
	3	15.4	0.231	0
PLGA (5% load)	1	15.7	0.785	0
	2	16	0.800	0
	3	14.2	0.710	0

* Sample drug content: expresses the amount of drug present in sample initially.

** Total Amount Remained: shows the total amount of drug remained in the samples at the end of *in vitro* studies.

Table 4.3. Investigation of the solubility of CPT in CL oligomers initiated with different initiators. It can be observed that all the synthesized oligomers were capable of dissolving CPT around 10 mg in every 100 mg of the oligomer.

Sample No.	Type of Initiator	CPT Mass (mg)	Oligomer Mass (mg)	Solubility Status
1	ethanol	9.2	100	yes
2	ethanol	9.8	100	no
3	oleyl alcohol	9	100	yes
4	oleyl alcohol	10.5	100	yes
5	oleyl alcohol	11	100	no
6	1-dodecanol	9	100	yes
7	1-dodecanol	11	100	yes
8	1-dodecanol	11.5	100	no
9	2-dodecanol	9	100	yes
10	2-dodecanol	10	100	yes
11	2-dodecanol	10.5	100	no
PLGA (50:50)	N/A	3	100	yes
PLGA (50:50)	N/A	3.5	100	no

Table 4.4. Effect of CPT loading on the melting point of unloaded CL oligomers. No significant difference was observed in terms of solubility of CPT in different oligomers. All samples were analyzed in triplicates.

CL oligomer	Initiator	CPT (mg)	Drug/Polmer ratio	T _m (°C)*
1	ethanol	0	0	46.1±0.1
2	ethanol	4	4/100	47.7±0.3
3	ethanol	7	7/100	47±0.2
4	ethanol	10	10/100	47.3±0.1
5	ethanol	20	20/100	47.3±0.2
6	oleyl alcohol	0	0	43.4±0.1
7	oleyl alcohol	4	4/100	45.3±0.1
8	oleyl alcohol	7	7/100	44.7±0.2
9	oleyl alcohol	10	10/100	44.6±0.3
10	oleyl alcohol	20	20/100	45±0.2

* T_m was determined based on the endotherm mid-point observed.

Table 4.5. Effects of viscosity and crystallinity on the diffusivity of CPT from different vehicles. No significant difference was observed in terms of degree of crystallinity among different oligomer/ drug mixtures. The slope of the line is an indicative of the rate of drug release. It can be observed that the lower the viscosity the higher the drug release rate.

Initiator	%crystallinity	Viscosity at 50 °C	Melting Point (°C)	Slope	S.D.	R ²
oleyl alcohol	65±8.6	0.11±0.005	37.9	8.72	0.1	0.997
2-dodecanol	65±7.4	0.13±0.005	39.5	6.79	0.06	0.998
1-dodecanol	73±8	0.10±0.030	39.6	8.65	0.05	0.978
ethanol	74±7.2	0.15±0.013	41.7	7.63	0.08	0.998

4.6. References

- [1]- B. Ertl , P. Platzer, M. Wirth, F. Gabor, Poly(D-L-lactic-co-glycolic acid) microspheres for sustained delivery of camptothecin. *J. Controlled Release* 61 (1999) 305-317.
- [2]- C. D. Conover, R. B. Greenwald, A. Pendri, K. L. Shum, Camptothecin delivery systems: the utility of amino acid spacers for the conjugation of camptothecin with polyethylene glycol to create prodrugs. *Anti-Cancer Drug Design* 14 (1999) 499-506.
- [3]- B.B. Lundberg, Biologically active camptothecin derivatives for incorporation into liposome bilayer and lipid emulsions. *Anti-Cancer Drug Design* 13 (1998) 453-461.
- [4]- J. O'leary, F. M. Muggia, Camptothecins: A review of their development and schedules of administration. *Eur. J. Cancer* 34 (1998) 1500-1508.
- [5]- S.C. Woodward, P.S. Brewer, A. Schindler, C.G. Pitt, The intracellular degradation of poly(ϵ -caprolactone). *J. Biomed. Mater. Res.* 19 (1985) 437-444.
- [6]- T. Ouhadi, C. Stevens, P. H. Teyssie, Study of poly- ϵ -caprolactone bulk degradation. *J. Appl. Polym. Sci.* 20 (1976) 2963-2970.
- [7]- C. G. Pitt, M. M. Gratzl, G. L. Kimmel, J. Surles, A. Schindler, Aliphatic polyesters II. The degradation of poly(DL-lactide), poly(ϵ -caprolactone), and their copolymers *in vivo*. *Biomaterials* 2 (1981) 215-220.
- [8]- C. G. Pitt, F. I. Chasalow, Y. M. Hibiondada, D. M. Klimas, A. Schindler, Aliphatic polyester II. The degradation of poly(DL-lactide), poly(ϵ -caprolactone) *in vivo*. *J. Appl. Polym. Sci.* 26 (1981) 3779-3784.
- [9]- D. E. Perrin, J. P. English, Poly glycolide and poly lactide. in: A. J. Domb, J. Kost, D.M. Wiseman (eds.), *Hand book of biodegradable polymers*. Amsterdam, The Netherlands, Harwood Academic Publishers, 1997, pp. 10.
- [10]- A. Schindler, R. Jeffcoat, G. L. Kimmel, C. G. Pitt, M. E. Wall, Biodegradable polymers for sustained drug delivery, *Contemp. Top. Polym. Sci.* 2 (1977) 251-289.

[11]- C. G. Pitt, A. Schindler, Capronor: A biodegradable delivery system for levonorgestrel, in: G. I. Zatuchni, A. Goldsmith, J. D. Shelton (eds.), long-acting contraceptive delivery systems, Harper and Row, Philadelphia, 1984, p. 48-63.

[12]- R. Langer, N. A. Peppas, Chemical and physical structure of polymers as carriers for controlled release of bioactive agents: A review, Rev. Macromol. Chem. Phys. C23 (1983) 61-126.

[13]- J. Siepmann, A. Gopferich, Mathematical modeling of bioerodible, polymeric drug delivery systems. Advanced Drug Delivery Reviews 48 (2001) 229-247.

[14]- R. M. Ginde, R. K. Gupta, *In vitro* chemical degradation of poly(glycolic acid) pellets and fibres. J. Appl. Polym. Sci. 33 (7) (1987) 2411-2429.

[15]- A. Browning, C. C. Chu, The effect of annealing on the tensile properties and hydrolytic degradative properties of poly glycolic acid sutures. J. Biomed. Mater. Res. 20 (5) (1986) 613-632.

[16]- C. G. Pitt, Poly ϵ -caprolactone and its copolymers, In: M. Chasin, R. Langer (eds.), Biodegradable polymers as drug delivery systems. Marcel Decker, New York, 1990.

[17]- M. Vert, S. Li, H. Garreau, More about the degradation of LA/GA-derived matrices in aqueous media. J. Controlled Release 16 (1-2) (1991) 15-26.

[18]- A. F. Kydonieus, Controlled release technologies: methods, theory and applications. Boca Raton, Florida, CRC Press, 1980, p. 7.

[19]- A. J. Domb, Implantable biodegradable polymers for site-specific drug delivery. In A. J. Domb (ed.), Polymeric site-specific pharmacotherapy. John Wiley & Sons, New York, 1994. p. 3.

[20]- R. S. Langer, N. A. Peppas, Present and future applications of biomaterials in controlled drug delivery. Biomater. 2 (1981) 201-214.

- [21]- X. Tongwen, H. Binglin, Mechanism of sustained release in diffusion-controlled polymer matrix-application of percolation theory. *Int. J. Pharm.* 170 (1998) 139-149.
- [22]- L. T. Fan, S. K. Singh, *Controlled release: A quantitative treatment*, Springer-Verlag, Berlin, 1989.
- [23]- E. Mathiowitz, *Encyclopaedia of controlled drug delivery*, John Wiley & Sons, New York, 1999, pp. 921-935.
- [24]- T. Higuchi, Rate of release of medicaments from ointment bases containing drug in suspensions, *J. Pharm. Sci.* 50 (1961) 874-875.
- [25]- M. Rosoff, *Controlled Release of Drugs: Polymers and Aggregate Systems*, VCH Publishers Inc., New York, 1989, pp. 62-63.
- [26]- J. Heller, R. W. Baker, Theory and practice of controlled drug delivery from bioerodible polymers, in: R. W. Baker (ed.), *Controlled release of bioactive materials*. Academic Press, New York, (1980), pp. 1-18.
- [27]- R. Baker, *Controlled release of bioactive materials*, Academic Press Inc., London, 1980.
- [28]- A. Shenderova, T. G. Burke, S. P. Schwendeman, Stabilization of 10-Hydroxycamptothecin in poly(lactide-co-glycolide) microsphere delivery vehicles. *Pharm Res* 14(10) (1997) 1406-1414.
- [29]- X. Zhang, J. K. Jackson, W. Wong, H. M. Burt, Development of biodegradable polymeric paste formulations for taxol: *in vitro* and *in vivo* study. *Int. J. Pharm.* 137 (1996) 199-208.
- [30]- B. Ertl, P. Platzer, M. Wirth, F. Gabor, Poly (DL-lactic-co-glycolic acid) microspheres for sustained delivery and stabilization of camptothecin. *J. Controlled Release* 61 (1999) 305-317.

[31]- F. Ahmed, V. Vyas, A. Saleem, High performance liquid chromatographic quantitation of total and lactone 20(S)camptothecin in patients receiving oral 20(S)camptothecin. *J. Chromatogr.* 707 (1998) 227-233.

[32]- J. H. Beijnen, High performance liquid chromatographic analysis of the antitumor drug camptothecin and its lactone ring-opened form in rat plasma. *J. Chromatogr.* 617 (1993) 111-117.

[33]- Y. F. Li, R. Zhang, Reversed phase high performance liquid chromatography method for the simultaneous quantitation of the lactone and carboxylate forms of the novel natural product anticancer agent 10-hydroxycamptothecin in biological fluids and tissues. *J. Chromatogr.* 686 (1996) 257-265.

[34]- D. L. Warner, T. G. Burke, Simple and versatile high performance liquid chromatographic method for the simultaneous quantitation of the lactone and carboxylate forms of camptothecin anticancer drugs. *J. Chromatogr.* 691 (1997) 161-171.

Chapter 5
General Discussion and Conclusions

5.1. History

Camptothecin, a plant alkaloid isolated from *Camptotheca acuminata*, is the prototype of a novel class of antitumor agents which exert their activities exclusively by inhibition of topoisomerase I (1). Topoisomerases are intranuclear enzymes that transiently break and rejoin DNA strands to facilitate processes like replication, recombination and transcription, and are essential for cell survival (1). During the initial phase I trials some promising responses were seen in colorectal carcinomas, melanoma and acute myeloid leukemia (2). Unfortunately, further clinical evaluation of camptothecin had to be discontinued due to its unpredictable toxicity profile including myelosuppression, gastrointestinal toxicity and haemorrhagic cystitis. In biological systems CPT undergoes a pH dependent equilibrium. The active lactone form, is present at acidic pH (4.0-5.0) and converts into the inactive carboxylated form in a more basic environment (3). Moreover, its poor water solubility was a problem in the pharmaceutical formulation of the drug and was considered to be the cause of the bladder toxicity. CPT is highly lipophilic and dissolves only in aprotic polar solvents or can be formulated as a suspension in Tween 80:saline or lipid (4). CPT injected intramuscularly induced complete remission in mice implanted with a variety of human cancer xenograft lines. However, antitumor and toxic effects were found to vary remarkably with schedule and route of administration (5). Despite its promising antitumor activity in animal models, clinical development of the drug was halted for unpredictable toxic events. Later O'Leary *et al.* (1998) (6), reported that large doses of CPT given on intermittent schedules are not effective and to be most effective they require a prolonged schedule of administration given continuously at low doses or frequent intermittent dosing schedules.

To serve this purpose, many different types of delivery systems have been devised such as polymer conjugated camptothecin (7,8), micro- and nanoparticle encapsulated camptothecin (9,10) and liposomes (11). Unfortunately, none of these systems was flawless and they suffered from many drawbacks as discussed in chapter 1.

Recently, the development of new injectable drug delivery systems such as thermoplastic pastes (12), *in situ* crosslinked systems (13,14) and *in situ* polymer

precipitation (15,16) has received considerable attention over the past few years. These systems can be used for local delivery of CPT to the tumor resection site or directly to a non-metastatic solid tumor. Among all these methods investigated, advantages such as lack of a potentially toxic solvent, no heat of reaction upon setting, facile syringeability, and degradability has made thermoplastic pastes the best candidate for CPT delivery.

5.2. General Discussion

A biodegradable short chain polymeric system (oligomer) was developed by using ϵ -caprolactone as a monomer, $\text{Sn}(\text{Oct})_2$ as a catalyst and different alcohols as initiator. It was shown that the optimum polymerization temperature is 110°C and the polymerization process needs at least 24hrs to complete.

It was hypothesized that the chemical structure of initiator can play a factor in characterizing the melting point, rheologic behaviour and degree of crystallinity in synthesized ϵ -caprolactone oligomers. To prove this hypothesis primary alcohols (i.e., 1-octanol, 1-dodecanol, stearyl alcohol) and secondary alcohols (i.e., 2-butanol, 2-octanol, 2-dodecanol) were used as an initiator while keeping the M/I ratio and M/C ratio constant at 8 and 1000 respectively.

The composition and theoretical \overline{Mn} of the synthesized oligomers was determined by using equation 3.7 and $^1\text{H-NMR}$. The results showed that number average molecular weight of the oligomers ranged between 1000 to 1300 daltons (Table 3.2) confirming the production of short chain ϵ -caprolactone polymer. By using the heat of fusion reported for 100% crystalline PCL (i.e., 139.5mJ/mg) (17) the degree of crystallinity of synthesized oligomers was calculated. DSC results revealed that by increasing the number of carbons in the structure of the primary alcohol initiators, heat of fusion and the crystallinity of the synthesized polymers increased whereas the melting point was not significantly affected (Table 3.3). Also, it was shown that the structure of the initiator, whether linear (primary alcohol) or branched (secondary alcohol), influenced the polymer melting point, heat of fusion and crystallinity (Table 3.3). All the results were analysed statistically and some of the differences observed were not significant ($p>0.05$). For example, in secondary alcohols the degree of crystallinity and melting point didn't change significantly when the number

of carbons in the initiator increased and in CL oligomers initiated by primary alcohols no significant difference was observed in terms of melting point while a significant difference was observed in terms of degree of crystallinity. Finally, a significant difference was observed between CL oligomers initiated by primary alcohols and secondary alcohols in terms of degree of crystallinity and melting point. Those oligomers initiated using secondary alcohols had significantly lower melting points and degrees of crystallinity. One of the reasons that no significant difference was observed could be attributed to the small sample size. Possibly, by increasing the number of samples a significant difference could be observed. Since the number of data obtained in each experiment was three (degree of freedom=2), it is possible that we made a type II error due to the insufficient number of data which has a significant impact on the power (not making type II error) of the test (18). Theoretically, we expected to observe a decrease in the degree of crystallinity and an increase in melting point as the number of carbons in the initiator's chain increased, especially in primary alcohols with a linear structure. As the number of carbons in the structure of initiator increases the melting point increases. For example, the melting point of 1-butanol is $-89.5\text{ }^{\circ}\text{C}$ whereas the melting point of stearyl alcohol is $61\text{ }^{\circ}\text{C}$. Inclusion of an initiator with higher melting point (i.e., stearyl alcohol) in the oligomer backbone can increase the melting point of the oligomer while the inclusion of 1-butanol may decrease the melting point of the oligomer. By introducing a non-polar hydrocarbon chain (i.e., initiator) to the polar structure of poly(ϵ -caprolactone) it is possible that the non-polar structure of the initiator interferes with the hydrogen bonds or any polar bonds between the CL units in the backbone of CL-oligomer. This interference could inhibit the polymer chain alignment as well as decreasing the number of polar bonds in the bulk causing a reduced degree of crystallinity.

Rheologic behaviour of these polymers also plays a significant role in this project. In order to be syringeable through a needle while heated slightly above its melting point, the polymer vehicle must have a low melt viscosity. Two factors such as the flexibility of the polymer backbone, which was discussed earlier, and the entanglement of the polymer chains with each other have a significant impact on the syringeability of the polymers (19). Primary alcohols can initiate the polymerization process of ϵ -caprolactone and produce a linear chain PCL. In the melt state these

polymer chains can slide over each other with minimum entanglement. This low entanglement between the polymer chains eases the passage of polymer through the needle. In contrast, secondary alcohols with an OH group positioned on the C₂ of the initiator's chain produce a PCL with a pendent CH₃ in the backbone which reduces the flexibility of the backbone chain as bond rotations are inhibited by steric hindrance. Moreover, the smaller number of carbons in the structure of primary alcohols (e.g., 1-dodecanol) in comparison to their corresponding secondary alcohol (i.e., 2-dodecanol) can reduce the flexibility of the PCL chain and hence, produce a higher melt viscosity [39]. This increased viscosity can make the polymer move through the needle with difficulty.

To test this theory, different polymers were synthesized (Table 3.4) and their rheologic behaviour was investigated. The results revealed that all the synthesized polymers behaved like Newtonian fluids at their melt state. To compare the viscosity of the polymers shown in Table 3.4. with each other at a constant temperature (e.g., 50 °C) a plot of shear stress versus shear rate was produced with the slope of the line being the viscosity. It was shown that by increasing the number of carbons in the structure of the initiator, the viscosity of the polymer decreases and overall primary alcohols produce lower viscosity polymers than secondary alcohols. This observation can be justified with the same argument delivered above. The introduction of a non-polar initiator into the polar structure of CL oligomers can interfere with the hydrogen bonds available between CL oligomer chains and facilitate their movement while it is melted. One goal of this project was to produce CL oligomers with melting points slightly above body temperature. Knowing that melting point can be influenced by molecular weight, different M/I ratios were used. By changing the M/I ratio, different CL oligomers were synthesized using various initiators, and purified to obtain oligomers with a melting point in the desired range (Table 3.5). The composition and molecular weight of the CL oligomers were determined by NMR spectroscopy (Table 3.6.). Also, the results of the calculated \overline{Mn} from the ¹H-NMR and GPC are compared in Table 3.6. \overline{Mn} values obtained with GPC were generally in agreement with those of NMR which confirm the production of oligo(ϵ -caprolactone). By comparing the \overline{Mn} obtained from GPC or

NMR after purification with theoretical \overline{Mn} which is calculated based on unpurified oligomers it is obvious that the theoretical \overline{Mn} was much lower. It was speculated that when the low M/I ratios were used (i.e., 2.1-4) a very heterogeneous oligomer bulk was produced comprised of mainly very low molecular weight chains which were removed after purification leaving only higher molecular weight oligomer chains.

DSC results revealed that the synthesized diblock oligomers had melting points between 38-42 °C, which is in the desired range. The GPC results showed that the molecular weight distribution of the oligomers was narrow and the molecular weight of all the oligomers were below 5000 daltons. A molecular weight of 5000 daltons is a critical point for caprolactone oligomers. It has been shown that at this molecular weight the caprolactone chains become small enough to diffuse out of the polymer bulk. Therefore, the polymer bulk becomes prone to fragmentation and faster degradation (20).

Table 3.7. summarizes the melt viscosity of the synthesized and purified oligomers. It is obvious that by increasing temperature the melt viscosity of oligomers decreases. Moreover, it can be observed that all the synthesized oligomers are in the melt state at 46 °C emphasizing the possibility of being syringeable at this temperature.

Among all these polymers, four were chosen as the best candidates for further studies. CL oligomers initiated by oleyl alcohol and 2-dodecanol were chosen due to their low degree of crystallinity. PCL initiated with ethanol was another candidate chosen as a comparison sample. CL oligomer initiated by 1-dodecanol was another candidate and was chosen to be compared with CL oligomer initiated with 2-dodecanol. In this latter case we can study the effect of the initiator on the drug release profile.

One hypothesis of this work is that incorporation of CPT into a generally hydrophobic polymer carrier would enhance the stability of the as-yet unreleased drug while within the polymer. Another hypothesis is that the incorporation of an alkane block to the caprolactone initiator would provide an increase in CPT solubility within the oligomer. To facilitate the implantation of the polymer-drug depot, an injectable system has been designed. To investigate the solubility of CPT in different CL oligomers and PLGA, the thermal behaviour of CL oligomers, PLGA and CPT was investigated separately. Four different candidates (i.e., CL oligomer initiated by ethanol, 1-dodecanol,

2-dodecanol and oleyl alcohol) were chosen to investigate the effect of different initiators with different hydrophobicity on the solubility of CPT (Table 4.3.). The CL oligomers can solubilize CPT up to 11mg in each 100mg of oligomer, which is at least 10000 times more than its solubility in water (2.5 μ g/mL) and 3 times more than PLGA. The results depicted in Table 4.3. do not show a clear difference of CPT solubility in the different CL oligomers. It was hypothesized that different CL oligomers with different hydrophobicity would show different CPT solubility. This lack of differentiation could be attributed to the insufficient sensitivity of our DSC instrument for this experiment, or may be an indication that CPT solubility is determined solely by its affinity for the CL component of the oligomer.

Since carboxylate conversion limits bioavailability and efficacy of CPT, maintenance of the lactone structure during preparation and release is a prerequisite for improved therapy using injectable implants. Based on a method developed for HPLC, we analyzed CPT after incorporation into the CL oligomers and at the time of release into the buffer media and no lactone to carboxylate conversion was observed (Appendix F, Figures 4-6). During long-term drug release studies in PBS (two months), no conversion of lactone to carboxylate was observed. This result proves that our delivery system was capable of preserving the lactone ring of CPT from water even after incubation for two months in PBS pH=7.4. This finding can be explained by considering the hydrophobicity of the CL oligomers which limits water penetration into the device and thus prevents hydrolysis of the CPT molecules.

For *in vitro* studies, drug-loaded oligomers with a concentration of 5mg CPT in 100mg of CL oligomer were prepared. This concentration is approximately 50% of the determined CPT saturation concentration in the oligomer. For the PLGA samples two different concentrations (i.e., 1.5mg CPT/100mg PLGA, & 5mg CPT/100mg PLGA) were prepared. In the early stages, where the drug concentration is high and there has not been a significant polymer degradation and thereby, constant diffusivity; the release of the drug follows the square root of time. As time goes by, the drug concentration in the polymer bulk decreases and therefore, the rate of the release decays exponentially and doesn't follow the square root of time anymore (equation 4.3). Meanwhile, the polymer starts to degrade into smaller molecular weight chains providing more free volume for

the drug molecules to diffuse, hence; increase in drug release rate. The CPT release profile (Figure 4.11) from CL oligomers and PLGA were analysed by using analysis of variance. The statistical analysis of results revealed that, overall, the drug release profiles from the oligomers were different ($p < 0.05$). As discussed earlier, the degree of crystallinity has a significant impact on drug release. The degree of crystallinity of the drug loaded oligomers was calculated and no significant difference among different oligomers was observed (Table 4.5). It is worth mentioning that all the samples that were prepared for *in vitro* studies had a melting point close to 37 °C and at this temperature it is plausible to assume that a great deal of the crystals are in melt state. Therefore, the effect of degree of crystallinity on drug release profile was considered insignificant. Oligomers with lower melt viscosity have more mobile chains, allowing the drug molecules to diffuse easier. Based on this fact the drug release profile of CPT from different oligomers was analysed. By comparing the slope of the release profile of CPT from different oligomers, the only non-significant difference was observed between CL-1-dodecanol (caprolactone oligomer initiated with 1-dodecanol) and CL-oleyl alcohol (caprolactone oligomer initiated with oleyl alcohol). It is obvious from Table 4.5. that CL-oleyl alcohol has almost the same melt viscosity as CL-1-dodecanol. This similarity can be interpreted into same free volume at a given temperature for both oligomers, allowing the drug molecules to release with the same pace. By analysing the rate of drug release from the other oligomers, it can be concluded that the lower the melt viscosity at a given temperature the higher the free volume and the faster the release rate (Table 4.5).

After 190 days of incubation in PBS (pH=7.4, 37 °C) it was only the CL-oleyl alcohol which showed signs of degradation while macroscopically the others remained intact. This faster rate of degradation can be attributed to the lower viscosity and lower melting point of the oligomer and thus a higher rate of water imbibition by the CL-oleyl alcohol block oligomers.

PLGA has a T_g of around 60 °C, therefore at the release conditions (37 °C) polymer is in its glassy state and drug release through the polymer chains is highly restricted (Figure 4.12.). This continues for a period of one month till water cleaves the esteric linkages inside the PLGA therefore \overline{M}_n and T_g of the oligomer decreases and it

swells. This swelling changes the mobility of polymer chains and increases the water imbibition and the diffusivity of drug. All these changes lead to a significant release of drug in the second phase. The final stage is related to the release of drug from the fragmented pieces of polymer. This pattern of drug release which consisted of releasing drug in very small doses for a period of 30 days followed by a burst in drug release does not seem to be suitable for effective camptothecin delivery.

5.3. Conclusions

- 1- The newly developed delivery system was syringeable at temperatures as low as 45 °C which provides a clear advantage over the other thermoplastic pastes discussed in Chapter 2.
- 2- This system provided a suitable carrier to preserve the active lactone form of CPT.
- 3- Active lactone form of CPT was released into the PBS media in a sustained fashion for a period of 190 days.
- 4- CL-oleyl alcohol seemed to be more suitable for CPT delivery than the other oligomers due to its lower degradation time.

5.4. Future Perspective

The developed and characterized injectable implant system showed that it is capable of solubilizing and stabilizing CPT to a significant extent while releasing the drug in a sustained fashion for 190 days. However, the implant composed of CL-oleyl alcohol showed signs of degradation after 4.5 months incubation in PBS. This time of degradation can be shortened by blending the synthesized CL-oleyl alcohol oligomer with other oligomers made of PLGA which possess short degradation time. In another approach, a mixture of ϵ -caprolactone with DLLA can be used as monomers to be polymerized and produce an oligomer with shorter degradation time. This is due to the

fact that DLLA is an amorphous and partially hydrophilic monomer which can increase the rate of water imbibition and thereby, shorter degradation time. Ultimately, our localized drug delivery system needs to be tested on animal models. Although the *in vitro* studies showed promising results, it is an *in vivo* study which can prove the efficacy our polymeric implant system in a biological environment. Two important factors need to be considered before injecting this delivery system into the body. First, the presence of residual solvent and second sterility. The presence of residual solvents in the delivery system is undesirable due to their harmful effects on tissues. This can be tested by using instruments such as Gas Chromatography or Thermal Gravimetric Assay. Before injection this delivery system needs to be sterilized and this purpose can be achieved by using γ -radiation (21).

5.4. References

- [1]- R. Zhang, Y. Li. Preclinical pharmacology of the natural product anticancer agent 10-hydroxycamptothecin, an inhibitor of topoisomerase I, *Cancer Chemother. Pharmacol.* 41 (1998) 257-267.
- [2]- M. E. Wall, M. Wani. Camptothecin and Taxol: Discovery to clinic, *Cancer Res.* 55 (1995) 753-760.
- [3]- R. P. Hertzberg, M. J. Caranfa, S. M. Hecht. On the mechanism of topoisomerase I inhibition by camptothecin:evidence for binding to an enzyme-DNA complex, *Biochemistry* 28 (1989) 4629-4638.
- [4]- B. C. Giovanella, H. R. Hinz, A. J. Kozielsi, M. Potmesil. Complete growth inhibition of human cancer xenografts in nude mice by treatment with 20-(S)-camptothecin, *Cancer Res.* 51 (1991) 3052-3055.
- [5]- U. Schaeppi, R. W. Fleischman, D. A. Cooney. Toxicity of camptothecin, *Cancer Chemother. Rep.* 2 (1974) 25-36.
- [6]- J. O'Leary, F. M. Muggia. Camptothecins: a review of their development and schedule of administration, *Europ. J. Cancer* 34 (1998) 1500-1508.
- [7]- M. Harada, J-I. Murata, Y. Sakamura, H. Sakakibara, S. Okuno, T. Suzuki, Carrier and dose effects on the pharmacokinetics of T-0128, a camptothecin analogue-carboxymethyl dextran conjugate, in non-tumor and tumor-bearing rats, *J. Controlled Release* 71 (2001) 71-86.
- [8]- J. W. Singer, R. Bhatt, J. Tulinsky, K. R. Buhler, E. Heasley, P. Klein, P. de Vreis. Water-soluble poly-(L-glutamic acid)-Gly-camptothecin conjugates enhance camptothecin stability and efficacy *in vivo*, *J. Controlled Release* 74 (2001) 243-247.
- [9]- B. Ertl, P. Platzer. Poly(D,L-lactide-co-glycolide) microspheres for sustained delivery and stabilization of camptothecin, *J. Controlled Release* 61 (1999) 305-317.
- [10]- V. Kumar, J. Kang, R. J. Hohi. Improved dissolution and cytotoxicity of camptothecin incorporated into oxidized-cellulose microspheres prepared by spray drying, *Pharm. Dev. Technol.* 6(3) (2001) 459-467.

- [11]- B. B. Lundberg. Biologically active camptothecin derivatives for incorporation into liposome bilayers and lipid emulsions, 13 (1998) 453-461.
- [12]- J. K. Jackson, W. Min, T. F. Cruz, S. Cindric, L. Arsenault, DD. Von Hoff, D. Degan, H. M. Burt, Polymer-based drug delivery system for the antineoplastic agent bis(maltolato)oxovanadium in mice. *Br. J. Cancer* 75 (7) (1997) 1014-1020.
- [13]- L. A. Moore, R. L. Norton, S. L. Whitman, R. L. Dunn, An injectable biodegradable drug delivery system based on acrylic terminated poly ϵ -caprolactone. The 21st Ann. Meeting Society Biomater., CA, USA, 1995.
- [14]- S. Lu, K. S. Anseth, Photopolymerization of multilaminated poly(HEMA) hydrogels for controlled release. *J. Controlled Release* 57 (1999) 291-300.
- [15]- N. H. Shah, A. S. Railkar, F. C. Chen, R. Tarantino, S. Kumar, M. Murjani, D. Palmer, M. H. Infeld, A. W. Malick, A biodegradable injectable implant for delivering micro and macromolecules using poly(lactic-co-glycolic)acid copolymers. *J. Controlled Release* 27 (1993) 139-147.
- [16]- B. Jeong, Y. H. Bae, S. W. Kim, In-situ gelation of PEG-PLGA-PEG triblock copolymer aqueous solutions and degradation thereof. *J. Biomed. Mater. Res.* 50 (2000) 171-177.
- [17]- V. Crescenzi, G. Manzini, G. Calzolari, C. Borri, Thermodynamics of fusion of poly- β -propiolactone and poly- ϵ -caprolactone. *Eur. Polym. J.* 8 (1972) 449.
- [18]- S. Bolton, *Pharmaceutical statistics*, Marcel Dekker Inc., New York, 1997.
- [19]- A. Martin, *Physical Pharmacy*. Lea & Febiger, Malvern, PA, USA (1993).
- [20]- S. C. Woodward, P. S. Brewer, F. Moatamed, The intracellular degradation of poly(ϵ -caprolactone). *J. Biomed. Mater. Res.* 19 (1985) 437-444.
- [21]- S. Einmahl, F. B. Cohen, J. Heller, R. Gurny, A viscous bioerodible poly(ortho ester) as a new biomaterial for intraocular application. *Biomed Mater Res* 50 (2000) 566-573.

Appendix A

(DSC Scans for Oligomers)

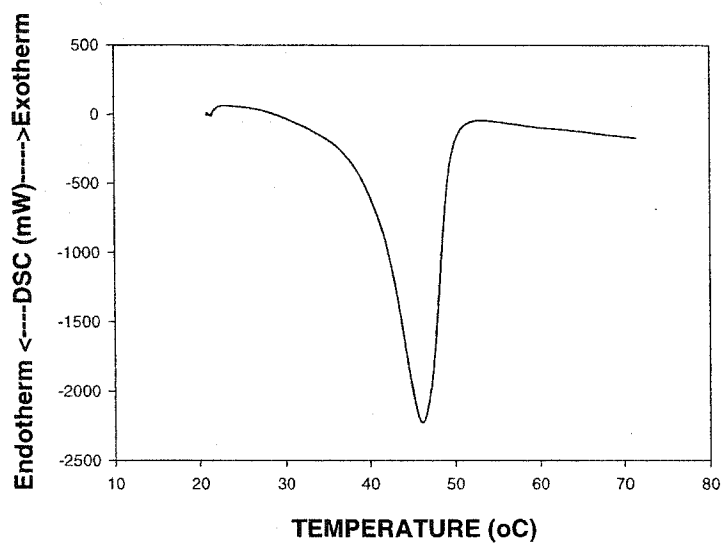


Figure 1: DSC scans for unpurified PCL initiated by 1-butanol (M/C= 1000; M/I= 8; Heat= 110 °C). Heating rate was set at 10 °C /minute. The midpoint of the endotherm was used to determine the melting point.

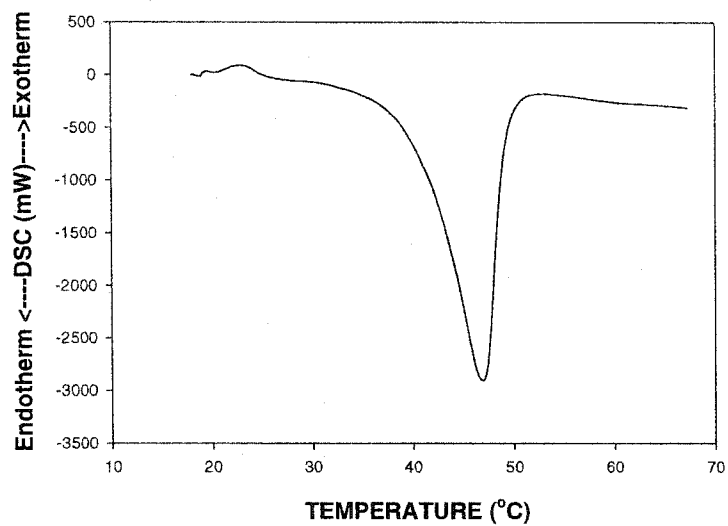


Figure 2: DSC scans for unpurified PCL initiated by 1-dodecanol (M/C= 1000; M/I= 8; Heat= 110 °C). Heating rate was set at 10 °C /minute. The midpoint of the endotherm was used to determine the melting point.

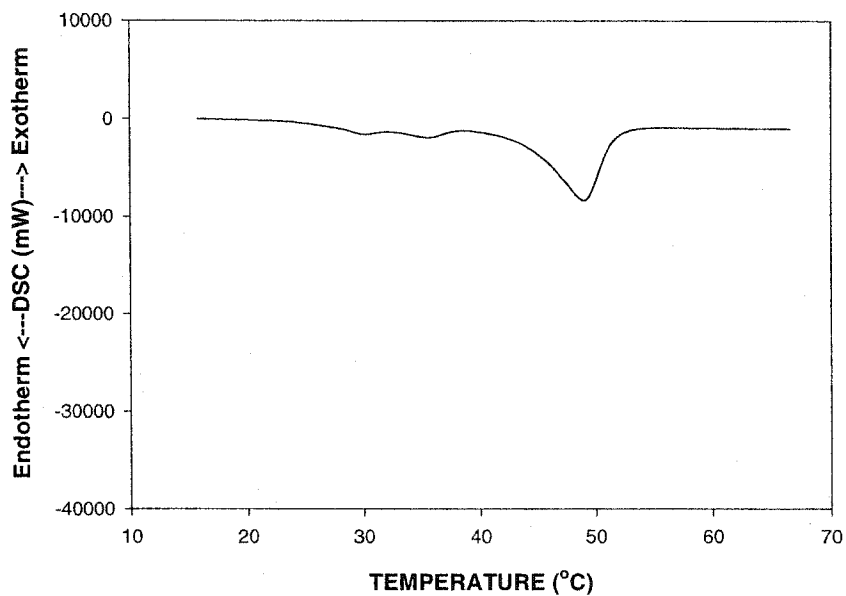


Figure 3: DSC scans for unpurified PCL initiated by stearyl alcohol (M/C= 1000; M/I= 8; Heat= 110 °C). Heating rate was set at 10 °C /minute. The midpoint of the endotherm was used to determine the melting point.

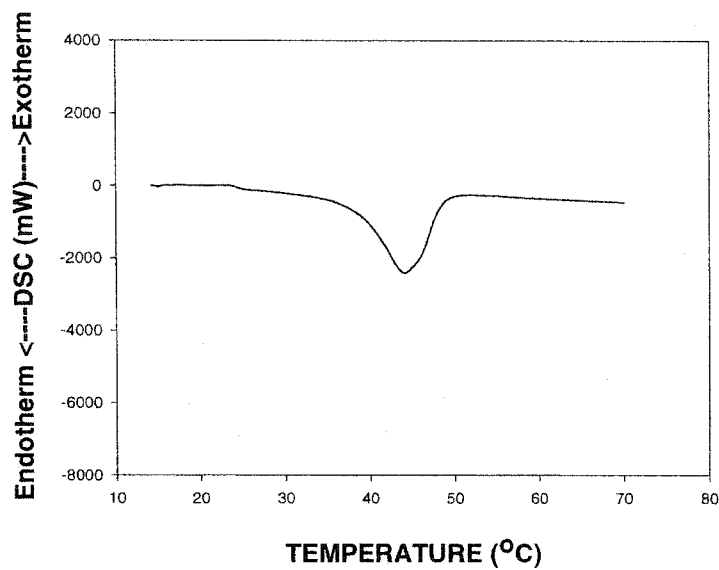


Figure 4: DSC scans for unpurified PCL initiated by 2-butanol (M/C= 1000; M/I= 8; Heat= 110 °C). Heating rate was set at 10 °C /minute. The midpoint of the endotherm was used to determine the melting point.

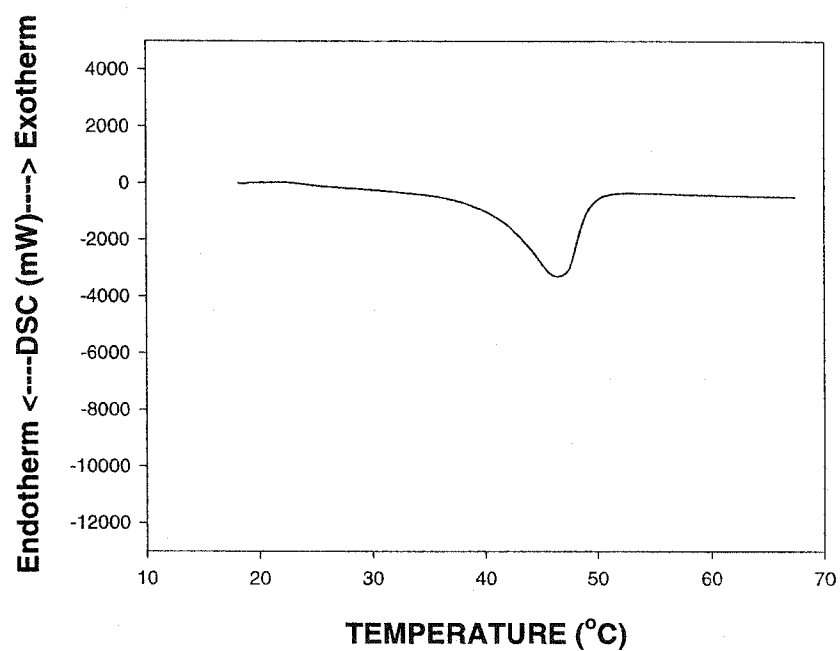


Figure 5: DSC scans for unpurified PCL initiated by 1-octanol (M/C= 1000; M/I= 8; Heat= 110 °C). Heating rate was set at 10 °C /minute. The midpoint of the endotherm was used to determine the melting point.

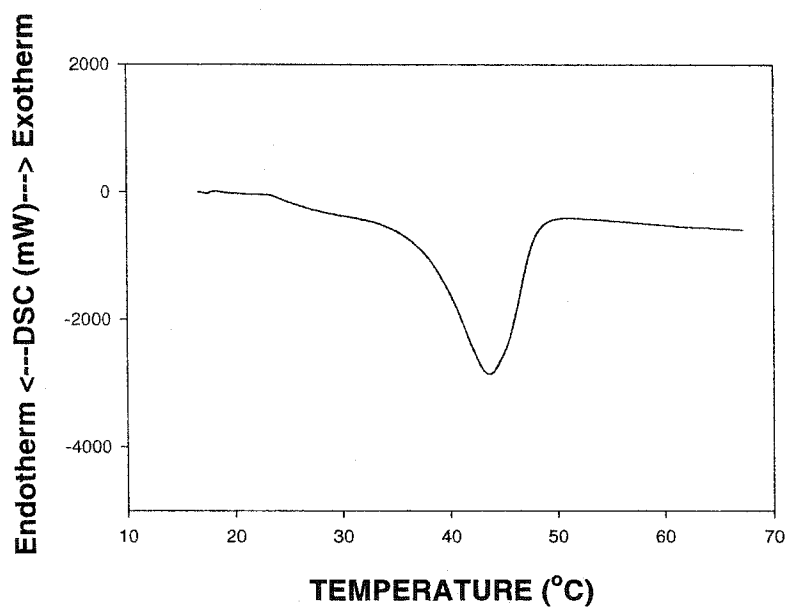


Figure 6: DSC scans for unpurified PCL initiated by 2-octanol (M/C= 1000; M/I= 8; Heat= 110 °C). Heating rate was set at 10 °C /minute. The midpoint of the endotherm was used to determine the melting point.

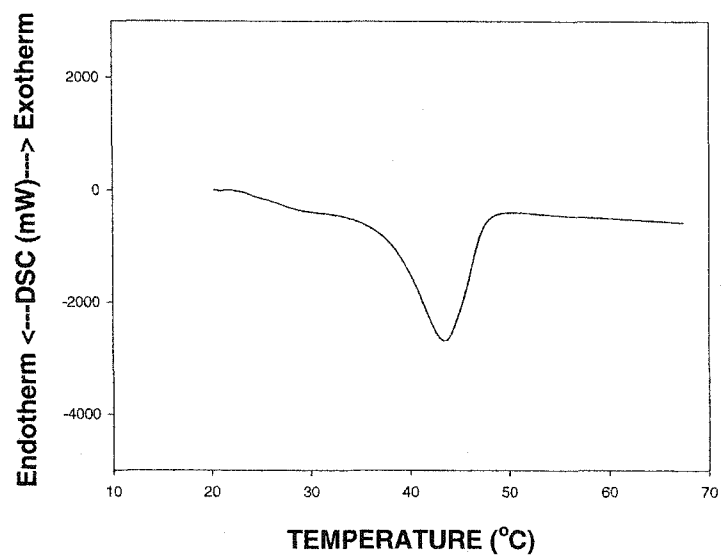


Figure 7: DSC scans for unpurified PCL initiated by 2-dodecanol (M/C= 1000; M/I= 8; Heat= 110 °C). Heating rate was set at 10 °C /minute. The midpoint of the endotherm was used to determine the melting point.

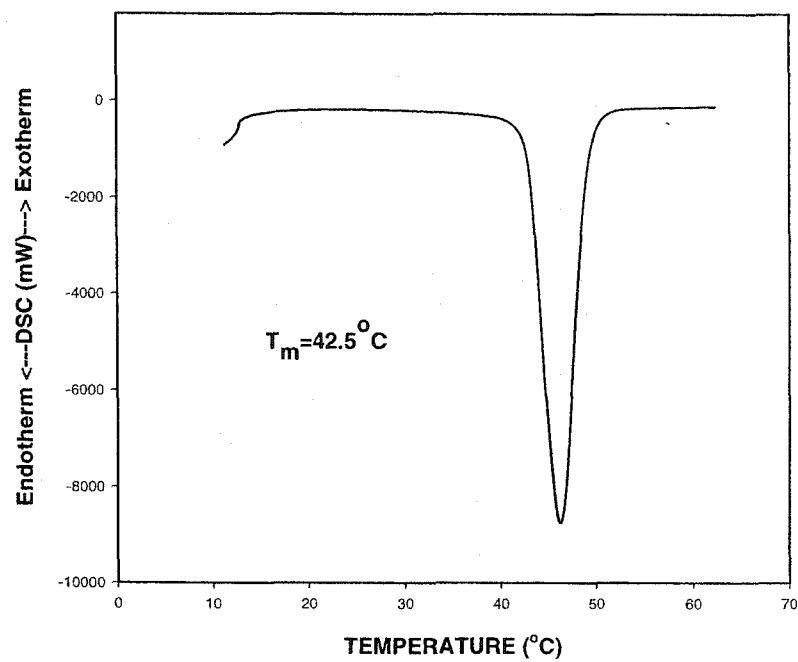


Figure 8: DSC scans for polymerized and purified PCL by using ethanol as an initiator. Heating rate was set at 10 °C /minute. The onset of melting was obtained from the endotherm.

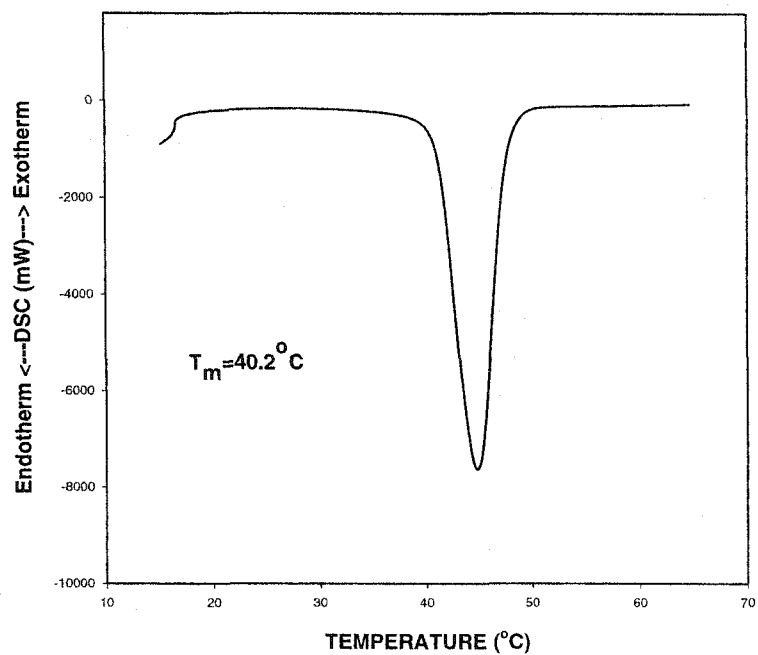


Figure 9: DSC scans for polymerized and purified PCL by using 1-butanol as an initiator. Heating rate was set at 10 °C /minute. The onset of melting was obtained from the endotherm.

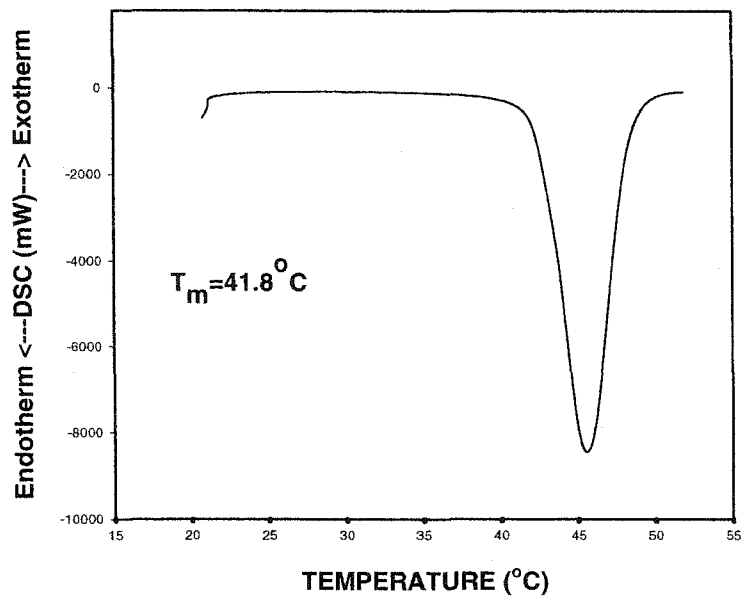


Figure 10: DSC scans for polymerized and purified PCL by using 2-butanol as an initiator. Heating rate was set at 10 °C /minute. The onset of melting was obtained from the endotherm.

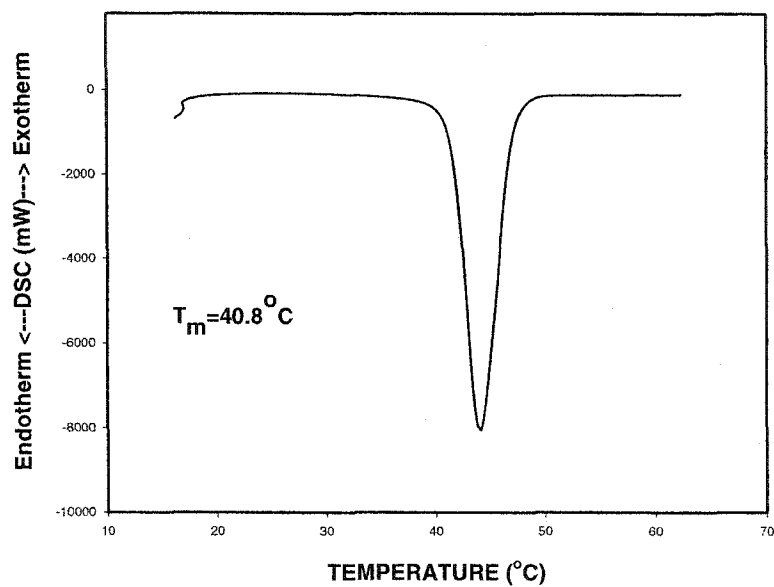


Figure 11: DSC scans for polymerized and purified PCL by using 1-octanol as an initiator. Heating rate was set at 10 °C /minute. The onset of melting was obtained from the endotherm.

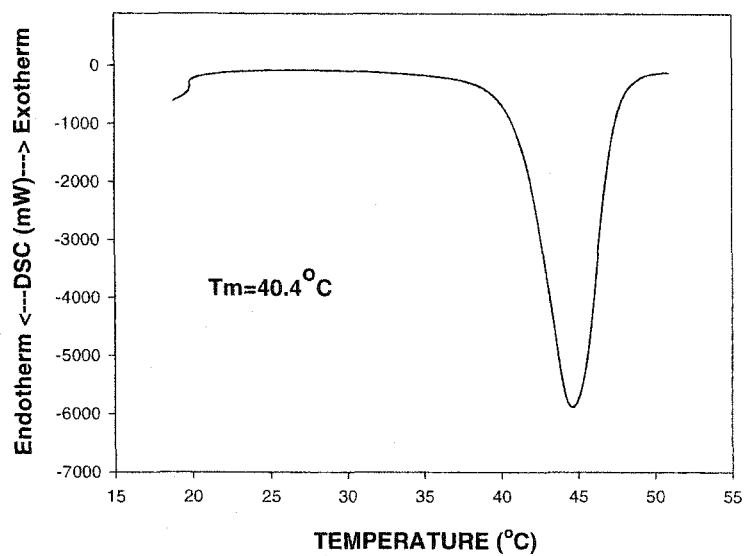


Figure 12: DSC scans for polymerized and purified PCL by using 2-octanol as an initiator. Heating rate was set at 10 °C /minute. The onset of melting was obtained from the endotherm.

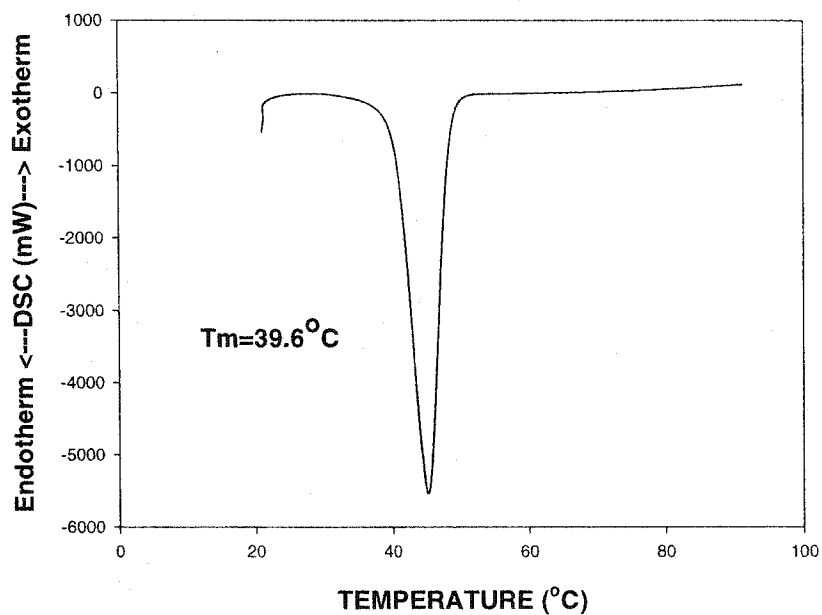


Figure 13: DSC scans for polymerized and purified PCL by using 1-dodecanol as an initiator. Heating rate was set at 10 °C /minute. The onset of melting was obtained from the endotherm.

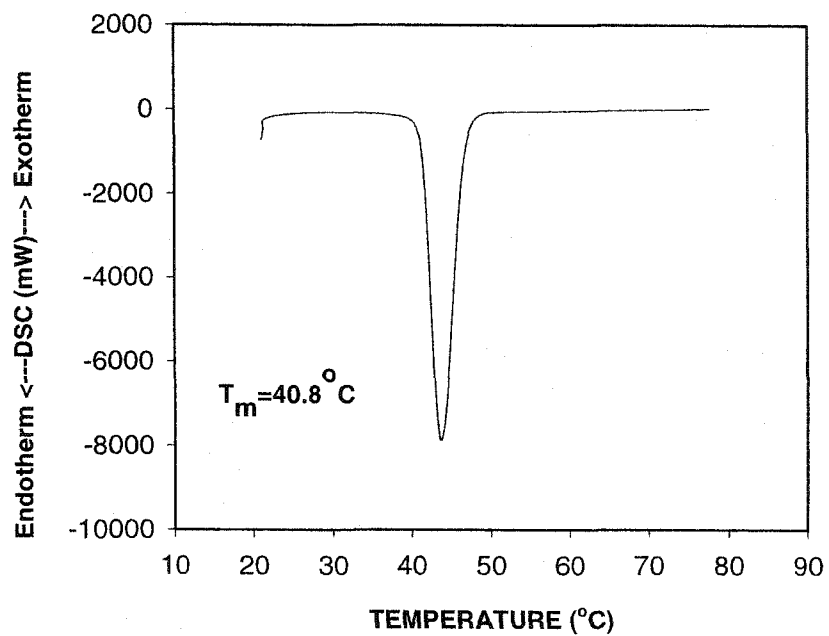


Figure 14: DSC scans for polymerized and purified PCL by using 2-dodecanol as an initiator. Heating rate was set at 10 °C /minute. The onset of melting was obtained from the endotherm.

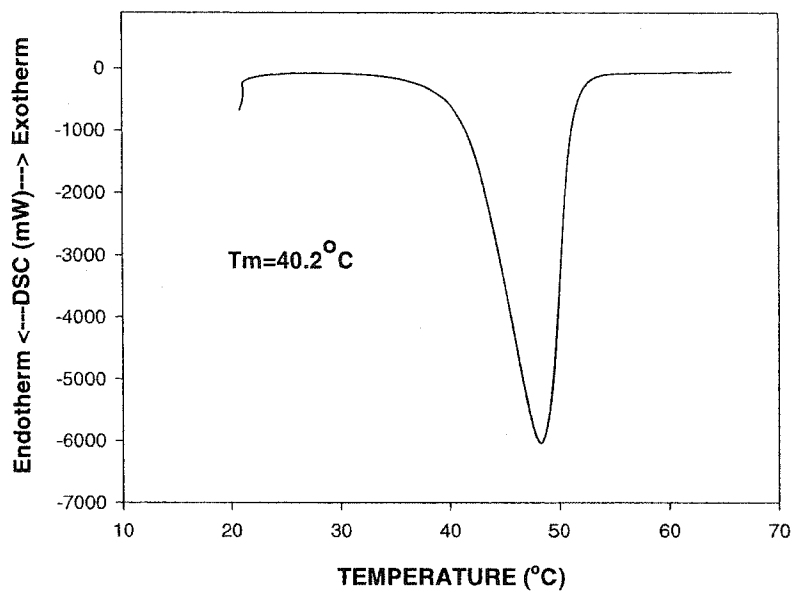


Figure 15: DSC scans for polymerized and purified PCL by using stearyl alcohol as an initiator. Heating rate was set at 10 °C /minute. The onset of melting was obtained from the endotherm.

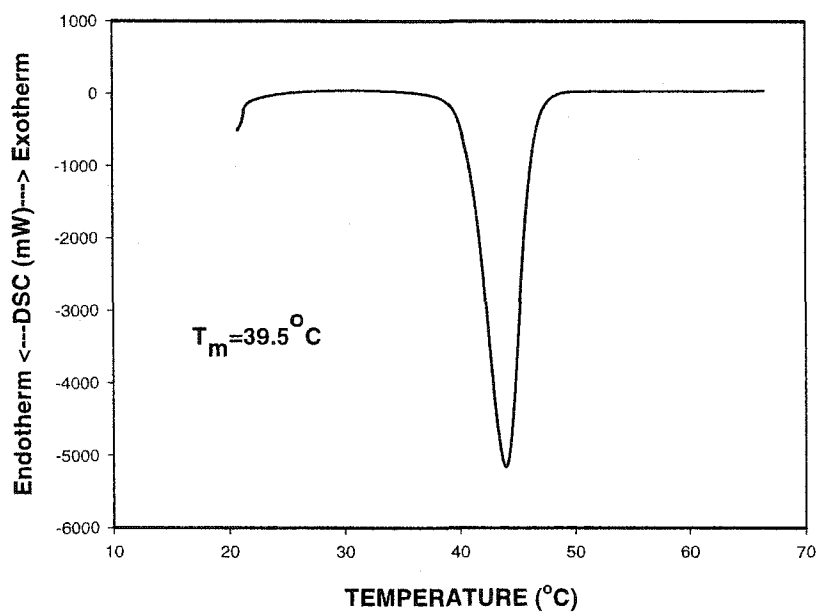


Figure 16: DSC scans for polymerized and purified PCL by using oleyl alcohol as an initiator. Heating rate was set at 10 °C /minute. The onset of melting was obtained from the endotherm.

Appendix B

(Rheometrics)

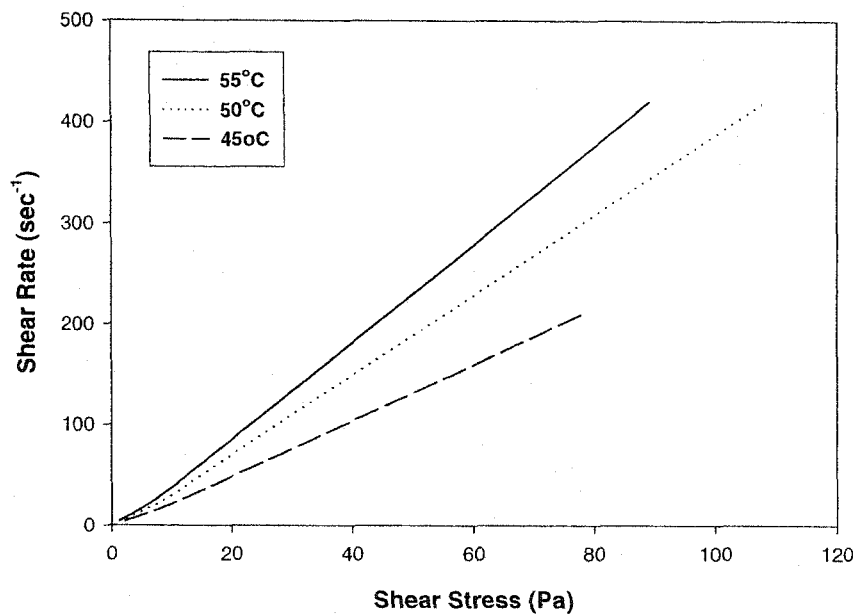


Figure 1: Rheologic behaviour of PCL initiated by 1-butanol at three different temperatures. As the temperature increases the oligomer becomes more fluid. Since plot of shear rate versus shear stress is a straight line, it was concluded that the oligomer behaves as a Newtonian fluid.

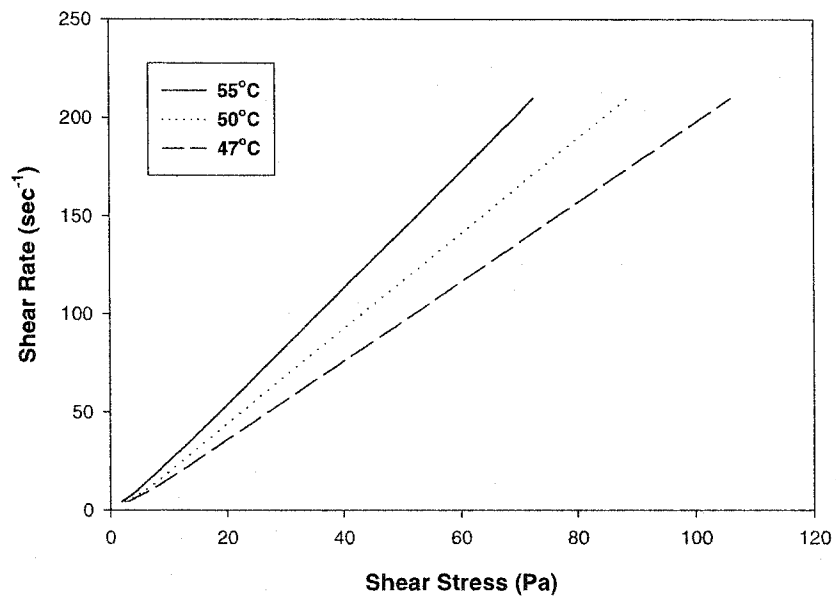


Figure 2: Rheologic behaviour of PCL initiated by 2-butanol at three different temperatures. As the temperature increases the oligomer becomes more fluid. Since plot of shear rate versus shear stress is a straight line, it was concluded that the oligomer behaves as a Newtonian fluid.

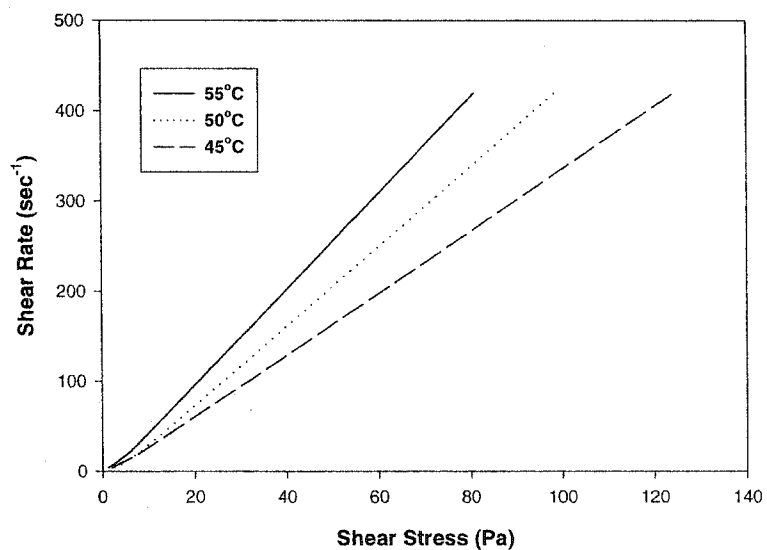


Figure 3: Rheologic behaviour of PCL initiated by 1-octanol at three different temperatures. As the temperature increases the oligomer becomes more fluid. Since plot of shear rate versus shear stress is a straight line, it was concluded that the oligomer behaves as a Newtonian fluid.

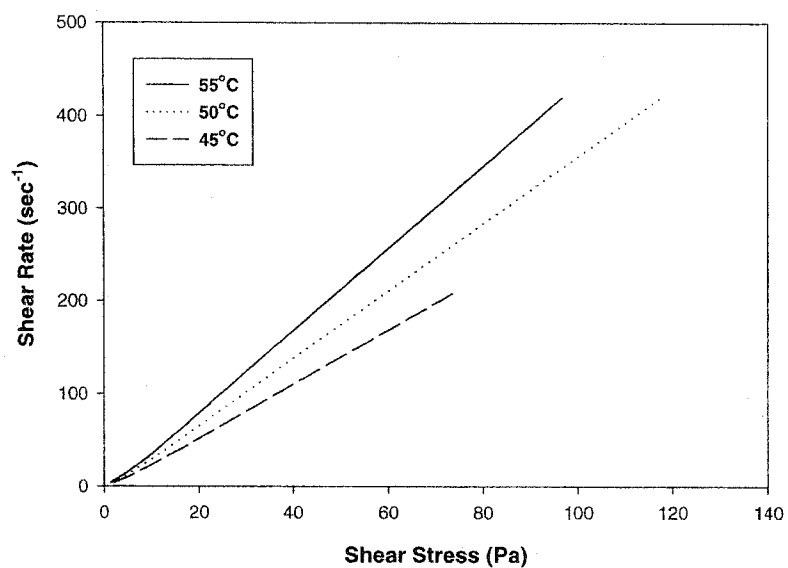


Figure 4: Rheologic behaviour of PCL initiated by 2-octanol at three different temperatures. As the temperature increases the oligomer becomes more fluid. Since plot of shear rate versus shear stress is a straight line, it was concluded that the oligomer behaves as a Newtonian fluid.

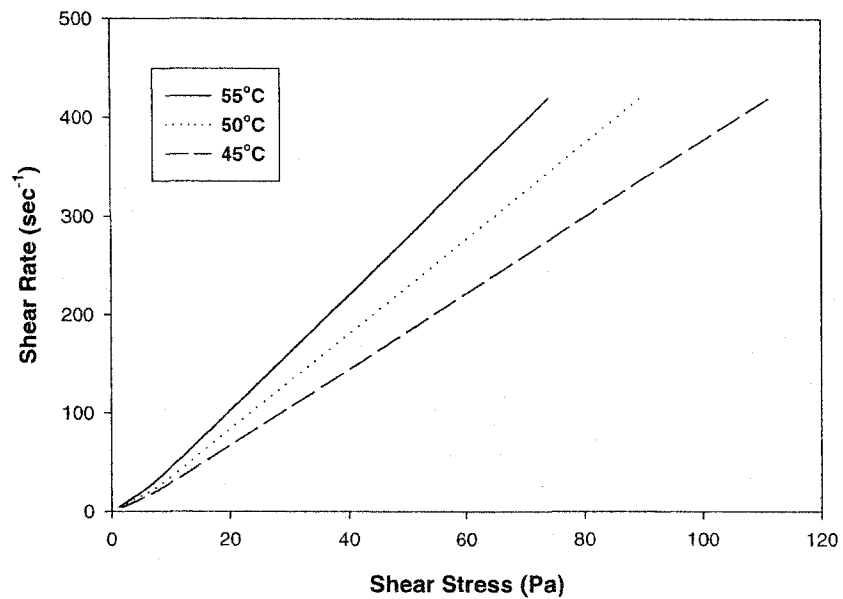


Figure 5: Rheologic behaviour of PCL initiated by 1-dodecanol at three different temperatures. As the temperature increases the oligomer becomes more fluid. Since plot of shear rate versus shear stress is a straight line, it was concluded that the oligomer behaves as a Newtonian fluid.

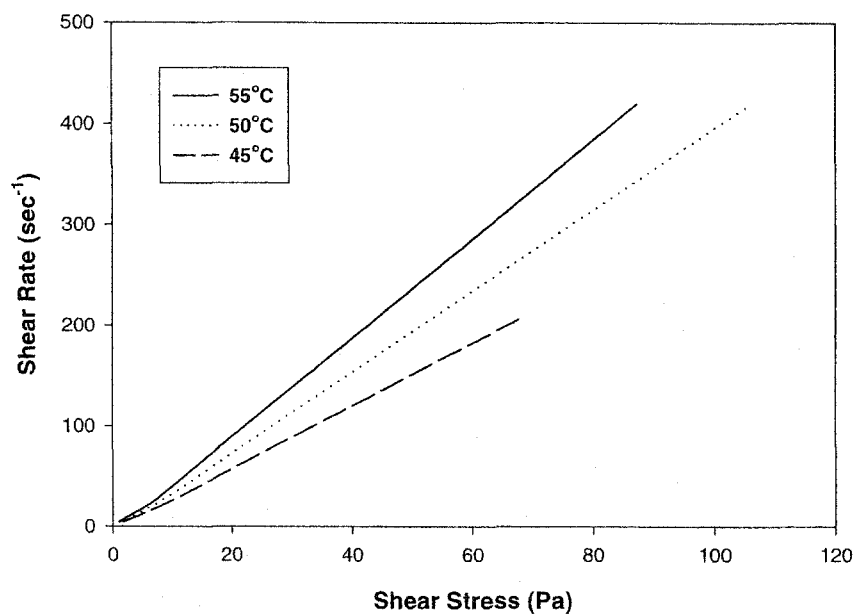


Figure 6: Rheologic behaviour of PCL initiated by 2-dodecanol at three different temperatures. As the temperature increases the oligomer becomes more fluid. Since plot of shear rate versus shear stress is a straight line, it was concluded that the oligomer behaves as a Newtonian fluid.

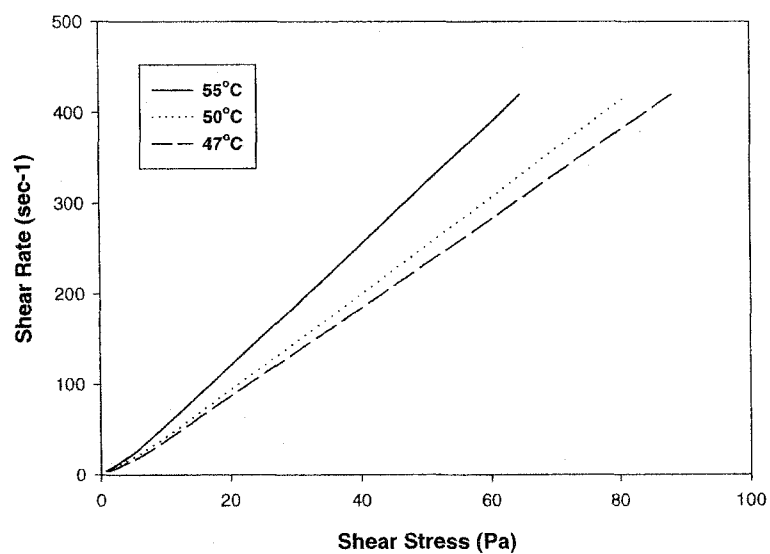


Figure 7: Rheologic behaviour of PCL initiated by stearyl alcohol at three different temperatures. As the temperature increases the oligomer becomes more fluid. Since plot of shear rate versus shear stress is a straight line, it was concluded that the oligomer behaves as a Newtonian fluid.

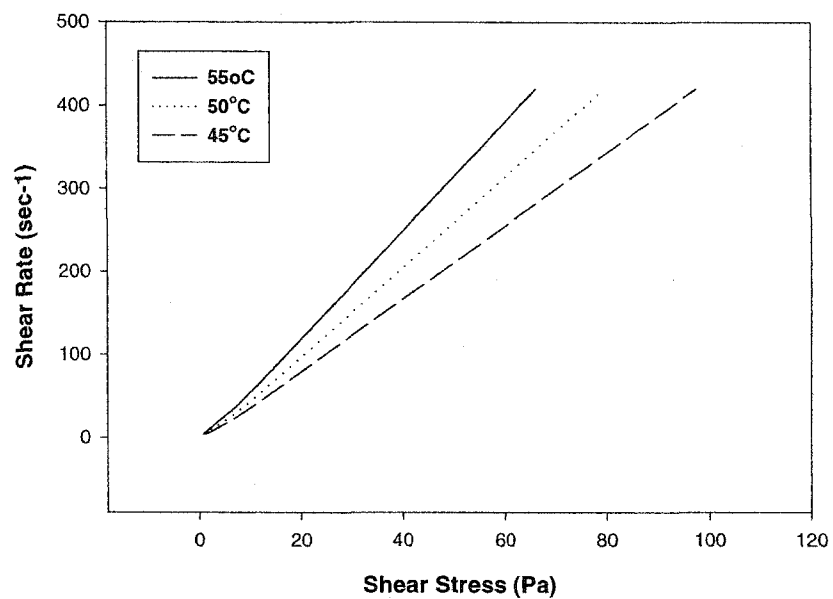


Figure 8: Rheologic behaviour of PCL initiated by oleyl alcohol at three different temperatures. As the temperature increases the oligomer becomes more fluid. Since plot of shear rate versus shear stress is a straight line, it was concluded that the oligomer behaves as a Newtonian fluid.

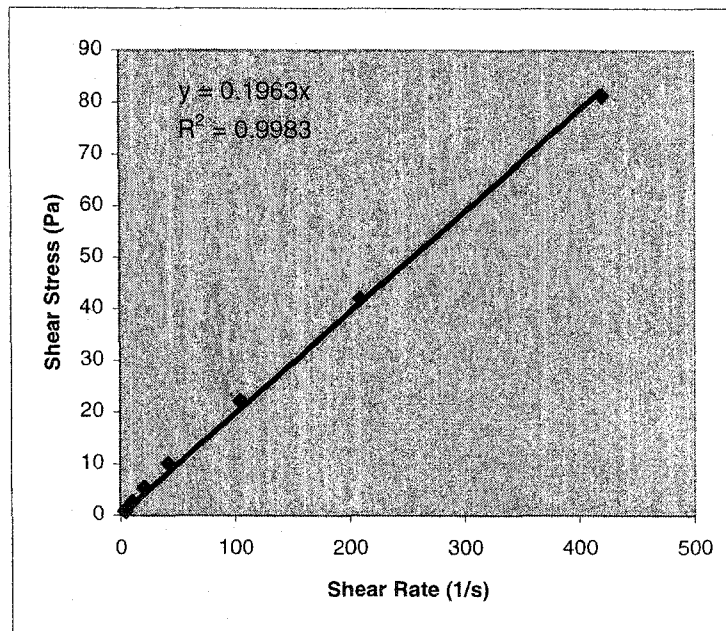


Figure 9: Plot of shear stress versus shear rate at 50°C for PCL initiated by stearyl alcohol. Slope of the line is viscosity (cP).

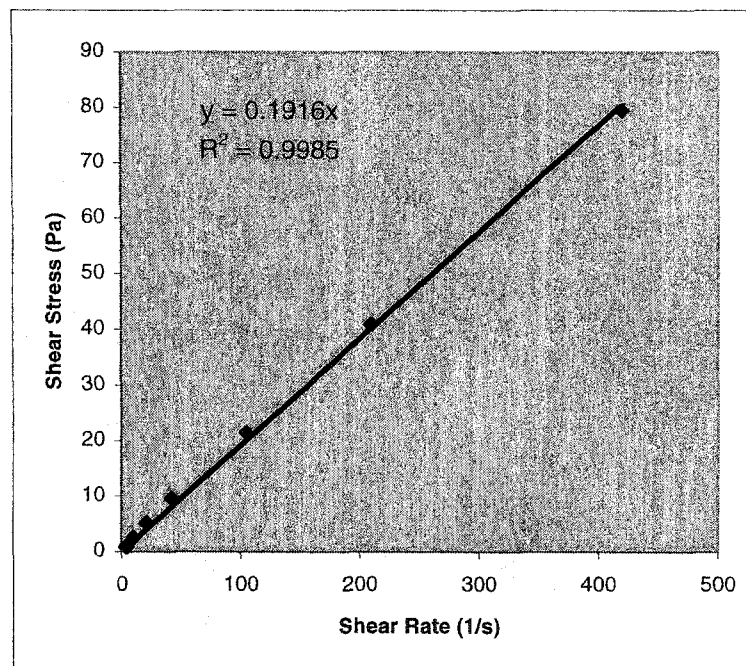


Figure 10: Plot of shear stress versus shear rate at 50 °C for PCL initiated by oleyl alcohol. Slope of the line is viscosity (cP).

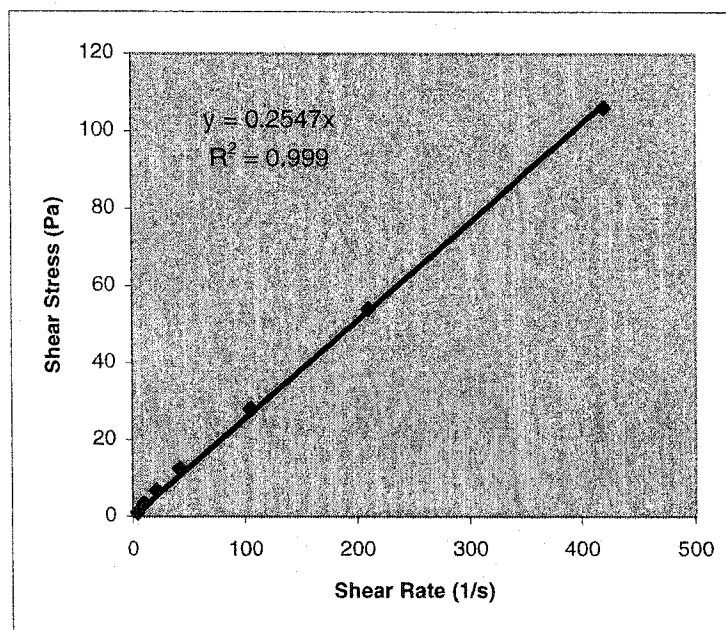


Figure 11: Plot of shear stress versus shear rate at 50 °C for PCL initiated by 2-dodecanol. Slope of the line is viscosity (cps).

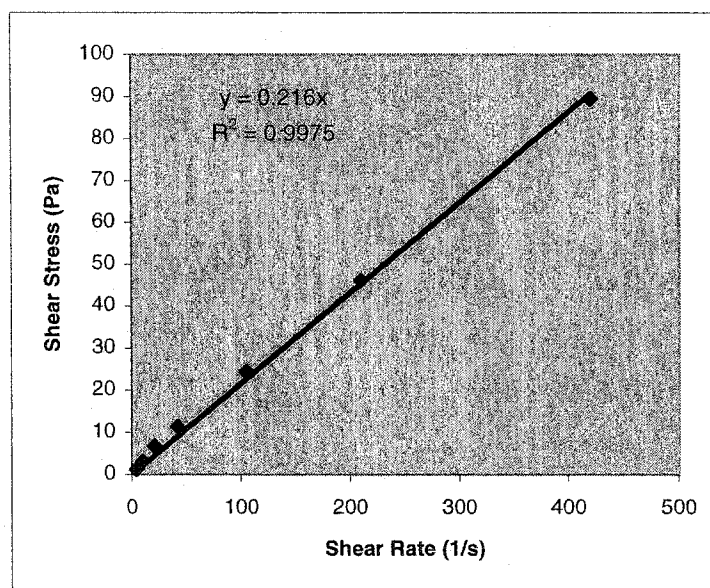


Figure 12: Plot of shear stress versus shear rate at 50 °C for PCL initiated by 1-dodecanol. Slope of the line is viscosity (cP).

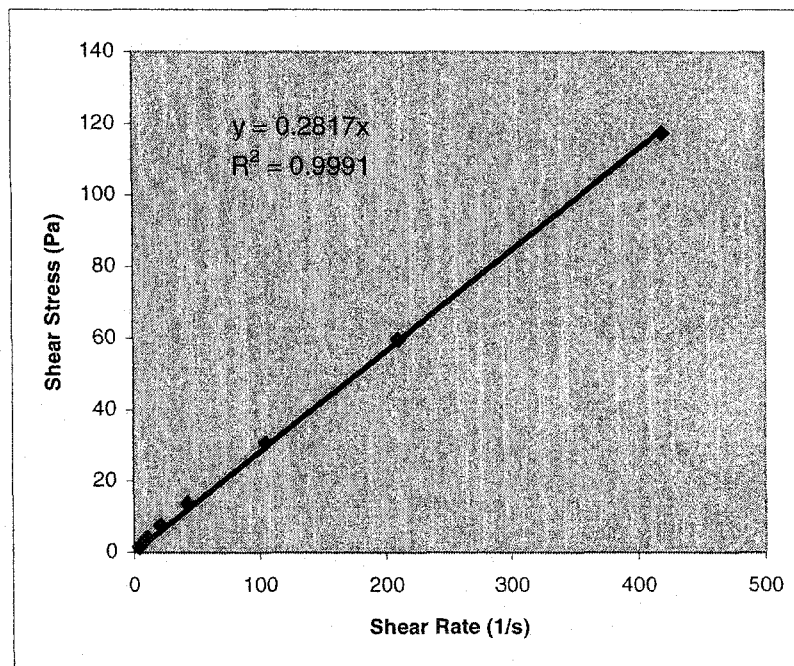


Figure 13: Plot of shear stress versus shear rate at 50 °C for PCL initiated by 2-octanol. Slope of the line is viscosity (cP).

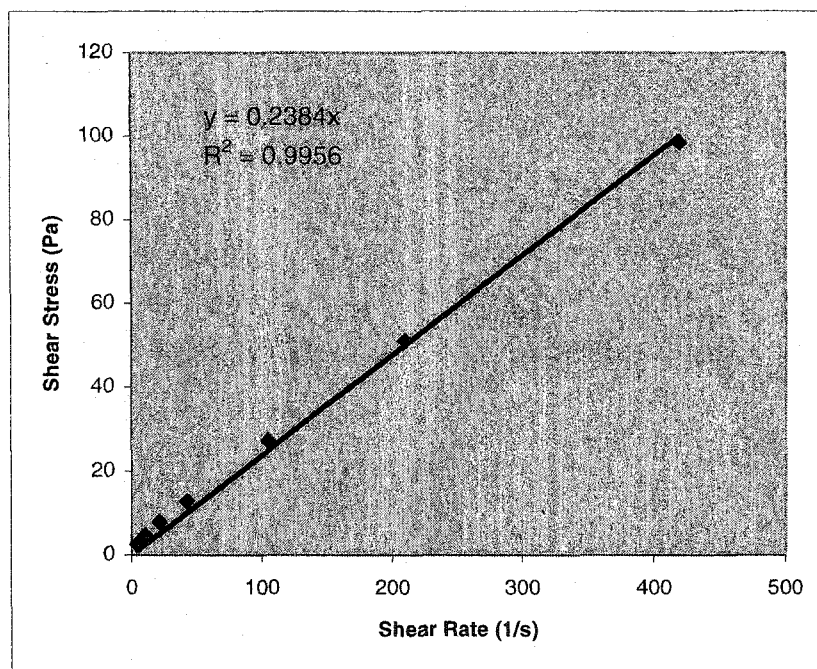


Figure 14: Plot of shear stress versus shear rate at 50 °C for PCL initiated by 1-octanol. Slope of the line is viscosity (cP).

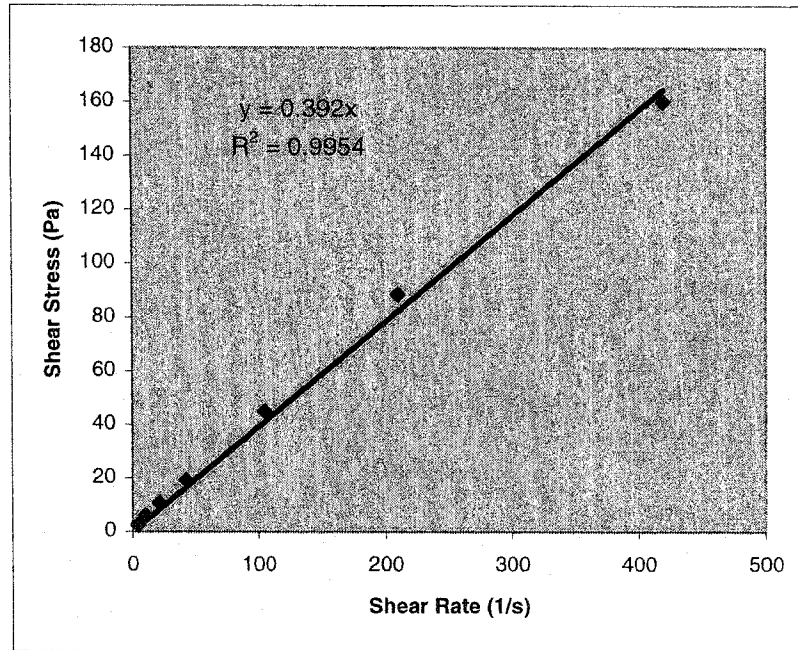


Figure 15: Plot of shear stress versus shear rate at 50 °C for PCL initiated by 2-butanol. Slope of the line is viscosity (cP).

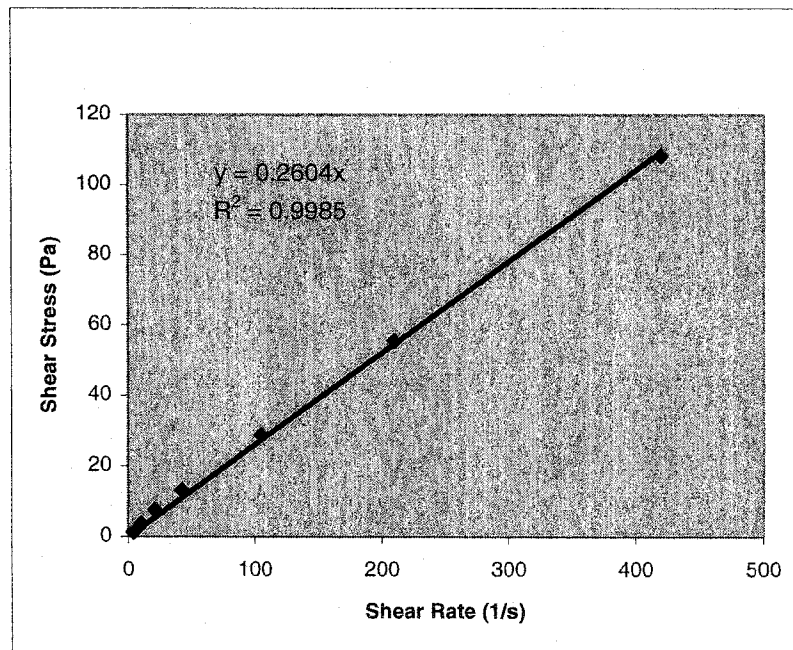
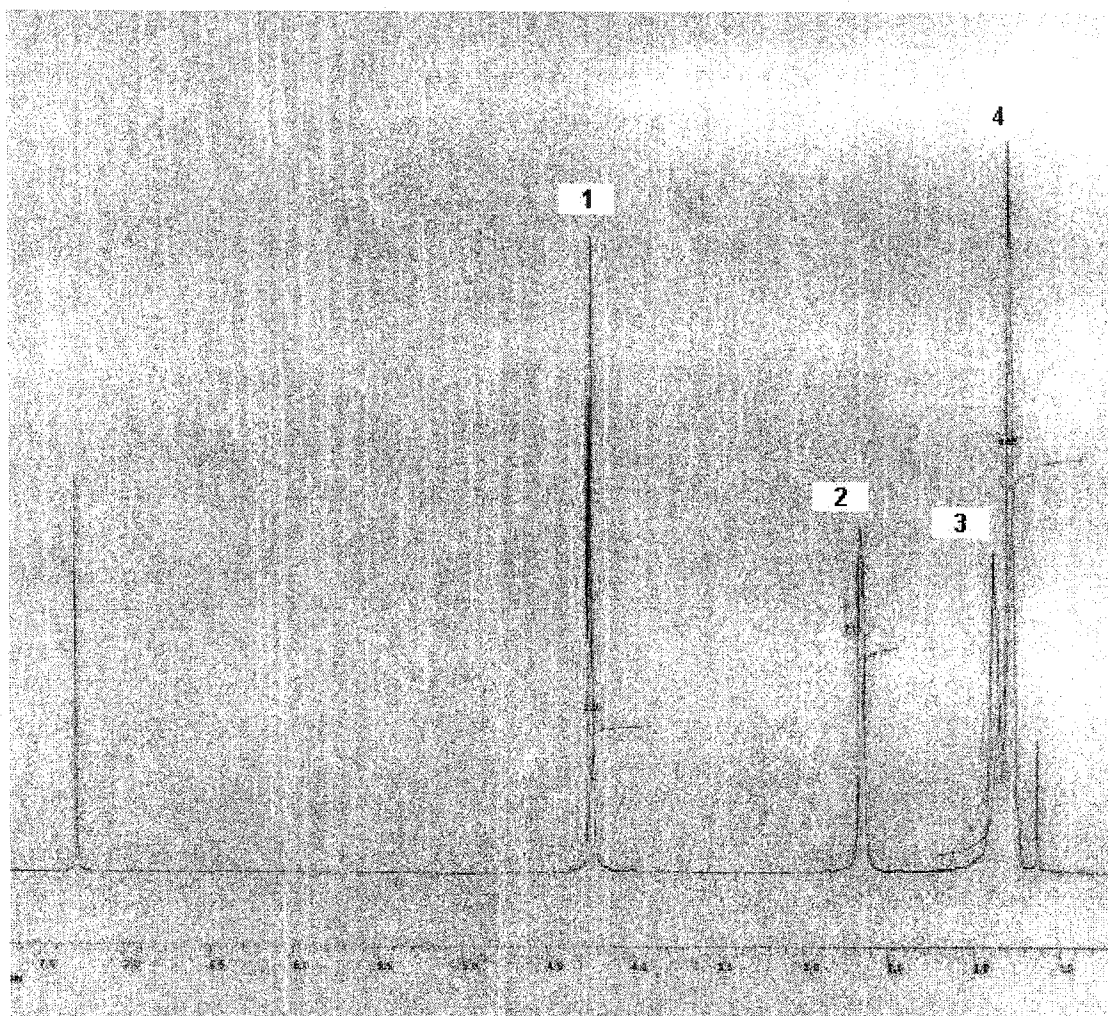
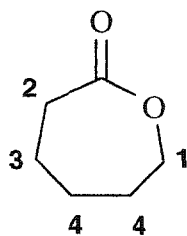


Figure 16: Plot of shear stress versus shear rate at 50 °C for PCL initiated by 2-butanol. Slope of the line is viscosity (cP).

Appendix C

(NMR Spectra)



Important Peak Integrations

- 1- Peak at 4.24 ppm with integration of 2.00
- 2- Peak at 2.65 ppm with integration of 2.13
- 3- Peak at 1.90 ppm with integration of 6.68

Figure 1: NMR spectrum of ϵ -caprolactone in CDCl_3 and its corresponding chemical structure.

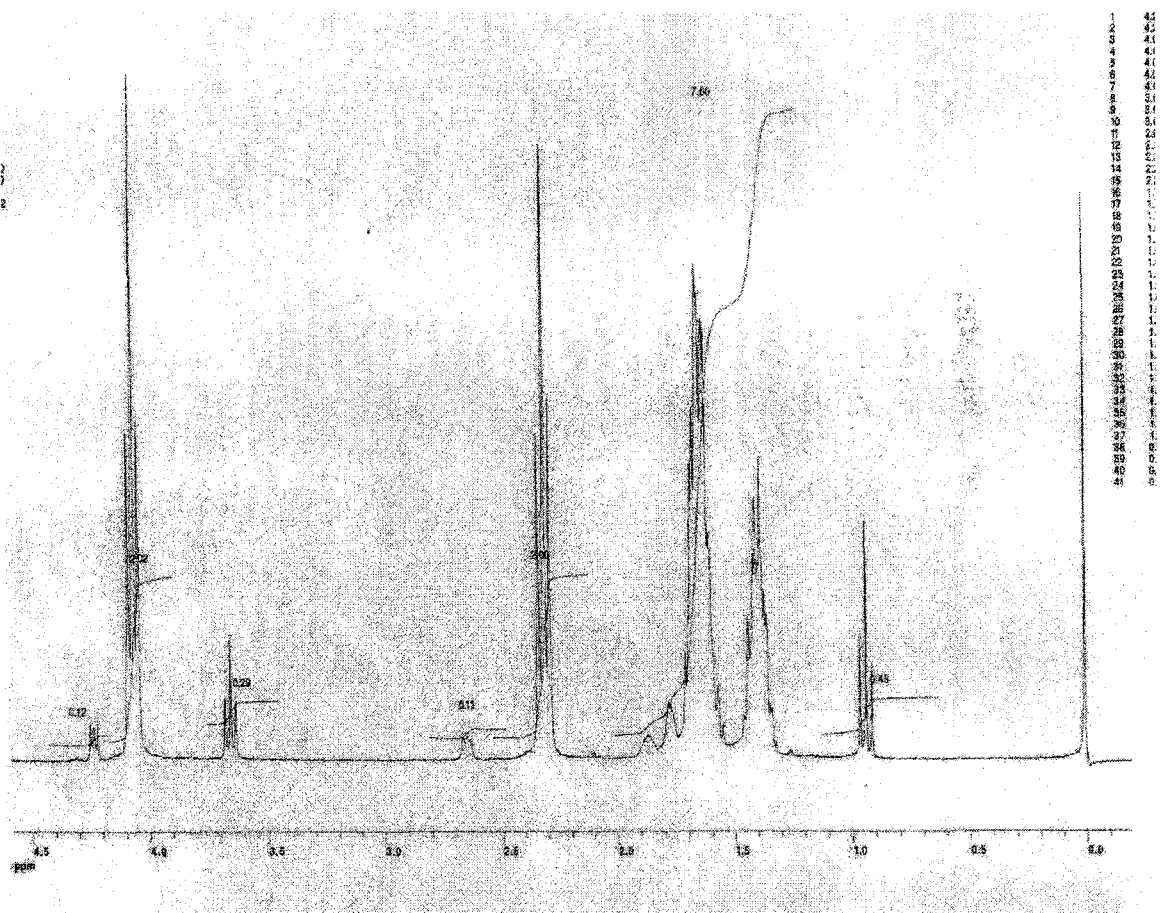
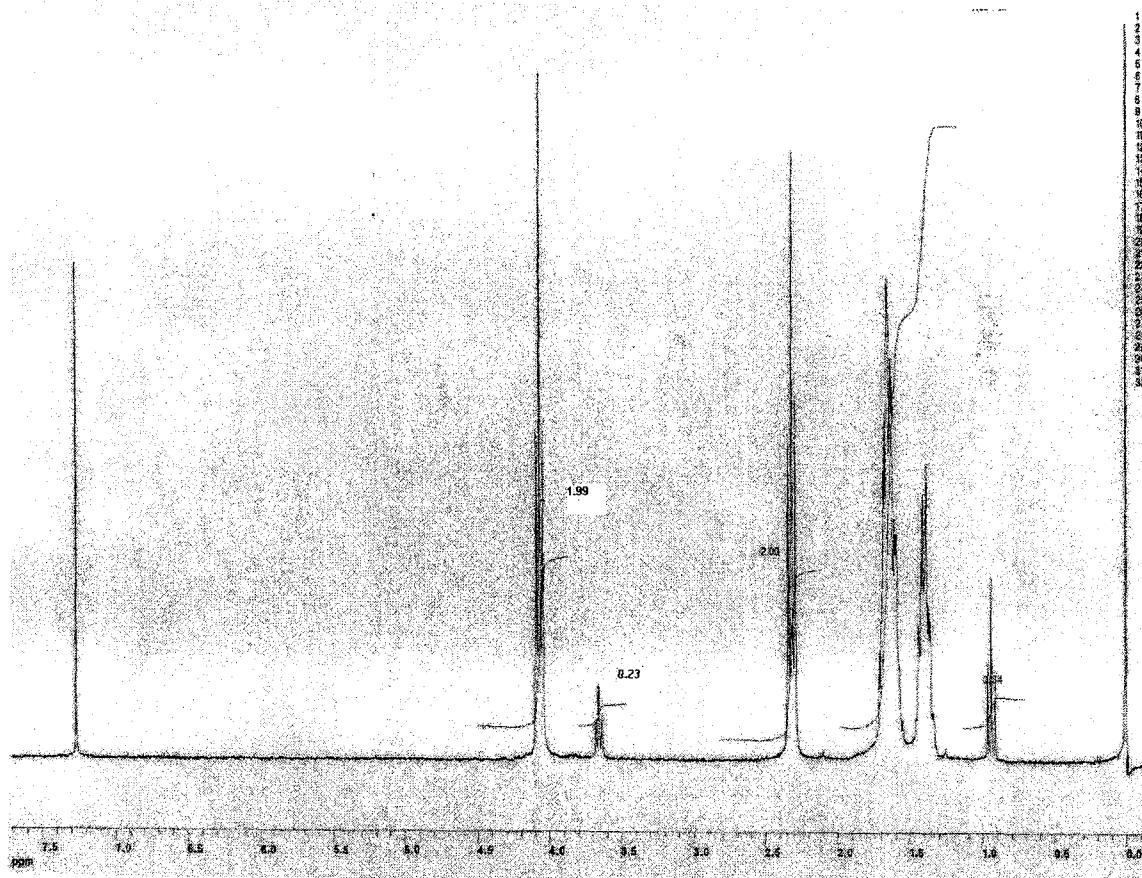


Figure 3: NMR spectrum of PCL initiated by 1-butanol in CDCl_3 . Polymerized for 24 hrs at 80°C with M/I and M/C ratio of 8 and 1000, respectively. The peaks at 2.65 ppm and 4.25 ppm correspond to unreacted ϵ -caprolactone monomer.



Chemical Shift

Integration

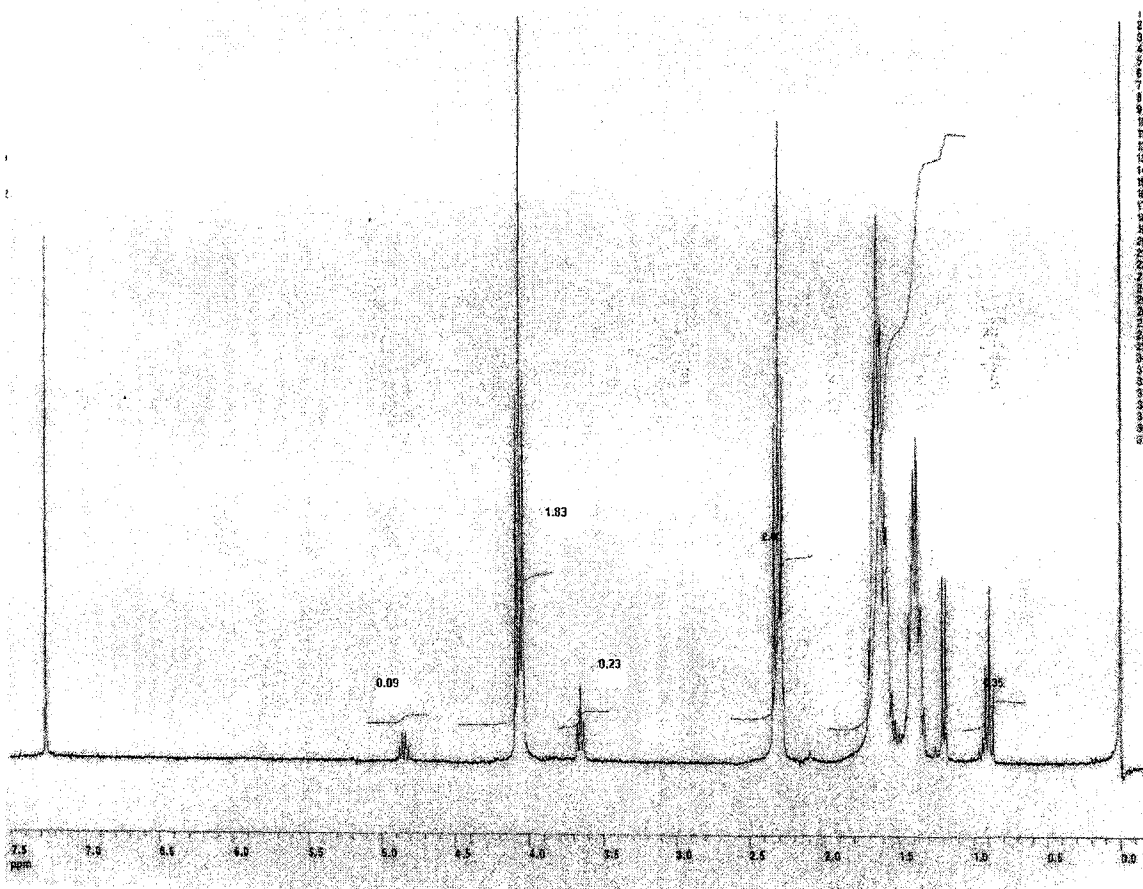
3.65

0.23

4.1

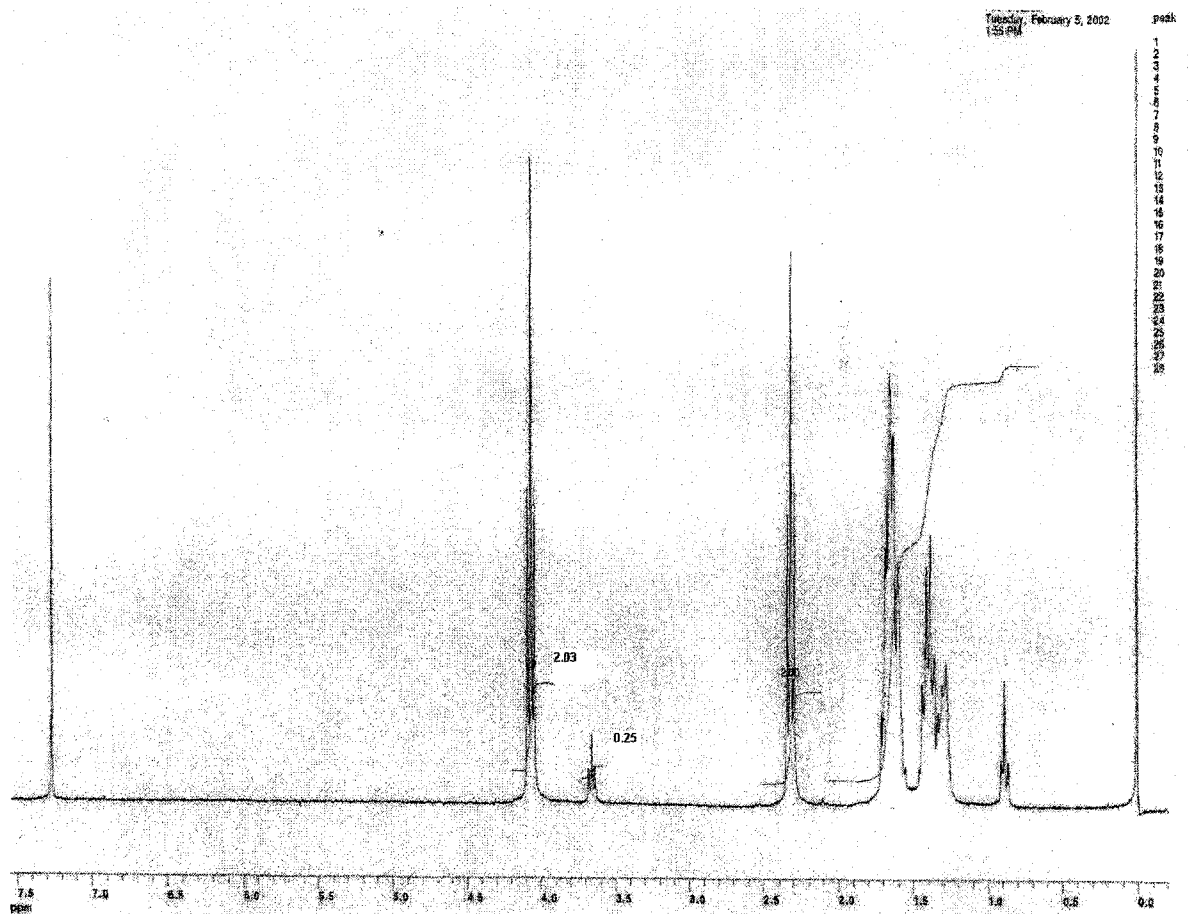
1.99

Figure 4: NMR spectrum in CDCl_3 for PCL initiated by 1-butanol without any purification. $M/I=8$, $M/C=1000$.



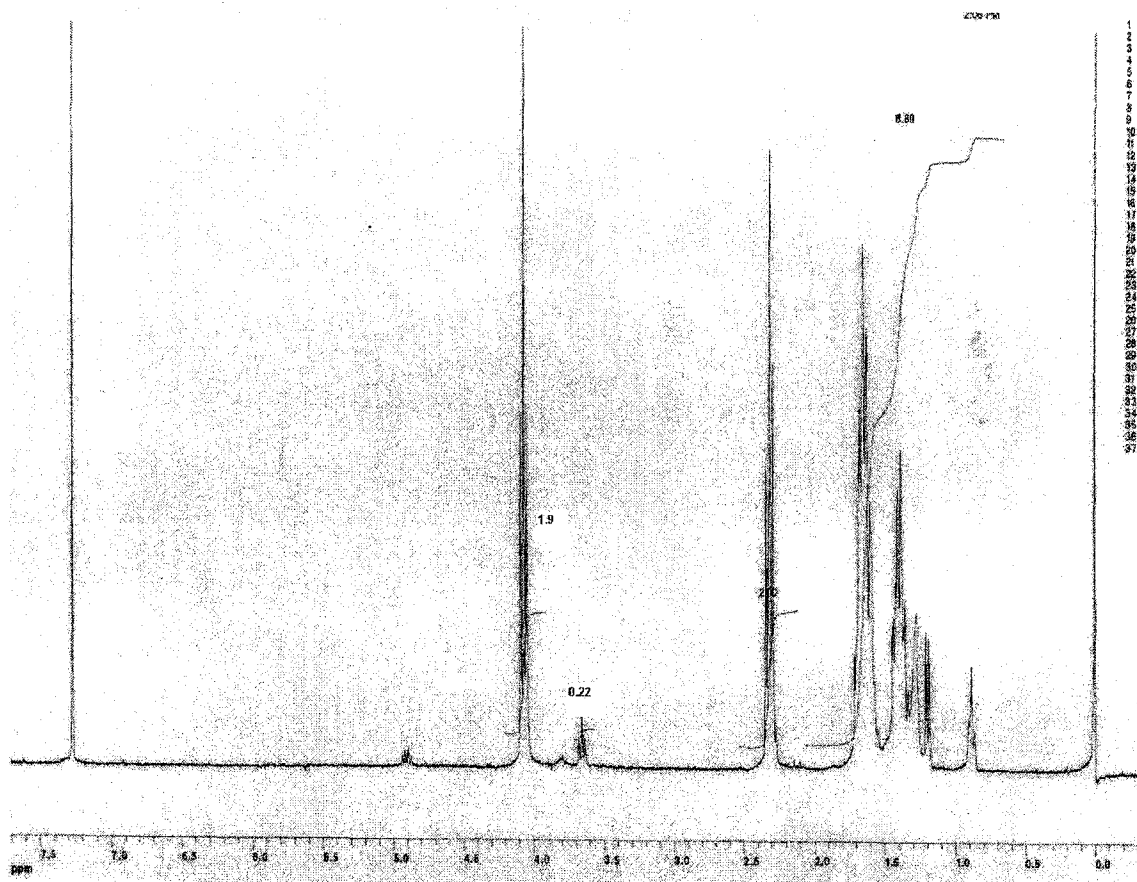
Chemical Shift	Integration
3.65	0.23
4.1	1.83

Figure 5: NMR spectrum in CDCl_3 for PCL initiated by 2-butanol without any purification.
 $M/I=8$, $M/C=1000$.



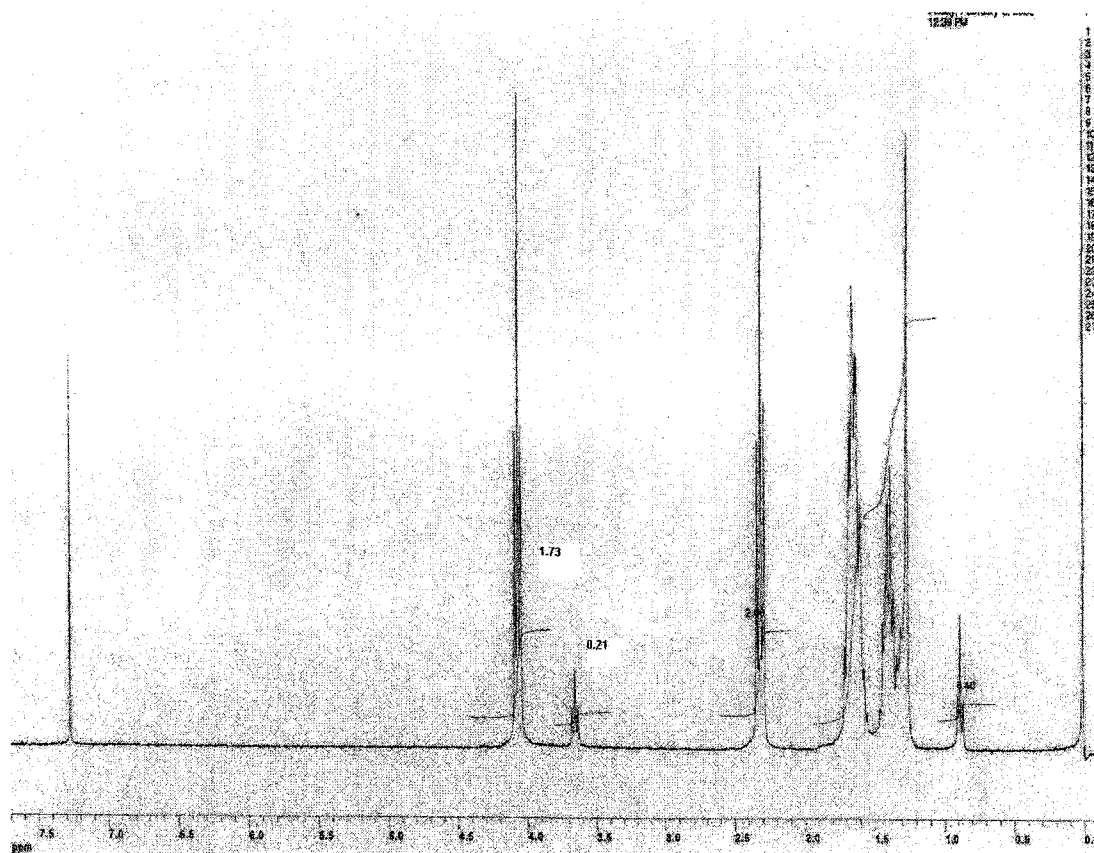
Chemical Shift	Integration
3.65	0.25
4.1	2.03

Figure 6: NMR spectrum in CDCl_3 for PCL initiated by 1-octanol without any purification.
 $M/I=8$, $M/C=1000$.



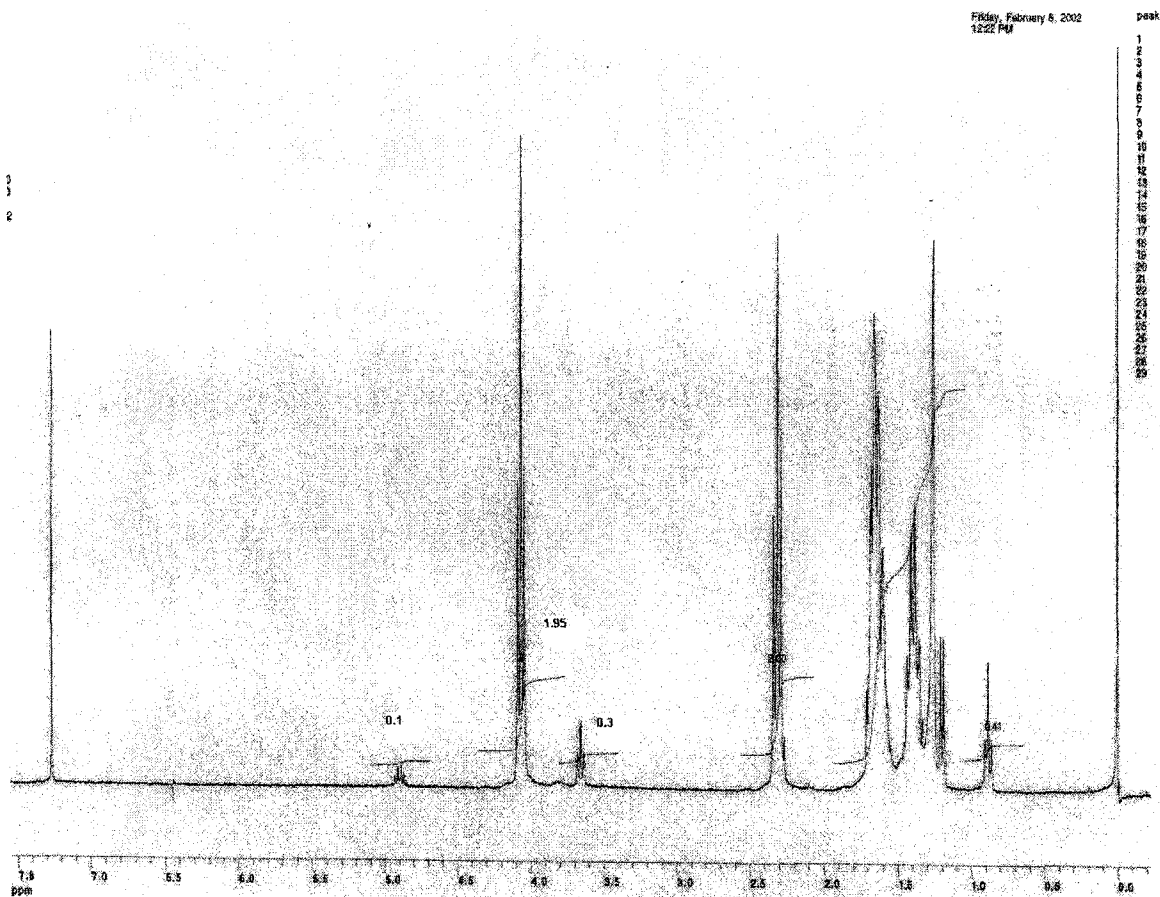
Chemical Shift	Integration
3.65	0.22
4.1	1.9

Figure 7: NMR spectrum in CDCl_3 for PCL initiated by 2-octanol without any purification.
 $M/I=8$, $M/C=1000$.



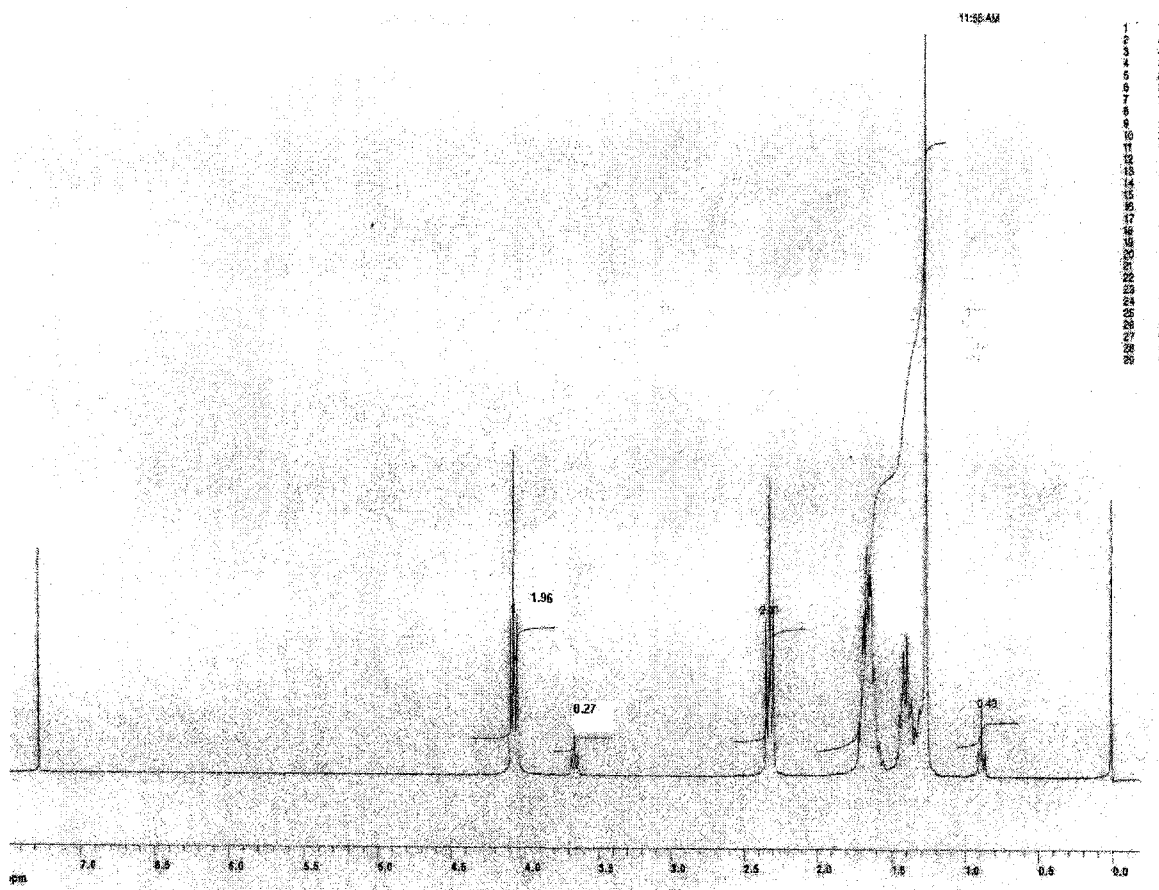
Chemical Shift	Integration
3.65	0.21
4.1	1.73

Figure 8: NMR spectrum in CDCl_3 for PCL initiated by 1-dodecanol without any purification.
 $M/I=8$, $M/C=1000$.



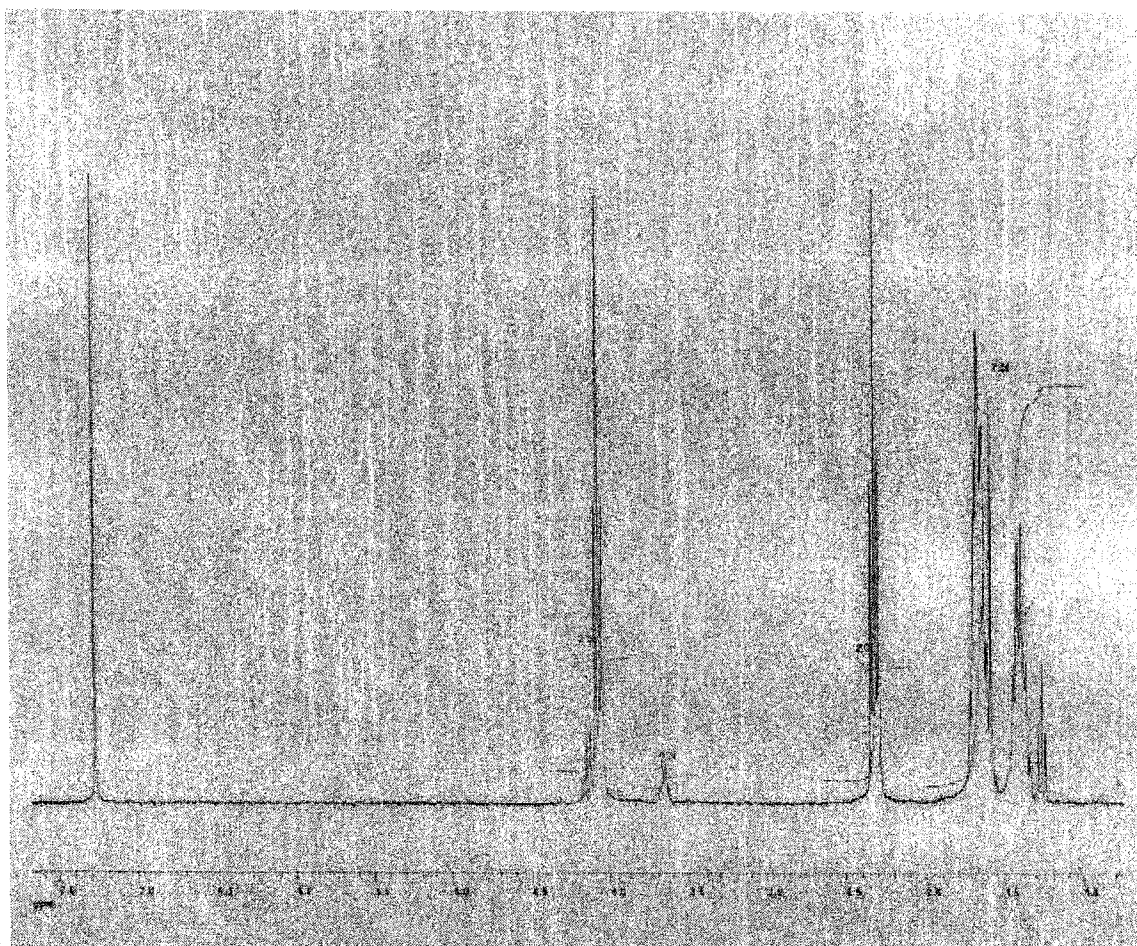
Chemical Shift	Integration
3.65	0.3
4.1	1.95

Figure 9: NMR spectrum in CDCl_3 for PCL initiated by 2-dodecanol without any purification.
M/I=8, M/C=1000.



Chemical Shift	Integration
3.65	0.27
4.1	1.96

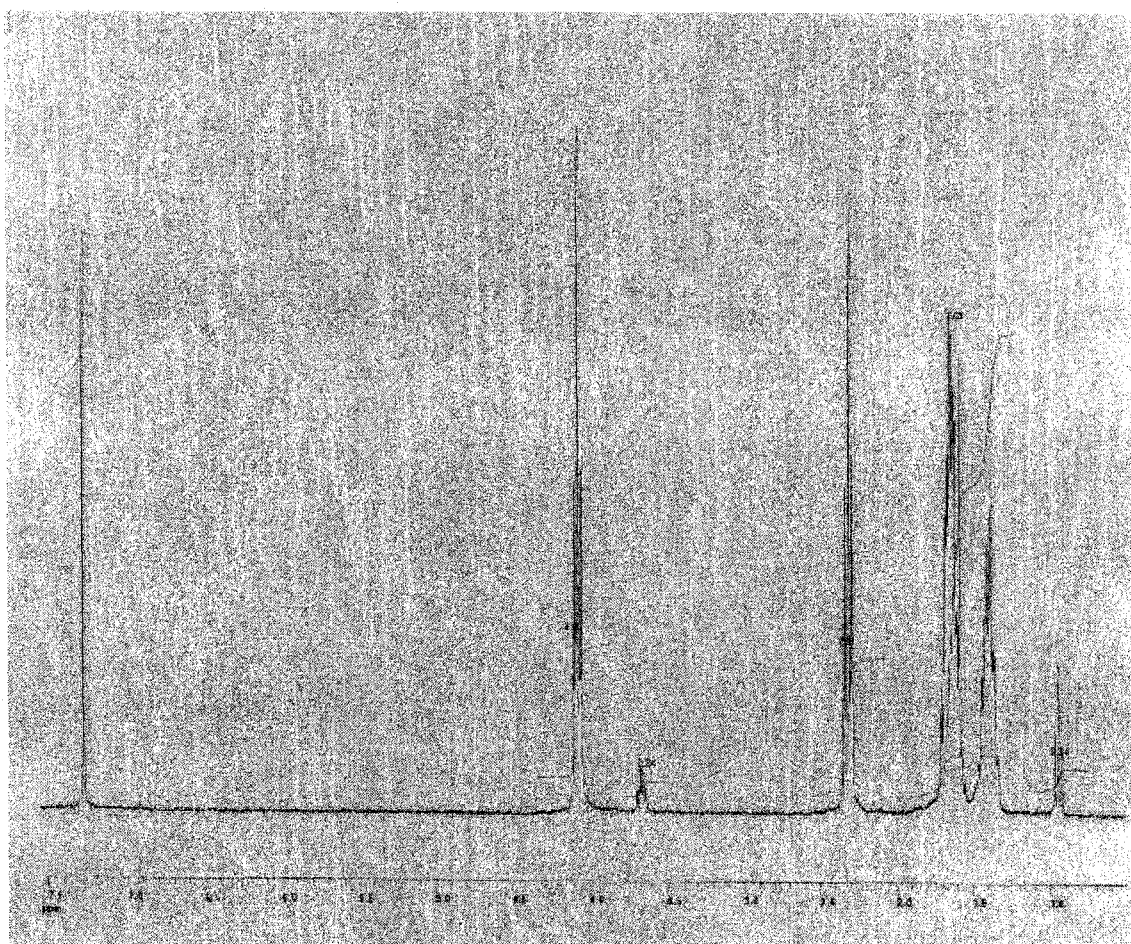
Figure 10: NMR spectrum in CDCl_3 for PCL initiated by stearyl alcohol without any purification.
 $M/I=8$, $M/C=1000$.



Important Peak Integrations:

- 1-Peak at 2.35 ppm with Integration of 2.01
- 2-Peak at 3.65 ppm with Integration of 0.21
- 3-Peak at 4.10 ppm with Integratoin of 2.00

Figure 11: NMR spectrum in CDCl_3 for CL oligomer initiated by ethanol after purification.
M/I=2.1, M/C=1000.



Important Peak Integrations:
1-Peak at 2.30 ppm with Integration of 2.01
2-Peak at 3.65 ppm with Integration of 0.24
3-Peak at 4.10 ppm with Integration of 2.00

Figure 12: NMR spectrum in CDCl_3 for CL oligomer initiated by 1-butanol after purification.
 $M/I=2.1$, $M/C=1000$.



Important Peak Integrations:

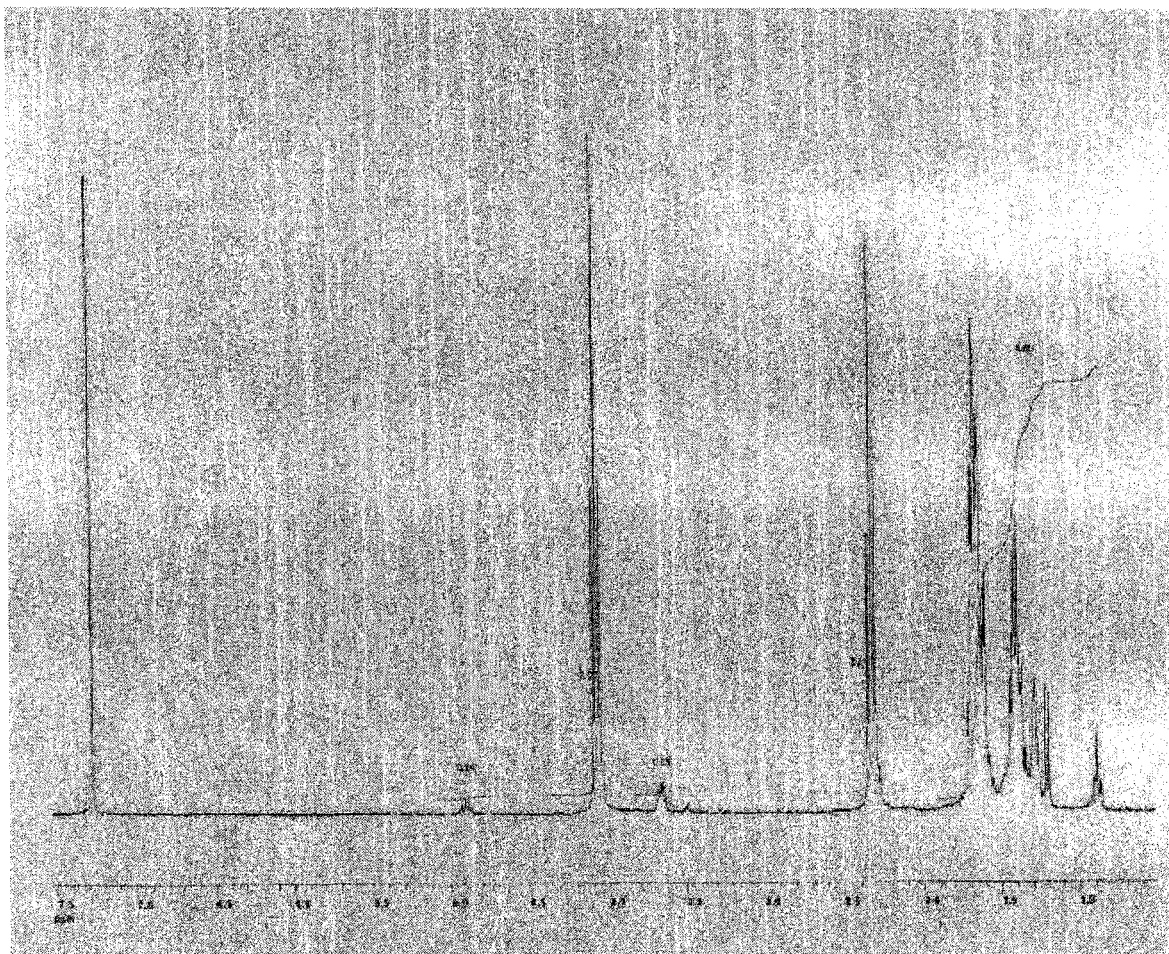
- 1- Peak at 2.30 ppm with Integration of 2.00
- 2- Peak at 3.65 ppm with Integration of 0.19
- 3- Peak at 4.05 ppm with Integration of 1.87
- 4- Peak at 4.85 ppm with Integration of 0.07

Figure 13: NMR spectrum in CDCl_3 for CL oligomer initiated by 2-butanol after purification.
 $M/I=2.1$, $M/C=1000$.



Important Peak Integrations:
1-Peak at 2.30 ppm with Integration of 2.08
2-Peak at 3.65 ppm with Integration of 0.23
3-Peak at 4.05 ppm with Integration of 2.00

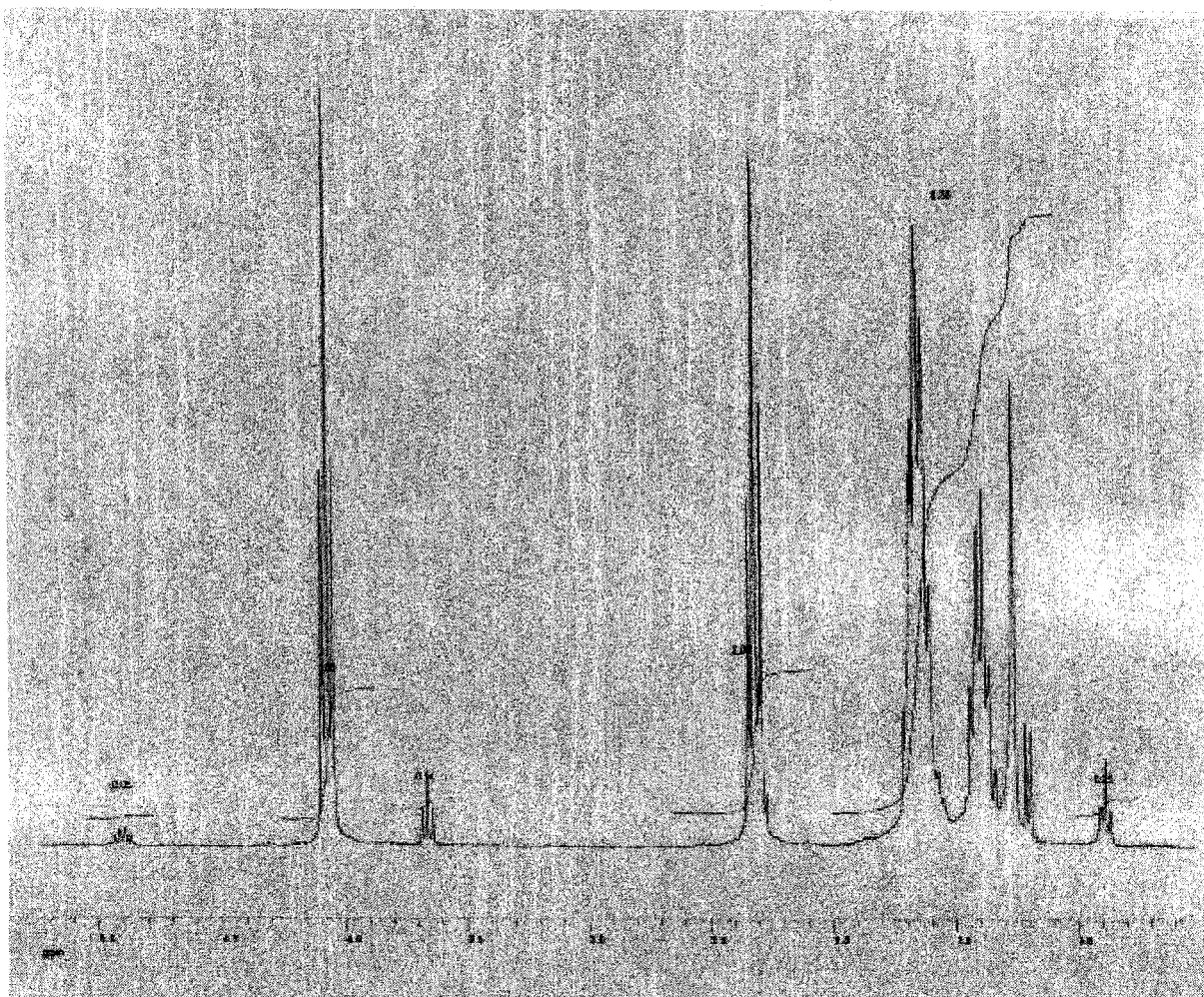
Figure 14: NMR spectrum in CDCl_3 for CL oligomer initiated by 1-octanol after purification.
 $M/I=2.1$, $M/C=1000$.



Important Peak Integrations:

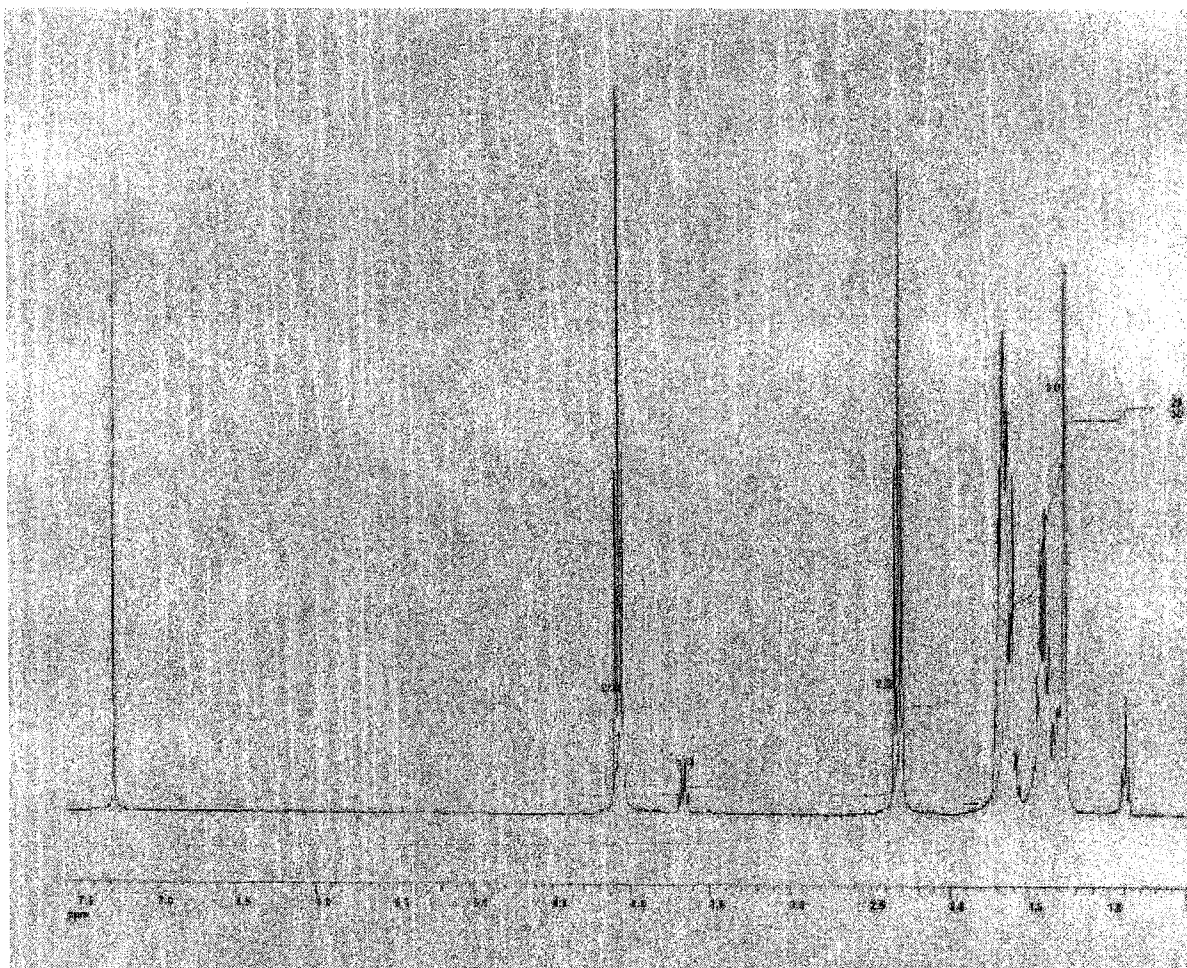
- 1- Peak at 2.35 ppm with Integration of 2.21
- 2- Peak at 3.65 ppm with Integration of 0.13
- 3- Peak at 4.10 ppm with Integration of 2.00
- 4- Peak at 4.90 ppm with Integration of 0.04

Figure 15: NMR spectrum in CDCl_3 for CL oligomer initiated by 2-octanol after purification.
 $M/I=2.1$, $M/C=1000$.



Important Peak Integrations:
1-Peak at 2.30 ppm with Integration of 2.00
2-Peak at 3.65 ppm with Integration of 0.14
3-Peak at 4.05 ppm with Integration of 1.83
4-Peak at 4.90 ppm with Integration of 0.05

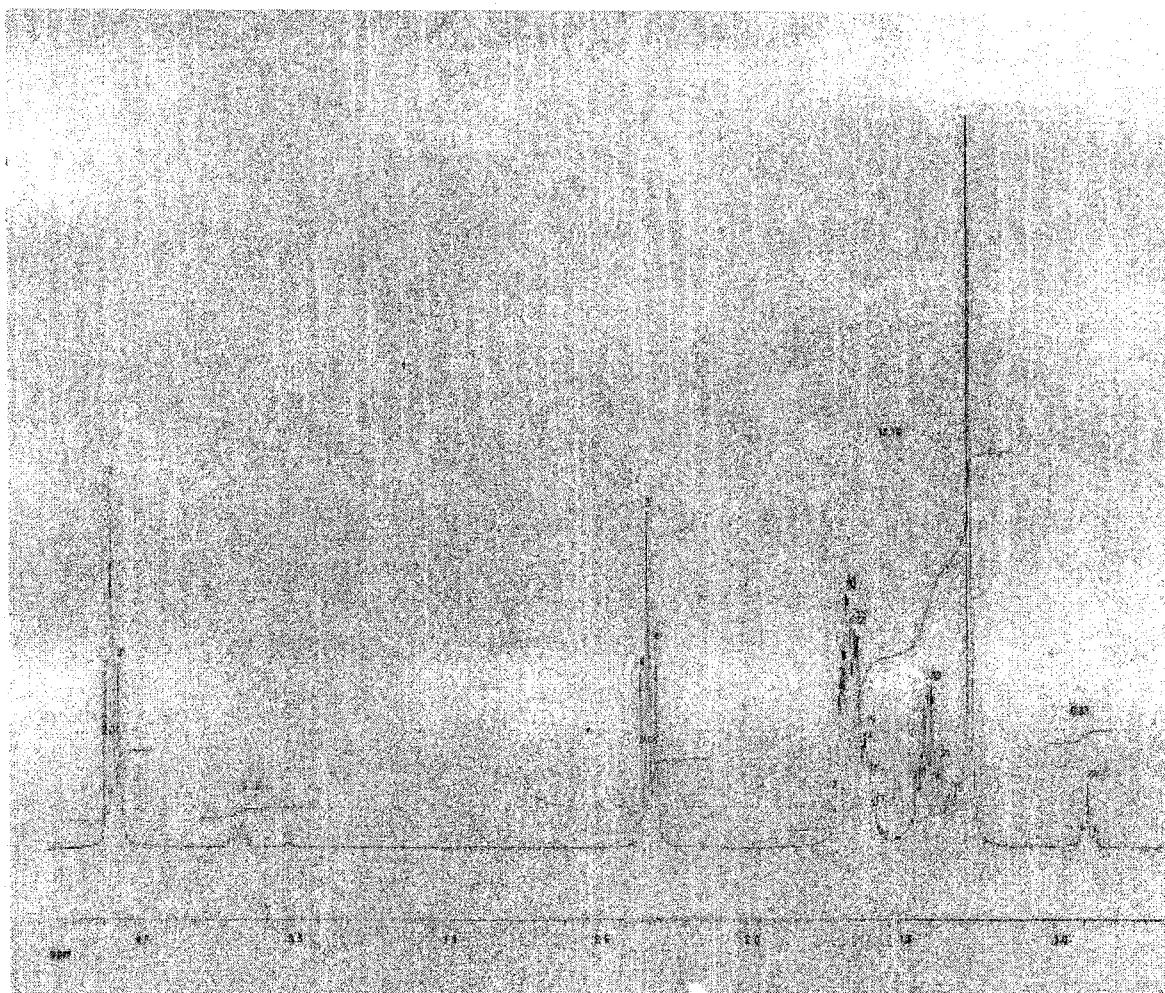
Figure 16: NMR spectrum in CDCl_3 for CL oligomer initiated by 2-dodecanol after purification.
 $M/I=2.6$, $M/C=1000$.



Important Peak Integrations:

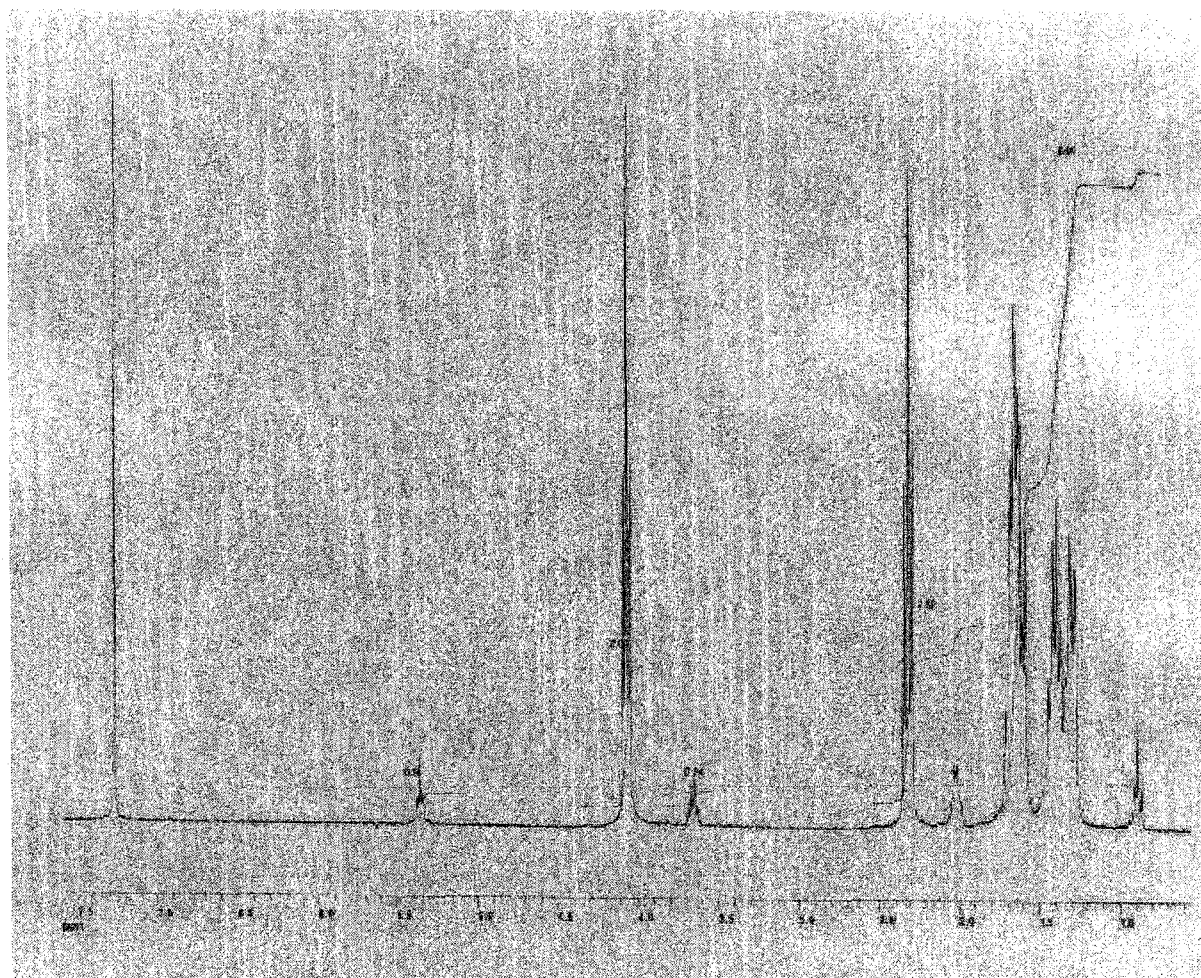
- 1- Peak at 2.35 ppm with Integration of 2.08
- 2- Peak at 3.65 ppm with Integration of 0.19
- 3- Peak at 4.1 ppm with Integration of 2.00

Figure 17: NMR spectrum in CDCl₃ for CL oligomer initiated by 1-dodecanol after purification.
M/I=3.4, M/C=1000.



Important Peak Integrations:
1-Peak at 2.30 ppm with Integration of 2.07
2-Peak at 3.65 ppm with Integration of 0.32
3-Peak at 4.05 ppm with Integration of 2.00

Figure 18: NMR spectrum in CDCl₃ for CL oligomer initiated by stearyl alcohol after purification.
M/I=4, M/C=1000.



Important Peak Integrations:

- 1-Peak at 2.30 ppm with Integration of 2.52
- 2-Peak at 3.65 ppm with Integration of 0.24
- 3-Peak at 4.10 ppm with Integration of 2.00
- 4-Peak at 5.35 ppm with Integration of 0.16

Figure 19: NMR spectrum in CDCl_3 for CL oligomer initiated by oleyl alcohol after purification.
M/I=3.2, M/C=1000.

Appendix D

(GPC Spectrums)

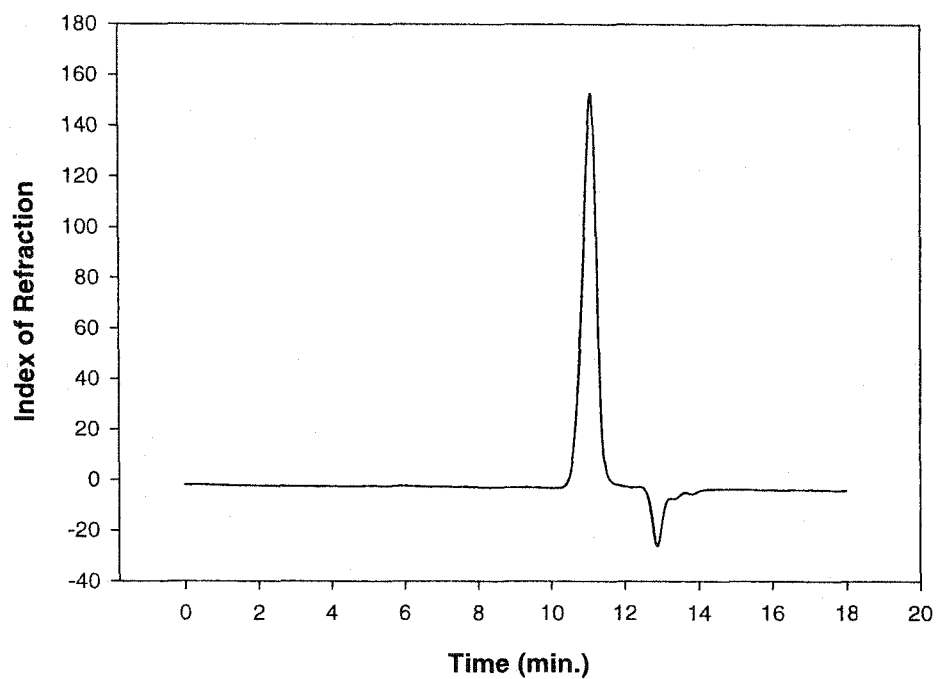


Figure 1: GPC spectrum for PCL initiated by ethanol. The peaks at 11 and 13 minutes correspond to oligomer and solvent, respectively.

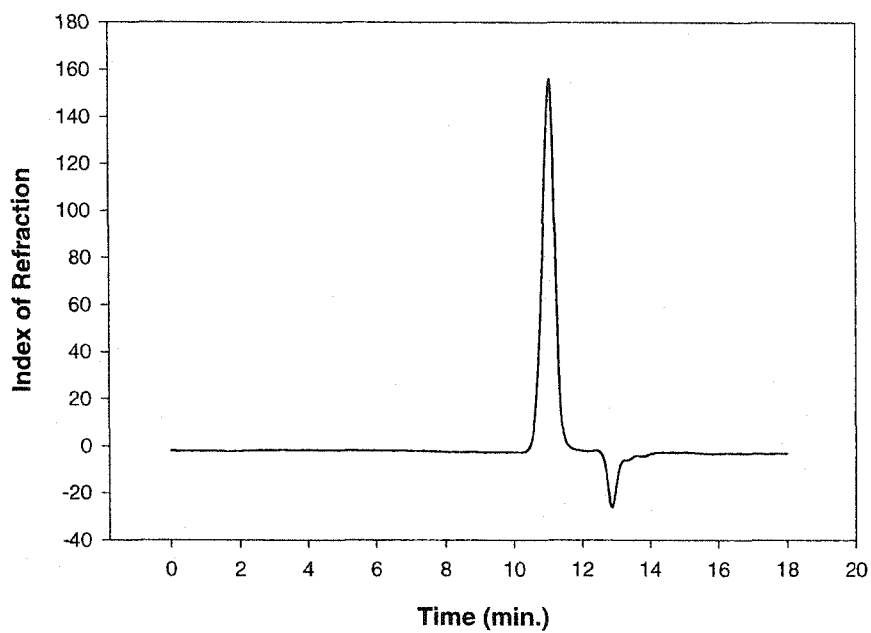


Figure 2: GPC spectrum for PCL initiated by 1-butanol. The peaks at 11 and 13 minutes correspond to oligomer and solvent, respectively.

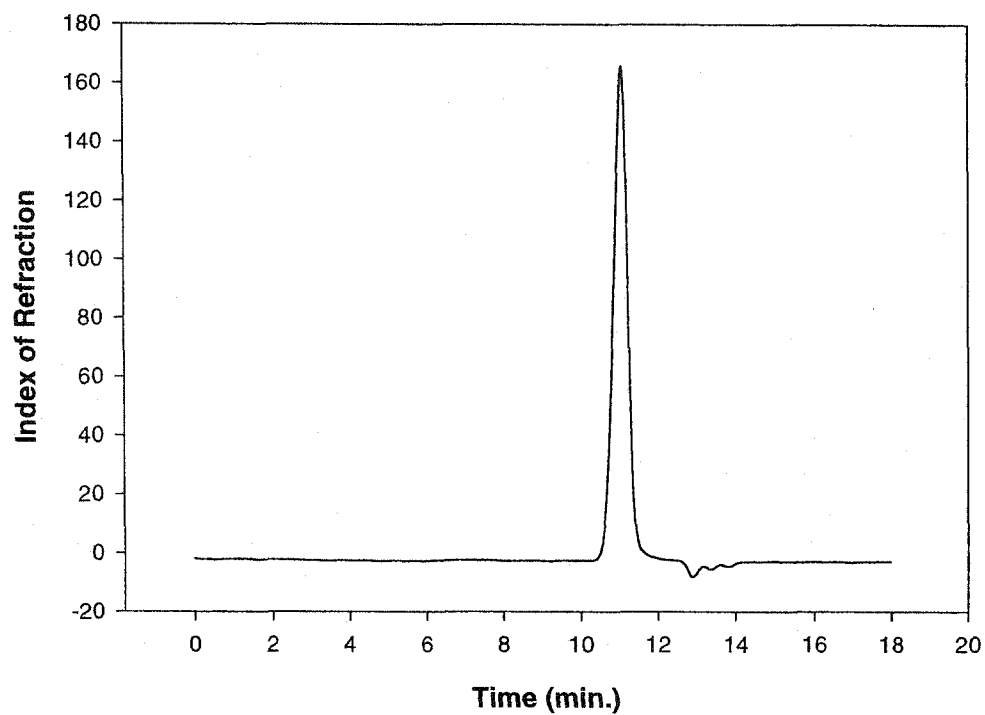


Figure 3: GPC spectrum for PCL initiated by 1-octanol. The peaks at 11 and 13 minutes correspond to oligomer and solvent, respectively.

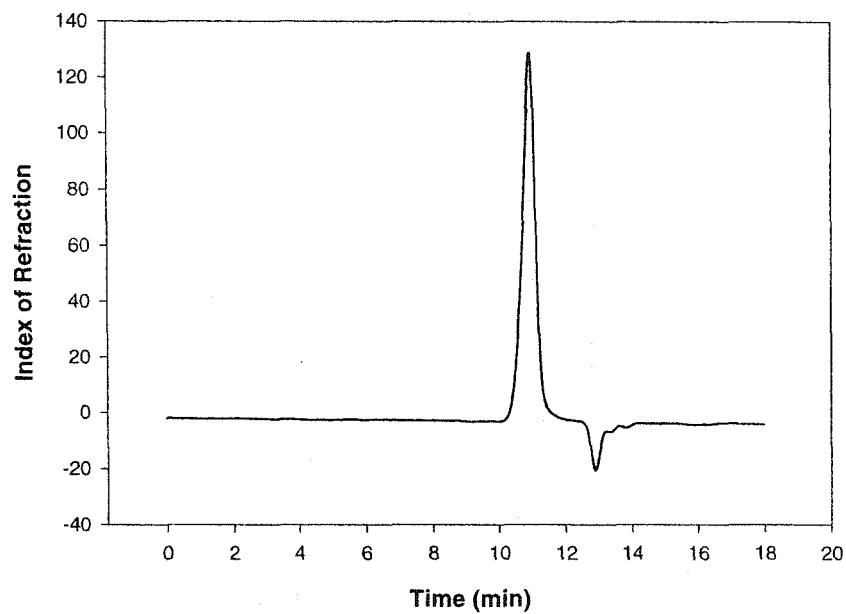


Figure 4: GPC spectrum for PCL initiated by 2-octanol. The peaks at 11 and 13 minutes correspond to oligomer and solvent, respectively.

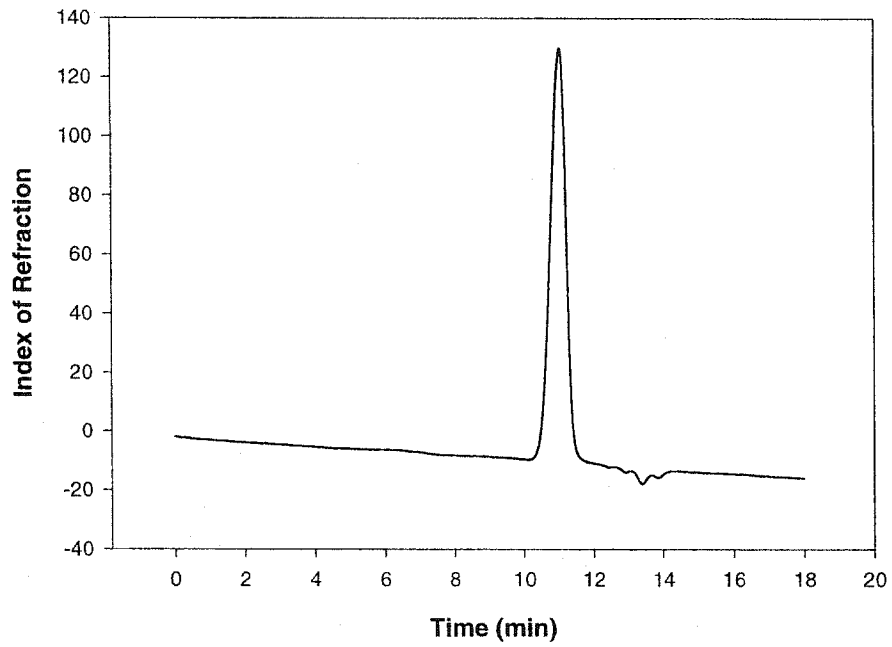


Figure 5: GPC spectrum for PCL initiated by 1-dodecanol. The peaks at 11 and 13 minutes correspond to oligomer and solvent, respectively.

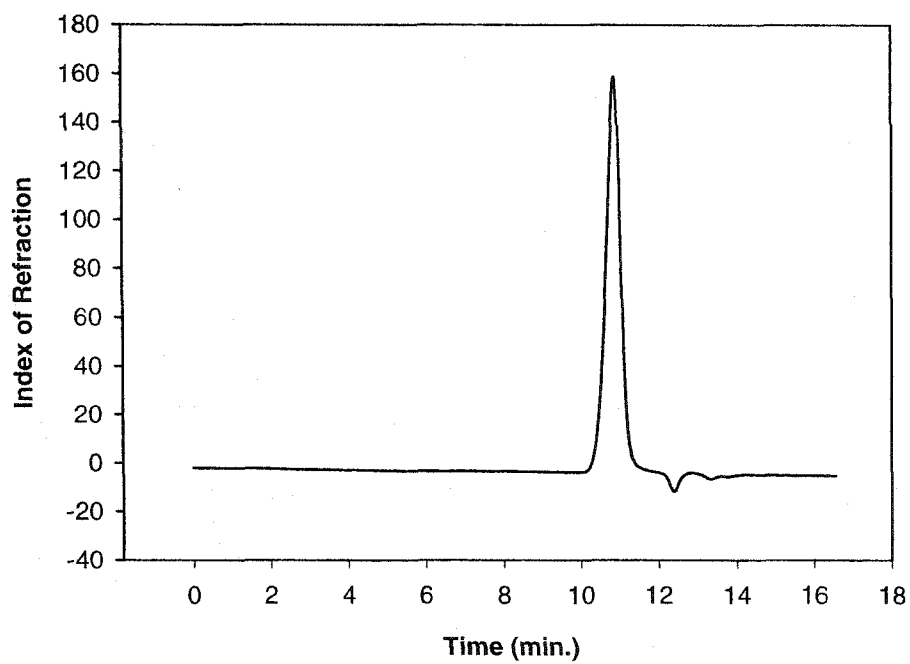


Figure 6: GPC spectrum for PCL initiated by 2-dodecanol. The peaks at 11 and 13 minutes correspond to oligomer and solvent, respectively.

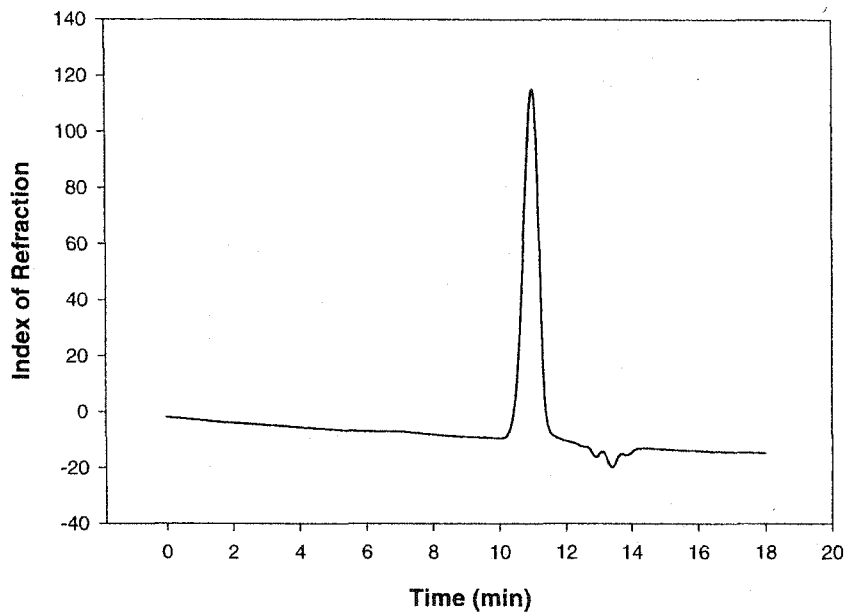


Figure 7: GPC spectrum for PCL initiated by stearyl alcohol. The peaks at 11 and 13 minutes correspond to oligomer and solvent, respectively.

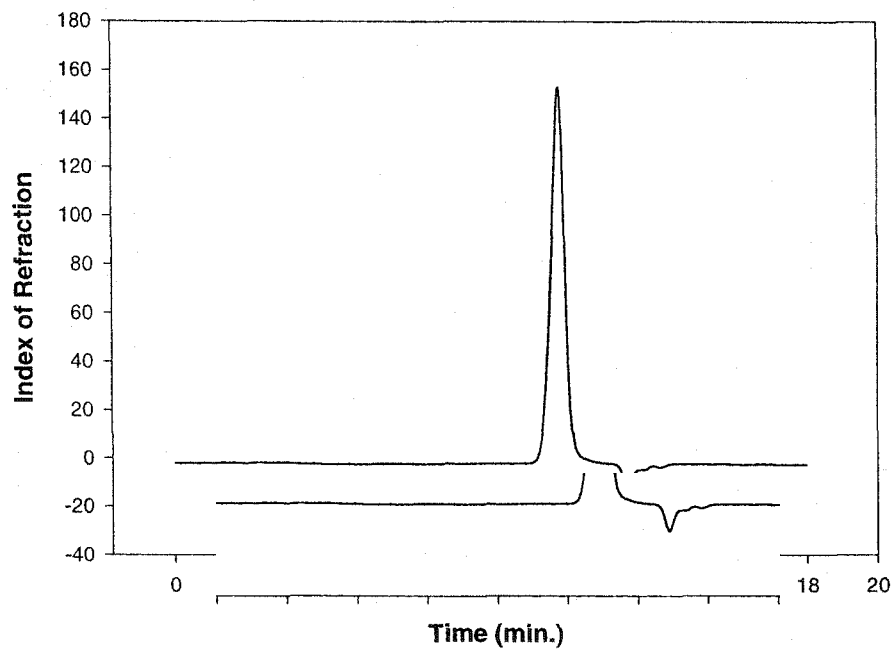
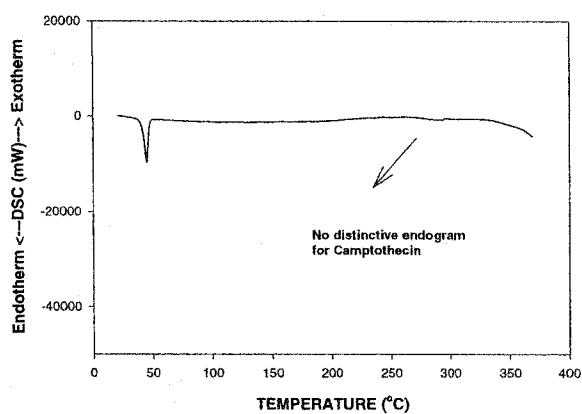


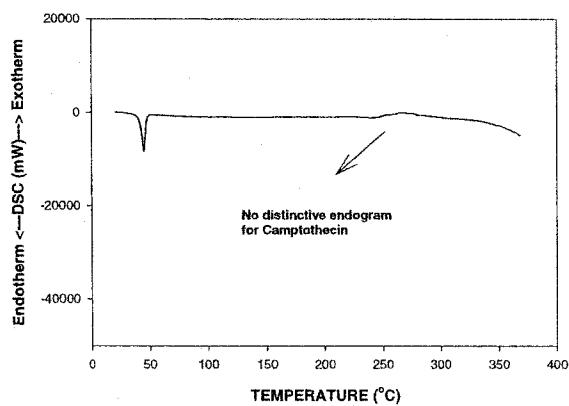
Figure 8: GPC spectrum for PCL initiated by oleyl alcohol. The peaks at 11 and 13 minutes correspond to oligomer and solvent, respectively.

Appendix E
(DSC Scans for Solubility Studies)

A)



B)



C)

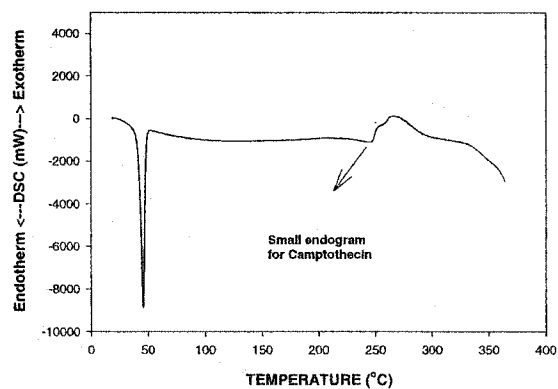
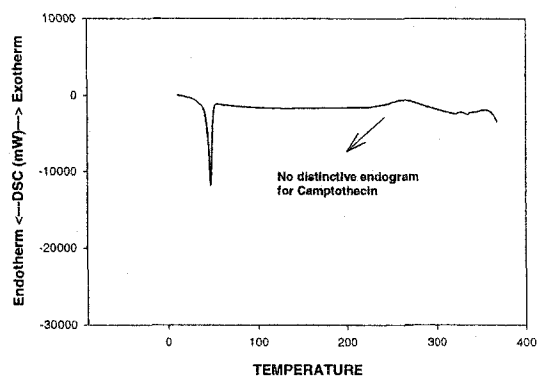
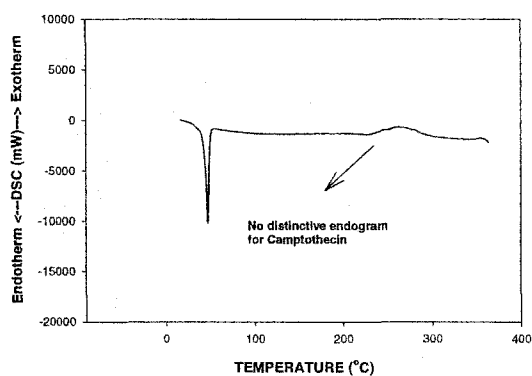


Figure 1: DSC analysis of CL oligomer initiated with oleyl alcohol mixed with CPT. Drug/ oligomer ratio of A) 9mg/100mg, B) 10.5mg/100mg, C) 11mg/ 100mg.

A)



B)



C)

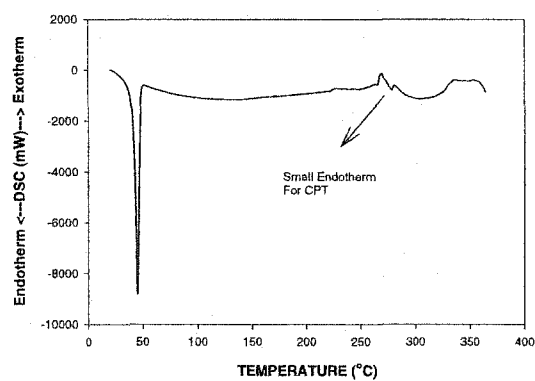
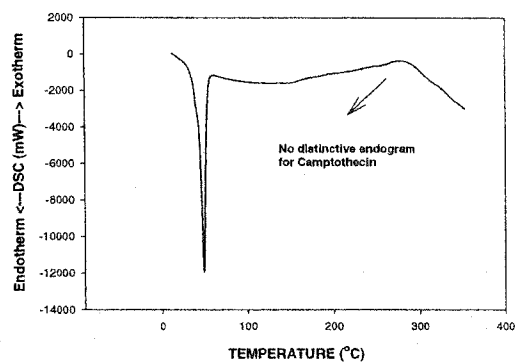
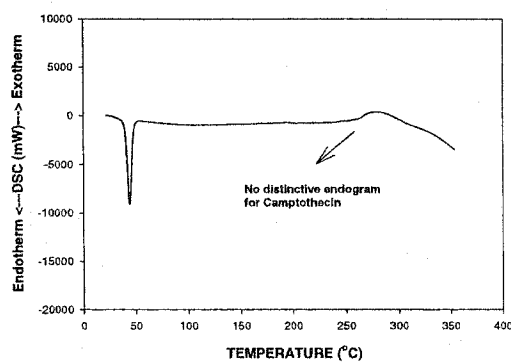


Figure 2: DSC analysis of CL oligomer initiated with 1-dodecanol mixed with CPT. Drug/ oligomer ratio of A) 9mg/100mg, B) 10mg/100mg, C) 11.5mg/ 100mg.

A)



B)



C)

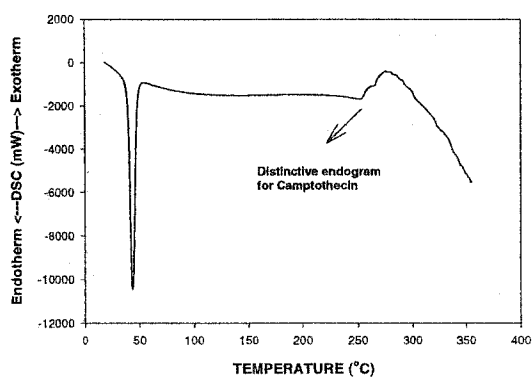
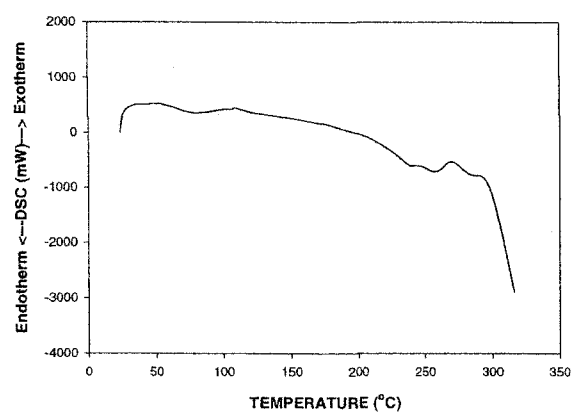


Figure 3: DSC analysis of CL oligomer initiated with 2-dodecanol mixed with CPT. Drug/ oligomer ratio of A) 8mg/100mg, B) 9mg/100mg, C) 10mg/100mg.

A)



B)

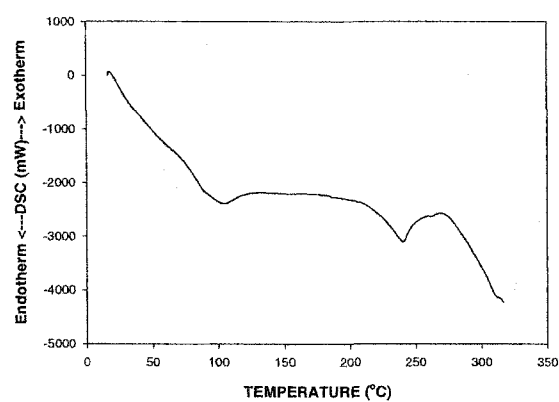


Figure 4: DSC analysis of PLGA mixed with CPT. Drug/ PLGA ratio of A) 3mg/100mg, B) 3.5mg/100mg.

Appendix F
(HPLC Spectra)

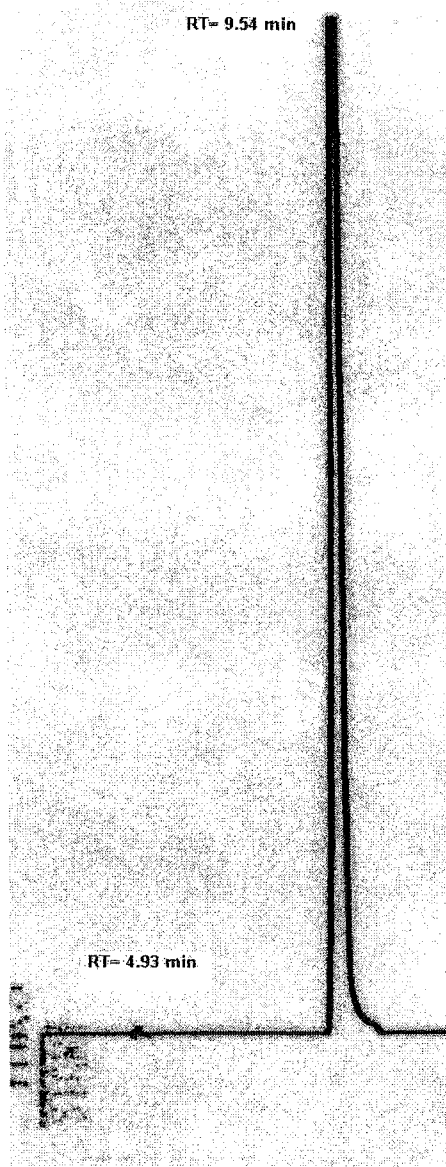


Figure 1: HPLC analysis of CPT at pH=6.1 after the first injection (first injection, time=0 min).

<u>Retention Time</u>	<u>Area %</u>	
4.93	0.05%	Carboxylate form
9.54	99.95%	Lactone form



Figure 2: HPLC analysis of CPT at pH=6.1 after the second injection (second injection, time=30 min).

<u>Retention Time</u>	<u>Area %</u>	
4.93	1.4%	Carboxylate form
9.54	98.6%	Lactone form

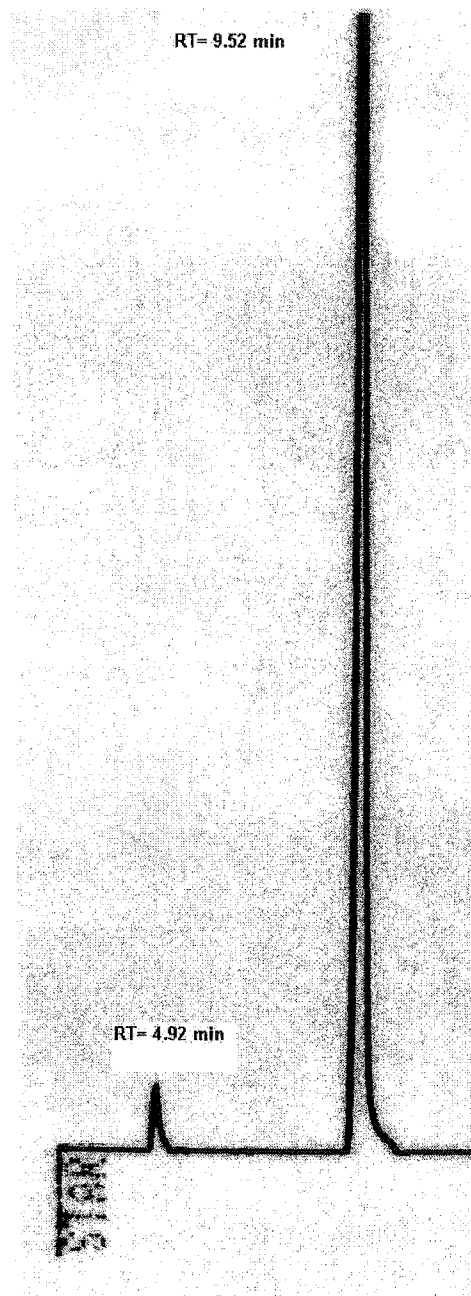


Figure 3: HPLC analysis of CPT at pH=6.1 after the second injection (third injection, time=60 min).

<u>Retention Time</u>	<u>Area%</u>	
4.92	5.5%	Carboxylate form
9.52	94.5%	Lactone form

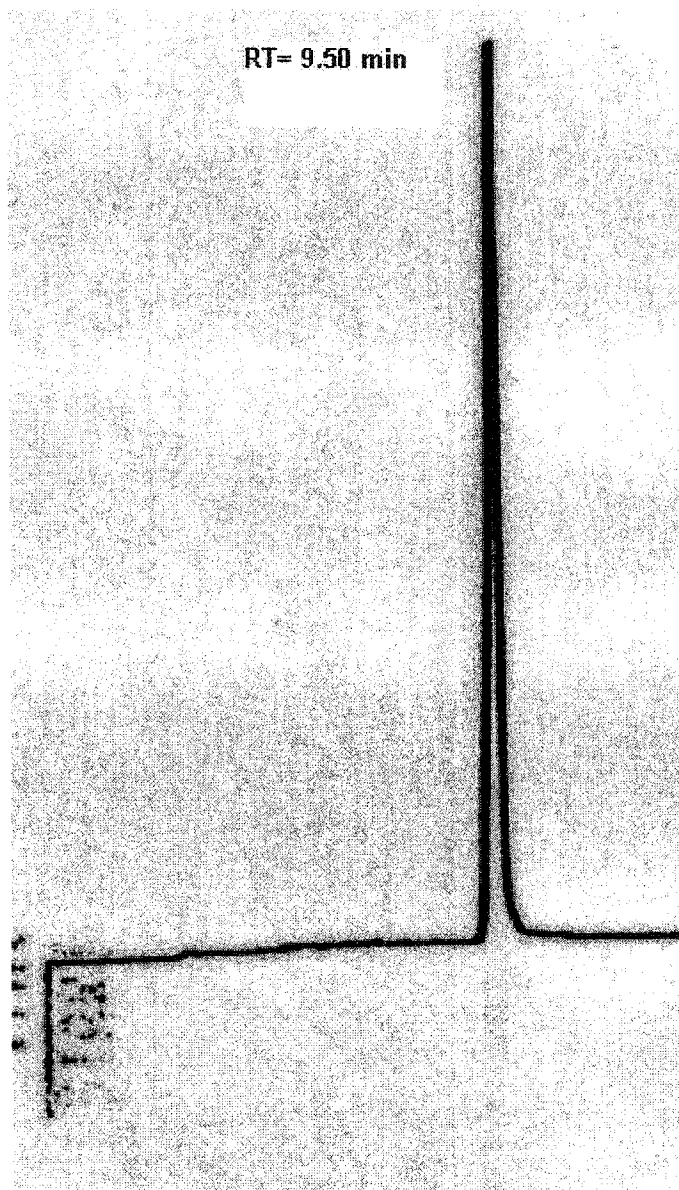


Figure 4: HPLC analysis of CPT at pH=6.1 after incorporation into CL oligomers. (first injection, time=0 min). No retention time for carboxylate form was observed.

<u>Retention Time</u>	<u>Area %</u>	
9.50	100%	Lactone form

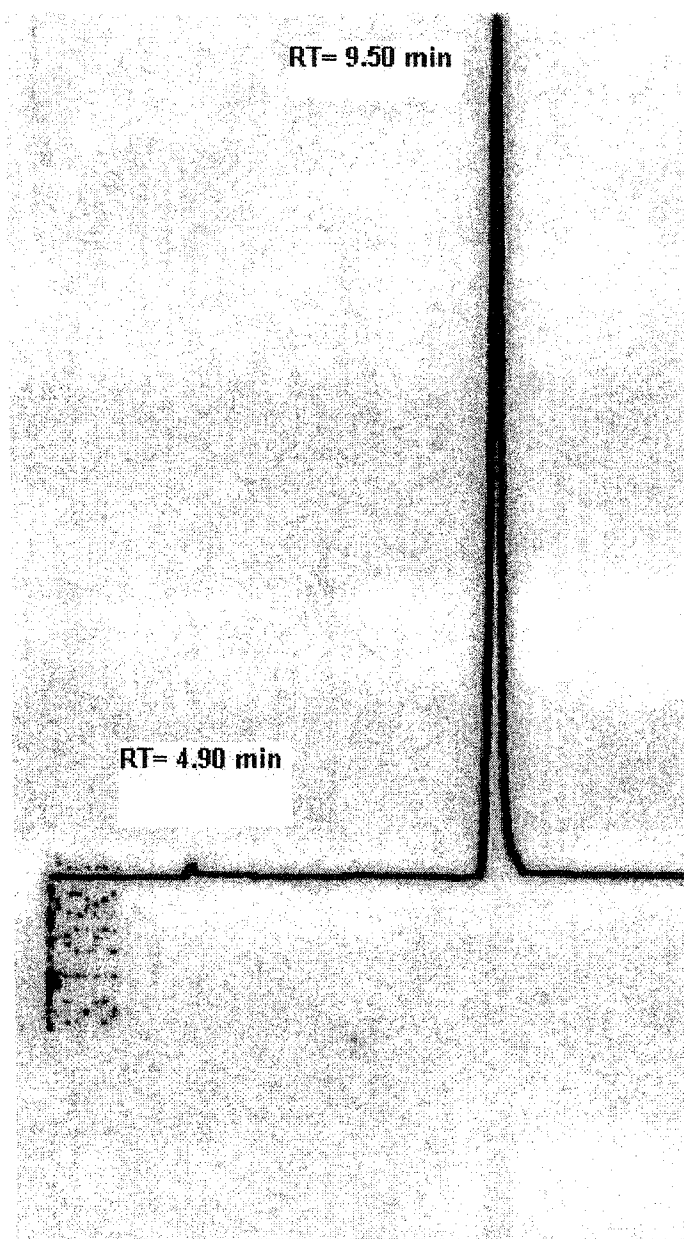


Figure 5: HPLC analysis of CPT at pH=6.1 after incorporation into CL oligomers. (second injection, time=30 min).

<u>Retention Time</u>	<u>Area %</u>	
4.90	0.5%	Carboxylate form
9.50	99.5%	Lactone form

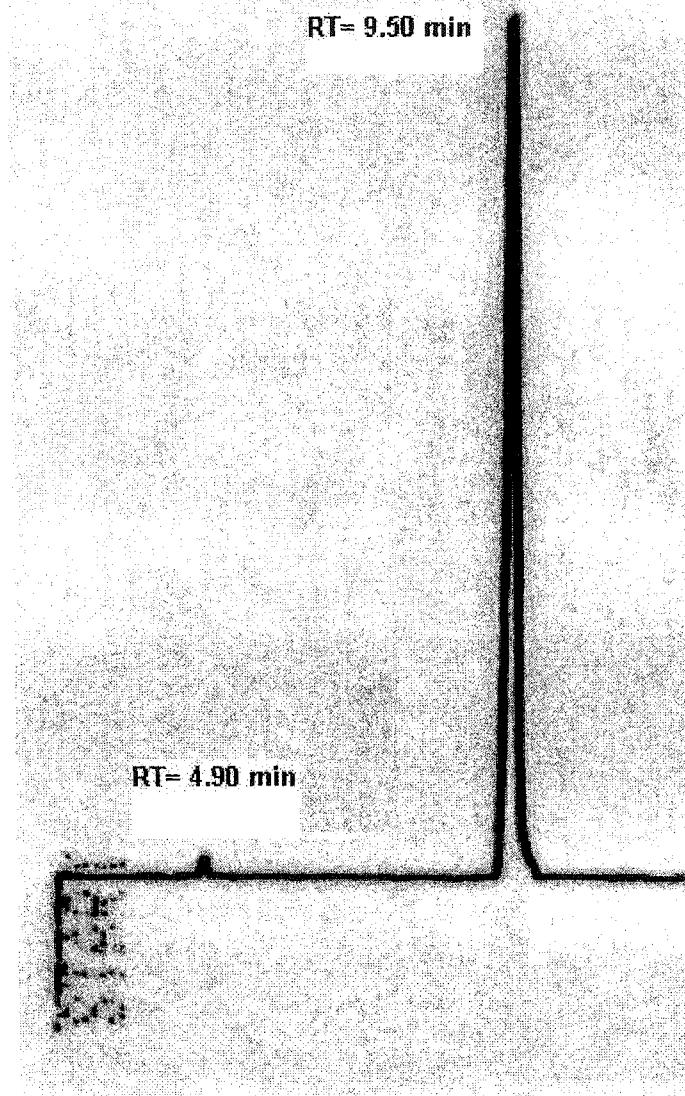


Figure 6: HPLC analysis of CPT at pH=6.1 after incorporation into CL oligomers. (third injection, time=60 min).

<u>Retention Time</u>	<u>Area%</u>	
4.90	1.5%	Carboxylate form
9.50	98.5%	Lactone form

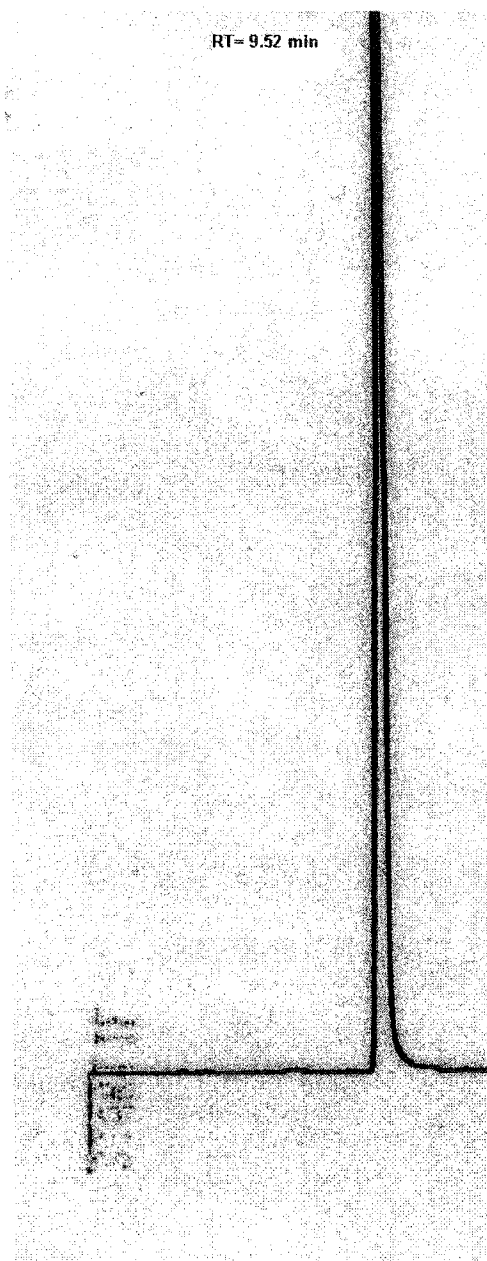


Figure 7: HPLC analysis of released CPT after incubation in PBS for 10 minutes in buffer pH=6.1 from CL oligomers. (first injection, time=0 min). No retention time for carboxylate form was observed.

<u>Retention Time</u>	<u>Area%</u>	
9.52	100%	Lactone form